PROPERTIES OF SUSPENSIONS OF INTERACTING PARTICLES

by

Richard Wyndham O'Brien

Gonville and Caius College

A dissertation submitted for the degree of Doctor of Philosophy within the University of Cambridge

March 1977

To Robyn

and our baby

PROPERTIES OF SUSPENSIONS OF INTERACTING PARTICLES - SUMMARY

The dissertation is divided into six chapters. The first chapter contains introductory remarks and sets the scene for the work that is to follow.

Chapter 2 is devoted to the conduction of heat or electricity through granular materials, the conductivity of the grains greatly exceeds that of the matrix and the grains are closely-packed. From an analysis of the temperature distribution near the point of contact between a pair of particles we derive an expression for the effective conductivity of this type of material.

In chapter 3 we study the conduction of heat across a bundle of fibres. It is shown that small deviations in fibre straightness or in fibre alignment have a marked effect on the conductivity of these types of materials, and expressions are obtained for the effective conductivity of two classes of fibre bundles.

The work in chapter 4 is concerned with general aspects of the determination of effective transport properties. A new method is described for obtaining the effective transport properties of suspensions of interacting spherical particles in both regular and random arrays. This new method does not encounter divergence difficulties, and provides a rigorous basis for the rather ad hoc procedures devised earlier to deal with divergence difficulties. Some old results are rederived by these new techniques and expressions are obtained for the effective modulus of compression of rigid spheres in random and regular arrays in an elastic matrix.

Chapter 5 is devoted to a study of the coagulation of particles in shear flow. We are mainly concerned with the coagulation of particles at "high" shear rates, in which case the Brownian motion of the particles is negligible and the Van der Waals forces between the particles only affect the motion of nearly touching particles. Expressions are obtained for the

rate at which single spherical particles coagulate for form doublets, per unit volume of suspension.

Finally, in chapter 6 we present the results of a numerical study on the effect of Van der Waals attraction and electrical repulsion on the motion of a pair of spherical particles in shear flow. It is shown that at very low shear rates, pairs execute closed orbits about each other. As the shear rate increases the pairs are pulled apart, and finally, at very high shear rates pairs are pushed together with such force by the flow that some are able to overcome the electrical repulsive forces and coagulation occurs.

rate at which single spherical particles coagulate for form doublets, per unit volume of suspension.

Finally, in chapter 6 we present the results of a numerical study on the effect of Van der Waals attraction and electrical repulsion on the motion of a pair of spherical particles in shear flow. It is shown that at very low shear rates, pairs execute closed orbits about each other. As the shear rate increases the pairs are pulled apart, and finally, at very high shear rates pairs are pushed together with such force by the flow that some are able to overcome the electrical repulsive forces and coagulation occurs.

CONTENTS

Chapter 4 : The Dipole field

Preface

With the exception of chapter 2, which contains work done in collaboration with Professor G.K. Batchelor, the work contained in this dissertation is entirely my own. Any unoriginal result cited in the thesis is accompanied by a reference to the article in which that result was first obtained. No part of this dissertation has been, or is currently being submitted for any other degree of diploma at any other university.

I would like to express my deepest gratitude to my supervisor, Professor G.K. Batchelor, who spent many hours giving direction to my research and converting my rather vague ideas into precise statements.

In addition I would like to thank Dr. P. Johnson of the Biochemistry department at Cambridge and Dr. J. Goodwin of the Chemistry department at Bristol University for their assistance during the experimental phase of my work.

Richard O'Brien

Cambridge, March 1977.

CHAPTER ONE

INTRODUCTION

1.1 Suspensions

A "suspension" is defined as a material composed of discrete particles embedded or immersed in a continuous matrix. The particles and matrix may be either solid or fluid, and it is assumed that each particle is large enough to be regarded as continuous. Examples of suspensions occur frequently in nature (blood, clay, mist) and in industry (latex paints, fibre reinforced materials, polymer solutions).

If a particle is placed in an infinite matrix the (temperature velocity or displacement) field in the matrix will be disturbed by the presence of the particle, and this disturbance field will vary on a length scale which is of the order of the particle dimensions. Thus the field in the neighbourhood of a particle in a suspension will be affected by the presence of a neighbouring particle unless the distance separating the pair is much greater than the particle size. We shall refer to this type of interaction as an "indirect interaction" since it is transmitted through the matrix material. In addition to this type of interaction between the particles in a suspension, there may be a "direct" interaction arising from the forces between the particles.

The work which we shall describe in the following chapters is concerned with suspensions in which the interactions, both direct and indirect, play a significant part. We shall only consider the case of solid particles suspended in a solid or liquid matrix. Both particles and matrix are composed of materials which are homogeneous and isotropic and it is assumed that each particle is composed of the same material.

The work divides into parts; chapters 2, 3 and 4 deal with the problems of determining the effective transport properties of suspension of interacting particles, and the remaining two chapters are devoted to the study of the effects of shear flow and interparticle forces on the motion of rigid spherical particles suspended in a Newtonian liquid.

In this chapter we describe the background to this work, beginning with the transport problem, and in §1.4 there is a brief description of some of the experiments with which I was concerned during my first two years at Cambridge.

1.2 The effective transport properties of suspensions

The transport properties of the particles are in general different from those of the matrix, and thus if a suspension is not in a state of equilibrium, the temperature, velocity or displacement varies in a complicated manner with position in the suspension. To determine the value of any of these quantities at each point in the suspensions we would require the position and shape of each particle, but such microstructural information is not usually available. Fortunately we are generally concerned with the behaviour of "microscopic" samples of the suspension which contain a large number of particles; the observable quantities with which we are concerned represent averages and the small scale fluctuations in the quantities are unimportant. For example, if a macroscopic sample is placed in a non-uniform temperature field, the fluctuations in the flux density $\underset{\sim}{F}$ are of less interest than the flux across portions of the surface of the sample which are much larger than the particle dimensions.

When viewed on this scale, the suspension appears to be a single phase continuum, with "effective" properties which vary in a continuous fashion with position in the material. Our aim is to determine the effective transport properties which characterize these macroscopic samples. The transport property of interest may be the conductivity (electrical or thermal), the viscosity, or the elastic moduli. We shall assume that the particles are force-free and therefore the only interactions are indirect.

The particles and matrix are characterized by (different) scalar conductivities. In discussing the effective conductivity it will be assumed that the matrix, if it is a liquid, is at rest and hence conduction is the only means of heat transfer. If the matrix is a liquid, it will be taken to be Newtonian, and if the particles or the matrix are composed of isotropic, linearly elastic materials we shall simply refer to them as being "elastic".

The concept of an effective transport property has been recently given a precise definition by Batchelor (see Batchelor 1974 for a review), who also derived an expression relating effective transport properties to an average over the particles of a quantity known as the "Particle dipole strength". We shall describe the derivation of this result here, as it will be referred to frequently in the following chapters. The derivation is the same, in principle, for each of the transport properties, and we will only give the details for the case of thermal conductivity. The conductivity of the matrix is denoted by k and that of the particles in αk.

In discussing the effective transport properties, Batchelor made use of the concept of an "ensemble average". If we perform experiments on a large number of samples of the same suspension under macroscopically identical conditions the value of any quantity (such as the temperature at a point in the suspension) will fluctuate randomly from one experiment to the next since the configuration of particles will not be the same for each sample. The average of a quantity, averaged over the ensemble of experiments, is defined as the ensemble average and is denoted by angle brackets. For the conduction problem, the averaged quantities with which we shall be concerned are the average flux density $\langle \underset{\sim}{F}(\underset{\sim}{x})\rangle$ and the average temperature gradient $\langle \nabla T(\underset{\sim}{x})\rangle$, at a point $\underset{\sim}{x}$.

Since the quantities $\underset{\sim}{F}$ and ∇T at a point in a suspension are linearly related, it is reasonable to assume that the ensemble averages of these quantities will also be linearly related, i.e.:

$$\langle \underset{\sim}{F} \rangle = -\underset{\approx}{k}^{*} \cdot \langle \nabla T \rangle \tag{2.1}$$

where the second rank tensor $\underset{\approx}{k}^{*}$ is defined as the effective conductivity. In the case of a material with a statistically isotropic structure, $\underset{\approx}{k}^{*}$ is proportional to the unit tensor and

$$\langle \underset{\sim}{F} \rangle = -k^{*} \langle \nabla T \rangle \ . \tag{2.2}$$

In general k^{*} may vary with position but we shall only be concerned with materials for which k^{*} is uniform.

If the temperature or flux density over the surface of the sample is known, then with the aid of the relation (2.1) or (2.2) and the heat conservation equation $\nabla \cdot \langle F \rangle = 0$, we can, in principle, determine the averaged quantities $\langle \underset{\sim}{F} \rangle$ and $\langle \nabla T \rangle$ at any point in the material. This would not be of much practical value if we could not then relate these ensemble averaged quantities to the quantities which would be measured in a single experiment, but fortunately these quantities are related for a large class of suspensions.

To demonstrate this relationship, we begin by noting that the quantities $F(\underset{\sim}{x})$ and $\nabla T(\underset{\sim}{x})$ vary randomly from one experiment to the next, reflecting the variations in the particle configuration. If the statistical properties of $F(\underset{\sim}{x})$ and $\nabla T(\underset{\sim}{x})$ do not vary with $\underset{\sim}{x}$, then by the Ergodic Hypothesis, the ensemble average of these quantitires is equal to an average obtained by "sampling" the values of $\underset{\sim}{F}$ and ∇T at a large number of points in a single suspension. This is of course only valid if the values of $\underset{\sim}{F}$ and ∇T at each sample point are statistically independent of the values at the other sample points; since these quantities fluctuate with position on a length scale of the order of the particle size, we conclude that the sample points must be separated by distances which are large compared to the particle size. Thus we may replace the ensemble average of $\underset{\sim}{F}$ and ∇T by the average over a single suspension if the variables are approximately statistically stationary over distances which greatly exceed the size of the particles.

Such suspensions are referred to as "locally statistically homogeneous". The work that follows deals only with this type of suspension. If we attempt to measure the value of a quantity in a suspension using a macroscopic measuring instrument we obtain an average of that quantity and for a statistically homogeneous suspension this average is equal to the local ensemble average. Thus the ensemble averages have a real meaning for this type of suspension, and the effective conductivity $\underset{\approx}{k}^*$ defined in (2.1) is consistant with the intuitive idea of an effective property.

Although the concept of an ensemble of experiments provides a useful framework in which to discuss the statistical nature of suspensions, the ensemble averages are less convenient for manipulation than the averages over regions of a single suspension. For a locally statistically homogeneous suspension the two averages are equal and in the work that follows we shall use the "volume average", which is defined as the integral average over a volume V which is large enough to contain many particles, but which has dimensions which are much less than the length scale over which the statistical properties of the quantity of interest vary. Thus for the conduction problem, the relevant averaged quantities are

$$\langle \underset{\sim}{F} \rangle = \frac{1}{V}\int_V \underset{\sim}{F}\, dV \tag{2.3}$$

and

$$\langle \nabla T \rangle = \frac{1}{V}\int_V \nabla T\, dV \,. \tag{2.4}$$

On dividing the volume of integration in (2.3) into matrix and particles and replacing $\underset{\sim}{F}$ by $-k\nabla T$ at points in the matrix and $-\alpha k\nabla T$ at points in the particles, we get ensemble average of $\underset{\sim}{F}$ and ∇T by the average over a single suspension if the variables are approximately statistically stationary over distances which greatly exceed the size of the particles.

Such suspensions are referred to as "locally statistically homogeneous". The work that follows deals only with this type of suspension. If we attempt to measure the value of a quantity in a suspension using a macroscopic measuring instrument we obtain an average of that quantity and for a statistically homogeneous suspension this average is equal to the local ensemble average. Thus the ensemble averages have a real meaning for this type of suspension, and the effective conductivity $\underset{\approx}{k}^*$ defined in (2.1) is consistant with the intuitive idea of an effective property.

Although the concept of an ensemble of experiments provides a useful framework in which to discuss the statistical nature of suspensions, the ensemble averages are less convenient for manipulation than the averages over regions of a single suspension. For a locally statistically homogeneous suspension the two averages are equal and in the work that follows we shall use the "volume average", which is defined as the integral average over a volume V which is large enough to contain many particles, but which has dimensions which are much less than the length scale over which the statistical properties of the quantity of interest vary. Thus for the conduction problem, the relevant averaged quantities are

$$\langle \underset{\sim}{F} \rangle = \frac{1}{V}\int_V \underset{\sim}{F}\, dV \qquad (2.3)$$

and

$$\langle \nabla T \rangle = \frac{1}{V}\int_V \nabla T\, dV \, . \qquad (2.4)$$

On dividing the volume of integration in (2.3) into matrix and particles and replacing $\underset{\sim}{F}$ by $-k\nabla T$ at points in the matrix and $-\alpha k\nabla T$ at points in the particles, we get

$$\langle \underset{\sim}{F} \rangle = -k\langle \nabla T \rangle + n\langle \underset{\sim}{S} \rangle \quad , \tag{2.5}$$

where n is the number of particles per unit volume and

$$\underset{\sim}{S} = (1-\alpha^{-1})\int_{V^i} \underset{\sim}{F}\, dV \tag{2.6}$$

is the dipole strength of the ith particle. The angle brackets about $\underset{\sim}{S}$ in (2.5) denote the average over the particles contained V.

If the particle is a perfect conductor ($\alpha = \infty$) it is not possible to calculate $\underset{\sim}{F}$ at points in the particle and a more convenient definition of the dipole strength is obtained by applying the divergence theorem to the volume integral in (2.6) which yields

$$\underset{\sim}{S} = (1-\alpha^{-1})\int_{A_p} \underset{\sim}{x}\, \underset{\sim}{F}\cdot\hat{n}\, dA \tag{2.7}$$

where Ap is the particle surface and $\hat{n}$ is the unit outward normal from Ap. This is the definition of $\underset{\sim}{S}$ which we shall use for the purposes of calculating the dipole strength.

For a statistically homogeneous suspension $\langle \underset{\sim}{S} \rangle$ is proportional to $\langle \nabla T \rangle$ and thus we may calculate the effective conductivity from (2.1) and (2.5), once $\langle \underset{\sim}{S} \rangle$ has been determined.

The corresponding results for the other transport problems are obtained by a similar procedure; the volume average stress $\langle \underset{\approx}{\sigma} \rangle$ in a suspension with an elastic or Newtonian liquid matrix is given by

$$\langle \underset{\approx}{\sigma} \rangle = \langle \underset{\approx}{\sigma}_0 \rangle + n\langle \underset{\approx}{S} \rangle \tag{2.8}$$

where $\underset{\approx}{\sigma}_0(\underset{\sim}{x}) = \underset{\approx}{\sigma}(\underset{\sim}{x})$ if $\underset{\sim}{x}$ lies in the matrix, and if $\underset{\sim}{x}$ lies in the particles $\underset{\approx}{\sigma}_0(\underset{\sim}{x})$ denotes the stress which would be obtained at $\underset{\sim}{x}$ if that particle could be replaced by matrix material with the strain or strain rate at $\underset{\sim}{x}$ held fixed. The dipole strength $\underset{\sim}{S}$ is here a second order tensor given by

$$\underset{\approx}{S} = \int_{V_p} (\underset{\approx}{\sigma}(\underset{\sim}{x}) - \underset{\approx}{\sigma}_0(\underset{\sim}{x}))\, dV \tag{2.9}$$

where V_p is the particle volume. For the case of a rigid particle, $\underset{\approx}{\sigma_o} = \underset{\approx}{0}$ at points in the particle, and on applying the divergence theorem to the volume integral in (2.9) we get

$$\underset{\approx}{S} = \int_{A_p} \underset{\sim}{x}\, \underset{\approx}{\sigma} \cdot \hat{n}\, dA \tag{2.10}$$

Thus the problem of determining the effective transport properties is equivalent to that of determining the average particle dipole strength.

Previous Theoretical investigations

If the volume fraction ϕ of the particles is small, the distance between neighbouring particles is, on average, much greater than the particle dimensions (provided there is no clustering), and hence most of the particles are effectively alone in an infinite matrix. In this case, the average dipole strength is equal to $\underset{\sim}{S}o$, the dipole strength of a lone particle immersed in an infinite matrix in which the temperature tends to $\langle \nabla T \rangle \cdot \underset{\sim}{x}$ at large distances from the particle.

The problem of determining $\underset{\sim}{S}o$ is simplest for the case of a spherical particle, and consequently the dilute suspensions of spherical particles were the first to receive theoretical attention. In 1873 Maxwell obtained an expression for the effective conductivity of such a suspension. The expression for the effective viscosity of a dilute suspension of rigid spheres was obtained by Einstein (1956) in 1905, and the corresponding result for a suspension of droplets of a second fluid held spherical by surface tension was obtained by Taylor (1932). Finally, in 1947, Dewey derived formulae for the effective elastic moduli of a dilute suspension of elastic spheres in an elastic matrix.

Subsequent investigations have yielded expressions for the effective transport properties of dilute suspensions of spheroidal particles. The problem of determining the effective viscosity of such a suspension is complicated by the fact that the orientation of a spheroid is affected by the bulk flow. Since the dipole strength of these particles depends on their orientation with respect to the flow field, the effective viscosity is affected by the bulk flow and such factors as the Brownian diffusivity of the particles. The problem of determining the orientation distribution of a dilute suspension of spheroidal particles has recently been solved by Leal and Hinch for a number of bulk flows and expressions for the effective viscosity have been obtained (see Batchelor 1974 for review).

Although the expressions for the effective transport properties of dilute suspensions help us to gain some insight into the effect of particle shape and composition, they are of little practical value, for the transport properties of these suspensions are only slightly different from those of the matrix. To obtain more useful expressions for the effective transport properties, we must be able to deal with the problems caused by particle interactions.

Since the average dipole strength $\langle \underset{\sim}{S} \rangle$ in a dilute suspension is independent of ϕ (for $\phi \ll 1$) it follows from the expressions (2.1) and (2.5) that the particles alter the effective conductivity by an amount that is proportional to ϕ. It is generally assumed that this is the leading term in a power series of ϕ^n, where the coefficients of the ϕ^2 and higher order terms reflect various particle interactions.

A great deal of effort has been expended on the determination of the ϕ^2 coefficient in the expressions for the effective transport properties of random arrays of spherical particles. This work was hampered by the occurance of non-convergent integrals, a problem which was finally overcome by Batchelor (see review article 1974).

By using Batchelor's "Particle Dipole method", Jeffrey (1973) was able to obtain the ϕ^2 term in the expression for the effective conductivity of a random array of spheres. The corresponding expression for the viscosity of a suspension of rigid spheres in a pure straining motion was obtained by Batchelor and Green (1972(b)), again by the Particle Dipole Method, and in the same paper, an expression was derived for the effective shear modulus of a suspension of incompressible elastic spheres in an incompressible elastic matrix. More recently, Batchelor (1977) has calculated the ϕ^2 term in the expression for the effective viscosity of rigid spherical particles suspended in a Newtonian liquid in shear flow, for the case of strong Brownian motion.

In addition to this work on random suspensions there have been a number of investigations into the effective conductivity of regular arrays of spheres embedded in a matrix. The initial work in this field was carried out by Rayleigh (1892), who derived an expression for the conductivity of a simple cubic array of spheres correct to $O(\phi^{13/3})$. This expression takes the form of a power series in $(^a/d)$, where a is the sphere radius and d is the distance between the centres of neighbouring spheres. The formula has been verified experimentally (Meredith and Tobias 1960). Recently, McKenzie and McPhedran (1977) have developed an algorithm for obtaining higher order terms in this power series, and with the aid of a computer they have calculated the effective conductivity of a simple cubic array at volume fractions which are near to the close-packing limit (ϕ = .524).

Expression have also been obtained for the effective conductivity of suspensions of spheres in body-centred-cubic and face-centred-cubic array (Bertaux et al 1975). These formulae were derived by essentially the same method as that developed by Rayleigh.

In the same paper in which he studied conduction through cubic arrays of spheres, Rayleigh also derived a formula for the components of k* associated with conduction across a square array of circular cylinders, but this formula appears to have aroused comparitively little interest.

Of the work which has so far been described, only that of McKenzie and McPhedran is valid for concentrated suspensions. These authors report that the series for k^* converges very slowly at volume fractions which are near to the close packing limit if the conductivity of the spheres is much greater than that of the matrix. This suggests that the problem of determining the conductivity becomes more complex as the volume fraction increases.

This apparent complexity arises from the fact that the power series formulation for k^* is inappropriate at high volume fractions if the conductivity of the spheres is much greater than that of the matrix. This was first realized by Keller (1962) who derived a simple formula for the conductivity of a cubic array of perfectly conducting spheres which are nearly in contact. Keller's formula is based on the observation that most of the heat which passes through the suspension flows along chains of particles which extend between the boundaries, and that most of the heat which passes between a pair of particles passes through the thin matrix layer which separates the parts of the particle surfaces that are nearly in contact. By a similar method, Keller also obtained an expression for the conductivity of a square array of nearly-touching parallel cylinders of infinite conductivity.

In addition to the work described above, there have been a number of investigations based on "cell models" (Happel and Brenner (1973)) or "self consistant schemes" (see Jeffrey (1974)), but we shall not describe these results here as they do not have a sound theoretical basis.

The work described in Chapters 2, 3 and 4

Chapters 2 and 3 deal with the problem of conduction (of heat or electricity) through suspensions of closely packed particles immersed in a matrix of relatively low conductivity. As in the case of perfectly conducting particles, most of the heat passes through these suspensions along chains of particles, but as neighbouring particles may be in contact, we cannot approximate the particles as perfect conductors (since the flux between a pair of perfect conductors diverges as they come into contact, if they are at different temperatures).

Chapter 2 deals with the problem of conduction through granular materials; expressions are obtained for the effective conductivity of suspensions of closely packed spherical particles in random or regular arrays. This work was done in collaboration with Professor Batchelor.

In Chapter 3 we study the conduction of heat across a bundle of fibres. It is shown that small deviations in fibre straightness or in fibre alignment have a marked effect on the conductivity of these type of materials, and expressions are derived for the effective conductivity of two classes of fibre bundles.

The work in Chapter 4 is concerned with general aspects of the determination of effective transport properties. I describe here a new method for obtaining the effective transport properties of suspensions of interacting spherical particles in both regular and random arrays. This new method does not encounter divergence difficulties, and provides a rigorous basis for the rather ad hoc procedures devised earlier to deal with divergence difficulties. Some old results are rederived by these new techniques and expressions are obtained for the effective modulus of compression of rigid spheres in random and regular arrays in an elastic matrix.

1.3 The effect of interparticle forces on the motion of suspended particles in shear flow

Particles suspended in a liquid tend to acquire an electric charge which may result from the absorption of ions from the solvent onto the particles surface, or from the migration of ions from the particle to the solvent. The sign of this charge is determined by the difference in chemical potential between the particles and the solvent, and thus there is generally an electrical repulsion between particles composed of the same material. Opposed to this repulsive force is the Van der Waals force of attraction between the particles, and it is the balance between these two forces which determines the stability of the suspension.

This balance can be altered by the addition of salt to the suspension, for the electrical forces diminish as the concentration of ions in the solvent is increased, and if sufficient salt is added, the particles will coagulate under the action of the Van der Waals forces. It has been found that the coagulation rate is enhanced if the suspension is stirred, and Chapter 5 is devoted to the study of this phenomenon, known as "Shear induced coagulation".

The earliest theoretical investigation into the problem of coagulation was carried out by Smoluchowski (1917), who studied the coagulation of spherical particles both in a suspension at rest and in a suspension in shear flow. At that time very little was known about the forces of attraction between colloidal particles, and Smoluchowski's work is based on the assumption that the Van der Waals force between a pair of particles is only significant if the particles are actually touching each other. Thus the particles are unaffected by this force unless they "collide", and furthermore it was assumed that the particles stick together after colliding.

Since an attractive force of this type cannot bring particles together, another mechanism is required. In a suspension at rest this is provided by the Brownian motion of the particles, and thus the coagulation rate is determined by the diffusivity of the particles.

If the suspension is undergoing shear flow, the coagulation rate increases because the shear flow provides an additional mechanism for bringing particles together.

In studying coagulation in a suspension in shear flow, Smoluchowski neglected the Brownian motion of the particles, an assumption which is valid if the shear rate is sufficiently high. In this analysis, the hydrodynamic interaction between the particles was neglected and thus it was assumed that particles simply translate with the bulk flow and coagulate on collision with other particles. With the aid of these assumptions, Smoluchowski derived expressionsfor the rate at which coagulated doublets, triplets and higher order groups of particles are formed per unit volume of suspension.

Clearly there was some room for improvement in Smoluchowski's analysis, but even the simpler problem of coagulation in a suspension at rest was not treated in an entirely satisfactory manner until 1967, when Derjaguin and Muller produced an analysis which took into account both the effects of Van der Waals attraction and hydrodynamic interaction on the coagulation rate.

In 1970 Curtis and Hocking studied the effect of Van der Waals attraction on the motion of a sphere-pair in a shear flow. By numerically integrating the equations of motion a sphere pair for a large number of initial conditions, they were able to determine which pairs would coagulate at a given shear rate. From this information Curtis and Hocking attempted to calculate the rate at which spheres coagulate to form pairs per unit volume of suspension, but their results are incorrect for reasons which we shall describe in § 5.9.

Most of the work in Chapter 5 deals with the problem of the coagulation of spherical particles at high shear rates. Like the previous authors, we neglect the Brownian motion of the particles, and in addition we make use of the observation that at these high shear rates, the Van der Waals forces only affect the motion of particles which are nearly touching each other. The equations which describe the motion of the centre of one member of a sphere-pair in a shear flow, relative to the centre of the other, have a particularly simple form if the pair are nearly in contact. We have been able to solve these equations and obtain expressions describing the relative trajectories of the nearly-touching sphere pairs which are influenced by the Van der Waals attraction.

The sphere pairs which are not nearly-touching are effectively force-free, and the motion of such pairs has been thoroughly analysed by Batchelor and Green (1972(a)). By linking Batchelor and Green's results with the expressions describing the relative trajectories of the nearly touching sphere-pairs, we have been able to calculate the rate at which single spheres coagulate to form doublets in a unit volume of suspension, for a number of shear rates. We have found that the coagulation rate approaches a limiting value at high shear rates, and we have calculated this value by two quite different methods.

Finally, by combining this high shear rate analysis with Derjaguin and Muller's (1967) work on coagulation in a suspension at rest, we have obtained a qualitative picture of the combined effects of Brownian motion and shear rate on coagulation.

If the concentration of electrolyte in the solvent is not sufficiently high, the electrical forces between the particles may have a significant effect on their motion in a shear flow. In Chapter 6 we present the results of a numerical study of the relative motion of sphere-pairs which are influenced by both electrical repulsion and Van der Waals attraction.

I have been unable to find any previous investigations on this subject in the literature, and the work presented in Chapter 6 is in the nature of a preliminary study. Consequently we have dispensed with complications such as the Brownian motion of the particles and the effect of retardation on the Van der Waals force.[+] Furthermore we assume that the

---

[+] The rate at which the Van der Waals force between a pair of particles drops off as the particles are separated increases when the minimum separation distance between the surfaces becomes of order λ , a wavelength (usually about 10^{-6} cms) associated with the material of which the particles are composed. This is known as the "retardation effect" (see Verwey and Overbeek (1948) for more details).

the other, have a particularly simple form if the pair are nearly in contact. We have been able to solve these equations and obtain expressions describing the relative trajectories of the nearly-touching sphere pairs which are influenced by the Van der Waals attraction.

The sphere pairs which are not nearly-touching are effectively force-free, and the motion of such pairs has been thoroughly analysed by Batchelor and Green (1972(a)). By linking Batchelor and Green's results with the expressions describing the relative trajectories of the nearly touching sphere-pairs, we have been able to calculate the rate at which single spheres coagulate to form doublets in a unit volume of suspension, for a number of shear rates. We have found that the coagulation rate approaches a limiting value at high shear rates, and we have calculated this value by two quite different methods.

Finally, by combining this high shear rate analysis with Derjaguin and Muller's (1967) work on coagulation in a suspension at rest, we have obtained a qualitative picture of the combined effects of Brownian motion and shear rate on coagulation.

If the concentration of electrolyte in the solvent is not sufficiently high, the electrical forces between the particles may have a significant effect on their motion in a shear flow. In Chapter 6 we present the results of a numerical study of the relative motion of sphere-pairs which are influenced by both electrical repulsion and Van der Waals attraction.

I have been unable to find any previous investigations on this subject in the literature, and the work presented in Chapter 6 is in the nature of a preliminary study. Consequently we have dispensed with complications such as the Brownian motion of the particles and the effect of retardation on the Van der Waals force.[+] Furthermore we assume that the

---

[+] The rate at which the Van der Waals force between a pair of particles drops off as the particles are separated increases when the minimum separation distance between the surfaces becomes of order λ , a wavelength (usually about 10^{-6} cms) associated with the material of which the particles are composed. This is known as the "retardation effect" (see Verwey and Overbeek (1948) for more details).

range of action of the electrical forces (the Debye length) is much smaller than the particle radius and thus we only deal with nearly-touching sphere pairs.

1.4 Unsuccessful Experiments

Although the work presented in this thesis is entirely theoretical, I had originally intended to carry out rheological measurements on concentrated suspensions. The experimental work I did during my first two years did not bear fruit, and in this section I shall briefly describe the aims of this work, and some of the problems which were encountered.

In the absence of Brownian motion, the bulk (i.e. volume averaged) stress in a suspension is determined by the bulk strain rate and the statistical aspects of the particle configuration which we term the "structure" of the suspension. We proposed to carry out an experiment in which the suspension has a known structure; in particular, we planned to measure the effective viscosity of a monodisperse suspension of particles with isotropic structure in an oscillatory shear flow of small amplitude. In this case the bulk flow only perturbs the structure from its equilibrium state, and therefore the suspension remains approximately isotropic during the experiment.

The first step was to obtain a monodisperse suspension. One such suspension which had been used in a number of experiments consists of rod-like particles, manufactured from fibre glass. The fibres are 3.5 microns in diameter, and the minimum length to which they can be accurately cut is about 100 microns (see Carter 1967 for details of manufacture of these suspensions). Unfortunately, these rods are too large for our purpose, for the time required for the Brownian rotation of these rods to impart an isotropic structure to the suspension is much larger than the time required for them to sediment out (the specific gravity of the rods is 2.5). Thus we could not be sure that this suspension would be isotropic at the start of the experiment.

A monodisperse suspension of smaller particles was required. Fortunately the suspensions known as "latices" appeared to be suitable. These consist of spherical polymer particles of radius 0.1 - 1 micron suspended in an aqueous solution. With the assistance of Dr. P. Johnson of the Department of Colloid Science I attempted to manufacture a latex, but it soon became apparent that the making of a monodisperse latex is something of an art. We then turned to Professor I.M. Krieger of Case WesternReserve University, Ohio who kindly supplied us with a monodisperse latex containing particles of 0.226 microns in diameter, with a volume fraction of 0.45.

In a review article on the rheology of monodisperse latices, Krieger (1972) describes a method for effectively eliminating the forces between the latex particles, based on the addition of certain amounts of surfactant and electrolyte to the latex. The latex which we had been given had been treated in this way, and so we assumed that the particles were effectively force-free, rigid spheres.

We proposed to measure the effective viscosity of this latex in an oscillatory shear flow, over a range of frequencies. In order to understand how the variation in frequency affects the viscosity we must consider the factors which determine the bulk stress in a suspension of rigid, force-free particles.

There are two components to the bulk stress in such a suspension. One component, known as the "hydrodynamic stress" is the stress that would be obtained in the absence of Brownian motion.[+] This component is proportional to the instantaneous strain rate with a constant of proportionality that is determined by the instantaneous structure. Since the structure is

---

[+] given that the suspension has the same instantaneous structure. This structure will be affected by the Brownian motion, and hence the hydrodynamic stress is indirectly affected by the Brownian motion.

approximately isotropic in the oscillatory flow, the component of the viscosity which arises from the hydrodynamic stress is not frequency dependent. The second component of the bulk stress, known as the "direct contribution due to the Brownian motion" arises from the fact that the flow slightly alters the structure of the suspension and as the particles diffuse through the liquid in an attempted to restore the equilibrium structure they generate a bulk stress.

The parameter which characterizes the relative magnitude of these two components is $\frac{\omega a^2}{D}$, where ω is the frequency of oscillation of the flow, a is the sphere radius and D is the diffusivity of the particles. At "low" frequencies $\frac{\omega a^2}{D} << 1$ the (nearly isotropic) structure of the suspension is determined by the instantaneous shear rate, and thus the effective viscosity is equal to the "zero-shear viscosity" μ_0 measured in a steadyshear flow (see figure (1.1)). As the frequency of oscillation increases (wht amplitude held fixed), the hydrodynamic component of the bulk stress increases in proportion to ω, but the direct contribution increases more slowly and hence the effective viscosity decreases as $\omega a^2/D$ increases until eventually the viscosity reaches the limiting value μ_1 (see figure (1.1)).

Similarly, the effective viscosity measured in a steady shear flow decreases with shear rate, (see figure (1.1)) but the high shear limiting value μ_2 will in general be different from μ_1, for in a steady shear flow the structure of the suspension is altered by the flow.

By measuring the quantities μ_0 and μ_1 we can determine the contribution to the zero shear viscosity from the Brownian motion of the particles. Furthermore, by measuring the high shear limiting viscosity μ_2 and comparing this with μ_1 we can study the effect of structure on the hydrodynamic component of the bulk stress.

Although this seemed to be a reasonable plan, even the steady shear measurements proved to be difficult at the higher volume fractions ($\emptyset > .4$),

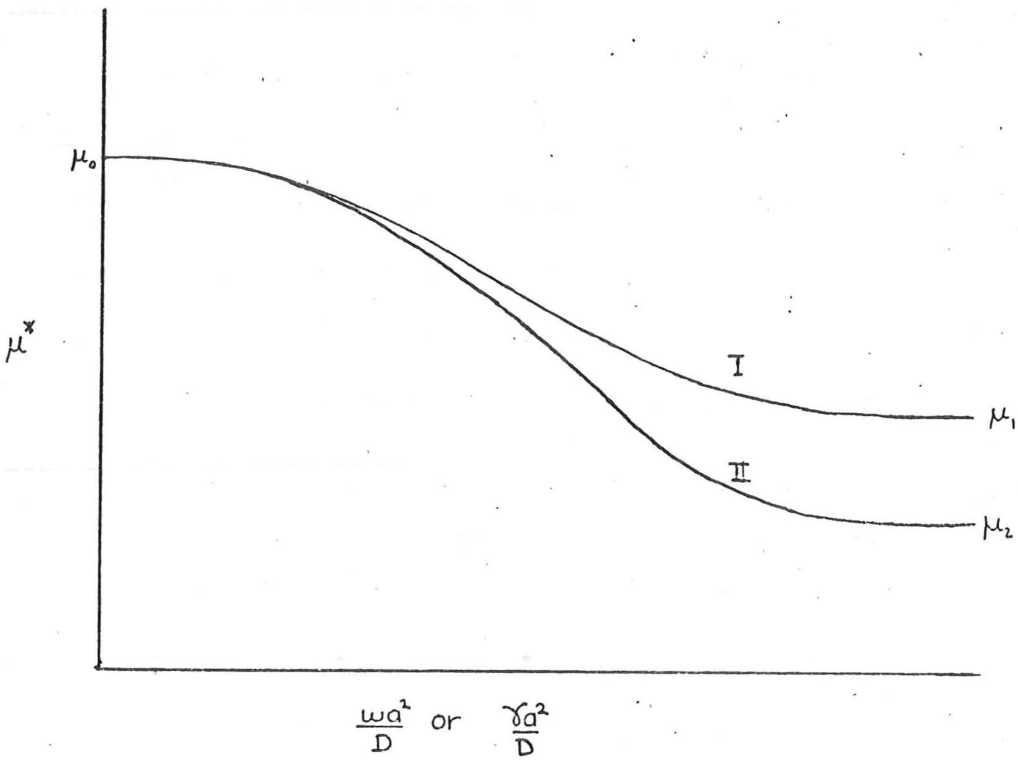

Figure 1.1 The expected form of the effective viscosity curves for a latex. Curve I represents the result for oscillatory shear and the parameter is $\omega a^2/D$ in this case. The dependence of μ^* on shear rate γ in steady shear flow is illustrated by curve II.

for the evaporation of the solvent from these suspensions causes a skin to form on the surface. At the Department of Chemistry at Bristol University there is a Weissenberg Rheogoneometer fitted with a "Mooney device"+ which is designed to overcome this evaporation problem, and it was at that department that I attempted to measure these quantities μ_0, μ_1 and μ_2.

With a great deal of assitance from Dr. Jim Goodwin I managed to obtain some reproducible measurements of μ_0 and μ_2. This required the most meticulous attention to cleanliness, between each run the Mooney device was taken apart and any solidified latex was washed away with distilled water.

Unfortunately, my attempts at measuring the high frequency viscosity μ_1, were totally unsuccessful. I had planned to measure this quantity by observing the decay rate in the oscillations of the upper platen of the Mooney device after it had been given an initial twist. The frequency of these oscillations is determined by the spring constant of the torsion bar which connects the platen to the frame of the Rheogoneometer. With the stiffest torsion bar, the frequency of oscillation is 38.6 cycles per second and although $\frac{\omega a^2}{D}$ is only of order 10 at this frequency, it was hoped that this would be sufficiently large for the direct contribution to the viscosity to be negligible.

Before testing the latex samples at this frequency, I carried out a trial run using distilled water, and it was at this point that the experiment floundered, for the measured decay rate differed significantly from the theoretical value (calculated on the assumption that the term $\underset{\sim}{u}\cdot\nabla\underset{\sim}{u}$ in the Navier-Stokes equations is negligible). Perhaps the flow is unstable at this frequency; if so, the measurement of μ_1 could be

---

+ this is a combination couette-cone and plate device.

carried out with a latex containing larger particles, since $\frac{\omega a^2}{D} \gg 1$ would then be satisfied for lower frequencies.

However, two years without success had dampened my enthusiasm for the project, and it was at this point that I began the work which is described in the remainder of this dissertation.

carried out with a latex containing larger particles, since $\frac{\omega a^2}{D} \gg 1$ would then be satisfied for lower frequencies.

However, two years without success had dampened my enthusiasm for the project, and it was at this point that I began the work which is described in the remainder of this dissertation.

CHAPTER TWO

THERMAL OR ELECTRICAL CONDUCTION THROUGH A GRANULAR MATERIAL

2.1 Introduction

In this chapter we try to derive the effective conductivity of a stationary granular material through which there is a steady transport of heat or electricity. The material consists of randomly arranged grains, in, or nearly in, contact with each other and immersed in a connected uniform matrix which may be fluid or solid. The matrix is characterized by a scalar conductivity k , and the material of the grains by a scalar conductivity αk. We shall study in particular the case $\alpha >> 1$, examples of which are conduction of heat through a packed bed of metal particles in water or of electricity through a pile of carbon particles in air. The case $\alpha >> 1$ is interesting theoretically because the amount of heat or electricity conducted is a delicate balance between the effects of the largeness of the conductivity of the grains and the smallness of the surface of contact between them. It is not at all evident whether the effective conductivity of the medium will be closer numerically to k or to αk.

As is customary in the analysis of properties of heterogeneous media with random structure, we shall assume that the granular medium is statistically homogeneous. It will be supposed that a uniform mean intensity gradient is set up in the medium, perhaps by imposing uniform and different values of the intensity at two distant parallel boundaries. Henceforth we shall use terms and notation appropriate to the case of thermal conduction for convenience; thus the mean intensity gradient will be written as $\langle\nabla T\rangle$, where ∇T is the temperature gradient at a point in the medium (not necessarily in the matrix) and the angle brackets denote an average over the ensemble of realisations of the random structure of the medium. The local thermal flux density $\underset{\sim}{F}$ is equal to $-k\nabla T$ at a point in the matrix and $-\alpha k \nabla T$ at a point in a grain or particle. At each point on the surface of a particle T and the normal components of $\underset{\sim}{F}$ are continuous; and at each point not on such a surface

$$\nabla \cdot \underset{\sim}{F} = 0 , \quad \text{i.e.} \quad \nabla^2 T = 0 . \tag{1.1}$$

All temperature differences are proportional to $\langle \nabla T \rangle$, and so for the mean flux density we have the linear relation

$$\langle \underset{\sim}{F} \rangle = -\underset{\approx}{k}^* \langle \nabla T \rangle ,$$

where the effective conductivity $\underset{\approx}{k}^*$ is a second-rank tensor, dependent on the structure of the medium. We shall be concerned only with granular materials with statistically isotropic structure, in which case $\underset{\approx}{k}^*$ is proportional to the unit tensor and

$$\langle \underset{\sim}{F} \rangle = -k^* \langle \nabla T \rangle . \tag{1.2}$$

Our objective is an expression for the scalar effective conductivity k^*. This problem is mathematically identical with that of determining the effective dielectric constant or the effective magnetic permeability of a disperse system in which the particles have electrical and magnetic properties different from those of the matrix.

The argument to be presented divides naturally into two main parts, one being concerned with the relation between the effective conductivity and the statistics of the structure of the medium and the other with the analysis of the temperature distribution in the neighbourhood of a point of contact between two particles.

Previous theoretical work on the problem of conduction through a packed bed of particles has assumed a regular array of spheres and will be referred to later. None of the previous results is accurate for touching particles.

2.2 The exact expression for the mean flux

In chapter one we described the formalism that has been developed in recent years for the transport properties of a statistically homogeneous medium. For these type of materials the ensemble average of the flux density $\underset{\sim}{F}$ and temperature gradient ∇T are equal to averages over a large volume, and $\langle \underset{\sim}{F} \rangle$ is given by

$$\langle \underset{\sim}{F} \rangle = -k\langle \nabla T \rangle + n\langle \underset{\sim}{S} \rangle . \tag{2.1}$$

The term $\underset{\sim}{S}$, called "the particle dipole strength" is defined by

$$\underset{\sim}{S} = (1-\alpha^{-1}) \int_{A_p} \underset{\sim}{x}\, \underset{\sim}{F} \cdot \hat{n}\, dA , \tag{2.2}$$

where A_o is the surface of the particle, $\hat{n}$ is the unit outward normal to A_o and $\underset{\sim}{x}$ is the position vector of a point on A_o. The angle brackets enclosing $\underset{\sim}{S}$ in (2.1) here denote an average over many particles in one realization. The expressions (2.1) and (2.2) are identical to equations (1 .2.5) and (1.2.7) respectively.

These relations are exact, and valid for any shape, orientation, concentration and spatial arrangement of the particles, either random or regular (the latter being a special case of the former), and they provide a convenient means of determining the effective conductivity. In the dilute limit $n \to 0$ the distribution of $\underset{\sim}{F}$ within a particle is unaffected by the presence of other particles, and may be obtained explicitly for simple particle shapes; for a sphere of radius a the value of $\underset{\sim}{S}$ in these circumstances is readily found to be

$$-\frac{4}{3}\pi a^3 \frac{3(\alpha-1)}{\alpha+2} k\langle \nabla T \rangle ,$$

giving Maxwell's (1873) expression for the effective conductivity for spherical inclusions correct to order ϕ, viz.

$$k^* = k\left\{1 + \frac{3(\alpha-1)}{\alpha+2}\phi\right\} ,$$

where $\phi = \frac{4}{3}\pi a^3 n$ is the fraction of the total volume that is occupied by particles. An improved estimate of the effective conductivity of a dilute dispersion of spherical inclusions which is correct to order ϕ^2 has recently been obtained from (2.1) and (2.2) by Jeffrey (1973) by taking into account the effect of interactions between pairs of particles on the value of $\underset{\sim}{S}$ for a particle.

Here we are concerned with the opposite limit, with ϕ close to its maximum value, for which an expansion of k^* in powers of ϕ is unlikely to exist, and unlikely to be useful if it did exist. The relations (2.1) and (2.2) are no less useful in this case.

2.3 An approximate expression for the particle dipole strength in the case of touching particles of high conductivity

We now make use of the assumption that $\alpha \gg 1$. This of course allows neglect of the term α^{-1} in the factor $1 - \alpha^{-1}$ in (2.2). There are in addition importance consequences for the integral over the particle surface A_o. When the conductivity of the particle material is relatively large, the temperature gradients within particles are relatively small. The temperature within one particle is approximately uniform, and in general is different for different particles. The thermal flux density across the surface of a particle is consequently of large magnitude near a point of contact with another particle. These points of contact on the surface of a particle are necessarily well separated, at any rate for particles without sharp protruberances. The quantity $\underset{\sim}{F}.\,\hat{n}$ thus has large magnitude near a few well separated points on the surface of a particle. This suggests, and later we shall confirm it analytically, that the total heat flux across the part of the surface of a particle that is near a contact point is determined by the local conditions and is large relative to the total flux across parts of the surface <u>not</u> near a contact point. In other words, the integral in (2.2) is approximately equal to the sum of contributions from the parts of A_o near each of the contact points.

Suppose that the ith contact point on A_o is at $\underset{\sim}{x} = \underset{\sim}{x}_i$. In the neighbourhood of this contact point $\underset{\sim}{x}$ is approximately constant, with the value $\underset{\sim}{x}_i$, and the outward heat flux across the particle surface in the neighbourhood of the contact point is

$$H_i = \int_{\mathcal{A}_i} \underset{\sim}{F} . \hat{n} \, dA$$

where $\mathcal{A}_i$ is an appropriately chosen portion of the surface A_o centred on the point $\underset{\sim}{x}_i$. Thus (2.2) becomes

$$\underset{\sim}{S} \approx \sum_i \underset{\sim}{x}_i H_i \ , \tag{3.1}$$

the summation being over the finite number of contact points on the surface A_o.

The flux H_i obviously depends on the difference between the temperatures at the centres of the reference particle with surface A_o and the particle that touches it at the point x_i. This temperature difference is determined by the requirement that

$$\sum_i H_i = 0 , \tag{3.2}$$

there being one such relation for each particle. In the case of a regular array of particles the temperature difference is a simple consequence of (3.2) and the geometry. But in the case of an irregular arrangement of spheres it is difficult to use (3.2) explicitly, and later we shall be obliged to make an ad hoc estimate of the difference between the temperatures of two touching particles in a random array.

It also follows from the largeness of the flux across the particle surface in the neighbourhoods of contact points that the first term on the right-hand side of (2.1) is negligible, whence

$$\langle \underset{\sim}{F} \rangle \approx n \langle \sum_i \underset{\sim}{x}_i H_i \rangle \ . \tag{3.3}$$

The relation (3.3) expresses the idea that most of the flux of heat between two parallel planes occurs through chains of particles and that the thermal resistance comes principally from the thin layers of matrix between adjoining particles. This idea has been used before to obtain an expression for the average heat flux by more heuristic arguments sometimes referred to as 'percolation theory'.

The next step is to consider the way in which H_i depends on α and on the conditions near the ith contact point. The next two sections are concerned with this local problem.

2.4 The thermal flux between two particles in, or nearly in, contact

We consider here the steady temperature distribution near the point of contact of two particles of high conductivity at different temperatures. More precisely, the temperature of one particle is uniform and equal to T_0 far from the contact point and that of the other to T_1 . Just how the temperature distribution within one particle remains steady despite the flux across the particle surface near the contact point is immaterial for our present purpose. The compensating flux across other parts of the particle surface might be concentrated near one or more points of contact with other particles or it might be spread widely over the surface. All that is relevant is that the temperature within a particle tends to a constant far from the contact point under discussion.

The particle surfaces are assumed to be rounded, with curvatures of the same order of magnitude. The two particle surfaces will be regarded as being not literally in contact but separated by a gap whose minimum width h (figure 2.1) is small compared with the radii of curvature of the particle surfaces; this additional generality involves no more mathematical difficulty, and enables us to examine separately the limits $\alpha \to \infty$ and $h \to 0$. The origin O of the coordinate system is at the centre of the minimum gap and the z-axis is normal to the two surfaces. The point

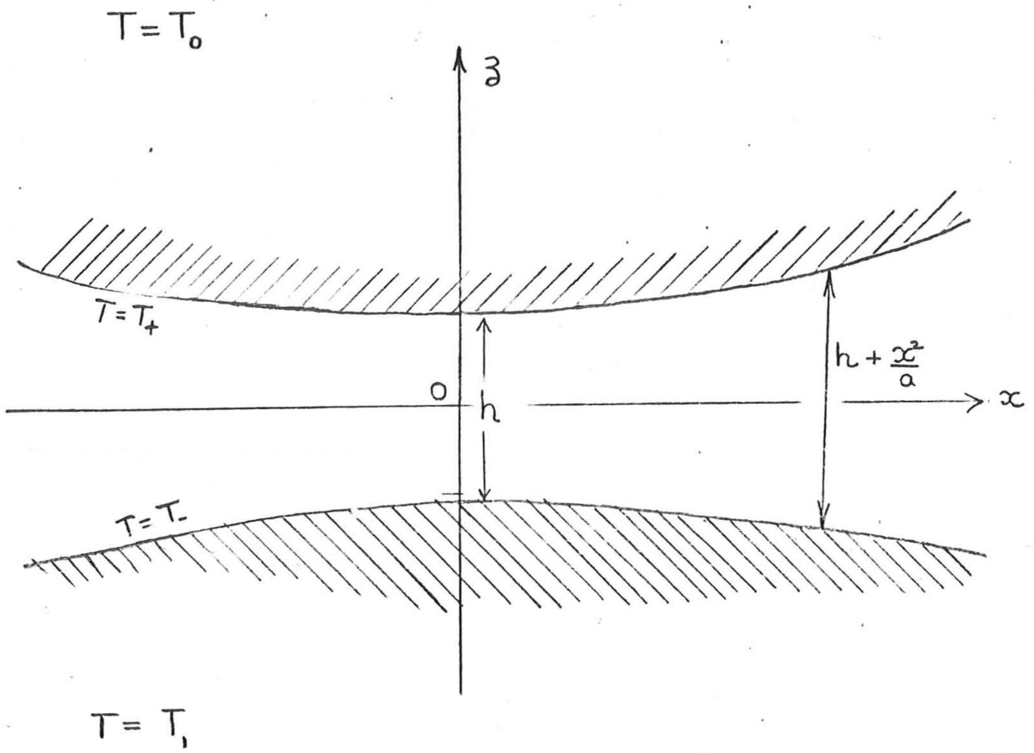

Figure 2.1 Two particle surfaces nearly in contact. The z-axis is normal to the two tangent planes at the points of closest approach.

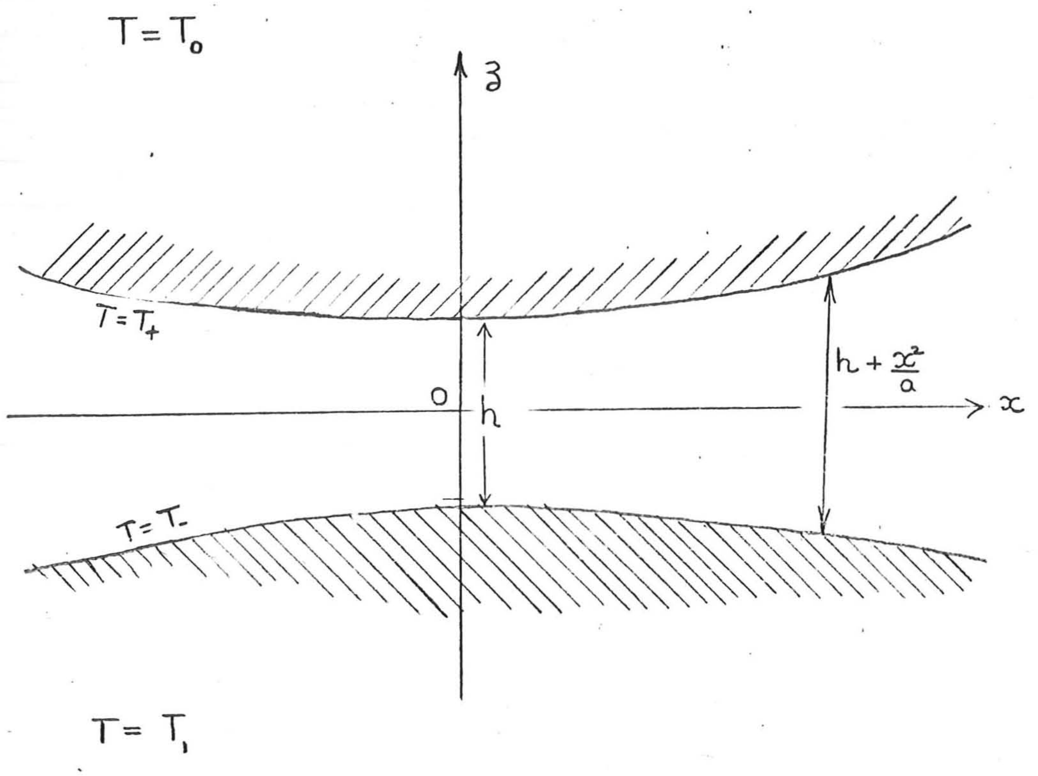

Figure 2.1 Two particle surfaces nearly in contact. The z-axis is normal to the two tangent planes at the points of closest approach.

on the surface of one particle that is closest to the other surface will still be referred to as the 'contact point'. The width of the matrix layer is approximately a quadratic function of x and y, and so for an appropriate choice of the directions of the x- and y-axes may be written as

$$h + \frac{x^2}{a} + \frac{y^2}{b} \quad , \tag{4.1}$$

when x << a, y << b; and in the particular case of two locally spherical surfaces of radii R_0 and R_1 ,

$$a = b = 2R_0R_1(R_0 + R_1)^{-1}.$$

Note that $h \ll (ab)^{\frac{1}{2}}$.

Perfectly conducting particles

The case $\alpha \to \infty$ is relatively simple, and will be considered first. The two particles here have uniform temperatures T_0 and T_1 , and the temperature in the matrix layer varies approximately linearly between the values T_0 and T_1 on the two sides. The z-component of the flux density at a point on one of the surfaces near O is thus approximately

$$\frac{k(T_1 - T_0)}{h + x^2/a + y^2/b} \quad , \tag{4.2}$$

and the total flux through a portion of the surface near O defined by $r^2 = (b/a)^{\frac{1}{2}}x^2 + (a/b)^{\frac{1}{2}}y^2 \leqslant R^2$ is given by

$$2\pi k(T_1 - T_0)\int_0^R \frac{r\,dr}{h + r^2(ab)^{-\frac{1}{2}}} = \pi k(T_1 - T_0)(ab)^{\frac{1}{2}}\log\left\{1 + \frac{R^2}{h(ab)^{\frac{1}{2}}}\right\}$$

$$\approx \pi k(T_1 - T_0)(ab)^{\frac{1}{2}}\left\{\log\frac{(ab)^{\frac{1}{2}}}{h} + \log\frac{R^2}{ab}\right\} \quad ,$$

on the surface of one particle that is closest to the other surface will still be referred to as the 'contact point'. The width of the matrix layer is approximately a quadratic function of x and y, and so for an appropriate choice of the directions of the x- and y-axes may be written as

$$h + \frac{x^2}{a} + \frac{y^2}{b} \quad , \tag{4.1}$$

when x << a, y << b; and in the particular case of two locally spherical surfaces of radii R_0 and R_1 ,

$$a = b = 2R_0R_1(R_0+R_1)^{-1}.$$

Note that $h \ll (ab)^{\frac{1}{2}}$.

<u>Perfectly conducting particles</u>

The case $\alpha \to \infty$ is relatively simple, and will be considered first. The two particles here have uniform temperatures T_0 and T_1 , and the temperature in the matrix layer varies approximately linearly between the values T_0 and T_1 on the two sides. The z -component of the flux density at a point on one of the surfaces near O is thus approximately

$$\frac{k(T_1 - T_0)}{h + x^2/a + y^2/b} \quad , \tag{4.2}$$

and the total flux through a portion of the surface near O defined by $r^2 = (b/a)^{\frac{1}{2}}x^2 + (a/b)^{\frac{1}{2}}y^2 \leqslant R^2$ is given by

$$2\pi k(T_1 - T_0)\int_0^R \frac{r\,dr}{h + r^2(ab)^{-\frac{1}{2}}} = \pi k(T_1 - T_0)(ab)^{\frac{1}{2}}\log\left\{1 + \frac{R^2}{h(ab)^{\frac{1}{2}}}\right\}$$

$$\approx \pi k(T_1 - T_0)(ab)^{\frac{1}{2}}\left\{\log\frac{(ab)^{\frac{1}{2}}}{h} + \log\frac{R^2}{ab}\right\} ,$$

provided we choose $R^2 \gg h(ab)^{\frac{1}{2}}$. The heat flux through the remainder of the surface is approximately independent of h. Hence the non-dimensional total flux across an extensive portion of the particle surface which includes this contact point and no other is approximately

$$\mathcal{H}_{\alpha\to\infty} = \frac{H}{\pi k(T_1 - T_0)(ab)^{\frac{1}{2}}} = \log\frac{(ab)^{\frac{1}{2}}}{h} + K \qquad (4.3)$$

where K is independent of h. The value of K depends on the precise specification of the extended portion of the surface and on the conditions far from the contact point, and is necessarily of order of magnitude unity. The logarithmic term in (4.3) may be said to be the contribution to the heat flux associated with the contact point.

The leading term in the asymptotic expression (4.3) was obtained by Keller (1963) for the case of two perfectly conducting spheres of equal radii a by essentially the above argument. It can also be found, as Keller pointed out by taking the limit (as $h/a \to 0$) of an expansion in terms of hyperbolic functions given by Jeffery (1912) for the total heat flux between two perfectly conducting spheres at different temperatures with a (distributed) heat source in the interior of one and a heat sink of equal magnitude in the other and uniform temperature in the matrix far from the spheres. The corresponding value of K for this case may be found from Jeffery's expansion to be 2.48.

Another relevant published result is the measurement by Meredith & Tobias (1960) of the electrical flux between two brass hemispheres of radius a at different temperatures in tap water with insulating plane boundaries so placed that the spheres were effectively part of an infinite simple cubic array. The gap width was $h/a = 9.6 \times 10^{-3}$, from which it is evident, as may be seen from the formulae given in the next section, that the spheres were each at uniform potential. The relation (4.3) is therefore applicable, and from Meredith & Tobias's measurement of the flux we find K = 0.2 for this particular outer field.

Particles with finite conductivity

If the two particles are not perfect conductors, the temperature distribution within each particle will depart from uniformity in the neighbourhood of the contact point because in that region the thermal flux density across the surface is large. For α large but finite the domain of non-uniform temperature will be small compared with the dimensions of the particle, and so it is permissible to regard the surface of the particle as plane. The heat conducted into a particle across an element of area of the surface thus spreads out in an effectively semi-infinite medium, and this allows the formulation of an integral equation for the distribution of temperature over the surface of the particle near the contact point. For the temperature at the surface of the upper particle in figure (2.1) we have

$$T_+(x,y) - T_0 = \frac{1}{2\pi\alpha k}\int_0^\infty\int_0^\infty \frac{F_3(x',y')\,dx'\,dy'}{\{(x'-x)^2+(y'-y)^2\}^{\frac{1}{2}}},$$

where $F_3(x,y)$ is the z-component of the flux density at a point on the surface. This local flux density may again be estimated from the assumption that the temperature varies linearly across the thin matrix layer, although here the temperature change across the layer as well as the layer thickness is variable. On writing

$$\left.\begin{aligned} T_+(x,y) &= T_0 + \tfrac{1}{2}(T_1-T_0)f(x,y), \\ T_-(x,y) &= T_1 - \tfrac{1}{2}(T_1-T_0)f(x,y) \end{aligned}\right\} \qquad (4.4)$$

for the temperatures at the surfaces of the upper and lower particles respectively, and using the approximation (4.1) for the thickness of the matrix layer, our integral equation for f(x,y) becomes and from Meredith & Tobias's measurement of the flux we find $K = 0.2$ for this particular outer field.

Particles with finite conductivity

If the two particles are not perfect conductors, the temperature distribution within each particle will depart from uniformity in the neighbourhood of the contact point because in that region the thermal flux density across the surface is large. For α large but finite the domain of non-uniform temperature will be small compared with the dimensions of the particle, and so it is permissible to regard the surface of the particle as plane. The heat conducted into a particle across an element of area of the surface thus spreads out in an effectively semi-infinite medium, and this allows the formulation of an integral equation for the distribution of temperature over the surface of the particle near the contact point. For the temperature at the surface of the upper particle in figure (2.1) we have

$$T_+(x,y) - T_0 = \frac{1}{2\pi\alpha k}\int_0^\infty\!\!\int_0^\infty \frac{F_z(x',y')\,dx'\,dy'}{\{(x'-x)^2+(y'-y)^2\}^{\frac{1}{2}}},$$

where $F_z(x,y)$ is the z-component of the flux density at a point on the surface. This local flux density may again be estimated from the assumption that the temperature varies linearly across the thin matrix layer, although here the temperature change across the layer as well as the layer thickness is variable. On writing

$$\left.\begin{aligned} T_+(x,y) &= T_0 + \tfrac{1}{2}(T_1 - T_0)f(x,y), \\ T_-(x,y) &= T_1 - \tfrac{1}{2}(T_1 - T_0)f(x,y) \end{aligned}\right\} \qquad (4.4)$$

for the temperatures at the surfaces of the upper and lower particles respectively, and using the approximation (4.1) for the thickness of the matrix layer, our integral equation for f(x,y) becomes

$$f(x,y) = \frac{1}{\pi\alpha}\int_0^\infty\int_0^\infty \frac{1-f(x',y')}{h+\frac{x'^2}{a}+\frac{y'^2}{b}} \frac{dx'dy'}{\{(x'-x)^2+(y'-y)^2\}^{\frac{1}{2}}} \cdot \tag{4.5}$$

We have obtained explicit results only for the case of particle surfaces which are spherical near the contact point, in which case a and b are equal, the temperature distribution is axisymmetric, and the integral equation (4.5) reduces to

$$f(r) = \frac{1}{\alpha}\int_0^\infty \frac{1-f(r')}{h+r'^2/a} I(\tfrac{r'}{r})\, dr' \tag{4.6}$$

where

$$I(\tfrac{r'}{r}) = \frac{1}{\pi}\int_0^{2\pi} \frac{r'd\phi}{\sqrt{r'^2+r^2-2rr'\cos\phi}} = \frac{4r'}{\pi(r'+r)} K\left(\frac{4r'r}{(r'+r)^2}\right),$$

K being the complete elliptic integral of the first kind. The function $I(r'/r)$ has an integrable singularity at $r'/r = 1$, and

$$I(\tfrac{r'}{r}) \sim \begin{cases} 2r'/r & \text{as } r'/r \to 0 \\ 2 & \text{as } r'/r \to \infty . \end{cases} \tag{4.7}$$

In non-dimensional form (4.6) becomes

$$f(\sigma) = \int_0^\infty \frac{1-f(\sigma')}{\lambda+\sigma'^2} I(\tfrac{\sigma'}{\sigma})\, d\sigma', \tag{4.8}$$

where

$$\sigma = \frac{\alpha r}{a}, \quad \lambda = \frac{\alpha^2 h}{a} .$$

This shows immediately that when $\lambda >> 1$ the particle temperature is approximately uniform, and that when $\lambda << 1$ the temperature distribution in the particle is approximately the same as if the two particles were touching; in other words we see how to judge whether a given small gap has practical significance.

It seems not to be possible to solve (4.8) analytically, but some useful deductions can be made immediately. The length scale on which the temperature in a particle varies is a/α, and in particular the radius of the circle on the particle surface centred on the contact point over which the departure of the temperature from T_0 is significant is of order a/α. The heat flux through a circular portion of the particle surface centred on the contact point is an integral of the form

$$\int 2\pi k(T_1 - T_0)\frac{1-f(r)}{h + r^2/a}\, r\,dr$$

$$= 2\pi k(T_1 - T_0)a\int \frac{1-f(\sigma)}{\lambda + \sigma^2}\,\sigma\, d\sigma\ , \tag{4.9}$$

and this integral would diverge logarithmically at the lower terminal as $\lambda \longrightarrow 0$, were it not for the fact that f takes values near unity in the neighbourhood of the contact point. The value of σ that cuts off this logarithmic divergence is of order unity, and so the approximate expression for the flux when $\lambda \ll 1$ is

$$\pi k(T_1 - T_0)a \log \alpha^2 . \tag{4.10}$$

On the other hand, when $\lambda \gg 1$ the estimate (4.3) is applicable, the difference being that the ... $\log \alpha^2$ in (4.10) is replaced by $\log a/h$. The expression (4.10) answers the question posed in § 2.1 about touching particles; it appears that the heat flux depends more sensitively on the conductivity of the matrix than on that of the particles.

The asymptotic form of the surface temperature increment, as $\alpha r/a \to \infty$ may be found from (4.8) by replacing $I(\sigma'/\sigma)$ by $2\sigma'/\sigma$ for values of σ' in the range $0 \leqslant \sigma' < \sigma$ and by 2 outside that range, and is given by

$$f(\sigma) \sim \frac{2\log\sigma}{\sigma} . \tag{4.11}$$

This asymptotic form shows incidentally that the difference between the heat flux through the particle surface and that for a perfectly conducting particle is a convergent integral which is independent of the boundary conditions far from the contact point.

In order to obtain more detailed results and to confirm the important asymptotic relation (4.10) we have solved the integral equation (4.8) numerically for several different values of λ. The integral in (4.8) was replaced by a sum involving the values of $f(\sigma)$ at N different values of σ by a generalised trapezoidal rule, and these N values of f were then determined from the N simultaneous equations expressing the satisfaction of (4.8) at each of the N points. A more detailed description of the method of solution is given in Appendix A1. Figure (2.2) shows the temperature distribution found with N = 90. As predicted, the curves for different values of λ have the common asymptotic form (4.11) as $\sigma \to \infty$. A convenient way of presenting the corresponding thermal flux across the matrix layer is in terms of the convergent integral

$$P(\lambda) = \int_0^\infty \frac{f(\sigma)}{\lambda + \sigma^2} 2\sigma d\sigma .$$

The non-dimensional flux across an extended portion of the particle surface which includes the neighbourhood of the contact point is then

$$\mathcal{H} = \frac{H}{\pi k(T_1 - T_0)a} = \log\frac{a}{h} + K - P(\lambda), \tag{4.12}$$

where K has the same meaning as in (4.3) and is independent of h and α. The computed values of P are shown in figure (2.3). As $\lambda \to 0$, P evidently tends to $\log \lambda^{-1}$, thereby confirming the asymptotic relation already found. The numerical results show further that

$$\log\frac{a}{h} - P \approx \log\alpha^2 - 3{\cdot}9 - 0{\cdot}1\lambda \tag{4.13}$$

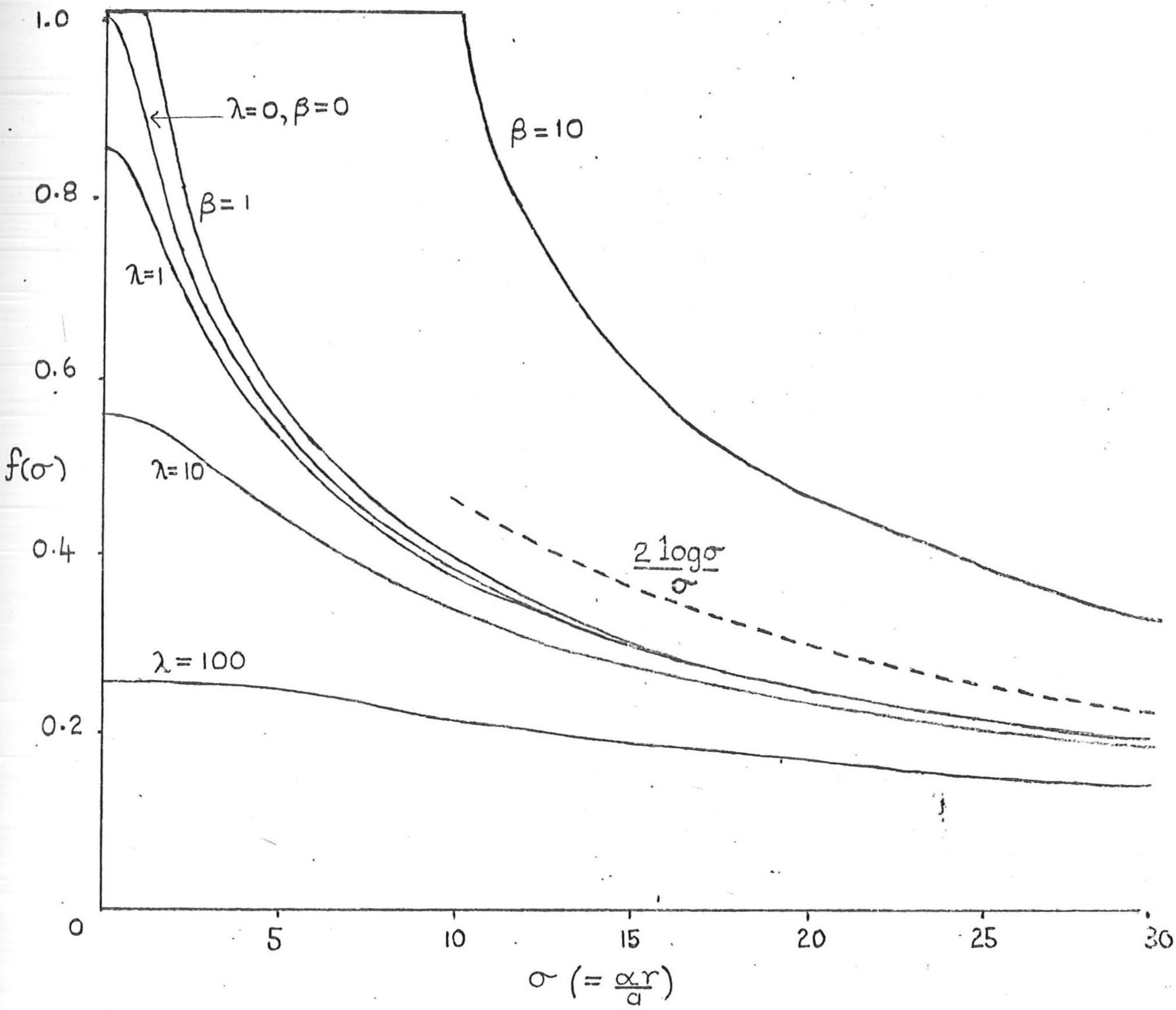

Figure 2.2 The calculated departure from uniformity of the temperature at the surface of a locally spherical particle either separated from another by a minimum distance h specified by λ $(= \alpha^2 h/a)$ or in contact with another over a circle of radius ρ specified by $\beta(= \alpha\rho /a)$.

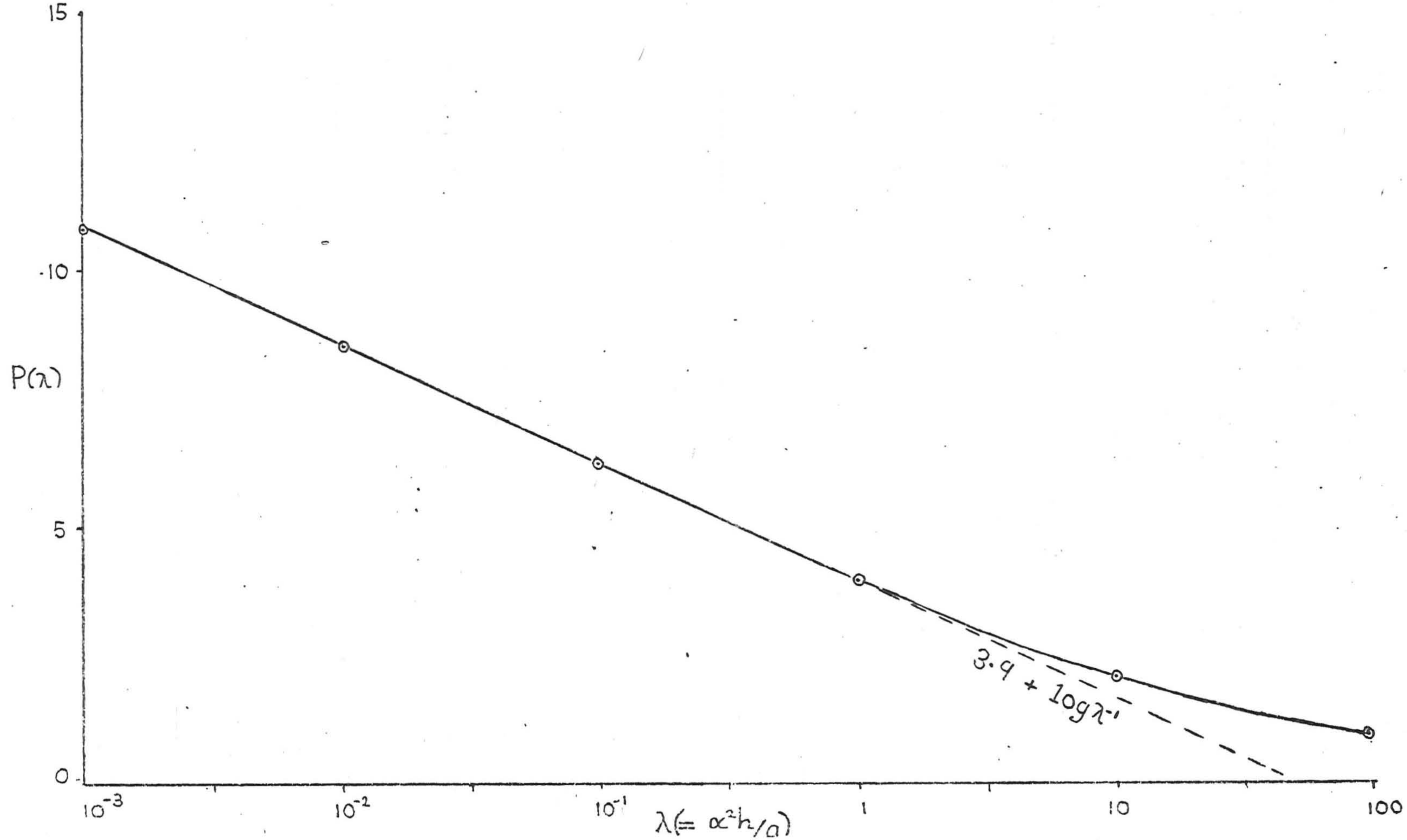

<u>Figure 2.3</u> The change in the heat flux between two particles due to non-uniformity of the temperature at the particle surface.

when λ << 1, and that this remains quite an accurate approximation for values of λ as large as unity. The constants 3.9 and 0.1 are parameters of the inner field, and are independent of conditions far from the contact point. The term linear in λ does not have practical value but plays a part in a later discussion (§2.5).

The non-dimensional heat flux between two touching particles with locally spherical surfaces is thus

$$\mathcal{H}_{h=0} = \log\alpha^2 + K - 3.9 , \tag{4.14}$$

where K is a number of order unity which depends on the outer field conditions and is independent of α and of whether the particles are actually touching.

Deissler and Boegli (1958) report having made a relaxation calculation of the temperature distribution inside and outside a sphere in point contact with a second sphere, with boundary conditions corresponding to the sphere being part of an infinite line of touching spheres in a circumscribing insulating cylinder, for several values of α up to about 10^3. They give their results in the form of a continuous curve, which we have replotted in figure (2.4) for comparison with (4.14). Deissler & Boegli's results are less accurate at the larger values of α, for which the temperature gradients are very steep, but they are consistent with the linear dependence of the heat flux on log α^2 at large values of α expected from (4.14). The value of the constant K corresponding to the linear asymptotic relationship drawn in figure 4 is - 0.2, which is not very different from the value 0.2 inferred from the measurement of heat flux by Meredith & Tobias (1960) for a slightly different outer field.

2.5 The thermal flux between two particles with a flat circle of contact

In practice it may happen that a compression load is imposed on a granular medium (perhaps arising from the weight of the particles) and that

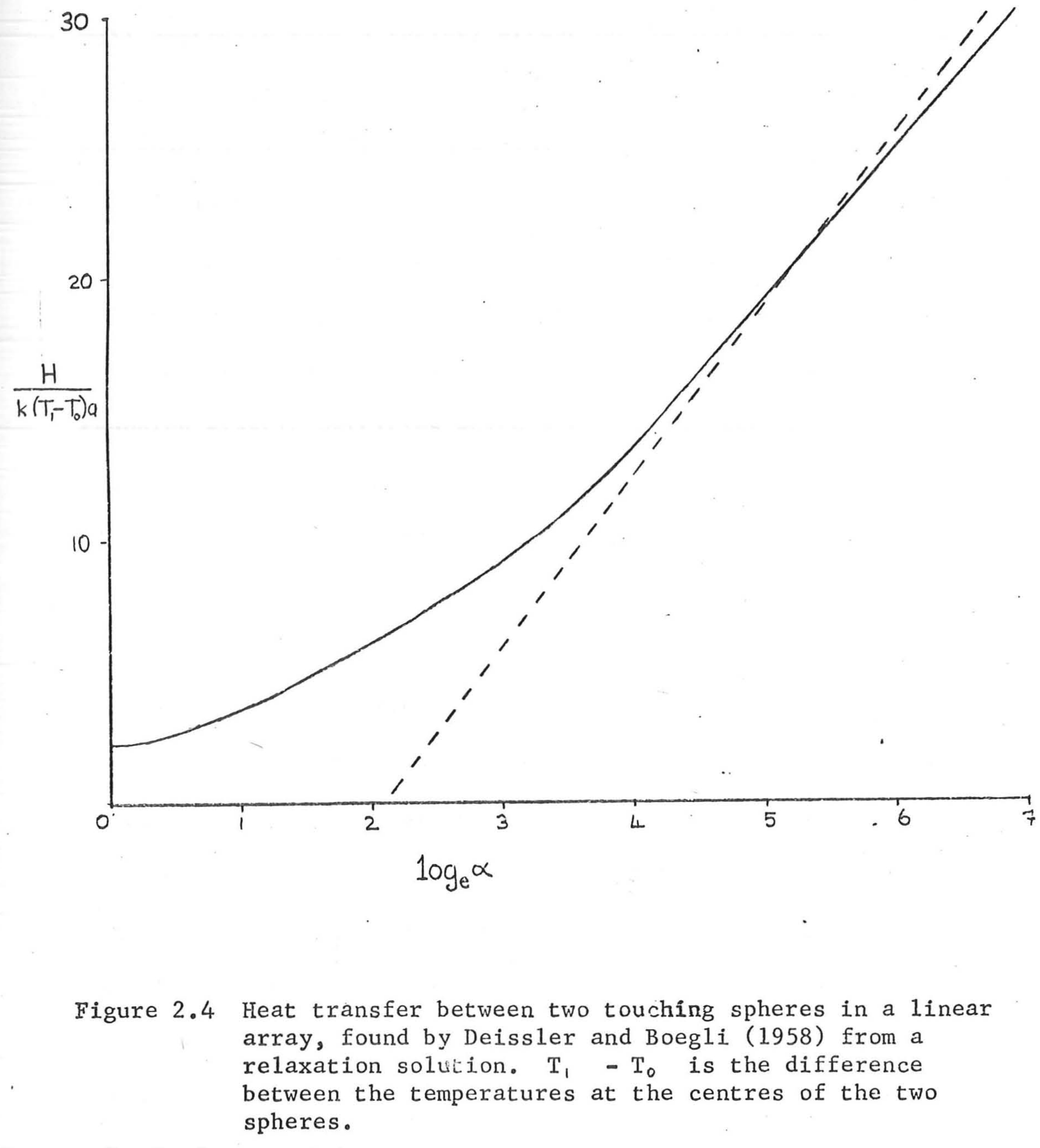

Figure 2.4 Heat transfer between two touching spheres in a linear array, found by Deissler and Boegli (1958) from a relaxation solution. $T_1 - T_0$ is the difference between the temperatures at the centres of the two spheres.

the particles are pressed together. If the particles are elastic they will deform slightly and will develop a flat circle of contact whose dimensions may be related to the load by the simple theory developed by Hertz many years ago. Such a change in the nature of the contact between particles will obviously have a radical effect on the bulk conductivity (an effect which is utilised in the old carbon microphone). The amount of the elastic deformation of particles in a random packed bed is unlikely to be either observable or calculable with much accuracy, but we shall consider here the thermal flux across a small flat circle of contact in order to illustrate the importance of deformation of particles.

According to the Hertz theory+ (see Landau & Lifshitz, 1959), two touching elastic particles which are locally spherical with radii R_o and R_1, and for which E is the Young's modulus and ν Poisson's ratio, will develop a flat contact circle of radius

$$\rho = P^{\frac{1}{3}}\left\{\frac{3(1-\nu^2)a}{4E}\right\}^{\frac{1}{3}}$$

when a compression force P acts on each particle normal to the common tangent plane at the point of contact, where $a = 2R_oR_1/(R_o+R_1)$ as before. (Formulae for the elliptic surface of contact between bodies which are not locally spherical are also available but are rather more complicated.) The theory also yields an expression for the deformation of the particles in the neighbourhood of the contact circle, and from this we find that the thickness of the matrix layer between the (deformed) surfaces of the two particles is $L(\eta)\,\rho^2/a$ for $\rho \leqslant r \ll a$ (see figure 25), where

$\eta = \frac{r}{\rho}$ and

$$L(\eta) = \frac{2}{\pi}\left\{\eta^2\tan^{-1}(\eta^2-1)^{\frac{1}{2}} + (\eta^2-1)^{\frac{1}{2}} - 2\tan^{-1}(\eta^2-1)^{\frac{1}{2}}\right\} \qquad (5.1)$$

+ Which is similar to that used in §2.4 for the thermal flux problem, in that the undeformed particle surface is regarded as plane and an integral equation for the surface displacment is solved.

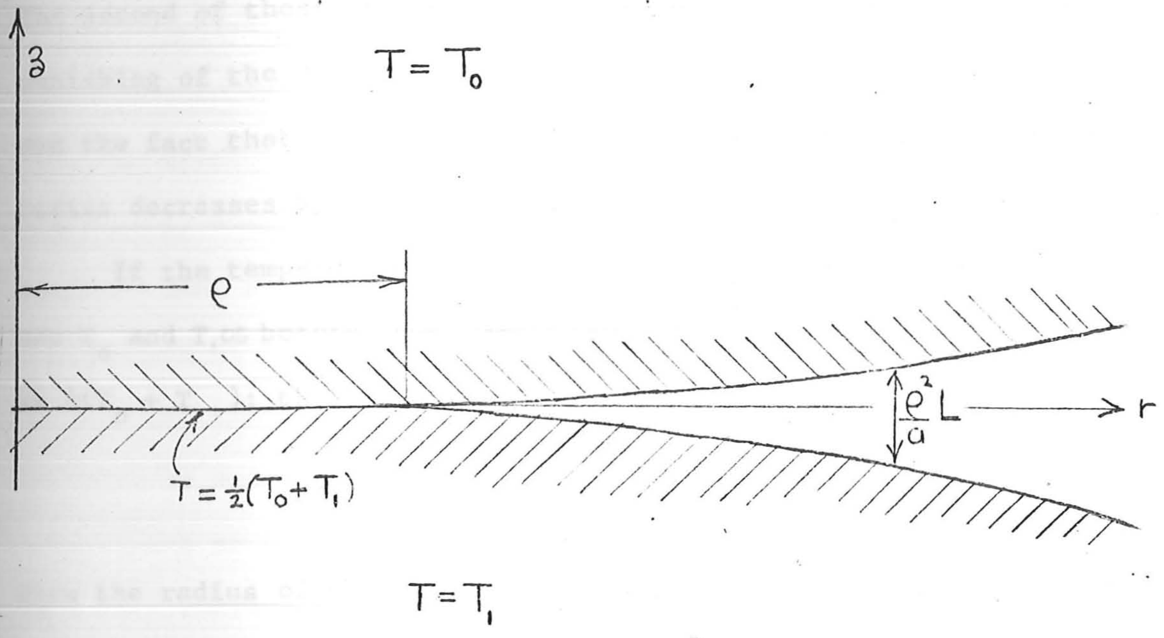

Figure 2.5 Definition sketch for two surfaces pressed together to form a flat circle of contact of radius ρ. In the undeformed state the surfaces are locally spherical, with radii of curvature R_0 and R_1, with $a = 2R_0R_1/(R_0 + R_1)$.

The function L has the asymptotic forms

$$L(\eta) = 2{\cdot}40(\eta-1)^{\frac{3}{2}} + O((\eta-1)^{\frac{5}{2}}) \quad \text{for } \eta-1 \ll 1 \tag{5.1a}$$

indicating the existence of a cusp at $\eta = 1$, and

$$L(\eta) = \eta^2 - 2 + O(\eta^{-1}) \quad \text{for } \eta \gg 1 . \tag{5.1b}$$

The second of these asymptotic expressions is a consequence of the vanishing of the deformation at large distances from the contact circle and the fact that the distance between the centres of volume of the two bodies decreases by $2\rho^2/a$ under the action of the compressive load.

If the temperatures of the two particles far from the contact region are T_0 and T_1 as before, the common temperature over the circle of contact is $\frac{1}{2}(T_0 + T_1)$; that is,

$$f(r) = 1 \quad \text{for } r \leqslant \rho .$$

When the radius of the circle of contact is so large that the heat flux through the thin annular matrix layer is negligible by comparison with that through the contact circle, the distribution of temperature inside the two particles is approximately the same as that of the velocity potential in irrotational flow of incompressible fluid through a circular hole in a plane wall. The solution to this latter problem is known(see Lamb 1932, §102), and shows that the normal flux density at the contact circle is

$$F_3(r) = \frac{\alpha k(T_1 - T_0)}{\pi(\rho^2 - r^2)^{\frac{1}{2}}} \tag{5.2}$$

and the total flux across the circle of contact is

$$H_c = \int_0^{\rho} F_3(r) 2\pi r dr = 2\alpha k(T_1 - T_0)\rho . \tag{5.3}$$

Comparison with (4.14) suggests that the value of the radius of the contact circle for which the flux across the contact circle is comparable with that between two particles in point contact is of order

$$\frac{a \log\alpha}{\alpha} \quad .$$

This may be an exceedingly small length in practice, indicating the extreme sensitivity of the bulk conductivity of a granular material to a little compression of the particles.

In order to obtain more general results for the total flux from one particle to another (the expression (5.3) being the flux only for ρ large in some sense), we reformulate the integral equation (4.6) for the temperature at the particle surface and again solve it mathematically. Outside the contact circle the normal flux density at the surface of either particle is approximately $k(T_- - T_+)\, a/\rho^2 L$. Hence the expression for the temperature at the particle surface, again regarded as plane, in terms of simple sources distributed over the surface is

$$f(\eta) = -\int_0^1 g(\eta') I(\eta'/\eta) d\eta' + \frac{1}{\beta}\int_1^\infty \frac{1 - f(\eta')}{L(\eta')} I(\eta'/\eta) d\eta' , \qquad (5.4)$$

where $\eta = r/\rho$, $\eta' = r'/\rho$, $\beta = \alpha\rho/a$ and

$$g(\eta) = \frac{-\rho F_3(r)}{\alpha k(T_1 - T_0)}$$

is the non-dimensional normal temperature gradient at the circle of contact.

The asymptotic form of f(r) for r large may be seen, by the same reasoning as led to (4.11), to be the same as in the case of particles in point contact, that is, in terms of the new non-dimensional variables,

$$f(\eta) \sim \frac{2 \log \beta\eta}{\beta\eta} \quad \text{as} \quad \eta \to \infty \, . \qquad (5.5)$$

Thus $f(r) - f_o(r)$, where f_o denotes the value of f for the case of particles in point contact, falls off more rapidly as r increases than f(r), which suggests that an integral equation for the difference $f(r) - f_o(r)$, will be more amenable to numerical solution than the one for f(r).

The integral equation for $f(\eta) - f_o(\eta)$, $= f_1(\eta)$ say, is found from (5.4) and (4.6) (with h = o) to be

$$f_1(\eta) = -\int_0^1 g_1(\eta') I(\eta'/\eta) d\eta' - \frac{1}{\beta}\int_1^\infty \frac{f_1(\eta')}{L(\eta')} I(\eta'/\eta) d\eta'$$

$$+ \frac{1}{\beta}\int_1^\infty \{1 - f_o(\eta')\}\left\{\frac{1}{L(\eta')} - \frac{1}{\eta'^2}\right\} I(\eta'/\eta) d\eta' , \qquad (5.6)$$

where

$$g_1(\eta) = g(\eta) + \frac{1 - f_o(\eta)}{\beta\eta^2} . \qquad (5.7)$$

This is not an integral equation for $f_1(\eta)$ in the analytic sense, since it involves also the temperature gradient $g_1(\eta)$ over the interval $o < \eta \leqslant 1$. However, over the same interval we have

$$f_1(\eta) = 1 - f_o(\eta) ,$$

so that there is no more than one unknown quantity at any given value of η. The set of simultaneous equations corresponding numerically to (5.6) may therefore be solved both for the value of $g_1(\eta)$ at a set of points in the range $o < \eta < 1$ and for the value of $f_1(\eta)$ at a set of points in the range $1 \leqslant \eta < \infty$. The details of the method of solution and the accuracy of the computed values are given in appendix A1.

The distributions of temperature at the particle surface found from this numerical solution of the integral equation for β = 1 and β = 10 are shown in figure (5.2) for comparison with the case of particles not in contact. (We have also solved the integral equation for β = 0.01, 0.1 and 100.)

Thus $f(r) - f_o(r)$, where f_o denotes the value of f for the case of particles in point contact, falls off more rapidly as r increases than f(r), which suggests that an integral equation for the difference $f(r) - f_o(r)$, will be more amenable to numerical solution than the one for f(r).

The integral equation for $f(\eta) - f_o(\eta)$, $= f_1(\eta)$ say, is found from (5.4) and (4.6) (with h = o) to be

$$f_1(\eta) = -\int_0^1 g_1(\eta') I(\eta'/\eta) d\eta' - \frac{1}{\beta}\int_1^\infty \frac{f_1(\eta')}{L(\eta')} I(\eta'/\eta) d\eta'$$

$$+\frac{1}{\beta}\int_1^\infty \{1 - f_o(\eta')\}\left\{\frac{1}{L(\eta')} - \frac{1}{\eta'^2}\right\} I(\eta'/\eta) d\eta' \ , \qquad (5.6)$$

where

$$g_1(\eta) = g(\eta) + \frac{1 - f_o(\eta)}{\beta\eta^2} . \qquad (5.7)$$

This is not an integral equation for $f_1(\eta)$ in the analytic sense, since it involves also the temperature gradient $g_1(\eta)$ over the interval $o < \eta \leqslant 1$. However, over the same interval we have

$$f_1(\eta) = 1 - f_o(\eta) \ ,$$

so that there is no more than one unknown quantity at any given value of η. The set of simultaneous equations corresponding numerically to (5.6) may therefore be solved both for the value of $g_1(\eta)$ at a set of points in the range $o < \eta < 1$ and for the value of $f_1(\eta)$ at a set of points in the range $1 \leqslant \eta < \infty$. The details of the method of solution and the accuracy of the computed values are given in appendix A1.

The distributions of temperature at the particle surface found from this numerical solution of the integral equation for $\beta = 1$ and $\beta = 10$ are shown in figure (5.2) for comparison with the case of particles not in contact. (We have also solved the integral equation for $\beta = 0.01$, 0.1 and 100.)

The results for the heat flux from one particle to another may conveniently be presented in terms of (a) the flux across the contact circle, which in non-dimensional form is

$$\mathcal{H}_c(\beta) = \frac{H_c}{\pi k(T_1 - T_0)} = \frac{1}{\pi k(T_1 - T_0)a}\int_0^{\rho} F_z(r)\,2\pi r\,dr \tag{5.8}$$
$$= -2\beta\int_0^1 g(\eta)\eta\,d\eta \quad ,$$

and (b) the difference between the flux across the matrix layer and the total flux between particles in point contact, viz.

$$\Delta\mathcal{H}_m(\beta) = \frac{\Delta H_m}{\pi k(T_1 - T_0)a} = 2\int_0^{\infty}\left\{\frac{1-f(\eta)}{L(\eta)} - \frac{1-f_0(\eta)}{\eta^2}\right\}\eta\,d\eta . \tag{5.9}$$

(The matrix layer for particles with a circle of contact extends over the range $\eta \geqslant 1$, but since $f(\eta) = 1$ for $\eta \leqslant 1$ in that case the contribution (b) can conveniently be written as a single integral over the range $0 \leqslant \eta < \infty$.) The total flux across an extended portion of the sphere surface which includes the contact circle is then seen from (4.14) to be

$$\frac{H}{\pi k(T_1 - T_0)a} = \mathcal{H}_c(\beta) + \Delta\mathcal{H}_m(\beta) + \log\alpha^2 + K - 3{\cdot}9 \quad , \tag{5.10}$$

where K is a constant determined by the outer field as before and $\mathcal{H}_c(\beta)$ and $\Delta\mathcal{H}_m(\beta)$ are independent of the outer field.

The values of $\mathcal{H}_c$ and $\Delta\mathcal{H}_m$ calculated for β = 0.01, 0.1, 1,10 and 100 are shown on a log - log plot in figure (2.6).

The asymptotic behaviour of $\mathcal{H}_c(\beta)$ as $\beta \to \infty$ has already been given in (5.3). And for $\Delta\mathcal{H}_m$ we note that the only part of the expression (5.9) which has large magnitude when $\beta \gg 1$ is the integral

$$-2\int_0^1 \frac{1 - f_0(\eta)}{\eta}\,d\eta$$

Since $f_0 \ll 1$ for $r \gg a/\alpha$, $(1 - f_0)/\eta$ is approximately equal to η^{-1} for

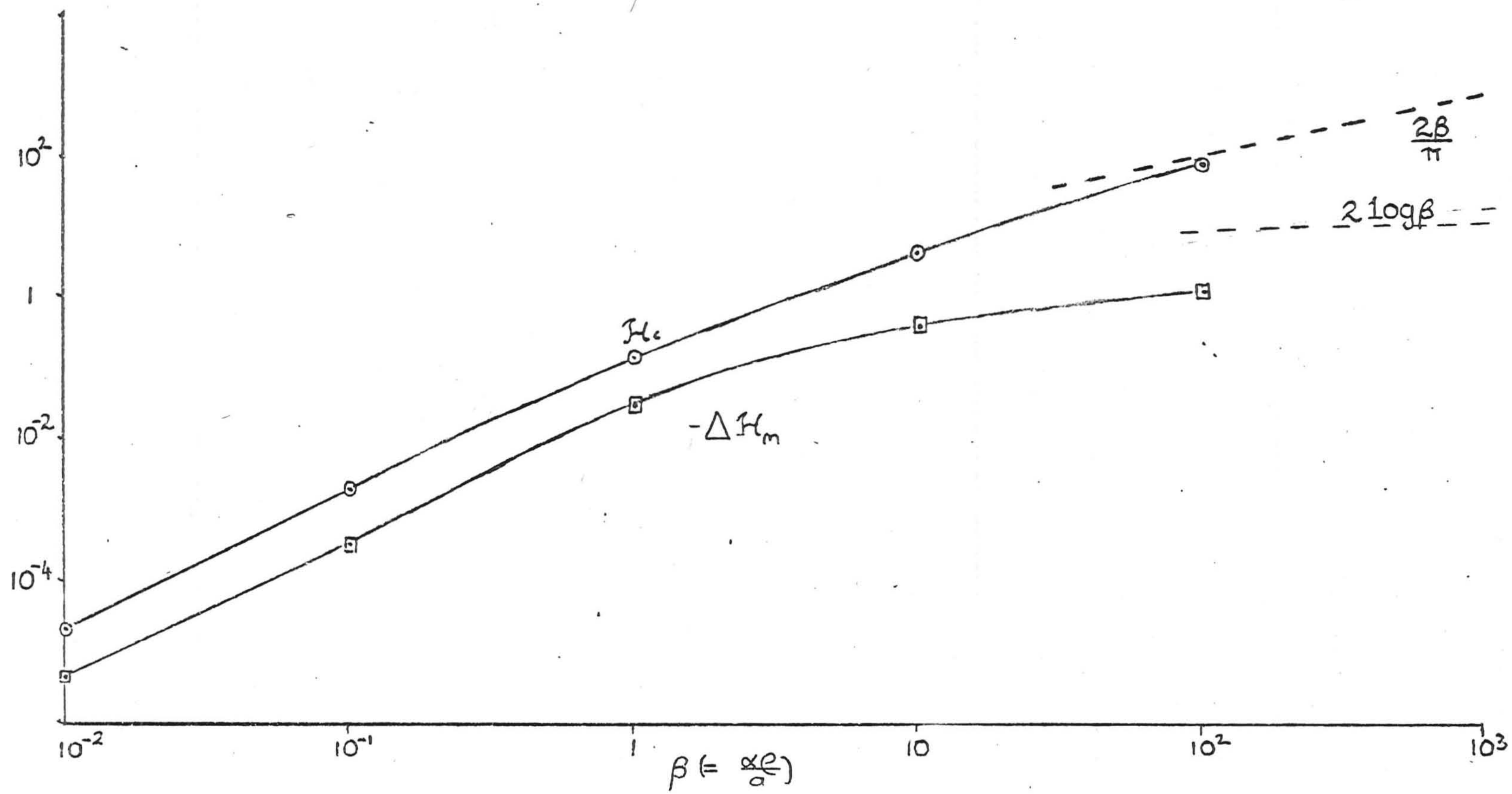

Figure 2.6 The thermal flux between two particles with a flat contact circle of radius ϱ .
$\mathcal{H}_c$ is the non-dimensional flux across the contact circle alone.

$\eta >> \beta^{-1}$ and the integral is asymptotically equal to -2 logβ as $\beta \rightarrow \infty$

We thus expect the numerical solution to be compatible with

$$\mathcal{H}_c(\beta) \sim \frac{2\beta}{\pi} \quad \text{and} \quad \Delta\mathcal{H}_m(\beta) \sim -2\log\beta \quad \text{as } \beta \rightarrow \infty. \tag{5.11}$$

As noted earlier, the total flux is dominated by that through the circle of contact, and $\mathcal{H} \sim 2\beta/\pi$, as $\beta \longrightarrow \infty$. We have not taken our numerical solution to large enough values of β to exhibit the asymptotic forms (5.11) although the trend of the values of $\mathcal{H}_c$ is clearly in accordance with (5.11). The difficulty in the numerical solution at large values of β is that a very large number of grid points are required for the solution of the integral equation (5.6) since the functions g and g_1 vary with increasing rapidity near the edge of the contact circle as $\beta \rightarrow \infty$

It appears from figure (2.6) that both $\mathcal{H}_c$ and $\Delta\mathcal{H}_m$ vary quadratically with β when β is small. More specifically

$$\mathcal{H}_c \approx 0.22\beta^2 \quad \text{and} \quad \Delta\mathcal{H}_m \approx -0.05\beta^2 \quad \text{for } \beta << 1. \tag{5.12}$$

This common behaviour is a consequence of the fact that for small β the length scale on which the normal flux density at the particle surface varies is a/α and that the flux density is approximately constant over the contact circle and independent of ρ. In the case of $\mathcal{H}_c$, the quadratic dependence on β then follows directly from the dependence of the area of the contact circle on ρ. In the case of $\Delta\mathcal{H}_m$, we need to refer back to the results (4.12) and (4.13) for the total flux between two particles with a gap h such that $\alpha^2h/a << 1$. Provided $\alpha^2h/a << 1$ for separated particles and $\alpha\rho/a << 1$ for particles with a circle of contact, the flux density distributions over the region $r < a/\alpha$ are approximately the same in the two cases and the total flux differs from that for two particles in point contact primarily because the matrix layer is thicker by a small amount h everywhere outside the region $r < a/\alpha$ in the case of separated particles and thinner by a small amount $2\rho^2/a$ (see 5.1b)) in the case of particles which a circle of contact. (This may be proved by comparing the integral equations for the normal flux density in the two cases.) The asymptotic formula (4.13) obtained from a previous numerical calculation holds regardless of the sign of h, from which we deduce that

$$\mathcal{H}_c(\beta) + \Delta\mathcal{H}_m(\beta) \approx 0.1\,\frac{\alpha^2}{a}\,\frac{2\rho^2}{a}\,, \quad \text{or} \quad 0.2\beta^2$$

when $\beta \ll 1$, which is in agreement with (5.12). The quadratic dependence of both $\mathcal{H}_c$ and $\Delta\mathcal{H}_m$ on β when $\beta \ll 1$ is thus accounted for.

2.6 The effective conductivity of a granular material

We return now to the formulae in §§ 2.2, 2.3 for the average thermal flux through a material consisting of touching, or nearly touching, particles of high conductivity embedded in a matrix. The expression (3.1) for the thermal dipole strength of a particle was based on the supposition that dominant contributions to the flux across the surface of a particle are made near each contact point. The analysis in the previous two sections has confirmed this supposition for the three cases, (a) particles separated by a gap of minimum width h, provided that $h/a \ll 1$ where a^{-1} is the mean curvature of the two locally-spherical surfaces, (b) particles making point contact, and (c) particles pressed together and in contact over a circle of radius ρ ($\ll a$). For all three of these types of contact the non-dimensional heat flux $H_i/\pi k(T_i-T_o)$ a across the particle surface in the neighbourhood of the ith contact point (connecting particles of temperature T_o and T_i) is large compared with unity, and the total flux across the much larger part of the particle surface that is not near a contact point is of order unity. In cases

(a) and (b) the heat flux through the contact region is only logarithmically large, and the arithmetical requirements on $^{a}/h$ and α respectively are that they must exceed unity by several powers of 10.

The expression (3.1) for $\underset{\sim}{S}$ may be written as

$$\underset{\sim}{S} \approx \pi k \sum_i \underset{\sim}{x}_i \frac{H_i}{\pi k (T_i - T_0) a_i} a_i (T_i - T_0) \qquad (6.1).$$

The factors $\underset{\sim}{x}_i$ and $(T_i - T_o)$ depend on the location of the contact point on the particle surface and a_i depends on the particle geometry, so that it will be difficult to obtain specific results without making restrictive assumptions about the geometry of the particle arrangement. It is therefore worth noticing at this stage that the only part of the expression (6.1) that depends on α is the flux H_i, and that in the case of an array of particles making point contact H_i is proportion to log α. This proportionality carries through to the average over a large number of particles, showing that $\langle \underset{\sim}{F} \rangle$ (see (3.3)) and k^* (see (1.2)) are proportional to log α, for any given shape and (statistical) arrangement of the particles in point contact.

We now make the following assumptions, mainly about the nature of the particle arrangement, in order to be able to determine the average value of $\underset{\sim}{S}$ over a large number of particles:

(a) The particles are spheres of the same radius a , so that $a_i = a$ for all contact points on all particle surfaces and $|\underset{\sim}{x}_i| = a$.

(b) The local geometry is the same at all contact points, i.e. there is the same minimum gap width h or the same contact-circle radius

(c) The temperature difference $T_i - T_o$ is equal to $2\underset{\sim}{x}_i . \langle \nabla T \rangle$, i.e. to the difference between the temperatures at the two sphere centres in a temperature field which is exactly linear with gradient $\langle \nabla T \rangle$ everywhere. This will not be correct for a random arrangement of spheres, although it is evidently true in some average sense.

With these assumptions (6.1) becomes

$$\underset{\sim}{S} = 2\pi a^3 k \mathcal{H} \sum_i \hat{n}_i \hat{n}_i \cdot \langle \nabla T \rangle \tag{6.2}$$

where $\hat{n}_i$ is the unit outward normal to the particle surface at the ith contact point and $\mathcal{H}$, the non-dimensional heat flux across the particle surface in the neighbourhood of a contact point, is a function only of α and of either $^h/a$ or ρ/a. The averaging of $\underset{\sim}{S}$ over a large number of particles is now concerned solely with the statistics of contact points.

The averaging is redundant in the case of a <u>regular</u> arrangement of spheres (and the above assumption (d) is here valid exactly), and the effective conductivity can be determined immediately from (2.1) and (6.2). For each of the three possible types of regular arrangement of close-packed spheres - simple cubic, body-centred cubic and face-centred cubic - $\sum_i \hat{n}_i \hat{n}_i$ is proportional to the unit tensor and

$$\sum_i \hat{n}_i \hat{n}_i \cdot \langle \nabla T \rangle = \langle \nabla T \rangle \sum_i (\hat{n}_i \cdot \underset{\sim}{m})^2 , \tag{6.3}$$

where $\underset{\sim}{m}$ is an arbitrary unit vector, whence it follows from (1.2) and (2.1) that

$$\frac{k^*}{k} \approx \frac{3}{2} \phi \mathcal{H} \sum_i (\hat{n}_i \cdot \underset{\sim}{m})^2 \tag{6.4}$$

where $\phi = \frac{4}{3}\pi a^3 n$ is the volume fraction occupied by the particles. From an elementary consideration of the geometry of the three types of array we find the results shown in table 2.1.

type of arrangement of spheres	volume fraction	number of contact points	$(n_i \cdot \dot{m})^2$	$k^*/k\mathcal{H}$
simple cubic array	0.524 ($\pi/6$)	6	2	1.57
body-centred " "	0.680 ($\sqrt{3}\pi/8$)	8	8/3	2.72
face-centred " "	0.740 ($\pi/3\sqrt{2}$)	12	4	4.45
random, isotropic	0.63	6.5	2.2	2.0

Table 2.1 The conductivity of close-packed beds of spheres.

We are interested primarily in the random arrays that are common in practice. It seems likely that many random close-packed arrays of uniform spheres are statistically isotropic in geometrical structure, and that contact points are distributed with uniform probability over the surface of a sphere, at any rate approximately. On this basis

$$\langle \underset{\sim}{S} \rangle = 2\pi a^3 k \mathcal{H} \tfrac{1}{3} p \langle \nabla T \rangle \tag{6.5}$$

where p is the average number of contact points at the surface of a particle, whence

$$\frac{k^*}{k} = \frac{1}{2}\phi p \mathcal{H}. \tag{6.6}$$

This formula is actually valid also for the above three types of regular arrangement of spheres, because, although the distribution of contact points over the surface of a sphere in one of these regular arrays is not statistically isotropic, it has a sufficient degree of uniformity to be indistinguishable from isotropy in a representation by a second-rank tensor.

A number of observations of the statistical properties of random close-packed (i.e. incompressible) arrays of hard spheres have been made, mostly in the context of the molecular structure of liquids. If many spheres of uniform size are simply poured into a vessel, preferably one with irregular walls to prevent regular arrangements from forming, it appears that the volume fraction of the spheres is likely to be about 0.60, and that if the vessel is shaken to allow some readjustment of the spheres the volume fraction may rise to about 0.64 (Scott 1960). The earliest count of contact points seems to have been made by Smith, Foote & Busang (1929), who found that the average number of contact points on a sphere varied with the volume fraction of the spheres, being larger for large volume fractions as one would expect. The values of ϕ for their different packed beds of spheres varied between 0.55 and 0.64, and the average number of contact points varied between 6.9 and 9.5, roughly linearly with ϕ. Bernal & Mason (1960) later made a count of the number of sphere pairs with separation less than 0.05a in a random array with ϕ equal to 0.64 and found that twice the average number per sphere was 6.4. A much larger number of spheres in a random close-packed array was generated by a computer (in a manner which simulated pouring into a vessel) by Adams and Matheson (1972), who found $\phi = 0.628$ and, judging by their figure 5, an average number of contact points per sphere (defined as a separation smaller than 0.04a) equal to 6.6. Our interest is in the average number of points on a sphere surface at which there is either actual contact or a separation very much less than 0.04a, which will be a little less than the numbers given by Bernal & Mason and Adams & Matheson but not by more than 0.1 if the probability of separations between 0 and 0.04a is estimated on the basis of a uniform pair distribution function. For a packed bed of spheres with $\phi = 0.63$ we thus have an estimate of 9.5 for the average number of contact points from the work of Smith, Foote & Busang, and much lower estimates of 6.3 and 6.5 from that of Bernal & Mason and Adams & Matheson respectively. Further work to resolve this discrepancy would be useful.

The volume fraction and the average number of contact points on a sphere surface in a random close-packed array of spheres no doubt vary with the method of manufacture, perhaps by 5 or 10 per cent, but for the purpose of comparison with regular arrays we shall adopt the values suggested by the work of Adams and Matheson, viz. $\phi = 0.63$ and $p = 6.5$, giving the value of k^*/k shown in table 2.1. The assumption (c) above concerning the temperature difference of spheres in contact is only an approximation in the case of a random arrangement, but seems unlikely to introduce an error in k^*/k of more than ten or twenty per cent. The effective conductivity depends on particle shape mainly through the dependence on the number and distribution of contact points on a particle surface, and should not vary much for different particle shapes provided they are rounded and globular.

The fact on which the bulk conductivity depends most sensitively is the non-dimensional heat flux across a particle surface in the neighbourhood of a contact point, and we conclude this section by summarizing the results obtained in §2.4,§2.5 for the flux across the region of contact between two locally-spherical surfaces:

	$\mathcal{H}\ \left(= \frac{H}{\pi a k(T_1-T_0)}\right)$
minimum gap h between surfaces	$\log \frac{a}{h} - P(\lambda)$
surfaces in point contact	$\log \alpha^2$
surfaces with a constact circle of radius ρ	$\mathcal{H}_c(\beta) + \Delta\mathcal{H}_m(\beta) + \log \alpha^2$

P is given as a function of λ $(= {}^{\alpha h}/a)$ in figure (2.3) and $\mathcal{H}_c$ and $\Delta\mathcal{H}_m$ as functions of β $(= {}^{\alpha\rho}/a)$ in figure (2.6). These expressions for $\mathcal{H}$ are approximate only, and the error in each of the three cases is an additive number of order unity which is not determined fully by the conditions near the contact point.

For the special case of a random array of uniform spherical particles making point contact with each other, and with Adams & Matheson's value of the average number of contact points, we have the simple approximate formula

$$\frac{k^*}{k} = 4.0 \log \alpha \,. \tag{6.7}$$

This is leading term in an asymptotic expansion of k^*/k as $\alpha \to \infty$, and the next term is a constant of order unity which depends on the (statistical) geometry of the arrangement of the spheres.

2.7 Observations of the effective conductivity of granular materials

A number of observations of either thermal or electrical conductivity of a bed of randomly packed spheres in contact have been reported in the literature. The experimental conditions for these observations are summarized in table 2.2, and the results are shown in figure 2.7. The beds were made in different ways, and the values of the particle volume fraction and average number of contact points probably vary from one to another. Some scatter of the points is therefore to be expected. It is also possible that the observations are subject to some uncertainity at the larger values of α, since the temperature or electrical potential gradients near points of contact between the spheres are of the order of α^2 times the mean gradient and so were exceedingly large for some of the measurements. Turner (1973, 1976), who was the only one to measure electrical conductivity, reported that it was very difficult to get reproducible results for values of α above 10^3.

We show on the figure the straight line

$$\frac{k^*}{k} = 4.0 \log \alpha - 11 \tag{7.1}$$

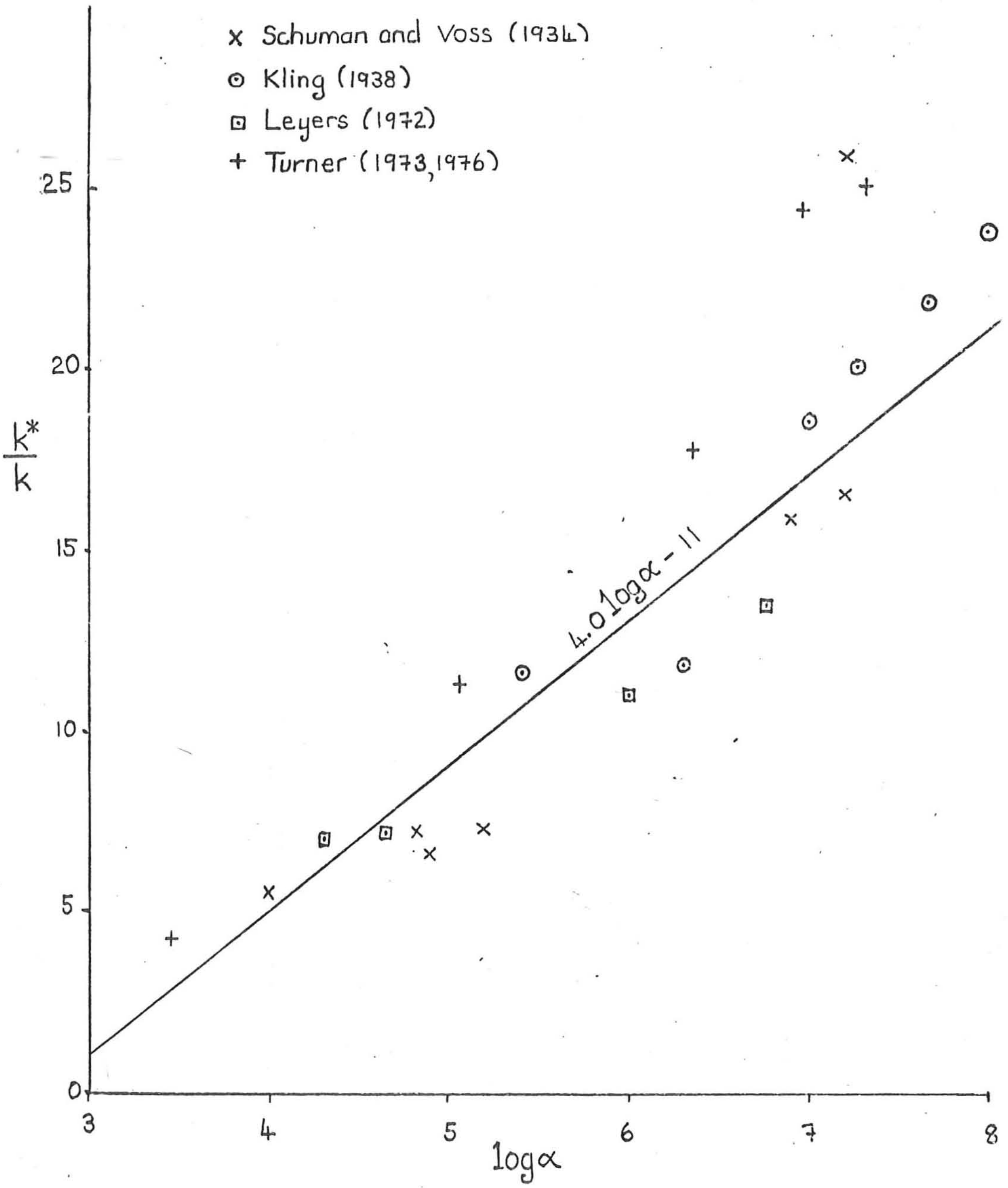

Figure 2.7 Measurements of the effective conductivity of random close-packed beds of spheres of uniform size immersed in fluid.

Authors	Type of conduction	Material	Vol. fraction of spheres.	Apparatus
Kling (1938)	thermal	steel spheres 3.8mm diam., in various gases.	0.62	Spheres contained between co-axial cylinders of radii 152mm and 352mm. Heat source in inner cylinder, steady state.
Leyers (1972)	thermal	steel spheres 1.1mm diam., in various gases.	0.605	As above, but cylinder radii 2mm and 7.5mm.
Schuman & Voss (1934)	thermal	steel shot, av. diam. 1.3mm, or lead shot, av. diam. 2.6mm, in various gases.	0.625	A long cylinder of radius 30mm containing the shot was plunged into hot water and the temperature on the cylinder axis measured as a function of time.
Turner (1973,1976)	electrical	resin beads, dia.m (i) 0.5-1.0mm or (ii) 0.15-0.30mm, in aqueous solution of NaCl.	(i) 0.60 (ii) 0.62	The resistance between two electrodes immersed in a packed bed in a cydliner was measured; alternating current.

Table 2.2 Observations of effective conductivity of random close-packed beds of spheres reported in the literature.

which has a slope given by the asymptotic relation (6.7) and an additive constant chosen to achieve a reasonable fit with the points. The formula (7.1) thus has partial theoretical basis, and provides a reasonable representation of the data for different packed beds of uniform touching spheres when $\alpha >> 1$. If we had accepted the estimate of the average number of contact points on a sphere in a packed bed given by Smith, Foote & Busang (1929), the coefficient of $\log\alpha$ in the asymptotic relation (6.7) would have been about 50 per cent greater. The agreement with the experimental points shown in figure 2.7 would then not have been as good.

There is even less reason to expect observations of the effective conductivity of beds of particles of non-spherical shape to show a dependence on α alone, but the extent of the variation of effective conductivity for given α is surprisingly small. Diessler & Boegli (1958) have reported some measurements of the conductivity of three different powders, the particles of which are generally rounded and globular, although not uniform in size and shape. The variation of α for each powder was obtained by change of the ambient gas. The measured values of the volume fraction of the particles varied by about 10 per cent for each of the powders, corresponding to different states of compaction, but all lay within the range 0.50 - 0.64. The observed effective conductivities tended to be higher for larger particle volume fractions of a given powder, and there is some scatter of the points, but all the measured values lie within 50 per cent of those given by the simple formula (7.1).

CHAPTER 3

CONDUCTION ACROSS FIBRE BUNDLES

3.1 Introduction

This chapter is concerned with the conduction of heat or electricity[+] through materials which consist of closely packed fibres immersed in a matrix of relatively low conductivity. It is assumed that each fibre has a circular cross-section of uniform radius R, and that the radius of curvature of the axis of each fibre is everywhere much greater than R. As a result of this curvature, the direction of the tangent to the axis of a fibre varies with position along the fibre, but we assume that these variations in direction are only slight, and that the fibres are approximately alligned. Transformer windings and electrical power cables are examples of this type of material.

If the fibres were straight and parallel, neighbouring fibres would be in contact along a line, but as the fibres are only nearly straight and nearly parallel, contact between neighbouring fibres occurs only at discrete points. It will be shown that this has a very significant effect on the conductivity.

We assume that both the bulk temperature gradient $\langle \nabla T \rangle$, and the bulk flux density $\underset{\sim}{F}$ are uniform and perpendicular to the mean fibre direction. If the arrangement of the fibre cross-sections is isotropic[++], the effective conductivity tensor k has the form

$$(\hat{e}_i \cdot \underset{\approx}{k}^* \cdot \hat{e}_j) = \begin{pmatrix} k^* & 0 & 0 \\ 0 & k^* & 0 \\ 0 & 0 & k_{33} \end{pmatrix} \qquad (1.1)$$

where $(\hat{e}_1, \hat{e}_2, \hat{e}_3)$ is a cartesian basis, and $\hat{e}_3$ is the unit vector in the mean fibre direction. We are concerned here with materials which are macroscopically two-dimensional, and therefore the components of $\underset{\approx}{k}^*$

\+ For the remainder of this chapter we will use thermal notation. Unless otherwise defined, symbols have the same meaning as in chapter 2.

++ i.e., the statistical properties of the cross-sectional geometry are invariant under rotations in the cross-sectional plane.

do not alter with position along the fibres. Our aim is to obtain an expression for k^*.

There have been relatively few investigations into the problem of conduction across materials composed of fibres, and in every case the fibres have been approximated by perfectly conducting parallel circular cylinders. Rayleigh (1892) derived an expression for the conductivity of a square array of cylinders which essentially provides the first few terms in an expansion of k^* in powers of R/c, where R is the cylinder radius and c is the distance between the centres of neighbouring cylinders. An additional term in the series was obtained by Runge (1925), but many more terms are needed if the expansion is to provide useful estimates of k^* at the volume fractions which concern us here.

The work of Keller (1962) is of more relevance to our investigation. He obtained an expression for the flux per unit length across the surface of one of a pair of nearly touching, perfectly conducting parallel cylinders, and from this derived a formula for the conductivity of a square array of such cylinders. In the following section we extend this work, and derive an expression for the flux per unit length between a pair of cylinders of finite conductivity which, unlike Keller's expression remains finite when the cylinders are touching.

As in chapter 2 we assume that most of the heat flow between the boundaries (in the plane normal to the mean fibre direction) occurs along chains of particles, and thus the dipole strength of each particle is dominated by the contributions from the small portions of the surface which are close to neighbouring fibres. These small portions of the fibre surfaces will be called "contact-regions".

With a suitably chosen cartesian coordinate system (x, y, z), the thickness of the matrix layer near the point of contact between a pair of fibres is given by

$$h(x,y) = \frac{x^2}{a} + \frac{y^2}{b} \quad , \tag{1.2}$$

where the z axis is perpendicular to the common tangent plane at the point of contact between the two surfaces. The quantities b and a are determined by the local fibre geometry, and we take

$$b > a$$

If the pair of fibres in the neighbourhood of the contact point can be approximated by a pair of cylinders with inclined and non intersecting axes, then b and a are given by

$$\left.\begin{aligned} a &= R/\cos^2(\theta/2) \, , \\ b &= R/\sin^2(\theta/2) \, , \end{aligned}\right\} \tag{1.3}$$

where θ is the angle of intersection of the projection of the cylinder axes on the (x,y) plane. This is illustrated in figure (3.1). For the type of materials that interest us, the fibres are nearly aligned, that is

$$\theta \ll 1$$

in which case

$$\left.\begin{aligned} a &\approx R \\ \text{and} \qquad b &\approx \frac{4R}{\theta^2} \, . \end{aligned}\right\} \tag{1.4}$$

If the axes of the pair of fibres are coplanar in the neighbourhood of the contact point, then it is the curvature of these axes which determines the thickness of the matrix layer. Denoting the local radii of curvature by b_1 and b_2 respectively, we have

$$\left.\begin{aligned} a &= R \\ b &= \frac{2b_1 b_2}{(b_1 + b_2)} \, . \end{aligned}\right\} \tag{1.5}$$

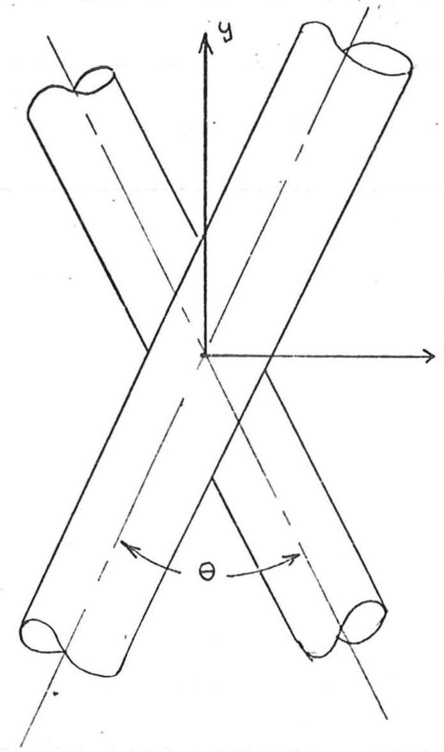

Figure 3.1 A pair of inclined cylinders. The origin of the x, y, z coordinate system is at the point of contact between the cylinders and the z axis is perpendicular to the plane which is tangential to the surfaces at the contact point. The angle θ is the angle between the projections of the cylinder axes on the x-y plane.

From (1.4) we see that the expressions (1.5) for a and b are valid if

$$\theta^2 \ll \frac{2R(b_1+b_2)}{b_1 b_2}.$$

The expressions (1.4) and (1.5) correspond to limiting cases, and in general the quantities a and b will depend on both the relative orientation of the fibre axes and their curvature.

For the type of materials which concern us here,

$$\theta \ll 1 \text{ and } (b_1, b_2) \gg R ,$$

and therefore

$$a \ll b. \tag{1.6}$$

for each contact point. The expression (2.4.12) for the flux across a contact region is only valid if a and b are the same order of magnitude, and in order to derive an expression for the flux in the case $a \ll b$, we begin by noting that this constraint implies that the temperature field is only slowly varying in the y direction. Therefore we may approximate the fibre surfaces locally by a pair of parallel circular cylinders of radius a, separated by a matrix layer of thickness

$$\left.\begin{aligned} & h(y) + \frac{x^2}{a} \\ \text{where } & h(y) = \frac{y^2}{b}. \end{aligned}\right\} \tag{1.7}$$

3.2 The Flux across a contact region for the case of parallel cylinders

The aim of this section is to derive an expression for the flux per unit length $H(\alpha,\frac{h}{a})$ passing between a pair of circular cylinders of radius a, conductivity αk, and minimum separation distance h. In §3.3 we integrate this expression (with $h = y^2/b$) with respect to y, and obtain a formula for the flux across the contact region of one of a pair of neighbouring fibres. Using this result, we derive an expression for the conductivity of a material composed of layers of parallel fibres, and in §3.4 we find the α dependence of k^* for the class of materials described in §3.1.

The temperature varies linearly across the matrix layer provided that both h and x are << a, and for a pair of perfectly conducting cylinders, H is therefore given by

$$H(\infty, \frac{h}{a}) = k(T_1 - T_0)\int_{-\infty}^{\infty} \frac{dx}{h + \frac{x^2}{a}} = \pi k (T_1 - T_0)\sqrt{\frac{a}{h}} \ , \qquad (2.1)$$

where T_1 and T_0 denote the temperatures of the fibre pair, as found by Keller (1962). The limits of integration in this expression can here be formally extended to $(\pm\infty)$, since the integral is dominated by the contribution from a small region surrounding the origin. There is no necessity to provide a precise definition of the contact region; it is sufficient to choose any portion of the surface provided that it includes that part which makes the dominant contribution to the integral for H.

The expression (2.1) for the flux per unit length across a contact region, shows a much stronger dependence on h than does the equivalent expression (2.4.3) for the flux between a pair of spheres, which varies as log(a/h). This implies that the thermal dipole strength of a cylinder is dominated by the contributions from the contact surfaces at much larger separations than are required for dominance in the case of spheres. However, the separation distance at which cylinders of finite conducitivity cease to have uniform temperatures is likely to be greater than (a/α^2), the value found for spheres, both because the flux density is much larger than for spheres with the same separation, and because the heat which passes through the surface of a cylinder can spread out only in two dimensions.

The Derivation of the Integral equation for the temperature on a contact region

To determine the flux per unit length H passing between a pair of cylinders for the case $\alpha \gg 1$, we must first determine the temperature distribution over the opposing surfaces of the two cylinders. As in the problem of two locally-spherical particles (§2.4) we formulate an integral equation for this temperature distribution.

The region surrounding the contact point is illustrated in figure (3.2). The fibre which lies in the region $z > 0$ will be called the "upper fibre", and the other will be called the "lower fibre". Far from the contact region the temperature of the upper fibre is approximately T_0 and similarly the temperature of the lower fibre approaches the constant value T_1 . The temperature varies linearly across the matrix layer and the heat flux across the layer is determined by the temperatures on the two fibre surfaces.

We assume that the region of non-uniform temperature within each of the fibres is so small that each fibre may be treated as a half-space. The temperature in the upper fibre, therefore satisfies the boundary condition

$$\frac{\partial T}{\partial z} = \frac{(T_+(x) - T_-(x))}{\alpha(h + x^2/a)} \qquad (2.2)$$

on $\qquad z = 0$

where T_+ and T_- denote the temperature on the surfaces of the upper and lower fibre respectively. The other boundary condition is

$$T \to T_0 \qquad (2.3)$$

far from the contact point.

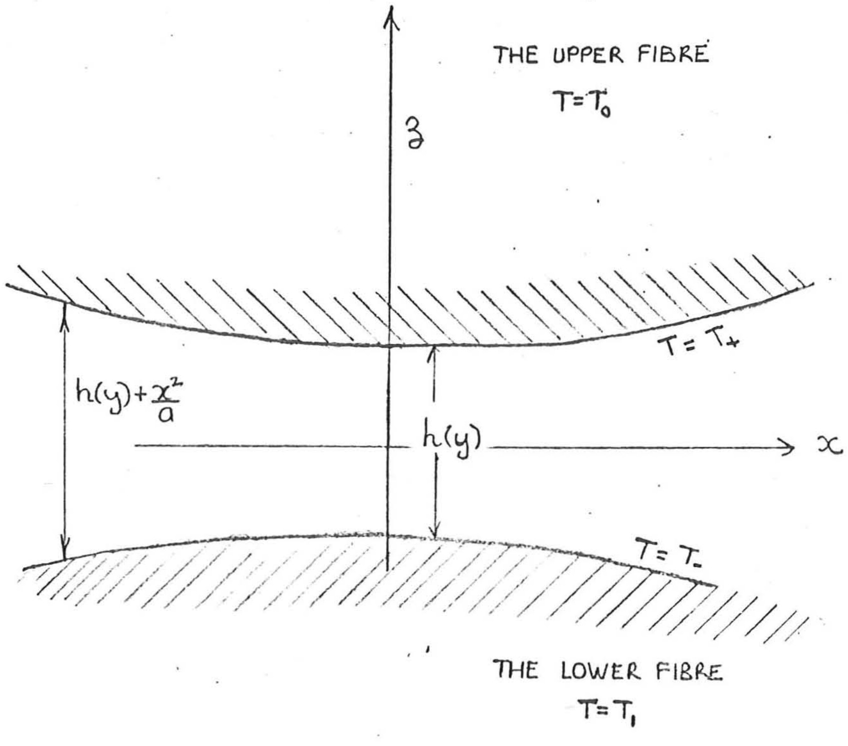

Figure 3.2 The thin matrix layer between a pair of nearly-touching parallel cylinders. The y-axis is parallel to the cylinder axes.

Unfortunately the two boundary conditions (2.2) and (2.3) are incompatible, for since most of the heat enters the cylinder through a small region surrounding the contact point, the temperature field far from this point is approximately that due to a line source. The temperature field of a line source diverges logarithmically at large distances and (2.3) is violated. However, at distances of order a from the origin, this logarithmic divergence is cancelled by similarly divergent contributions from the other contact regions on the surface of the fibre, and thus the boundary condition (2.3) is invalid.

An appropriate matching condition is required if T is to be determined uniquely, but as the outer solution is not available, we replace the boundary condition (2.3) by the constraint

$$\left| \frac{T(x,z) - T_0}{T_+(0) - T_0} \right| \ll 1 \tag{2.4}$$

if $\sqrt{x^2 + z^2}$ is of order a.

Although this is not sufficiently precise to enable us to determine T_+ uniquely, it will be shown that the uncertainty in $T_+(x)$ which results is negligible if α is sufficiently large.

A solution of Laplaces equation in two-dimensions, which satisfies the boundary condition (2.2) is given by

$$\begin{aligned} T(x,z) - T_0 = \frac{1}{2\pi} \Bigg\{ & \int_{-\infty}^{\infty} \frac{T_+(x') - T_-(x')}{\alpha(h + x'^2/a)} \log\left(\beta\sqrt{(x-x')^2 + z^2}\right) dx' \\ & - \int_{-\infty}^{\infty} (T_+(x') - T_0) \frac{\partial}{\partial z} \log\sqrt{(x-x')^2 + z^2}\,\Big|_{z=h} dx' \Bigg\}, \end{aligned} \tag{2.5}$$

where β is a constant. The value of β is not determined by the "inner boundary conditions" but we can estimate it as follows. At large distances from the boundary (z = 0), (2.5) becomes, approximately

$$T(x,z) - T_0 \approx \frac{1}{2\pi}\left\{\int_{-\infty}^{\infty} \frac{T_+(x') - T_-(x')}{\alpha(h + x'^2/a)}\, dx'\right\} \log \beta\sqrt{x^2+z^2}\, dx'$$

$$= \frac{H(\alpha, h/a)}{2\pi k\alpha} \log \beta\left(\sqrt{x^2+z^2}\right), \tag{2.6}$$

which is the temperature field of a line source. At distances of order a from the origin the condition (2.4) must be satisfied, and as $T_+(0) - T_0$ is of order $T_1 - T_0$, we obtain, with the aid of (2.6), the constraint

$$\left|\frac{H(\alpha, \frac{h}{a}) \log(\beta N a)}{2\pi\alpha k(T_1 - T_0)}\right| \ll 1,$$

where N is a number of order 1. If we choose $\beta = \frac{1}{a}$, $\log(\beta N a)$ is of order 1 and the constraint becomes

$$\left|\frac{H(\alpha, h/a)}{2\pi\alpha k(T_1 - T_0)}\right| \ll 1. \tag{2.7}$$

For the remainder of this section we take $\beta = \frac{1}{a}$, and later we will show that the condition (2.7) is satisfied if α is sufficiently large. This choice of β is obviously not unique; $\beta = \frac{M}{a}$ where M is a number of order 1, would be an equally appropriate choice. Later in this section it will be shown that if the condition (2.7) is satisfied, then the effect of such a change in β on the value of H is negligible.

If the point (x, z) lies on the surface of the upper fibre, the integral equation (2.5) reduces to

$$T_+(x) - T_0 = \frac{1}{\pi\alpha}\int_{-\infty}^{\infty} \frac{T_+(x') - T_-(x')}{h + \frac{x'^2}{a}} \log\left[\frac{|x - x'|}{a}\right] dx', \tag{2.8}$$

where we have replaced β by $1/a$. A similar equation may be formulated for the temperature on the surface of the lower fibre, and combining this expression with (2.8) we obtain

$$T_+(x) - T_-(x) - [T_0 - T_1] = \frac{2}{\pi\alpha}\int_{-\infty}^{\infty} \frac{T_+(x') - T_-(x')}{h + \frac{x'^2}{a}} \log\left|\frac{x-x'}{a}\right| dx'. \tag{2.9}$$

On introducing $\eta = \frac{x}{a}$ as the non-dimensional distance, and defining the non-dimensional flux density $g(\eta)$, by

$$g(\eta) = \frac{(T_+ - T_-)a}{\alpha(T_0 - T_1)(h + \frac{x'^2}{a})}, \tag{2.10}$$

we get an integral equation for $g(\eta)$:

$$1 = \alpha\left(\frac{h}{a} + \eta^2\right)g(\eta) - \frac{2}{\pi}\int_{-\infty}^{\infty} g(\eta')\log|\eta - \eta'|\,d\eta'. \tag{2.11}$$

The numerical solution of the Integral equation (2.11)

We have solved equation (2.11) by a quadrature technique, similar to that employed for the solution of equations (2.4.8) and (2.5.6). The details of the method of solution are given in appendix A2.

A convenient way of presenting the numerical solution is in terms of the non dimensional flux $\mathcal{H}(\alpha, \frac{h}{a})$ defined by

$$\mathcal{H}(\alpha, \frac{h}{a}) = \frac{H(\alpha, h/a)}{k(T_1 - T_0)} = \alpha\int_{-\infty}^{\infty} g(\eta)\,d\eta. \tag{2.12}$$

The computed values of $\mathcal{H}(\alpha, \frac{h}{a})$ are illustrated in figure (3.3) for the case $\alpha = 10^4$. From the computed values of $\mathcal{H}(10^4, h/a)$ it is possible to obtain the value of $\mathcal{H}(\alpha, h/a)$ for any α and h/a without having to solve equation (2.11) again. To show this, we introduce another non-dimensional coordinate

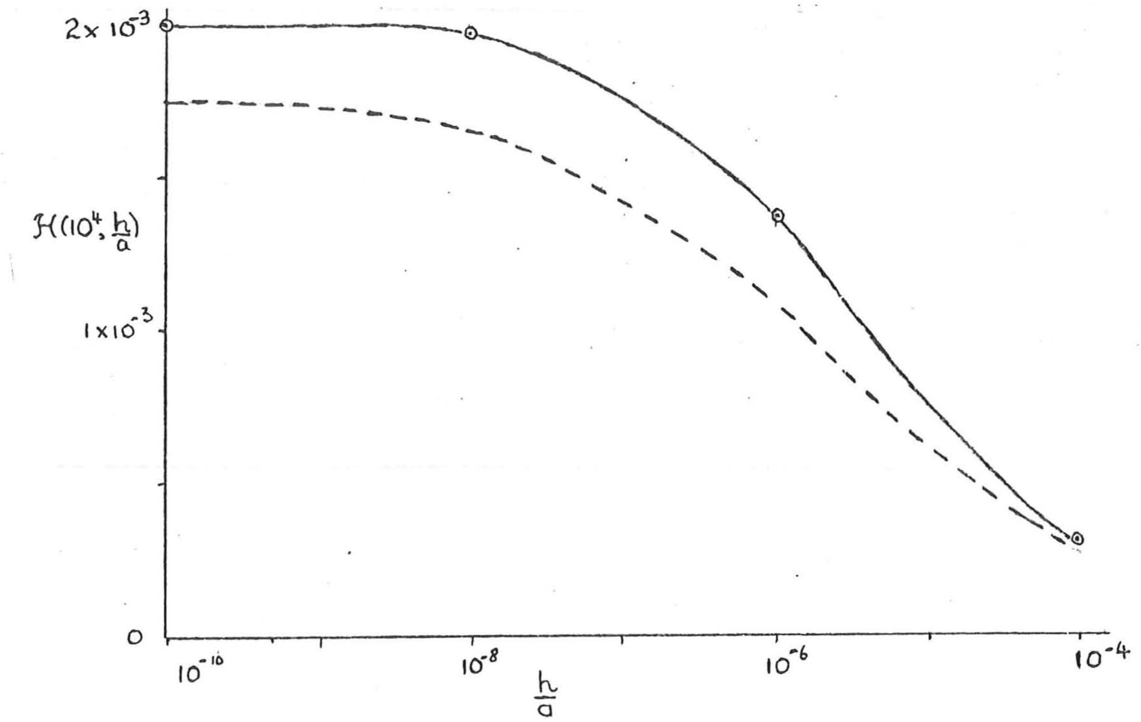

Figure 3.3. The non dimensional flux $\mathcal{H}(\alpha, \frac{h}{a})$ between a pair of parallel cylinders as a function of separation h, for $\alpha = 10^4$ The points represent computed values. The asymptotic approximation (2.26) for $\alpha = 10$ is shown by the broken line.

$$\sigma = \alpha\eta . (= \frac{\alpha x}{a})$$

and non-dimensional flux density

$$g' = g/\alpha$$

in equation (2.11), which becomes

$$1 - \frac{2}{\pi}\frac{\mathcal{H}(\alpha, h/a)}{\alpha}\log\alpha = (\lambda + \sigma^2)g'(\sigma) - \frac{2}{\pi}\int_{-\infty}^{\infty} g'(\sigma')\log|\sigma - \sigma'|\,d\sigma', \tag{2.13}$$

where $\lambda = \frac{\alpha^2 h}{a}$.

The right-hand side of (2.13) has the same form as the right-hand side of (2.11), and the two are identical if h/a is replaced by λ and α is replaced by 1 in equation (2.11). Both equations are linear, and therefore

$$g'(\sigma) = \left(1 - \frac{2}{\pi}\frac{\mathcal{H}(\alpha, h/a)}{\alpha}\log\alpha\right)g^*(\sigma),$$

where $g^*(\sigma)$ denotes the solution of equation (2.11) for the case $\alpha = 1$, $h/a = \lambda$. On integrating both sides of this identity with respect to σ between the limits $\pm\infty$ we obtain

$$\frac{\alpha}{\mathcal{H}(\alpha, h/a)} - \frac{1}{\mathcal{H}(1,\lambda)} = \frac{2}{\pi}\log\alpha .$$

Thus the non-dimensional fluxes $\mathcal{H}(\alpha_1, h_1/a)$ and $\mathcal{H}(\alpha_2, h_2/a)$ are related by

$$\frac{\alpha_1}{\mathcal{H}(\alpha_1, h_1/a)} - \frac{\alpha_2}{\mathcal{H}(\alpha_2, h_2/a)} = \frac{2}{\pi}\log\left(\frac{\alpha_1}{\alpha_2}\right), \tag{2.14}$$

provided

$$\alpha_1^2 h_1 = \alpha_2^2 h_2 . \tag{2.15}$$

With the aid of equation (2.14) we are able to calculate $\mathcal{H}(\alpha, h/a)$ from the computed values of $\mathcal{H}(10^4, h/a)$. This result was only realised after I had computed $H(\alpha,0)$ for a number of values of α and found that the computed values appeared to satisfy a relationship of the form (2.14).

From the identity (2.14) we can find the asymptotic behaviour of $\mathcal{H}$ for a pair of touching cylinders as $\alpha \to \infty$. Putting $h_1 = h_2 = 0$ in (2.14), we get

$$\frac{\alpha_1}{\mathcal{H}(\alpha_1,0)} = \frac{\alpha_2}{\mathcal{H}(\alpha_2,0)} + \frac{2}{\pi}\log\left(\frac{\alpha_1}{\alpha_2}\right)$$

and letting $\alpha_1 \longrightarrow \infty$ with α_2 fixed, we find

$$\mathcal{H}(\alpha_1,0) \sim \frac{\pi\alpha_1}{2\log\alpha_1} \quad \text{as} \quad \alpha_1 \to \infty. \tag{2.16}$$

With the aid of the identity (2.14) and the computed values of $\mathcal{H}(10^4, h/a)$, we have calculated values of $\mathcal{H}(\alpha,h/a)$ for $\alpha = 10^3$, 10^5 and 10^6, over the range of separations

$$10^{-14} \leqslant \frac{h}{a} \leqslant 10^{-4}.$$

These functions are shown in a log-log plot in figure (3.4), together with the asymptotic approximation for touching cylinders, given by (2.16). In that figure we have also shown the non-dimensional flux between a pair of perfectly conducting cylinders, which from (2.1) and (2.12), is given by

$$\mathcal{H}\left(\infty, \frac{h}{a}\right) = \pi\sqrt{\frac{a}{h}}. \tag{2.17}$$

As mentioned previously, the temperature on the contact region cannot be determined precisely, since an exact value of β is not available. If we choose $\beta = M/a$, where M is a number of order 1, then instead of

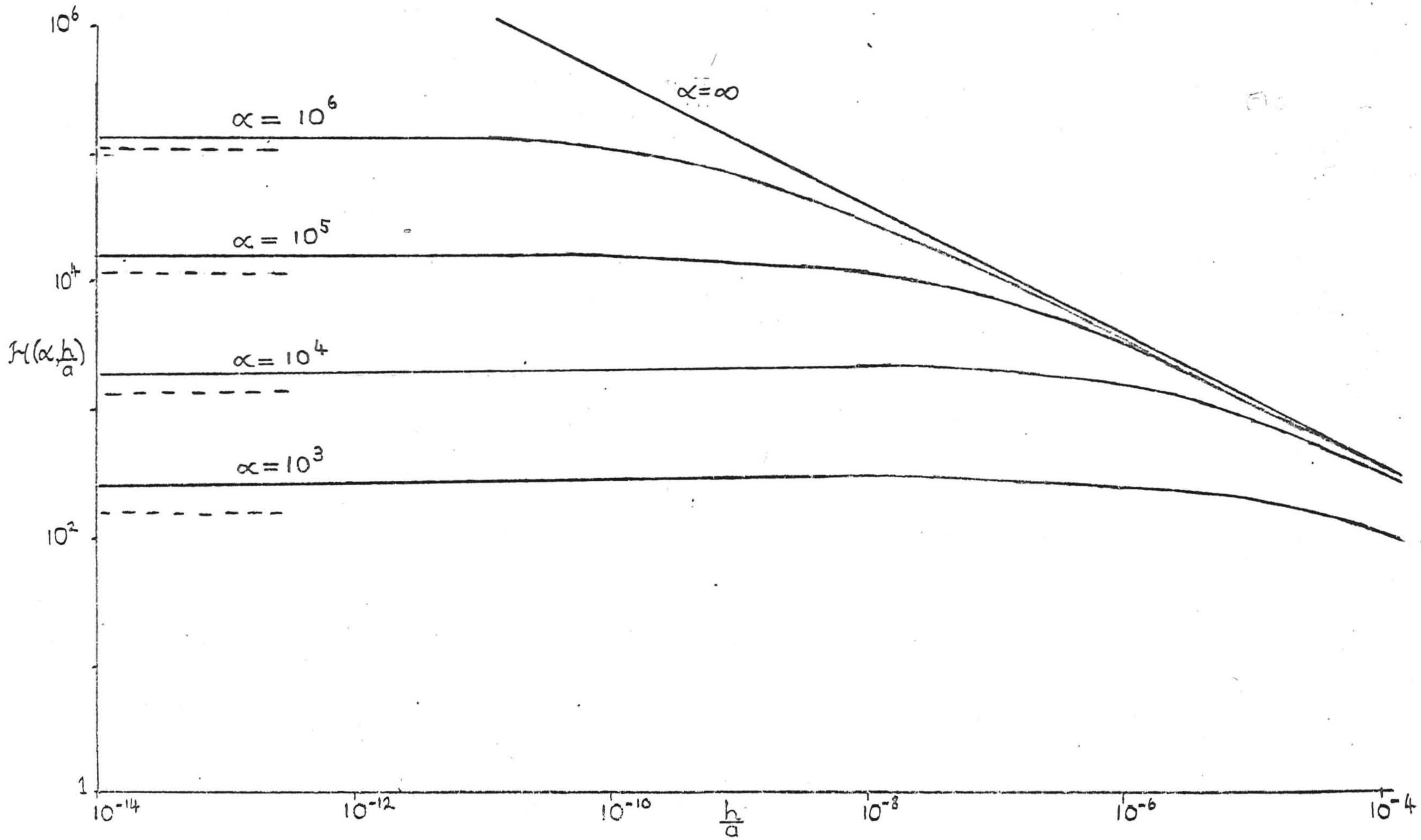

Figure 3.4 The non dimensional flux $\mathcal{H}(\alpha, h/a)$ for various values of the cylinder conductivity, α. The curves for $\alpha = 10^3$, 10^5 and 10^6 were obtained from the $\alpha = 10^4$ curve with the aid of equation (2.14). The asymptotic expression (2.18) for $\mathcal{H}$ for touching cylinders $\alpha \gg 1$ is shown by the broken line.

equation (2.11) we obtain

$$1 = \alpha\left(\frac{h}{a} + \eta^2\right)g(\eta) - \frac{2}{\pi}\int_{-\infty}^{\infty} g(\eta')\log(M|\eta-\eta'|)d\eta',$$

or

$$1 + \frac{2}{\pi}(\log M)\frac{\mathcal{H}_M(\alpha, h/a)}{\alpha} = \alpha\,(h/a + \eta^2)g(\eta) - \frac{2}{\pi}\int_{-\infty}^{\infty} g(\eta')\log|\eta-\eta'|d\eta',$$

where the subscript M denotes the value of $\mathcal{H}(\alpha, h/a)$ computed with $\beta = \frac{M}{a}$. Again using the fact that the integral equations are linear, we find that the solutions $\mathcal{H}_1$ and $\mathcal{H}_M$ are related by

$$\frac{\mathcal{H}_M(\alpha, h/a)}{\left(1 + \frac{2}{\pi}(\log M)\frac{\mathcal{H}_M(\alpha, h/a)}{\alpha}\right)} = \mathcal{H}_1(\alpha, h/a)$$

Thus the relative uncertainty in $\mathcal{H}$ is of order $\frac{\mathcal{H}}{\alpha}$ and the solutions to equation (2.11) are only accurate if $\frac{|\mathcal{H}|}{\alpha} \ll 1$, which is merely a restatement of the condition (2.7). If the cylinders are in contact, we may approximate H in (2.7) by the asymptotic expression (2.16), in which case the constraint becomes

$$\log\alpha \gg 1\,. \tag{2.18}$$

The quantity $\mathcal{H}(\alpha, h/a)$ decreases with increasing h/a, and thus if the condition (2.18) holds, the calculated values of H are accurate over the entire range of separations $\frac{h}{a}$.

A Uniformly Valid Asymptotic Expression for $\mathcal{H}(\alpha, h/a)$

From figure (3.4) it can be seen that a pair of cylinders of finite conductivity may be approximated by perfect conductors if their separation h is sufficiently large. We let $h'/a(\alpha)$ denote the value of h/a at which this approximation ceases to be valid, and from (2.17) we have

$$\mathcal{H}\left(\alpha, \frac{h}{a}\right) \approx \pi\sqrt{\frac{a}{h}}. \tag{2.19}$$

provided that

$$\frac{h}{a} > \frac{h'}{a}(\alpha) \cdot$$

We also introduce the function $\frac{h''}{a}(\alpha)$ as the maximum value of (h/a) at which a pair of cylinders are effectively in contact, so that (from (2.16))

$$\mathcal{H}(\alpha, \frac{h}{a}) \approx \frac{\pi\alpha}{2\log\alpha} \quad (\text{provided } \alpha \gg 1) \tag{2.20}$$

for $\frac{h}{a} < \frac{h''}{a}(\alpha) \cdot$

To obtain the non-dimensional flux $\mathcal{H}(\alpha, h/a)$, for the intermediate range of separations

$$\frac{h''}{a}(\alpha) < \frac{h}{a} < \frac{h'}{a}(\alpha) \tag{2.21}$$

we must use the identity (2.14) together with the numberical solutions of (2.11) for $\alpha = 10^4$.

In this section we shall obtain an approximate expression for $\mathcal{H}$ which is valid for all separations, provided that α is sufficiently large, and which may be evaluated without the need for numerical solutions of equation (2.11). To derive this expression, we must find the way in which $\frac{h'}{a}(\alpha)$ and $\frac{h''}{a}(\alpha)$ depend on α. Since the curves given by (2.19) and (2.20) intersect at

$$\frac{h}{a} = 4\left(\frac{\log\alpha}{\alpha}\right)^2$$

we assume that $\frac{h'}{a}$ and $\frac{h''}{a}$ are proportional to $\left(\frac{\log\alpha}{\alpha}\right)^2$. This assumption will be verified after we have obtained the asymptotic expression for $\mathcal{H}$.

We derive this asymptotic expression from the identity (2.14) by letting $\alpha_1 \to \infty$, with α_2 fixed. When

$$\log\alpha_1 \gg \log\alpha_2 \tag{2.22}$$

(2.14) becomes approximately

$$\frac{\alpha_1}{\mathcal{H}(\alpha_1, \frac{h_1}{a})} \approx \frac{\alpha_2}{\mathcal{H}(\alpha_2, \frac{h_2}{a})} + \frac{2}{\pi}\log\alpha_1 \quad , \tag{2.23}$$

and if $\frac{h_2}{a} > \frac{h'(\alpha_2)}{a}$, we can replace $\mathcal{H}(\alpha_2, h_2/a)$ in this expression by the approximation (2.19), which gives

$$\frac{\alpha_1}{\mathcal{H}(\alpha_1, \frac{h_1}{a})} \approx \frac{\alpha_2}{\pi}\sqrt{\frac{h_2}{a}} + \frac{2}{\pi}\log\alpha_1$$

Eliminating α_2 and h_2, with the aid of (2.15), we get

$$\frac{\alpha_1}{\mathcal{H}(\alpha_1, \frac{h_1}{a})} \approx \frac{\alpha_1}{\pi}\sqrt{\frac{h_1}{a}} + \frac{2}{\pi}\log\alpha_1 \ . \tag{2.24}$$

This result holds if

$$\frac{h_2}{a} > \frac{h'}{a}(\alpha_2),$$

and from (2.15), we see that the minimum separation h_1, for which (2.24) is valid is given by

$$\frac{h_1}{a} = \left(\frac{\alpha_2}{\alpha_1}\right)^2 \frac{h'}{a}(\alpha_2) \, .$$

This quantity is proportional to $\frac{1}{\alpha_1^2}$, and since the function $\frac{h''}{a}(\alpha_1)$ decreases at the slower rate of $\left(\frac{\log\alpha_1}{\alpha_1}\right)^2$, as $\alpha_1 \to \infty$, the constraint

$$\left(\frac{\alpha_2}{\alpha_1}\right)^2 \frac{h'}{a}(\alpha_2) < h''(\alpha_1) \tag{2.25}$$

will be satisfied if α_1 is sufficiently large.

If the constraint (2.25) holds, then the expression (2.24) is valid for all $\frac{h_1}{a}$. This is because the $\log\alpha_1$ term dominates both in the identity (2.14) and in (2.24) and thus both equations give

$$\mathcal{H}(\alpha_1, \frac{h_1}{a}) \approx \frac{\pi\alpha_1}{2\log\alpha_1}$$

for $$\frac{h_1}{a} < \frac{h'(\alpha_2)}{a}\left(\frac{\alpha_2}{\alpha_1}\right)^2 .$$

Thus equation (2.24) is the uniformly valid asymptotic expression for $\mathcal{H}$, which we rewrite as

$$\mathcal{H}(\alpha, \frac{h}{a}) \sim \frac{1}{\frac{2}{\pi}\frac{\log\alpha}{\alpha} + \frac{1}{\pi}\sqrt{\frac{h}{a}}} \quad \text{as } \alpha \to \infty . \qquad (2.26)$$

This asymptotic approximation is shown, for $\alpha = 10^4$, by the broken line in figure (3.3).

From (2.26) we see that

$$\mathcal{H}(\alpha, \frac{h}{a}) \approx \pi\sqrt{\frac{a}{h}} \quad \text{if} \quad h \gg a\left(\frac{\log\alpha}{\alpha}\right)^2$$

and

$$\mathcal{H}(\alpha, \frac{h}{a}) \approx \frac{\pi\alpha}{2\log\alpha} \quad \text{if} \quad h \ll a\left(\frac{\log\alpha}{\alpha}\right)^2$$

and this is consistent with the assumption that $\frac{h'}{a}$ and $\frac{h''}{a}$ are proportional to $\left(\frac{\log\alpha}{\alpha}\right)^2$. We have seen, in §2.4, that the separation at which a pair of locally spherical particles cease to behave as perfect conductors is of order a/α^2, and thus we verify the statement made earlier (§3.2), that the perfect conductor approximation breaks down at larger separations for cylinders than for spheres.

3.3 The conductivity of a material composed of layers of parallel fibres

We have assumed that the temperature field in the neighbourhood of a contact point between a pair of fibres is approximately two-dimensional, and thus the flux Q across the contact region of either fibre can be found by integrating the expression for the flux between a pair of cylinders, viz

$$Q = \int H dy = k\Delta T \int \mathcal{H}(\alpha, \tfrac{h(y)}{a}) dy \,, \tag{3.1}$$

where ΔT denotes the temperature difference between the axes of the cylinders which form the contact, and the integral extends over a suitably chosen neighbourhood of the contact point. The function h(y) denotes the minimum separation distance between the surfaces at the given value of y, and from the expression (1.7) for the thickness of the matrix layer near a contact point, we have

$$h(y) = y^2/b \,. \tag{3.2}$$

To calculate the integral in equation (3.1) we require the values of a and b. Since the fibres are nearly straight and parallel, a is approximately equal to R, the cross-sectional radius of the fibres+. The quantity b is more difficult to determine, since it depends on the radii of curvature of the fibre axes in the neighbourhood of the contact point, and the relative orientation of the fibres (see (1.4) and (1.5)). To determine the conductivity of a fibre-bundle we need details of the statistical distribution function for b which is associated with the material. For most of the commonly occuring fibre-bundles, it is unlikely

---

\+ As mentioned in §3.1, we assume that each fibre has the same circular cross section, of radius R.

that such detailed microstructural information would be available.

There is however, one class of materials for which we can easily calculate b. These materials consist of plane layers of parallel cylindrical fibres. Although the cylinders within each layer are parallel, the orientation of the fibres may vary from layer to layer. Each layer of fibres bears against the adjoining plane layer and thus every fibre makes contact with fibres in neighbouring layers. Our aim is to derive an expression for the component of the conductivity tensor associated with conduction across the layers. The bulk temperature gradient is taken to be perpendicular to the layers and of magnitude G. The temperature on the axis of each fibre is therefore uniform along the length of the fibres, and this temperature is the same for all fibres which lie in the same layer. The difference in temperature between the axes of fibres in subsequent layers is

$$\Delta T = 2RG \tag{3.3}$$

where as usual R denotes the fibre radius.

It is assumed that most of the heat passes between adjacent layers through the contact regions, and therefore the flux F across unit area of a plane parallel to the fibres layers is

$$F = N_c Q \tag{3.4}$$

where N_c is the number of contacts per unit area between adjacent layers. With the aid of figure (3.5) it can be seen that the number of contacts per unit area of the plane touching two adjacent layers is given by

$$N_c = \frac{\sin\theta}{4R^2} , \tag{3.5}$$

where θ denotes the difference in radians between the orientation of subsequent layers. If the fibre are nearly aligned, and $\theta \ll 1$,

$$N_c \approx \frac{\theta}{4R^2} . \tag{3.6}$$

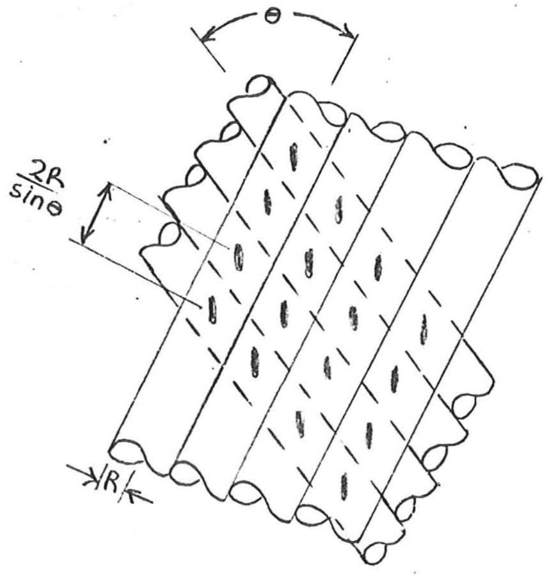

Figure 3.5 A sketch of the contact regions between the fibres in subsequent layers.

It will be shown that F is independent of θ (for $\theta \ll 1$) and therefore the difference in orientation between adjacent layers need not be uniform.

The flux across a contact surface is given by (3.1), and on replacing h(y) by the quadratic expression (3.2), and $H(\alpha, \frac{h(y)}{a})$ by the asymptotic approximation (2.26), we get

$$Q = \pi k \Delta T \int \frac{dy}{\frac{2\log\alpha}{\alpha} + \frac{|y|}{\sqrt{ab}}} . \tag{3.7}$$

The contribution to this integral from the Δy neighbourhood of the contact point is

$$\int_{-\Delta y}^{\Delta y} \frac{dy}{\frac{2\log\alpha}{\alpha} + \frac{|y|}{\sqrt{ab}}} = 2\sqrt{ab}\, \log\left\{1 + \frac{\Delta y}{\sqrt{ab}} \frac{\alpha}{2\log\alpha}\right\}$$

$$\sim 2\sqrt{ab}\, \log\left(\frac{\alpha}{\log\alpha}\right) \quad \text{as } \alpha \to \infty . \tag{3.8}$$

On replacing a and b in (3.8) by the expressions (1.4), and substituting in (3.7), we obtain the asymptotic expression

$$Q \sim \frac{4\pi R}{\theta} k \Delta T \left\{ \log\left(\frac{\alpha}{\log\alpha}\right) \right\} . \tag{3.9}$$

Combining this result with the expression (3.4) for the average flux density F, and substituting the expressions (3.3) and (3.6) for ΔT and N_c, we get

$$F \sim 2\pi k \left(\frac{\alpha}{\log\alpha}\right) G \quad \text{as } \alpha \to \infty .$$

The conductivity associated with the transport of heat across the layers is therefore given by,

$$k^* \sim 2\pi k \log\left(\frac{\alpha}{\log\alpha}\right) \quad \text{as } \alpha \to \infty \tag{3.10}$$

in the case $\theta \ll 1$.

It will be shown that F is independent of θ (for $\theta \ll 1$) and therefore the difference in orientation between adjacent layers need not be uniform.

The flux across a contact surface is given by (3.1), and on replacing h(y) by the quadratic expression (3.2), and $H(\alpha, \frac{h(y)}{a})$ by the asymptotic approximation (2.26), we get

$$Q = \pi k \Delta T \int \frac{dy}{\frac{2\log\alpha}{\alpha} + \frac{|y|}{\sqrt{ab}}} \, . \tag{3.7}$$

The contribution to this integral from the Δy neighbourhood of the contact point is

$$\int_{-\Delta y}^{\Delta y} \frac{dy}{\frac{2\log\alpha}{\alpha} + \frac{|y|}{\sqrt{ab}}} = 2\sqrt{ab}\,\log\left\{1 + \frac{\Delta y}{\sqrt{ab}}\frac{\alpha}{2\log\alpha}\right\}$$

$$\sim 2\sqrt{ab}\,\log\left(\frac{\alpha}{\log\alpha}\right) \quad \text{as } \alpha \to \infty \, . \tag{3.8}$$

On replacing a and b in (3.8) by the expressions (1.4), and substituting in (3.7), we obtain the asymptotic expression

$$Q \sim \frac{4\pi R}{\theta} k \Delta T \left\{ \log\left(\frac{\alpha}{\log\alpha}\right) \right\} . \tag{3.9}$$

Combining this result with the expression (3.4) for the average flux density F, and substituting the expressions (3.3) and (3.6) for ΔT and N_c, we get

$$F \sim 2\pi k \left(\frac{\alpha}{\log\alpha}\right) G \quad \text{as } \alpha \to \infty \, .$$

The conductivity associated with the transport of heat across the layers is therefore given by,

$$k^* \sim 2\pi k \log\left(\frac{\alpha}{\log\alpha}\right) \quad \text{as } \alpha \to \infty \tag{3.10}$$

in the case $\theta \ll 1$.

We can also find the asymptotic form of k^* as $\alpha \to \infty$. for $\theta = \frac{\pi}{2}$. In this case, a and b are equal, and from (1.3) we find

$$a = b = 2R \tag{3.11}$$

The matrix layer thickness is here axisymmetric and the expression (2.4.14) for the flux between a pair of locally spherical particles is valid, namely

$$Q \sim 2\pi k a \Delta T \log\alpha \quad \text{as} \quad \alpha \to \infty. \tag{3.12}$$

Replacing a by 2R, and ΔT by 2RG, we get

$$Q \sim 8\pi k R^2 G \log\alpha \quad \text{as} \quad \alpha \to \infty. \tag{3.13}$$

From the expression (3.5) for the number of contacts per unit area, we get

$$N_c = \frac{1}{4R^2} \quad \text{for } \theta = \frac{\pi}{2},$$

and combining this result with (3.13) and (3.4) we find

$$F \sim 2\pi k G(\log\alpha) \quad \text{as} \quad \alpha \to \infty.$$

Thus the asymptotic expression for the conductivity is

$$k^* \sim 2\pi k(\log\alpha) \quad \text{as} \quad \alpha \to \infty, \tag{3.14}$$

when $\theta = \frac{\pi}{2}$.

Comparing this result with (3.10) we see that the conductivity is only weakly dependent on the relative orientation of the layers.

3.4 The Conductivity of a two-dimensional, isotropic fibre bundle

In this section we consider the problem of conduction through the macroscopically two-dimensional material described in §3.1. Since the material has an isotropic cross-sectional geometry, the conductivity associated with the conduction of heat across the fibres is characterized by a single variable k^* (see (1.1)), and our aim is to derive an expression for this quantity. It is likely that this type of material will occur more commonly in practice than the fibre-layer material discussed in the previous section

It is assumed that the material is statistically homogeneous and therefore the ensemble average of a quantity may be replaced by the volume average of a single realisation. As the material is macroscopically two-dimensional, we can choose for our averaging volume V a cylinder of length L and cross-sectional area A. The axis of the cylinder is parallel to the mean fibre direction, the cross section is sufficiently large to enclose many fibres, and the length L is much greater than the length scale characterising the fluctuations in temperature.

The average flux density is given by

$$\langle \underset{\sim}{F} \rangle = -k \langle \nabla T \rangle + \frac{1}{V} \sum_i \underset{\sim}{S}^i, \tag{4.1}$$

where $\underset{\sim}{S}^i$ is the dipole strength associated with the ith fibre in V, defined by

$$\underset{\sim}{S}^i = (1-\alpha^{-1}) \int_{A_i} \underset{\sim}{x}\, \underset{\sim}{F} \cdot \hat{n}\, dA , \tag{4.2}$$

and the integral extends over the portion of the surface of the ith fibre contained in V. The contribution to this integral from the areas formed by the intersection of the fibre and the surface of V is negligible, since these areas represent only a small portion of A_i.

The assumption that $\alpha >> 1$, enables us to neglect the α^{-1} term in (4.2), and assuming that $k^* >> k$, we rewrite (4.1) as

$$\langle \underset{\sim}{F} \rangle \approx \frac{1}{V} \sum \underset{\sim}{S}^i = \frac{n}{L} \langle \underset{\sim}{S} \rangle , \tag{4.3}$$

where n is the average number of fibres which intersect a unit cross-sectional plane, and $\langle \underset{\sim}{S} \rangle$ is the average dipole strength of the fibres in V.

As in the previous chapter, we assume that the dipole strength of each particle is dominated by the contributions from the contact regions on the particle surface, and the expression (4.2) for $\underset{\sim}{S}$ becomes

$$\underset{\sim}{S} \approx \sum_i \underset{\sim}{x}^i Q^i , \tag{4.4}$$

where $\underset{\sim}{x}^i$ is the vector to the ith contact point and Q^i is the flux across the ith contact region. The latter quantity is given by the expression (3.1), which we write as

$$Q^i = k \Delta T^i \int_{\substack{\text{ith contact} \\ \text{region}}} \mathcal{H}(\alpha, \tfrac{h(y)}{a}) \, dy .$$

Replacing $\mathcal{H}$ in the integral by the asymptotic approximation (2.26), and using (3.8), we get

$$Q^i \approx 2\pi k \Delta T^i \sqrt{Rb^i} \log\left(\frac{\alpha}{\log \alpha}\right) \tag{4.5}$$

provided $\alpha >> 1$. In deriving this result we have used the fact that $a \approx R$ for this type of material (see (1.4) and (1.5)).

An expression relating the temperature differences ΔT^i can be obtained from the identity

$$\sum_i Q^i = 0 ,$$

where the sum extends over the contact points on the surface of a fibre. Combining this expression with the approximate formula (4.5) for Q^i we obtain

$$\sum \Delta T^i \sqrt{b^i} = 0 . \tag{4.6}$$

If α is sufficiently large, the temperature is approximately constant along the axis of each fibre, and the equations (4.6) (one for each particle) together with appropriate boundary conditions, are sufficient to determine ΔT^i. We shall assume that this is the case. Since α does not appear in (4.6), the temperature differences ΔT^i are independent of α.

The particle dipole strength is found from (4.4) and (4.5) to be

$$\underset{\sim}{S} = \{\sum_i \underset{\sim}{x}^i \Delta T^i \sqrt{b^i}\} 2\pi k \sqrt{R} \log(\frac{\alpha}{\log\alpha}) , \tag{4.7}$$

and since ΔT^i is independent of α, the dipole strength is proportional to log $(\alpha/\log\alpha)$. Thus the conducitivity k^* has the asymptotic form

$$\frac{k^*}{k} \sim (\text{constant}) \log(\frac{\alpha}{\log\alpha}) \quad \text{as } \alpha \to \infty . \tag{4.8}$$

where the value of the constant is determined by the fibre geometry. This is not very different from the asymptotic form of the conductivity of granular materials (see 2.6.7), and it appears that a weak α dependence is characterisitic of materials composed of highly conducting particles with point contact.

If the fibres are perfectly cylindrical and parallel, the expression for k^* takes a very different form from that of (4.8). From the asymptotic expression (2.16) for the flux between a pair of touching cylinders, we see that k^* is proportional to $(\alpha/\log\alpha)$ in this case. The material which we have studied contains nearly cylindrical and nearly parallel fibres and these slight imperfections have a very significant effect on the conductivity because they convert the line contact of parallel perfectly straight cylinders into point contact.

To show the way in which the constant in the asymptotic expression (4.8) for k^* depends on the microstructure of the material, we shall derive an expression for the conductivity of a particular type of fibre bundle.

The material under consideration is composed of "nearly straight" fibres, that is, we assume that the amount by which the axis of any fibre deviates from a straight line is much less than the fibre radius R. This straight line will be called the "mean axis", and it is assumed that the mean axes of the fibres are parallel. This material is intended to provide a model for the windings of transformers or electric motors.

Since we are concerned with conduction across the fibres, we need only consider the component of the particle dipole strength which lies in the cross-sectional plane. We denote this component by $\underset{\sim}{S}_P$, and from (4.7) we have

$$\underset{\sim}{S}_P (= \underset{\sim}{S} - \underset{\sim}{S} \cdot \hat{e}_3 \hat{e}_3) = \Big\{ \sum_{\substack{i \\ \text{contacts}}} \underset{\sim}{r}^i \Delta T^i \sqrt{b^i} \Big\} 2\pi k \sqrt{R} \, \log\Big(\frac{\alpha}{\log\alpha}\Big) , \qquad (4.9)$$

where

$$\underset{\sim}{r}^i = \underset{\sim}{x}^i - (\underset{\sim}{x}^i \cdot \hat{e}_3)\hat{e}_3 ,$$

is a vector orthogonal to the mean fibre axis and extending from the mean axis to the ith contact point. Each pair of fibres make contact at many points along their length and $\underset{\sim}{r}^i$ is approximately the same for each of these points.

To evaluate the average of $\underset{\sim}{S}_p$ we make the following assumptions:

(1) The temperature at the centre of any fibre cross section differs from that of any neighbouring fibre by an amount

$$2R\langle\nabla T\rangle\cdot\hat{r}^i ,$$

where $\hat{r}^i$ is the unit vector in the direction of the line of centres $(= \underset{\sim}{r}^i/R)$;

(2) The shape of the matrix layer surrounding the point of contact is the same for each contact, that is

$$b^i = b \qquad \text{for all contact points.}$$

With the aid of these assumptions, (4.9) becomes

$$\underset{\sim}{S}_p = -\Big\{\sum_{\substack{i\\ \text{contacts}}} \hat{r}^i\hat{r}^i\Big\}\cdot\langle\nabla T\rangle 4\pi R^3\sqrt{\frac{b}{R}}\,k\log\Big(\frac{\alpha}{\log\alpha}\Big) . \tag{4.10}$$

Taking the average of this expression, we get

$$\langle \underset{\sim}{S}_p\rangle = -4\pi R^3 k\sqrt{\frac{b}{R}}\log\Big(\frac{\alpha}{\log\alpha}\Big)\langle\sum_{\text{contacts}}\hat{r}^i\hat{r}^i\rangle\cdot\langle\nabla T\rangle . \tag{4.11}$$

If the cross-section geometry is isotropic,

$$\langle\sum\hat{r}^i\hat{r}^i\rangle = \tfrac{1}{2}\Big(\sum\hat{r}^i\cdot\hat{r}^i\Big)\underset{\approx}{I} \tag{4.12}$$

where $\underset{\approx}{I}$ is a 2 x 2 unit tensor.

The vectors $\hat{r}^i$ have unit magnitude, and (4.12) may be written as

$$\langle\sum\hat{r}^i\hat{r}^i\rangle = \frac{L}{2}\langle N_c\rangle\underset{\approx}{I} , \tag{4.13}$$

where $\langle N_c \rangle$ is the average number of contact points, per unit length, on the surface of a fibre, and, as usual L denotes the length of fibre in the averaging volume. We may write $\langle N_c \rangle$ as

$$\langle N_c \rangle = \langle p \rangle \langle \mathcal{N}_c \rangle \tag{4.14}$$

where $\langle p \rangle$ is the average number of near neighbours surrounding the reference fibre, and $\langle \mathcal{N}_c \rangle$ is the average number of points of contact, per unit length, between the reference fibre and a neighbouring fibre.

With the aid of equations (4.13) and (4.14), the expression (4.11) for the average dipole strength becomes

$$\langle \underset{\sim}{S}_p \rangle = -2\pi R^3 k \sqrt{\frac{b}{R}}\, \log\left(\frac{\alpha}{\log\alpha}\right) \langle p \rangle \langle \mathcal{N}_c \rangle L \langle \nabla T \rangle$$

Combining this result with the approximate expression (4.3) for $\langle \underset{\sim}{F} \rangle$ we get

$$\langle \underset{\sim}{F} \rangle = -2\phi k \sqrt{\frac{b}{R}} \langle p \rangle R \langle \mathcal{N}_c \rangle \log\left(\frac{\alpha}{\log\alpha}\right) \langle \nabla T \rangle, \tag{4.15}$$

where ϕ is the fibre volume fraction $(= \pi R^2 n)$

The quantities ϕ and $\langle p \rangle$ are determined by the type of packing. For a square array,

$$\phi \langle p \rangle = \pi$$

and for the more closely-packed triangular array

$$\phi \langle p \rangle = \pi\sqrt{3}.$$

I have been unable to find, from the literature, estimates of ϕ and $\langle p \rangle$ for the case of a two-dimensional random array, but it seems certain that $\frac{\phi\langle p \rangle}{\pi}$ lies between 1 and $\sqrt{3}$ for this type of array.

The quantities $\langle \underset{\sim}{F} \rangle$ and $\langle \nabla T \rangle$ are related by

$$\langle \underset{\sim}{F} \rangle = -\underset{\approx}{k}^* \langle \nabla T \rangle \quad ,$$

and using the expression (1.1) for $\underset{\approx}{k}^*$, together with the fact that $\langle\nabla T\rangle$ is orthogonal to $\hat{e}_3$, we get

$$\langle \underset{\sim}{F} \rangle = -k^* \langle \nabla T \rangle \ .$$

Comparing this expression with (4.15), we find that k^* is given by the asymptotic formula

$$\frac{k^*}{k} \sim 2\phi \langle p \rangle \log\left(\frac{\alpha}{\log\alpha}\right)\sqrt{\frac{b}{R}}\langle N_c \rangle R \qquad (4.16)$$

as $\alpha \to \infty$.

It is unlikely that the microstructural information required for the evaluation of the expression (4.16) would be available in practice. Thus the main result of this section is the formula (4. 8) for k^* , for even though we are unable to determine the constant in that expression, it shows the α dependence of k^* , and the result is valid for any material of the type described in § 3.1.

The expressions (3.10), (3.14) and (4.8) should now be compared with experimental observation, but unfortunately I have been unable to find any relevant observations of k^* in the literature.

CHAPTER 4

THE DIPOLE FIELD

4.1 Introduction

The previous two chapters have been devoted to the study of materials composed of closely packed particles immersed in a matrix of relatively low conductivity. The effective conductivity of such materials can be determined because the particle dipole strength is dominated by the contributions from the regions near points of contact between particles, and the flux across these regions is a locally determined quantity. At lower volume fractions the problem of determining the average dipole strength is more difficult, and past work has been concerned with two classes of suspensions.[+]

(1) Materials composed of spherical particles in a regular array, and

(2) Dilute suspensions of randomly placed spheres.

In this chapter we present new methods for calculating the effective transport properties of these types of suspensions. The relevant transport property may be the conductivity, the viscosity or the elastic moduli.

The earliest theoretical investigation into the problem of conduction through a regular array was carried out by Rayleigh (1892), who obtained an expression for the conductivity of a cubic array of spheres. This expression takes the form of a power series in $(^a/d)$, where a is the sphere radius, and d denotes the centre-to-centre distance between nearest neighbours in the array. In order to calculate the effect of surrounding particles on the dipole strength of a reference sphere, Rayleigh assumed that the temperature gradient "seen" by the reference sphere (that is, the temperature gradient which determines the particle

---

+ We are not concerned here with the work on two-dimensional composites, some of which has been described in § 3.1.

dipole strength) is simply the sum of the field produced by the surrounding spheres. Unfortunately, this sum is non-absolutely convergent.+ Rayleigh noted this, but nevertheless summed the contributions in a particular order, giving no real justification for doing so.

Subsequent investigations into the effective conductivity of regular arrays of spheres have been concerned either with obtaining more terms in the expansion for the conductivity of a cubic array, (Meredith and Tobias (1960), McKenzie and McPhedran (1976)), or with deriving similar expressions for other types of arrays (Bertaux et al (1975)). In each case, Rayleigh's unjustified procedure for the evaluation of the non-absolutely convergent sum has been adopted without comment. In this chapter we show why this convergence problem arises, and in §4.4 we present an alternative method for calculating the effective conductivity of a regular array of spherical particles.

The problem of determining the effective transport properties of a random suspension of interacting spheres is more difficult, since the dipole strength is different for each sphere, and neighbouring spheres may be so close to the reference sphere that they cannot adequately be approximated by a dipole and a sum of several higher order poles. However, if the volume fraction of the particles is small, it is possible to calculate the perturbation in the average dipole strength* $\langle S \rangle$ caused by particle interaction.

+ That is, the result depends on the order in which the contributions from the (infinite number of) surrounding spheres are summed.

* We have not specified the order of the tensor S, since we are concerned both with the conduction problem, for which S is a vector, and with the viscosity and elasticity problems, for which S is a second order tensor.

The probability that a particle will have n neighbours within a distance of several radii is of order ϕ^n, and if we assume that only the close particles interact, we find that the perturbation in $\langle S \rangle$ is due mainly to pair interactions (n = 1). Provided that this assumption is valid, the average dipole strength may apparently be written as

$$\langle S \rangle = S_0 + \int S_1(\underset{\sim}{r}) p(\underset{\sim}{r}|0) dV(\underset{\sim}{r}) \quad , \tag{1.1}$$

where $p(\underset{\sim}{r}|0)dV(\underset{\sim}{r})$ is the probability that the centre of a particle lies within the volume dV surrounding the point $\underset{\sim}{r}$, given that the centre of the reference sphere is at the origin o. The term S_0 denotes the dipole strength in the absence of particle interaction, and S_1 is the amount by which the dipole strength of the reference sphere is altered by the presence of another sphere at $\underset{\sim}{r}$, neglecting all other particles.

Unfortunately the term $S_1(\underset{\sim}{r})$ falls off as $1/|\underset{\sim}{r}|^3$ as $|\underset{\sim}{r}| \to \infty$, and the integral in equation (1.1), like the sum encountered by Rayleigh, is not absolutely convergent.

In order to obtain an expression for $\langle S \rangle$ in terms of convergent integrals, Batchelor (see (1974) for review) devised a technique based on the observation that for each of the transport problems, there is a quantity which has the same far-field dependence as S_1 and which has a known average. We shall call this quantity "the renormalizing quantity". The integral of the difference of S_1 and the renormalizing quantity converges, and it is possible to relate this integral to $\langle S \rangle$. This method, called here the "renormalization technique" has been employed in the derivation of expressions for the average velocity of sedimentation of spheres to order ϕ (Batchelor, 1972), the effective viscosity to order ϕ^2 of a suspension of rigid spheres in a Newtonian liquid (Batchelor and Green 1972), and the effective conductivity of a random suspension of spheres to order ϕ^2 (Jeffrey 1973).

Although this procedure is undoubtedly correct, it is difficult to see why it works, and furthermore it is not clear why the assumption which led to equation (1.1) is wrong. It is hoped that the alternative procedure described in this chapter may help to clear away some of this obscurity.

The new procedures described here for determining the effective transport properties of regular and random arrays are based on equations, derived in §4.2, which relate the temperature, velocity or displacement at a point $\underset{\sim}{x}$ in a suspension to an integral over the surrounding particles together with an integral over a "macroscopic boundary" Γ_b which encloses $\underset{\sim}{x}$.

In §4.3 we use these equations to obtain expressions for the dipole strength of a spherical particle, in terms of the dipole and higher order multipoles of the surrounding particles, together with an integral over Γ_b. On applying the divergence theorem to this integral over Γ_b we obtain a term which may be regarded as the field due to a continuous distribution of dipoles throughout the volume enclosed by Γ_b. The contribution to the dipole strength of the reference sphere from spheres which lie in a distant volume are cancelled by the contribution from the continuous distribution of dipoles contained in that volume. Thus it is the dipole field term which causes the expression for the dipole strength of a reference sphere to converge, and it is shown that Rayleighs convergence difficulties arose simply because he neglected this term.

In §4.4 we describe a procedure for obtaining the effective transport properties of a suspension containing spheres in a regular array, and we illustrate this method by deriving an expression for the effective conductivity of such a material. Another application of this method is described in §4.5, where we derive an expression for the effective modulus of compression of a material composed of rigid spheres in a regular array in an elastic matrix.

The final two sections of the chapter are concerned with random suspensions of interacting particles. In § 4.6 we re-derive Jeffrey's (1973) expression for the effective conductivity, using an alternative procedure, and in § 4.7 we obtain an expression, correct to $O(\phi)$ for the average particle dipole strength in a suspension of rigid spheres in an elastic matrix.

<u>Notation</u>: Since we shall be concerned with suspensions which have an elastic or Newtonian liquid matrix, we introduce here some notation associated with these materials.

Both the velocity and the displacement at a point $\underset{\sim}{x}$ will be denoted by $\underset{\sim}{u}(\underset{\sim}{x})$, the meaning of the symbol will be clear from the context.

In a linear and isotropic elastic material, the stress tensor $\underset{\approx}{\sigma}$ is related to the displacement field by the constitutive equation

$$\underset{\approx}{\sigma} = E(\underset{\approx}{e} + \frac{\nu}{1-2\nu}\nabla\cdot\underset{\sim}{u}\,\underset{\approx}{I}), \tag{1.2}$$

where

$$\underset{\approx}{e} = \frac{1}{2}(\nabla\underset{\sim}{u} + (\nabla\underset{\sim}{u})^T), \tag{1.3}$$

and ν and E are Poisson's ratio, and Young's modulus respectively. The constitutive equation for a Newtonian liquid is

$$\underset{\approx}{\sigma} = -p\underset{\approx}{I} + 2\mu\underset{\approx}{e}, \tag{1.4}$$

where the rate of strain tensor $\underset{\approx}{e}$ is given by (1.3) (with $\underline{u}$ denoting the velocity field), p is the pressure and μ the viscosity.

If a force $\underset{\sim}{F}$ is applied to a point $\underset{\sim}{x}$ in an infinite elastic material, the displacement at $\underset{\sim}{x}'$ is given by

$$\underset{\sim}{u}(\underset{\sim}{x}') = \underset{\approx}{G}(\underset{\sim}{x}-\underset{\sim}{x}')\cdot\underset{\sim}{F}, \tag{1.5}$$

where

$$\underset{\approx}{G}(\underset{\sim}{x}) = \frac{1+\nu}{8\pi E(1-\nu)}\left[\frac{(3-4\nu)}{|\underset{\sim}{x}|}\underset{\approx}{I} + \frac{\underset{\sim}{x}\underset{\sim}{x}}{|\underset{\sim}{x}|^3}\right], \tag{1.6}$$

(Landau and Lifshitz(1970), pp 29). The tensor $\underset{\approx}{G}$ is the Greens function for the elasticity equations in an infinite region.

Similarly, the velocity field due to a force $\underset{\sim}{F}$ at a point $\underset{\sim}{x}$ in an infinite Newtonian liquid is also given by equation (1.5), where

$$\underset{\approx}{G}(\underset{\sim}{x}) = \frac{1}{8\pi\mu}\left[\underset{\approx}{I}\cdot\frac{1}{|\underset{\sim}{x}|} + \frac{\underset{\sim}{x}\underset{\sim}{x}}{|\underset{\sim}{x}|^3}\right]. \tag{1.7}$$

This expression for $\underset{\sim}{u}$ is valid provided that the inertia forces in the liquid may be neglected.

4.2 The integral expression for the temperature in a statistically homogeneous suspension

In this section we derive an equation which relates the temperature $T(\underset{\sim}{x})$ at a point in a suspension to an integral over the volumes of the suspended particles and an integral over the "macroscopic boundary" of the sample. For a statistically homogeneous suspension we show that this macroscopic boundary integral involves only the average temperature and flux density, and it is this observation which enables us to formulate the procedures for calculating the effective transport properties, described in the following sections.

The analogous results for the other transport problems can be obtained by similar methods to those described here for the conduction problem and therefore we will state these results without proof.

If the temperature field $T(\underset{\sim}{x})$ satisfies Laplace's equation

$$\nabla^2 T = 0$$

at each point in a volume V, then the temperature at any point $\underset{\sim}{x}$ in V is related to the flux density $\underset{\sim}{F}$ and the temperature over the surface of

V by the identity

$$T(\underset{\sim}{x})=\frac{1}{4\pi}\int_{\Gamma}\left\{\frac{\underset{\sim}{F}'\cdot\hat{n}}{kr}+T'\nabla'\frac{1}{r}\cdot\hat{n}\right\}dA(\underset{\sim}{x}'), \tag{2.1}$$

where

$$\underset{\sim}{F}'\equiv F(\underset{\sim}{x}'),\quad T'\equiv T(\underset{\sim}{x}'),$$

$$r\equiv|\underset{\sim}{x}-\underset{\sim}{x}'|,$$

$$\nabla_i'\equiv\frac{\partial}{\partial x_i'},$$

and k is the conductivity of the material. The surface of V is denoted by Γ, and $\hat{n}$ is the unit normal directed into V. The identity (2.1) is an example of Greens Second Indentity (Protter and Weinberger (1967) pp 82).

If $\underset{\sim}{x}$ denotes a point in the matrix of a suspension, we write the expression (2.1) in the form

$$T(\underset{\sim}{x})=\frac{1}{4\pi}\sum_i\oint_{\Gamma_i}\left\{\frac{\underset{\sim}{F}'\cdot\hat{n}}{kr}+T'\nabla'\frac{1}{r}\cdot\hat{n}\right\}dA+\frac{1}{4\pi}\oint_{\Gamma_b}\left\{\frac{\underset{\sim}{F}\cdot\hat{n}}{kr}+T'\nabla'\frac{1}{r}\cdot\hat{n}\right\}dA, \tag{2.2}$$

where Γ_b denotes a closed surface enclosing the point $\underset{\sim}{x}$ and Γ_i denotes the surface of the ith particle contained in Γ_b. If the surface Γ_b passes through the ith particle, then Γ_i denotes the closed surface formed by the part of the particle which lies inside Γ_b, together with the part of Γ_b which lies inside the particle.

With the aid of the divergence theorem we can convert the integrals over the surfaces of the particles to volume integrals:

$$\oint_{\Gamma_i}\left\{\frac{\underset{\sim}{F}'\cdot\hat{n}}{kr}+T'\nabla'\frac{1}{r}\cdot\hat{n}\right\}dA=\int_{V_i}\frac{\underset{\sim}{\tau}'}{k}\cdot\nabla'\frac{1}{r}\,dV, \tag{2.3}$$

where V^i is the volume of the ith particle, and

$$\underset{\sim}{\tau}(\underset{\sim}{x}) = \underset{\sim}{F}(\underset{\sim}{x}) + k\nabla T(\underset{\sim}{x}) \tag{2.4}$$

is called the "extra flux density". With the aid of (1.2.6) we see that this quantity is related to the dipole strength $\underset{\sim}{S}^i$ of a particle, by

$$\underset{\sim}{S}^i = \int_{V_i} \underset{\sim}{\tau}' dV. \tag{2.5}$$

In deriving the result (2.3) we have used the fact that both $\underset{\sim}{F}$ and $\nabla'\frac{1}{r}$ have zero divergence at each point in Γ_i. Replacing the integrals over Γ_i in equation (2.2) by the equivalent volume integrals given by (2.3), we get

$$T(\underset{\sim}{x}) = \sum_i \frac{1}{4\pi k}\int_{V_i} \underset{\sim}{\tau}'\cdot\nabla'\frac{1}{r}\,dV + \frac{1}{4\pi}\oint_{\Gamma_b}\left\{\frac{\underset{\sim}{F}'\cdot\hat{n}}{kr} + T'\nabla'\frac{1}{r}\cdot\hat{n}\right\}dA. \tag{2.6}$$

The corresponding expression for the velocity or displacement is+

$$\begin{aligned} u_j(\underset{\sim}{x}) = \sum_i \int_{V_i} \frac{\partial G_{ji}}{\partial x'_k}(\underset{\sim}{x}-\underset{\sim}{x}')\tau_{ik}(\underset{\sim}{x}')dV(\underset{\sim}{x}') \\ + \int_{\Gamma_b}\{G_{ji}(\underset{\sim}{x}-\underset{\sim}{x}')\sigma_{ik}(\underset{\sim}{x}') - u_i(\underset{\sim}{x}')J_{ikj}(\underset{\sim}{x}-\underset{\sim}{x}')\}n_k dA(\underset{\sim}{x}'), \end{aligned} \tag{2.7}$$

where $\underset{\approx}{\tau}$ is the "extra stress", defined by

$$\underset{\approx}{\tau} = \underset{\approx}{\sigma} - \frac{E}{1+\nu}\left(\underset{\approx}{e} + \frac{\nu}{1-2\nu}\nabla\cdot\underset{\sim}{u}\,\underset{\approx}{I}\right)$$

in the case of an elastic matrix, and

$$\underset{\approx}{\tau} = \underset{\approx}{\sigma} - 2\mu\,\underset{\approx}{e}$$

for a Newtonian liquid matrix. The term $J_{ikj}(\underset{\sim}{x}-\underset{\sim}{x}')F_j$ is the stress at $\underset{\sim}{x}'$ caused by the application of a force $\underset{\sim}{F}$ at $\underset{\sim}{x}$, and thus J_{ikj} may be related to the Green's function $\underset{\approx}{G}$ with the aid of

---

+ This result follows from the reciprocal theorem if one of the velocity or displacement fields taken to be the field due to a point force at $\underset{\sim}{x}$ given by (1.5).

the constitutive equation (1.2) or (1.4).

The equations (2.6) and (2.7) hold for any closed surface Γ_b enclosing $\underset{\sim}{x}$, and we now consider the form which these equations take if Γ_b has the following properties:

(1) It is sufficiently large to contain many particles, and

(2) At each point on Γ_b, the local radii of curvature of the surface are much greater than the length scales associated with the fluctuations in the temperature field (typically of the order of the particle diameter).

A surface with these properties is called here a "macroscopic surface", since the length scales associated with the surface are much larger than those associated with the microstructure. If the distance from $\underset{\sim}{x}$ to the nearest point on Γ_b is much greater than the particle diameter then the functions $\frac{1}{r}$ and $\nabla' \frac{1}{\underset{\sim}{r}} \cdot \hat{n}$ are approximately constant over portions of Γ_b which are large enough to be regarded as Sample Areas.+ If ΔA^i denotes such a portion of Γ_b then for a statistically homogeneous material, we have

$$\int_{\Delta A^i} \underset{\sim}{F} \cdot \hat{n} \, dA \approx \int_{\Delta A^i} \langle \underset{\sim}{F} \rangle \cdot \hat{n} \, dA ,$$

and

$$\int_{\Delta A^i} T \, dA \approx \int_{\Delta A^i} \langle T \rangle \, dA ,$$

and thus the integral over Γ_b in equation (2.6) becomes

$$\frac{1}{4\pi} \oint_{\Gamma_b} \left\{ \frac{\langle \underset{\sim}{F}' \rangle \cdot \hat{n}}{kr} + \langle T' \rangle \nabla' \frac{1}{r} \right\} \cdot n \, dA .$$

Substituting this result in equation (2.6) we find that the temperature at a point in the matrix of a statistically homogeneous suspension is given by

---

+ A "Sample Area" is an area which passes through a representative sample of the material. In a statistically homogeneous material, the averages of $\underset{\sim}{F}$ and ∇T over a sample area are equal to the local ensemble averages.

$$T(\underset{\sim}{x}) = \sum_i \frac{1}{4\pi k} \int_{V_i} \underset{\sim}{\tau}' \cdot \nabla' \frac{1}{r}\, dV + \frac{1}{4\pi k} \oint_{\Gamma_b} \left\{ \frac{\langle \underset{\sim}{E}' \rangle}{r} \cdot \hat{n} + k \langle T' \rangle \nabla' \frac{1}{r} \cdot \hat{n} \right\} dA \, . \tag{2.8}$$

The equivalent result for the elastic or Newtonian matrix is

$$\begin{aligned} u_j(\underset{\sim}{x}) = {} & \sum_i \int_{V_i} \frac{\partial G_{ji}}{\partial x'_k}(\underset{\sim}{x} - \underset{\sim}{x}')\, \tau_{ik}(\underset{\sim}{x}')\, dV(\underset{\sim}{x}) \\ & + \int_{\Gamma_b} \left\{ G_{ji}(\underset{\sim}{x} - \underset{\sim}{x}') \langle \sigma_{ik}(\underset{\sim}{x}') \rangle n_k - \langle u_i(\underset{\sim}{x}') \rangle J_{ikj}(\underset{\sim}{x} - \underset{\sim}{x}') n_k \right\} dA(\underset{\sim}{x}') \, . \end{aligned} \tag{2.9}$$

Although it may appear that we have only made a slight step forward in deriving (2.8) from (2.6), it will become apparent in the following sections that the step is a very significant one, for the results which are obtained in the remainder of this chapter are derived in a straightforward manner from the expressions (2.8) and (2.9) obtained here.

4.3 The Dipole Strength of a Sphere in a Statistically Homogeneous suspension

The method for determining the effective transport properties of a regular array of spheres, is quite different from that required for a random array. There is however, one step which is common to both techniques, namely the derivation of an expression which relates the dipole strength of a particle to the dipole and higher order multipole strengths of the surrounding particles. In this section we derive this expression for the particle dipole strength, and in subsequent sections we describe the procedures for finding the average dipole strength of spheres in a regular array (§4.4) and (§4.5) and in a random array (§4.6 and §4.7).

To derive this expression for the dipole strength, we combine one of the equations(2.8) or (2.9) (depending on which transport problem we are concerned with) with a Faxén type formula for the dipole strength of a sphere placed in an ambient field. As in the previous section, we shall concentrate on the conduction problem.

To obtain the Faxén-type expression for the thermal dipole strength of a sphere we begin by writing the expression (2.8) for the temperature at a point in the matrix in the form

$$T(\underset{\sim}{x}) = \frac{1}{4\pi k}\int_{V_j} \underset{\sim}{\tau}'\cdot\nabla'\frac{1}{r}\,dV + T_E(\underset{\sim}{x})\,, \tag{3.1}$$

where

$$T_E(\underset{\sim}{x}) = \sum_{\substack{i\\ i\neq j}} \frac{1}{4\pi k}\int_{V_i} \underset{\sim}{\tau}'\cdot\nabla'\frac{1}{r}\,dV + \frac{1}{4\pi k}\oint_{\Gamma_b}\left\{\frac{\langle \underset{\sim}{F}'\rangle\cdot\hat{n}}{r} + k\langle T'\rangle\nabla'\frac{1}{r}\cdot n\right\}dA\,. \tag{3.2}$$

The form of (3.1) is the same as that of the expression for the temperature field surrounding a single particle in an infinite matrix, with $T_E(\underset{\sim}{x})$ taking the place of the temperature field in the absence of the particle. We seek an expression for the dipole strength of sphere j in terms of the field $T_E(\underset{\sim}{x})$, called here "the external field".

The reference particle (sphere j) has conductivity αk , and from the expression (2.4) for $\underset{\sim}{\tau}$ we get

$$\underset{\sim}{\tau}(\underset{\sim}{x}) = (1-\alpha^{-1})\underset{\sim}{F}(\underset{\sim}{x}) \tag{3.3}$$

at points which lie in the particles.

Combining this result with (3.1) and using the divergence theorem, we obtain

$$T(\underset{\sim}{x}) = \frac{(1-\alpha^{-1})}{4\pi k}\oint_{\Gamma_j}\frac{\underset{\sim}{F}\cdot\hat{n}}{r}\,dA + T_E(\underset{\sim}{x})\,, \tag{3.4}$$

for points $\underset{\sim}{x}$ in the matrix.

The expression (3.4) is also valid for points which lie inside the reference sphere. To show this, we apply Green's second identity (2.1) to the volume enclosed by the reference sphere, with k replaced by αk , and we get

$$T(\underset{\sim}{x}) = -\frac{1}{4\pi}\oint_{\Gamma_j}\left\{\frac{\underset{\sim}{F}'\cdot\hat{n}}{\alpha k r} + T'\nabla'\frac{1}{r}\cdot\hat{n}\right\}dA\,, \tag{3.5}$$

where, as usual, $\hat{n}$ denotes the unit normal directed into the matrix, and $\underset{\sim}{x}$ is a point in the reference sphere. By applying Green's second identity to the volume of matrix enclosed by Γ_b and combining the resulting expression for $\oint T'\nabla'\frac{1}{r}\cdot\hat{n}\,dA$ with (3.5) we obtain equation (3.4).

Taking the gradient of (3.4) and setting $\underset{\sim}{x}=\underset{\sim}{x}_0$; where $\underset{\sim}{x}_0$ denotes the position of the centre of the reference sphere, we get

$$\begin{aligned}\nabla T(\underset{\sim}{x}_0) &= \frac{(1-\alpha^{-1})}{4\pi k a^3}\oint_{\Gamma_j}(\underset{\sim}{x}'-\underset{\sim}{x}_0)\underset{\sim}{E}'\cdot\hat{n}\,dA + \nabla T_E(\underset{\sim}{x}_0) \\ &= \frac{\underset{\sim}{S}^j}{4\pi k a^3} + \nabla T_E(\underset{\sim}{x}_0) \quad ,\end{aligned} \tag{3.6}$$

where a is the radius of the reference sphere and $\underset{\sim}{S}^j$ is its dipole strength. If the reference sphere is a perfect conductor,

$$\nabla T(\underset{\sim}{x}_0)=0$$

and from (3.6) we get

$$\underset{\sim}{S}^j = -4\pi k a^3\nabla T_E(\underset{\sim}{x}_0).$$

For the case of a sphere of finite conductivity, we require an additional expression for $\nabla T(\underset{\sim}{x}_0)$ in order to find $\underset{\sim}{S}^j$. This is obtained by taking the gradient of equation (3.5) and putting $\underset{\sim}{x}=\underset{\sim}{x}_0$ which gives

$$\nabla T(\underset{\sim}{x}_0) = \frac{-\underset{\sim}{S}^j}{4\pi k a^3(\alpha-1)} + \frac{1}{4\pi}\oint_{\Gamma_j} T'\nabla'\nabla'\frac{1}{r}\cdot\hat{n}\,dA \tag{3.7}$$

Expanding T in the integral in this expression in a Taylor series about $\underset{\sim}{x}=\underset{\sim}{x}_0$, and using the fact that $\nabla^2 T=0$ in V_j , we get

$$\int T\nabla'\nabla'\frac{1}{r}\cdot\hat{n}\,dA = \frac{8\pi}{3}\nabla T(\underset{\sim}{x}_0)$$

and on substituting this result in (3.7), we find,

$$\nabla T(\underset{\sim}{x}_o) = \frac{-3\, \underset{\sim}{S}^j}{4\pi k a^3(\alpha-1)} \cdot \tag{3.8}$$

The Faxén-type formula for the dipole strength of the reference sphere is found by equating (3.6) and (3.8), which gives

$$\underset{\sim}{S}^j = -4\pi a^3 k \frac{(\alpha-1)}{(\alpha+2)} \nabla T_E(\underset{\sim}{x}_o) \,. \tag{3.9}$$

The corresponding expression for the dipole strength of a rigid sphere suspended in a Newtonian liquid[+] (with inertia forces neglected), is given by (Batchelor and Green 1972(a)):

$$\underset{\approx}{S}^j = \frac{20}{3}\pi a^3 \mu \left(\underset{\approx}{e}_E(\underset{\sim}{x}_o) + \frac{1}{10} a^2 \nabla^2 \underset{\approx}{e}_E(\underset{\sim}{x}_o) \right), \tag{3.10}$$

where

$$\underset{\approx}{e}_E = \frac{1}{2}\left(\nabla \underset{\sim}{u}_E + (\nabla \underset{\sim}{u}_E)^T \right), \tag{3.11}$$

and $\underset{\sim}{u}_E$ is the external velocity field. From equation (2.9) we have

$$u_E(\underset{\sim}{x})_n = \sum_{\substack{i \\ i\neq j}} \int_{V_i} \frac{\partial G_{nm}(\underset{\sim}{x}-\underset{\sim}{x}')}{\partial x'_k} \tau_{mk}(\underset{\sim}{x}) dV(\underset{\sim}{x}')$$

$$+ \int_{\Gamma_b} \{ G_{nm}(\underset{\sim}{x}-\underset{\sim}{x}') \langle \sigma_{mk}(\underset{\sim}{x}') \rangle n_k - \langle u_m(\underset{\sim}{x}') \rangle J_{mkn}(\underset{\sim}{x}-\underset{\sim}{x}') n_k \} dA(\underset{\sim}{x}'). \tag{3.12}$$

and from this expression we can calculate the external strain field $\underset{\approx}{e}_E$.

Using a similar method to that employed by Batchelor and Green (1972(a)) for the derivation of (3.10), we have found that the dipole strength of a rigid sphere in an elastic matrix is given by[+]

$$\underset{\approx}{S} = \frac{10\pi a^3 E(1-\nu)}{(4-5\nu)(1+\nu)} \left[\underset{\approx}{e}_E(\underset{\sim}{x}_o) + \frac{a^2}{10} \nabla^2 \underset{\approx}{e}_E(\underset{\sim}{x}_o) + \underset{\approx}{I} \frac{\nabla\cdot \underset{\sim}{u}_E(\underset{\sim}{x}_o)}{5(1-2\nu)} \right], \tag{3.13}$$

[+] For a rigid particle in an elastic or newtonian liquid matrix, the dipole strength S is given by (1.2.10).

where E and ν are Young's modulus and Poisson's ratio for the matrix, and the strain tensor $\underset{\approx}{e}_E$ is given by equations (3.11) and (3.12) in the case of a statistically homogeneous suspension. The derivation of (3.13) is given in the appendix A3.+

By combining the Faxen-type formula (3.9) for the thermal dipole strength, with the expression (3.2) for T_E, we get

$$\underset{\sim}{S}^j = \sum_{\substack{i\\ i\neq j}} \frac{(\alpha-1)}{(\alpha+2)} a^3 \int_{V_i} \underset{\sim}{\tau}' \cdot \nabla\nabla' \frac{1}{r} dV + \frac{(\alpha-1)a^3}{(\alpha+2)} \oint_{\Gamma_b} \left\{ \nabla' \frac{1}{r} \langle \underset{\sim}{F}' \rangle + k \langle T' \rangle \nabla\nabla' \frac{1}{r} \right\} \cdot \hat{n}\, dA \,. \quad (3.14)$$

With the aid of the expression (3.3) for $\underset{\sim}{\tau}$, and the divergence theorem, we find

$$\int_{V_i} \underset{\sim}{\tau} \cdot \nabla\nabla' \frac{1}{r} dV = (1-\alpha^{-1}) \oint_{\Gamma_i} \nabla' \frac{1}{r} \underset{\sim}{F}' \cdot \hat{n}\, dA \quad (3.15)$$

Expanding $\nabla' \frac{1}{r}$ in (3.15) in a Taylor series about $r = |\underset{\sim}{x}_0 - \underset{\sim}{x}_i|$, where $\underset{\sim}{x}_i$ is the centre of sphere i, we get

$$(1-\alpha^{-1}) \oint_{\Gamma_i} \nabla' \frac{1}{r} \underset{\sim}{F}' \cdot \hat{n}\, dA = \underset{\sim}{S}^i \cdot \nabla'\nabla' \frac{1}{r^i} + \sum_{k=2}^{\infty} \frac{\mathcal{M}_k^i}{k!} \overset{(1)}{\nabla} \overset{(2)}{\nabla'} \cdots \overset{(k+1)}{\nabla'} \frac{1}{r^i} \,, \quad (3.16)$$

where $r^i = |\underset{\sim}{x}_i - \underset{\sim}{x}_0|$,

$$\nabla'\nabla' \ldots \nabla' \frac{1}{r^i} \equiv \left[\nabla\nabla' \ldots \nabla' \frac{1}{|\underset{\sim}{x}' - \underset{\sim}{x}_0|} \right]_{\underset{\sim}{x}' = \underset{\sim}{x}_i}$$

and

$$\mathcal{M}_k^i = (1-\alpha^{-1}) \oint_{\Gamma_i} \overset{(1)}{(\underset{\sim}{x} - \underset{\sim}{x}_i)} \overset{(2)}{(\underset{\sim}{x} - \underset{\sim}{x}_i)} \ldots \overset{(k)}{(\underset{\sim}{x} - \underset{\sim}{x}_i)} \underset{\sim}{F}(\underset{\sim}{x}) \cdot \hat{n}\, dA(\underset{\sim}{x}) \,, \quad (3.17)$$

+ It seems likely that the Faxén type formula for an elastic sphere can be found by a similar, but more arduous procedure. Since our main aim is to illustrate methods for finding the effective transport properties, we shall only consider the simpler problem of rigid particles.

is a kth order tensor, called here the "kth multipole strength of sphere i". This is a straightforward generalization of the concept of a dipole strength. The term

$$\mathcal{M}^i_k \overset{(1)}{\nabla'}\overset{(2)}{\nabla'}\cdots\overset{(k+1)}{\nabla'}\frac{1}{r^i}$$

is the vector formed by the contraction of the tensors $\mathcal{M}^i_k$ and $\overset{(1)}{\nabla'}\overset{(2)}{\nabla'}\cdots\overset{(k+1)}{\nabla'}\frac{1}{r^i}$.

To obtain an equation relating the dipole strength of the reference sphere to the dipole and higher order multipole strengths of the surrounding spheres, we substitute (3.16) in (3.15) and replace the integrals over V_i in (3.14) by the resulting expression, which gives

$$\underset{\sim}{S}^j = \frac{(\alpha-1)}{(\alpha+2)}a^3\Big\{\sum_{\substack{i\\ i\neq j}}\Big(\underset{\sim}{S}^i\cdot\nabla'\nabla'\frac{1}{r^i} + \sum_{k=2}^{\infty}\frac{\mathcal{M}^i_k}{k!}\overset{(1)}{\nabla'}\overset{(2)}{\nabla'}\cdots\overset{(k+1)}{\nabla'}\frac{1}{r^i}\Big) + \oint_{\Gamma_b}\Big[\nabla'\frac{1}{r}\langle \underset{\sim}{E}\rangle\cdot\hat{n} + k\langle T\rangle\nabla'\nabla'\frac{1}{r}\cdot\hat{n}\Big]dA\Big\} \tag{3.18}$$

Rayleigh (1892) assumed that the field "seen" by the reference sphere (in our notation this is the external field T_E) is equal to the average field $\langle\nabla T\rangle\cdot\underset{\sim}{x}$ plus a contribution from the surrounding spheres. He then obtained an expression for the dipole strength of a sphere (equation (62) of that paper) which contained the first term on the right hand side of (3.18), but not the second. From (3.18) it can be seen that the contributions to this first term from far-off spheres drop off as $1/(r^i)^3$, and as mentioned in §4.1, the sum is non-absolutely convergent. We shall now show that the term which Rayleigh neglected, namely the integral over Γ_b in (3.18), cancels out the effect of the far off particles and gives a convergent expression for $\underset{\sim}{S}^j$.

Applying the divergence theorem to the integral over Γ_b in equation (3.18), we get

$$\oint_{\Gamma_b}\Big\{\nabla'\frac{1}{r}\langle \underset{\sim}{E}'\rangle\cdot\hat{n} + k\langle T'\rangle\nabla'\nabla'\frac{1}{r}\cdot\hat{n}\Big\}dA = -\oint_{V'}\{\langle\underset{\sim}{E}\rangle + k\nabla\langle T\rangle\}\cdot\nabla'\nabla'\frac{1}{r}\,dV - \oint_{\Gamma_E}\Big\{\nabla'\frac{1}{r}\langle \underset{\sim}{E}'\rangle\cdot\hat{n} + k\langle T'\rangle\nabla'\nabla'\frac{1}{r}\cdot\hat{n}\Big\}dA \,, \tag{3.19}$$

where Γ_ϵ denotes the surface of a small sphere of radius ϵ, centred on $\underset{\sim}{x}_0$, and V' denotes the volume which lies between the surfaces Γ_b and Γ_ϵ. From the expression (1.2.5) for the bulk flux density, we see that the volume integral in (3.19) may be written as

$$\int_{V'} n\langle \underset{\sim}{S}\rangle\cdot\nabla'\nabla'\frac{1}{r}\,dV\,. \tag{3.20}$$

This integral, divided by $4\pi k$, gives the temperature gradient at $\underset{\sim}{x}_0$ due to a continuous distribution of dipoles throughout V'.

To estimate the integral over Γ_ϵ in (3.19), we expand $\langle \underset{\sim}{F}\rangle$ and $\langle T\rangle$ in a Taylor series about $\underset{\sim}{x}_0$, and this gives

$$\oint_{\Gamma_\epsilon}\Big\{\nabla'\frac{1}{r}\langle \underset{\sim}{F}'\rangle\cdot\hat{n} + k\langle T'\rangle\nabla'\nabla'\frac{1}{r}\cdot\hat{n}\Big\}dA = -\frac{4\pi}{3}\langle \underset{\sim}{F}(\underset{\sim}{x}_0)\rangle + \frac{8\pi k}{3}\langle\nabla T(\underset{\sim}{x}_0)\rangle + O(\epsilon).$$

Combining this result with (3.19) and (3.20), we find

$$\oint_{\Gamma_b}\Big\{\nabla'\frac{1}{r}\langle \underset{\sim}{F}'\rangle\cdot\hat{n} + k\langle T'\rangle\nabla'\nabla'\frac{1}{r}\cdot\hat{n}\Big\}dA = -\int_{V'} n\langle \underset{\sim}{S}\rangle\cdot\nabla'\nabla'\frac{1}{r}\,dV + \frac{4\pi n}{3}\langle \underset{\sim}{S}(\underset{\sim}{x}_0)\rangle$$
$$- 4\pi k\langle\nabla T(\underset{\sim}{x}_0)\rangle + O(\epsilon)\,,$$

and replacing the integral over Γ_b in (3.18) by the above expression we obtain

$$\underset{\sim}{S}^j = \frac{(\alpha-1)}{(\alpha+2)}a^3\Big\{\sum_{\substack{i\\ i\neq j}}\Big(\underset{\sim}{S}^i\cdot\nabla'\nabla'\frac{1}{r_i} + \sum_{k=2}^{\infty}\frac{\mathcal{M}_k^i}{k!}\,\overset{(1)}{\nabla'}\,\overset{(2)}{\nabla'}\cdots\overset{(k+1)}{\nabla'}\frac{1}{r_i}\Big)\Big\}$$
$$+ \underset{\sim}{S}_0 + \phi\frac{(\alpha-1)}{(\alpha+2)}\langle \underset{\sim}{S}(\underset{\sim}{x}_0)\rangle - \frac{(\alpha-1)}{(\alpha+2)}a^3\int_{V'} n\langle \underset{\sim}{S}\rangle\cdot\nabla'\nabla'\frac{1}{r}\,dV, \tag{3.21}$$

where

$$\underset{\sim}{S}_0 = -4\pi a^3 k\frac{(\alpha-1)}{(\alpha+2)}\langle\nabla T(\underset{\sim}{x}_0)\rangle\,, \tag{3.22}$$

is the dipole strength of the reference sphere in the absence of particle interaction. In deriving (3.21) we have neglected terms $O(\epsilon)$.

From equation (3.21), we see that the contribution to the dipole strength of the reference sphere from the spheres contained in a distant volume δV, is given, to leading order, by+

$$\frac{(\alpha-1)}{(\alpha+2)} a^3 n \langle \underset{\sim}{S} \rangle \cdot \nabla' \nabla' \frac{1}{r} \delta V ,$$

where $\langle \underset{\sim}{S} \rangle$ is the average dipole strength of the particles in δV, and r is the distance from $\underset{\sim}{x}_0$ to a point in δV. This term is cancelled, to leading order, by the contribution to (3.21) from the integral over the continuous distribution of dipoles contained in δV. Thus the expression (3.21) converges and the result is independent of the shape of the macroscopic volume V'.

Equation (3.21) is the expression for the dipole strength referred to at the beginning of this section. The methods for finding the average thermal dipole strength of a sphere in a regular, and in a random array, both begin with this equation.

To find the corresponding expression relating the elastic dipole strength of a rigid sphere to the multipoles strengths of the surrounding spheres, we re-write the Faxén type expressions (3.13) for $\underset{\approx}{S}^j$ as

$$\underset{\approx}{S}^j = \eta_1 \left(\underset{\approx}{e}_E(\underset{\sim}{x}_0) + \frac{a^2}{10} \nabla^2 \underset{\approx}{e}_E(\underset{\sim}{x}_0) + \frac{\underset{\approx}{I}\, \text{trace}\, \underset{\approx}{e}_E(\underset{\sim}{x}_0)}{5(1-2\nu)} \right), \qquad (3.23)$$

where

$$\eta_1 = \frac{10\pi a^3 E(1-\nu)}{(4-5\nu)(1+\nu)} . \qquad (3.24)$$

Substituting the expression (3.12) for $\underset{\sim}{u}_E$ into the defining expression (3.11) for $\underset{\approx}{e}_E$, and using the divergence theorem to convert the integral over Γ_b to a volume integral, we get

---

+ We assume that δV contains a large number of particles, that is, $\delta V \gg \frac{1}{n}$ and also that $\delta V^{1/3} \ll r$.

$$e_E(\underset{\sim}{x}_0)_{pq} = \langle e_{pq}\rangle + \eta_2\langle S_{pq}\rangle + \eta_3\,\delta_{pq}\langle S_{mm}\rangle$$

$$+\sum_{\substack{i\\ i\neq j}}\int_{V_i} P(\underset{\sim}{x}-\underset{\sim}{x}_0)_{pqmk}\,\tau_{mk}(\underset{\sim}{x})\,dV(\underset{\sim}{x}) - n\int_{V'} P(\underset{\sim}{x}-\underset{\sim}{x}_0)_{pqmk}\langle S_{mk}\rangle dV, \qquad (3.25)$$

where
$$\left.\begin{aligned} \eta_2 &= \frac{n(1+\nu)(13-20\nu)}{30(1-\nu)E} \\ \eta_3 &= \frac{n(1+\nu)}{15(1-\nu)E} \end{aligned}\right\} \qquad (3.26)$$

$$P_{pqmk} = \frac{1}{2}\left(\frac{\partial^2 G_{pm}}{\partial x_q \partial x_k} + \frac{\partial^2 G_{qm}}{\partial x_p \partial x_k}\right), \qquad (3.27)$$

and $\underset{\approx}{G}$ is given by (1.6).

To obtain an expression for $\nabla^2 \underset{\approx}{e}_E(\underset{\sim}{x}_0)$, we combine the expression (3.12) for $\underset{\sim}{u}_E$ with equation (3.11), and apply the ∇^2 operator to the resulting equation, which becomes

$$\nabla^2 e_E(\underset{\sim}{x}_0)_{pq} = \sum_{\substack{i\\ i\neq j}}\int \nabla^2 P(\underset{\sim}{x}-\underset{\sim}{x}_0)_{pqmk}\,\tau_{mk}(\underset{\sim}{x})\,dV$$
$$+\frac{1}{2}\int_{\Gamma_b}\left\{\nabla^2\left(\frac{\partial G_{pm}}{\partial x_q}+\frac{\partial G_{qm}}{\partial x_p}\right)\langle\sigma_{mk}\rangle - \langle u_m\rangle\nabla^2\left(\frac{\partial J_{mkp}}{\partial x_q}+\frac{\partial J_{mkq}}{\partial x_p}\right)\right\} n_k\,dA. \qquad (3.28)$$

The integral over Γ_b in this expression may be neglected if Γ_b is sufficiently large. To show this, we note that

$$\nabla^2\left(\frac{\partial G_{pm}(\underset{\sim}{x})}{\partial x_q} + \frac{\partial G_{qm}(\underset{\sim}{x})}{\partial x_p}\right) \text{ is } O(1/|\underset{\sim}{x}|^4) \text{ as } |\underset{\sim}{x}|\to\infty.$$

and

$$\nabla^2\left(\frac{\partial J_{mkp}}{\partial x_q} + \frac{\partial J_{mkq}}{\partial x_p}\right) \text{ is } O(1/|\underset{\sim}{x}|^5) \text{ as } |\underset{\sim}{x}|\to\infty.$$

Furthermore, the term $\langle\underset{\approx}{\sigma}\rangle\cdot\hat{n}$ is bounded on Γ_b (since we generally take $\langle\underset{\approx}{e}\rangle$ to be uniform), and $\langle\underset{\sim}{u}(\underset{\sim}{x})\rangle - \langle\underset{\sim}{u}(\underset{\sim}{x}_0)\rangle$ $(= \nabla\langle\underset{\sim}{u}\rangle\cdot(\underset{\sim}{x}-\underset{\sim}{x}_0))$ increases linearly with $|\underset{\sim}{x}-\underset{\sim}{x}_0|$. If Γ_b is a large sphere, of radius R, centred on $\underset{\sim}{x}_0$, the integral in (3.28) is $O(1/R^2)$ as $R\to\infty$.

and may therefore be neglected. Thus (3.28) becomes

$$\nabla^2 \underset{\approx}{e}_E(\underset{\sim}{x}_0) = \sum_i \int_{V_i} \nabla^2 P(\underset{\sim}{x}-\underset{\sim}{x}_0)_{pqmk}\, \tau(\underset{\sim}{x})_{mk}\, dV(\underset{\sim}{x}). \tag{3.29}$$

This sum converges and there is no dipole field term.

To express the integrals over the particles in the expression (3.25) and (3.29) in terms of the multipole strengths of those particles, we make use of the fact that

$$\underset{\approx}{\tau} = \underset{\approx}{\sigma}$$

in a rigid particle. From the divergence theorem, we find

$$\int_{V_i} P_{pqmk} \tau_{mk} dV = \frac{1}{2} \int_{\Gamma_i} \left(\frac{\partial G_{pm}}{\partial x_q} + \frac{\partial G_{qm}}{\partial x_p} \right) \sigma_{mk} n_k dA \quad .$$

Expanding G in the above integral in a Taylor series about $(\underset{\sim}{x}_i - \underset{\sim}{x}_0)$ we get

$$\begin{aligned}\int_{V_i} P_{pqmk}\tau_{mk} dV = {} & \frac{1}{2}\frac{\partial}{\partial x_a}\left(\frac{\partial}{\partial x_q} G(\underset{\sim}{x}_i-\underset{\sim}{x}_0)_{pm} + \frac{\partial G}{\partial x_p}(\underset{\sim}{x}_i-\underset{\sim}{x}_0)_{qm}\right) S^i_{am} \\ & + \frac{1}{2}\sum_{k=2}^{\infty} \frac{1}{k!} \overset{(1)}{\frac{\partial}{\partial x_a}} \overset{(2)}{\frac{\partial}{\partial x_b}} \cdots\cdots \overset{(k)}{\frac{\partial}{\partial x_c}} \left(\frac{\partial}{\partial x_q} G_{pm} + \frac{\partial}{\partial x_p} G_{qm}\right) (\mathcal{M}^i_k)_{ab \ldots cm} ,\end{aligned} \tag{3.30}$$

where

$$(\mathcal{M}^i_k)_{ab\ldots cm} = \int_{\Gamma_i} \overset{(1)}{(\underset{\sim}{x}-\underset{\sim}{x}_i)_a} \overset{(2)}{(\underset{\sim}{x}-\underset{\sim}{x}_i)_b} \cdots\cdots \overset{(k)}{(\underset{\sim}{x}-\underset{\sim}{x}_i)_c}\, \sigma_{mp} n_p dA. \tag{3.31}$$

Substituting (3.30) in (3.25), we obtain

$$\begin{aligned} e_E(\underset{\sim}{x}_0)_{pq} = {} & \langle e_{pq}\rangle + \eta_2\langle S_{pq}\rangle + \delta_{pq}\eta_3\langle S_{mm}\rangle - n\int_{V'} P(\underset{\sim}{x}-\underset{\sim}{x}_0)_{pqam}\langle S_{am}\rangle dV \\ & \sum_{\substack{i \\ i\neq j}} \left\{ P(\underset{\sim}{x}_i-\underset{\sim}{x}_0)_{pqam} S^i_{am} + \sum_{k=2}^{\infty} \frac{1}{k!}\frac{\partial}{\partial x_b}\cdots\cdots\frac{\partial}{\partial x_c} P(\underset{\sim}{x}_i-\underset{\sim}{x}_0)_{pqam}(\mathcal{M}^i_k)_{ab\ldots cm}\right\}, \end{aligned} \tag{3.32}$$

and combining (3.30) with the expression (3.29) for $\nabla^2 \underset{\approx}{e}_E$, we find

$$\begin{aligned}\nabla^2 e_E(\underset{\sim}{x}_0)_{pq} = \sum_{\substack{i \\ i\neq j}} \Big\{ & \nabla^2 P(\underset{\sim}{x}_i-\underset{\sim}{x}_0)_{pqam} S^i_{am} \\ & + \sum_{k=2}^{\infty} \frac{1}{k!} \frac{\partial}{\partial x_b}\cdots\frac{\partial}{\partial x_c} \nabla^2 P(\underset{\sim}{x}_i-\underset{\sim}{x}_0)_{pqam} (\mathcal{M}^i_k)_{ab\ldots cm} \Big\} .\end{aligned} \tag{3.33}$$

By substituting (3.32) and (3.33) for $\underset{\approx}{e}_E$ and $\nabla^2 \underset{\approx}{e}_E$ in the expression (3.23) for $\underset{\approx}{S}^j$, we obtain the required equation relating the dipole strength of the reference sphere to the multipoles of the surrounding spheres, but since this equation is rather long, we shall work with each of the component equations (3.23), (3.32) and (3.33) separately.

For the case of rigid spheres suspended in a Newtonian liquid, the dipole strength of a reference sphere is related to the "external strain rate" $\underset{\approx}{e}_E$ by equation (3.10), and using a similar method to that described above, we find

$$e_E(\underset{\sim}{x}_0)_{pq} = \langle e_{pq} \rangle + \frac{n}{10\mu} \langle S_{pq} \rangle - \int_{V'} P_{pqam} \langle S_{am} \rangle \, dV \qquad (3.34)$$
$$+ \sum_{\substack{i \\ i \neq j}} \left\{ P(\underset{\sim}{x}_i - \underset{\sim}{x}_0)_{pqam} S^i_{am} + \sum_{k=2}^{\infty} \frac{1}{k!} \frac{\partial}{\partial x_b} \cdots \frac{\partial}{\partial x_c} P_{pqam}(\underset{\sim}{x}_i - \underset{\sim}{x}_0)(M^i_k)_{ab \ldots cm} \right.,$$

and $\nabla^2 \underset{\approx}{e}_E$ is given by equation (3.33)

4.4 Conduction through a Regular Array of Spheres

We now turn to the problem of determining the effective transport properties of a material composed of spheres in a regular array, immersed in a matrix.

The technique for calculating the transport properties of such a material makes use of the fact that each of the spheres has the same dipole and higher order multipole strength.+ To illustrate the method, we shall consider the problem of conduction through a regular array of spheres.

We assume that the material is subjected to a uniform mean temperature gradient $\langle \nabla T \rangle$. Since the multipole tensors are the same for each particle, we may drop the superscripts of these terms, and equation (3.21) becomes

---

+ This is true for all spheres in a volume within which $\langle \nabla T \rangle$ does not vary significantly.

$$\underset{\sim}{S}\left(1-\frac{\phi(\alpha-1)}{(\alpha+2)}\right)=\underset{\sim}{S}_0+\frac{(\alpha-1)}{(\alpha+2)}a^3\Big[\underset{\sim}{S}\cdot\Big\{\sum_{\substack{i\\ i\neq j}}\nabla'\nabla'\frac{1}{r^i}-n\int_{V'}\nabla'\nabla'\frac{1}{r^i}dV\Big\} + \sum_{k=2}^{\infty}\frac{\mathcal{M}_k}{k!}\sum_{\substack{i\\ i\neq j}}\overset{(1)}{\nabla'}\overset{(2)}{\nabla'}\dots\overset{(k+1)}{\nabla'}\frac{1}{r^i}\Big], \tag{4.1}$$

where $\underset{\sim}{S}_0$ is given by (3.22), and as before, the sum is over the spheres surrounding the reference sphere and contained in the macroscopic volume V'.

We can obtain an approximate expression for $\underset{\sim}{S}$ from equation (4.1) by neglecting the contributions from the second and higher order multipoles associated with the surrounding spheres, in which case (4.1) becomes

$$\underset{\sim}{S}=\frac{(\alpha-1)}{(\alpha+2)}\phi\underset{\sim}{S}+\underset{\sim}{S}_0+\frac{(\alpha-1)}{(\alpha+2)}a^3\underset{\sim}{S}\cdot\Big\{\sum_{\substack{i\\ i\neq j}}\nabla'\nabla'\frac{1}{r^i}-n\int_{V'}\nabla'\nabla'\frac{1}{r}dV\Big\}. \tag{4.2}$$

As mentioned in the previous section, the term

$$\Big\{\sum_{\substack{i\\ i\neq j}}\nabla'\nabla'\frac{1}{r^i}-n\int_{V'}\nabla'\nabla'\frac{1}{r}dV\Big\}$$

converges absolutely as the volume V' becomes infinite. For a given type of lattice, this term is proportional to $1/d^3$, where d is the centre-to-centre distance between nearest neighbours in the array. Thus if

$$\left(\frac{\alpha-1}{\alpha+2}\right)\frac{a^3}{d^3}\ll 1,$$

the expression (4.2) for the particle dipole strength becomes, approximately

$$\underset{\sim}{S}=\underset{\sim}{S}_0\Big\{1+\frac{(\alpha-1)}{(\alpha+2)}\phi\Big\}+\frac{(\alpha-1)}{(\alpha+2)}a^3\underset{\sim}{S}_0\cdot\Big[\sum_{\substack{i\\ i\neq j}}\nabla'\nabla'\frac{1}{r^i}-n\int_{V'}\nabla'\nabla'\frac{1}{r}dV\Big] \tag{4.3}$$

For an "orthotropic" lattice (that is, one which is invariant under $\pi/2$ rotations), the square bracketed term in (4.3) is zero. To show this, we choose V to be a large sphere centred on $\underset{\sim}{x}_0$. In this case, the second order tensors

$$\sum_{\substack{i\\ i\neq j}}\nabla'\nabla'\frac{1}{r^i} \quad\text{and}\quad \int\nabla'\nabla'\frac{1}{r}dV$$

are isotropic, and since

$$\nabla^2 \frac{1}{r} = 0 \qquad (r \neq 0)$$

these tensors are identically zero. Thus the dipole strength of a sphere in an orthotropic array is found from (4.3) to be

$$\underset{\sim}{S} \approx \underset{\sim}{S}_0 \left\{ 1 + \frac{(\alpha-1)}{(\alpha+2)} \phi \right\} . \tag{4.4}$$

Combining this result with the expression (1.2.5) for the bulk flux density, using the definition (1.2.2) of k^* and replacing $\underset{\sim}{S}_0$ by the expression (3.22) we find that the conductivity of an isotropic array is given by

$$\frac{k^*}{k} = 1 + 3\phi \frac{(\alpha-1)}{(\alpha+2)} \left(1 + \frac{(\alpha-1)}{(\alpha+2)} \phi \right) \tag{4.5}$$

correct to $O(\phi^2)$. For the remainder of this section we shall only be concerned with orthotropic arrays.

To obtain a more accurate estimate of $\underset{\sim}{S}$, we must include the contributions to equation (4.1) from the second and higher order multipoles. From symmetry considerations, we find

$$\mathcal{M}_k = 0$$

if k is even, and to find a more accurate value for $\underset{\sim}{S}$, we can approximate the surrounding spheres by a dipole and a third order multipole. The equation (4.1) thenbecomes

$$\underset{\sim}{S} \left(1 - \phi \frac{(\alpha-1)}{(\alpha+2)} \right) = \underset{\sim}{S}_0 + \frac{(\alpha-1)}{(\alpha+2)} \frac{a^3 \mathcal{M}_3}{6} \sum_{\substack{i \\ i \neq j}} \nabla \nabla' \nabla' \nabla' \frac{1}{r_i} , \tag{4.6}$$

where we have used the fact that the term in curly bracket in (4.1) is zero for an isotropic array.

To evaluate $\underset{\sim}{S}$ from (4.6) we require an expression for the tensor $\mathcal{M}_3$. This is obtained in appendix A4 by the same type of method as that used for the derivation of the expression (3.21) for the dipole strength. The required expression is:

$$\mathcal{M}_3^j = -\frac{a^7(\alpha-1)}{15(\alpha+4/3)}\left\{\sum_{\substack{i \\ i\neq j}}\left[\underset{\sim}{S}^i\cdot\nabla\nabla\nabla\nabla\frac{1}{r^i} + \sum_{k=2}^{\infty}\frac{1}{k!}\mathcal{M}_k^i\overset{(1)}{\nabla'}\overset{(2)}{\nabla'}\ldots\overset{(k+3)}{\nabla'}\frac{1}{r^i}\right]\right\}. \tag{4.7}$$

There are no convergence problems here, since the contribution from far off dipoles is $O(1/r^5)$, and there is also no dipole field term.

The expression (4.7) is valid for any statistically homogeneous suspension of spherical particles, and for a regular array, the expression becomes

$$\mathcal{M}_3 = -\frac{a^7(\alpha-1)}{15(\alpha+4/3)}\left\{\underset{\sim}{S}\cdot\sum_{\substack{i \\ i\neq j}}\nabla\nabla\nabla'\nabla'\frac{1}{r^i} + \sum_{k=2}^{\infty}\frac{\mathcal{M}_k}{k!}\sum_{\substack{i \\ i\neq j}}\overset{(1)}{\nabla'}\overset{(2)}{\nabla'}\ldots\overset{(k+1)}{\nabla'}\frac{1}{r^i}\right\}. \tag{4.8}$$

To leading order we may neglect the contributions from the second and higher order multipoles to (4.8), and the first approximation to $\mathcal{M}_3$ is given by

$$\mathcal{M}_3 = -\frac{a^7(\alpha-1)}{15(\alpha+4/3)}\underset{\sim}{S}\cdot\sum_{\substack{i \\ i\neq j}}\nabla'\nabla'\nabla'\nabla'\frac{1}{r^i}\ .$$

Substituting this expression for $\mathcal{M}_3$ in (4.6) we get

$$\underset{\sim}{S} = \underset{\sim}{S}_o + \frac{(\alpha-1)}{(\alpha+2)}\phi\underset{\sim}{S} - \frac{a^{10}(\alpha-1)^2}{90(\alpha+2)(\alpha+4/3)}\underset{\sim}{S}\cdot\left[\left(\sum_{i\neq j}\nabla'\nabla'\nabla'\nabla'\frac{1}{r^i}\right):\left(\sum_{i\neq j}\nabla'\nabla'\nabla'\nabla'\frac{1}{r^i}\right)\right].$$

Expanding $\underset{\sim}{S}$ in a power series in $(^a/d)$, and equating the coefficients of like powers, we find

$$\underset{\sim}{S} = \left(1 + \frac{(\alpha-1)}{(\alpha+2)}\phi + \left(\frac{\alpha-1}{\alpha+2}\right)^2\phi^2 + \left(\frac{\alpha-1}{\alpha+2}\right)^3\phi^3\right)\underset{\sim}{S}_o + \frac{(\alpha-1)^2}{90(\alpha+2)(\alpha+4/3)}\left(\frac{a}{d}\right)^{10}\underset{\sim}{S}_o\cdot\underset{\approx}{C}\ , \tag{4.9}$$

where

$$\underset{\approx}{C} = d^{10}\left(\sum_{\substack{i \\ i\neq j}}\nabla'\nabla'\nabla'\nabla'\frac{1}{r^i} : \sum_{\substack{i \\ i\neq j}}\nabla'\nabla'\nabla'\nabla'\frac{1}{r^i}\right), \tag{4.10}$$

is determined by the type of lattice.

From (4.9) it can be seen that, to $O((a/d)^9)$, the dipole strength is only a function of volume fraction and thus the effect of lattice type on conductivity only becomes significant at fairly high volume fractions.

To evaluate the tensor $\underset{\approx}{C}$, we use the fact that the array is orthogonally invariant, to obtain

$$d^5 \sum_{\substack{i \\ i \neq j}} \nabla'_m \nabla'_j \nabla'_k \nabla'_\ell \frac{1}{r_i} = \lambda(\delta_{mj}\delta_{k\ell} + \delta_{mk}\delta_{j\ell} + \delta_{m\ell}\delta_{jk}) + \beta(v_{ijk\ell}) \quad , \qquad (4.11)$$

where $v_{ijk\ell}$ = 1 if i = j = k = ℓ, and is zero otherwise. The constants λ and β are related by

$$\sum_{i \neq j} \frac{\partial}{\partial x_k}\frac{\partial}{\partial x_\ell} \nabla^2 \frac{1}{r_i} = \delta_{k\ell}(5\lambda + \beta) = 0 ,$$

i.e. $5\lambda + \beta = 0$.

Using this relation to eliminate λ from (4.11) and substituting the resulting equation in the expression (4.10) for $\underset{\approx}{C}$ we get

$$\underset{\approx}{C} = \frac{2}{5}\beta^2 \underset{\approx}{I} ,$$

and thus (4.9) becomes

$$\underset{\sim}{S} = \left(1 + \left(\frac{\alpha-1}{\alpha+2}\right)\phi + \left(\frac{\alpha-1}{\alpha+2}\right)^2\phi^2 + \left(\frac{\alpha-1}{\alpha+2}\right)^3\phi^3\right)\underset{\sim}{S}_0 + \frac{(\alpha-1)^2\ \beta^2\ \underset{\sim}{S}_0}{(\alpha+2)(\alpha+4/3)225}\left(\frac{a}{d}\right)^{10}. \quad (4.12)$$

For a cubic array, β can be related to the constant S_4 evaluated by Rayleigh (1892 pp 497), and we find

$$\beta (= 60 S_4) = 186 \cdot 6$$

The volume fraction of spheres in a cubic array is given by

$$\phi = \frac{4}{3}\pi\frac{a^3}{d^3}$$

and substituting this result in (4.12) and replacing $\underset{\sim}{S}_0$ by the formula (3.22), we obtain

$$\underset{\sim}{S} = \frac{4\pi a^3(\alpha-1)}{(\alpha+2)}k\left\{1 + \left(\frac{\alpha-1}{\alpha+2}\right)\phi + \left(\frac{\alpha-1}{\alpha+2}\right)^2\phi^2 + \left(\frac{\alpha-1}{\alpha+2}\right)^3\phi^3 + \frac{1 \cdot 3\,(\alpha-1)^2\,\phi^{10/3}}{(\alpha+2)(\alpha+4/3)}\right\}\langle\nabla T\rangle. \quad (4.13)$$

Thus from (1.2.2) and (1.2.5) we find that the conductivity of a cubic array is given by

$$\frac{k^*}{k} = 1 + 3\phi\frac{(\alpha-1)}{(\alpha+2)}\left\{1 + \left(\frac{\alpha-1}{\alpha+2}\right)\phi + \left(\frac{\alpha-1}{\alpha+2}\right)^2\phi^2 + \left(\frac{\alpha-1}{\alpha+2}\right)^3\phi^3 + \frac{1.3(\alpha-1)^2\phi^{10/3}}{(\alpha+2)(\alpha+4/3)}\right\}. \qquad (4.14)$$

This is identical to Rayleigh's[+] expression for the conductivity of a cubic array. It appears that in estimating the non-convergent sum for $\underset{\approx}{S}$, Rayleigh chose a value which gave the correct expression for k^*.

To show why Rayleigh obtained the correct result, we must compare his expression for the dipole strength with the expression (4.1). In our notation, Rayleigh's expression is[++]

$$\underset{\sim}{S} = \underset{\sim}{S}_0 + \frac{(\alpha-1)}{(\alpha+2)}a^3\left[\underset{\sim}{S}\cdot\sum_{\substack{i \\ i\neq j}}\nabla'\nabla'\frac{1}{r^i} + \sum_{k=2}^{\infty}\frac{m_k}{k!}\sum_{\substack{i \\ i\neq j}}\overset{(1)}{\nabla'}\overset{(2)}{\nabla'}\ldots\overset{(k+1)}{\nabla'}\frac{1}{r^i}\right], \qquad (4.15)$$

and on comparing this with (4.1) we see that the dipole field term and the term $\phi\frac{(\alpha-1)}{(\alpha+2)}\underset{\sim}{S}$ are both absent.

The square bracketed term in (4.15) is non-absolutely convergent and unless the order of summation is specified the expression (4.15) is meaningless. Without justification, Rayleigh summed the terms in (4.15) in the following way: he first calculated the sum over the spheres contained in an infinitely long cylinder of square cross section. The axis of the cylinder was chosen to coincide with one of the axes of the lattice and in addition $\langle\nabla T\rangle$ was taken to be parallel to this axis. By letting the cross section of the cylinder become infinite, Rayleigh obtained a value for the square bracketed term in (4.15).

With the aid of (4.1) we can now see why this particular order of summation led to the correct result for $\underset{\sim}{S}$. We let the volume V' in (4.1) denote the volume of the cylinder described above. On applying the divergence theorem to the dipole field term in (4.1) we get

---

[+] Rayleigh made some numerical errors in deriving the expression for k*. These errors have been corrected by Bertaux et al (1975) and their result is identical to (4.14).

[++] The term B_1 in Rayleigh's paper is $|\underset{\sim}{S}|/4\pi k$. If we eliminate A_1 from equation (62) of that paper with the aid of equation (52), we obtain the result quoted here.

$$\underset{\sim}{S} \cdot \int_{V'} \nabla' \nabla' \frac{1}{r} dV = -|\underset{\sim}{S}| \int_{\Gamma_b} \frac{\partial}{\partial x}\left(\frac{1}{r}\right) \hat{n}\, dA - \underset{\sim}{S} \cdot \int_{\Gamma_\epsilon} \nabla'\left(\frac{1}{r}\right) \hat{n}\, dA, \tag{4.16}$$

where x denotes the component of $\underset{\sim}{r}$ in the direction of $\underset{\sim}{S}$, Γ_b denotes the surface of the cylinder, and as usual Γ_ϵ is a small sphere centred on the point r = o. If the lattice is orthotropic $\underset{\sim}{S}$ is parallel to <∇T> and as <∇T> is parallel to the cylinder axis it can be seen from symmetry considerations that the integral over Γ_b in (4.16) is zero. Evaluating the integral over Γ_ϵ in (4.16) we get

$$\underset{\sim}{S} \cdot \int_{V'} \nabla' \nabla' \frac{1}{r} dV = \frac{4\pi}{3} \underset{\sim}{S}$$

and on substituting this result in (4.1) we obtain Rayleighs expression (4.15) for the dipole strength. Thus by summing the terms in a special way, Rayleigh was able to obtain the correct value for the dipole strength from an improper expression.

The expressions for the conductivity of other types of isotropic arrays only differ from (4.14) in the coefficient of the $\phi^{13/3}$ term. Using Rayleigh's method, Bertraux et al (1975) have studied conduction through other types of isotropic arrays and their expressions for k* can be obtained by replacing the term 1.3 in equation (4.14) by:

.132 in the case of a body centred cubic array, and by .078 for a face centred cubic array

The methods for determining the other transport properties of a regular array of spheres immersed in a matrix are similar to that used for the conduction problem, and we shall now outline the general procedure for obtaining any of the effective transport properties of such a material.

To determine the particle dipole strength[+] S to a given accuracy, it is necessary to obtain a set of equations which relate the multipoles $S, \mathcal{M}_1, \ldots, \mathcal{M}_N$ of the reference sphere to the dipole and higher order

---

[+] As in §4.1, S here denotes either a vector or a tensor.

multipoles of the surrounding spheres. Then by expanding each of the multipoles in a power series in $(^a/d)^n$ and equating the coefficients of like powers in the expressions for $S, \mathcal{M}_1, \ldots, \mathcal{M}_N$, we get an approximate formula for S. The number of terms in this series for S increases with N, the number of multipole equations.

In the following section we will show how we can use this method to obtain an approximate expression for the effective modulus of compression of an elastic suspension.

4.5 The Effective Modulus of Compression of a Regular orthotropic array of Rigid Spheres embedded in an Elastic Matrix

The material under consideration consists of rigid spheres in a regular orthotropic array, embedded in elastic matrix.

The aim is to derive an expression for the effective modulus of compression K* of this material, correct to $O(\phi^2)$, where K* is defined by

$$K^* = \frac{\langle \sigma_{ii} \rangle}{3\langle e_{ii} \rangle} . \tag{5.1}$$

With the aid of the expression (1.2.8) for the bulk stress and the constitutive equation (1.2) for elastic material we can write (5.1) as

$$\begin{aligned} K^* &= \frac{1}{3}\frac{E}{(1+\nu)}\left(1 + \frac{3\nu}{1-2\nu}\right) + \frac{n}{3}\frac{S_{ii}}{\langle e_{ii} \rangle} \\ &= K + nS_{ii}/3\langle e_{ii} \rangle, \end{aligned} \tag{5.2}$$

where the dipole strength $\underset{\sim}{S}$ is the same for each sphere in the array, and K is the modulus of compression of the matrix. As usual, the Youngs modulus and Poissons ratio of the matrix are denoted by E and ν respectively.

We assume that the material is subjected to a uniform bulk compression, given by

$$\langle e_{ij} \rangle = -\varepsilon \delta_{ij} \tag{5.3}$$

and therefore $\underset{\approx}{S}$ has the form

$$S_{ij} = -\mathcal{S}\,\delta_{ij} \tag{5.4}$$

for an orthotropic array. Substituting (5.3) and (5.4) in (5.2) gives

$$K^{*} = K + \frac{n\mathcal{S}}{3\mathcal{E}} \;. \tag{5.5}$$

The coefficient of $\mathcal{S}$ in this expression is $O(\phi)$, and to find K^{*} to $O(\phi)^2$ we therefore require an expression for $\mathcal{S}$ to $O(\phi)$.

The expression relating the dipole strength of a sphere in a regular array to the dipole and higher order multipoles of the surrounding spheres can be found from the equation

$$S_{ij} = \eta_1\Big(e_E(\underset{\sim}{x}_0)_{ij} + \frac{a^2}{10}\nabla^2 e_E(\underset{\sim}{x}_0)_{ij} + \frac{\delta_{ij}}{5(1-2\nu)} e_E(\underset{\sim}{x}_0)_{mm}\Big), \qquad \text{(3.23) repeated}$$

where the constant η_1 is given by the expression (3.24). Taking the trace of the above expression, and using (5.4), we get

$$-\mathcal{S} = \frac{\eta_1}{3}\Big(e_E(\underset{\sim}{x}_0)_{ii}\big(1 + \frac{3}{5(1-2\nu)}\big) + \frac{a^2}{10}\nabla^2 e_E(\underset{\sim}{x}_0)_{ii}\Big) . \tag{5.6}$$

The external strain field is given by equation (3.32), and as we only require $\mathcal{S}$ to $O(\phi)$, we can neglect the contribution from the second and higher order multipoles to that equation, which then becomes

$$\begin{aligned} e_E(\underset{\sim}{x}_0)_{pq} = {} & \langle e_{pq}\rangle + \eta_2 S_{pq} + \eta_3 \delta_{pq} S_{mm} \\ & + S_{mn}\sum_{\substack{i\\ i\neq j}} P(\underset{\sim}{x}_i - \underset{\sim}{x}_0)_{pqmn} - S_{mn}\int_{V'} P(\underset{\sim}{x} - \underset{\sim}{x}_0)_{pqmn}\, dV(\underset{\sim}{x}) \end{aligned}$$

where η_2 and η_3 are given by (3.26) and P_{pqmn} is defined by (3.27). Taking the trace of this expression and using (5.3) and (5.4), we obtain

$$e_E(\underset{\sim}{x}_0)_{qq} = -3\mathcal{E} - 3(\eta_2 + 3\eta_3)\mathcal{S} - \mathcal{S}\sum_{i\neq j} P^{i}_{qqmm} + \mathcal{S}\int P_{qqmm}\, dV \tag{5.7}$$

From the definitions (3.27) for P_{pqmn} and (1.6) for G_{mn} we find

$$P_{qqmm} = 0 , \tag{5.8}$$

and (5.7) becomes

$$e_E(\underset{\approx}{x}_0)_{qq} = -3\mathcal{E} - 3(\eta_2 + 3\eta_3)\mathcal{S} . \tag{5.9}$$

Similarly, taking the trace of the expression (3.33) for $\nabla^2 \underset{\approx}{e}_E$ and neglecting the second and higher order multipoles of the surrounding spheres, we get

$$\nabla^2 e_E(\underset{\approx}{x}_0)_{qq} = -\sum_{i \neq j} \nabla^2 P^i_{qqmm} = 0 ,$$

where we have used the identity (5.8). Combining this result with the expressions (5.9) and (5.6) for $(\underset{\approx}{e}_E)_{qq}$ and $\mathcal{S}$, we obtain

$$\mathcal{S} = \eta_1 \left[\mathcal{E}\left(1 + \frac{3}{5(1-2\nu)}\right) + \mathcal{S}(\eta_2 + 3\eta_3)\left(1 + \frac{3}{5(1-2\nu)}\right)\right] , \tag{5.10}$$

and using the expression (3.24) and (3.26) for η_1, η_2 and η_3 this becomes

$$\mathcal{S} = \frac{10\pi a^3 E(1-\nu)}{(4-5\nu)(1+\nu)}\left(1 + \frac{3}{5(1-2\nu)}\right)\mathcal{E} + \frac{\phi(19-20\nu)\mathcal{S}}{(10-20\nu)} . \tag{5.11}$$

Neglecting $O(\phi^2)$ terms, we get

$$\mathcal{S} = \frac{4\pi a^3 E(1-\nu)}{(1-2\nu)(1+\nu)}\left(1 + \frac{\phi(19-20\nu)}{(10-20\nu)}\right)\mathcal{E} ,$$

and from the expression (5.5) for the effective modulus of compression, we obtain

$$K^* = K\left(1 + 3\phi\frac{(1-\nu)}{(1+\nu)}\left[1 + \phi\frac{(19-20\nu)}{(10-20\nu)}\right]\right) . \tag{5.12}$$

To obtain more terms in the series for K*, we require expressions for the higher order multipole strengths $\mathcal{M}_N$ of the reference sphere. Although we have not obtained such expressions, it can be seen from symmetry considerations, that

$$\mathcal{M}_2 = \underset{\approx}{0},$$

and by analogy with the expression (4.8) for the thermal multipole $\mathcal{M}_3$ we expect that the contribution from $\mathcal{M}_3$ to the expression (5.6) for $\mathcal{S}$ will be $O((^a/d)^{10})$. If this is so, then by expanding $\mathcal{S}$ in powers of $(^a/d)$ in (5.11) and equating the coefficients of like powers, we get

$$\mathcal{S} = 12\pi a^3 K\frac{(1-\nu)}{(1+\nu)}\left(1 + \sum_{m=1}^{3}\left(\frac{19-20\nu}{10-20\nu}\right)^m \phi^m + O\left(\frac{a}{d}\right)^{10}\right)\mathcal{E}.$$

From (5.5), we find that the corresponding expression for the effective modulus of compression is

$$K^* = K\left(1 + 3\phi\frac{(1-\nu)}{(1+\nu)}\left[1 + \sum_{m=1}^{3}\left(\frac{19-20\nu}{10-20\nu}\right)^m \phi^m\right] + O(\phi^{13/3})\right). \tag{5.13}$$

4.6 Conduction through a random array of spheres

In this section we shall describe a procedure for obtaining the effective transport properties of a statistically homogeneous suspension of spheres with random structure. As for the case of the regular array in § 4.4, we begin by illustrating the procedure for the conduction problem.

Our objective is an expression for the conductivity k*, correct to $O(\phi^2)$. From the expression (1.2.5) for the bulk flux density, it can be seen that to obtain the required formula for k*, we need an expression for the average dipoles strength $\langle \underset{\sim}{S} \rangle$ correct to $O(\phi)$. This in turn can be obtained from equation (3.21), which relates the dipole strength of a reference sphere to the multipoles of the surrounding spheres. Taking the average+ of (3.21), we get++

$$\langle \mathbf{S}\rangle\left(1-\frac{(\alpha-1)}{(\alpha+2)}\phi\right) = \mathbf{S}_0 + a^3\frac{(\alpha-1)}{(\alpha+2)}\Big[\int_{|\mathbf{r}|=2a}^{\infty}\{\langle \mathbf{S}(\mathbf{r}|0)\rangle p(\mathbf{r}|0) - n\langle \mathbf{S}\rangle\}\cdot\nabla\nabla\frac{1}{r}\,dV$$
$$+\sum_{k=2}^{\infty}\frac{1}{k!}\int_{|\mathbf{r}|=2a}^{\infty}\langle \mathcal{M}_k(\mathbf{r}|0)\rangle\overset{(1)}{\nabla}\overset{(2)}{\nabla}\cdots\overset{(k+1)}{\nabla}\frac{1}{r}\,p(\mathbf{r}|0)\,dV\Big], \qquad (6.1)$$

where $p(\mathbf{r}|0)dV$ is the probability that the centre of a particle lies in the volume dV surrounding $\mathbf{r}$, given that there is a particle at the origin o. The term $\langle \mathbf{S}(\mathbf{r}/o)\rangle$ denotes the average dipole strength of a sphere at $\mathbf{r}$, given that there is a sphere at the origin. If there is no long range order in the suspension,

$$p(\mathbf{r}|0)\to n \text{ and } \langle \mathbf{S}(\mathbf{r}|0)\rangle \to \langle \mathbf{S}\rangle \text{ as } |\mathbf{r}|\to\infty \quad ,$$

and the integral

$$\int_{|\mathbf{r}|=2a}^{\infty}\{\langle \mathbf{S}(\mathbf{r}|0)\rangle p(\mathbf{r}|0) - n\langle \mathbf{S}\rangle\}\cdot\nabla\nabla\frac{1}{r}\,dV$$

converges.

We can write the expression (6.1) in a more convenient form with the aid of the relation

$$\langle \mathbf{S}(0|\mathbf{r})\rangle - \mathbf{S}_0 = a^3\frac{(\alpha-1)}{(\alpha+2)}\Big\{\langle \mathbf{S}(\mathbf{r}|0)\rangle\cdot\nabla\nabla\frac{1}{r} + \sum_{k=2}^{\infty}\frac{\langle \mathcal{M}_k(\mathbf{r}|0)\rangle\overset{(1)}{\nabla}\cdots\overset{(k+1)}{\nabla}\frac{1}{r}}{k!}\Big\} + O(\phi) \quad , \qquad (6.2)$$

+ This may be either an ensemble average, or an average over a large number of particles in a single realization.

++ The integral

$$\int_{v''}\langle \mathbf{S}\rangle\cdot\nabla\nabla\frac{1}{r}\,dV = 0$$

if v" is the volume between a pair of concentric spheres, centred on the origin, and therefore we are free to take the lower limit of integration to be $|\mathbf{r}| = 2a$ in (6.I).

obtained by taking the average of (3.21) over all configurations for which there is a sphere at O and one at $\underset{\sim}{r}$. Substituting (6.2) in (6.1) we get

$$\langle \underset{\sim}{S}\rangle\left(1-\frac{(\alpha-1)}{(\alpha+2)}\phi\right) = \underset{\sim}{S}_o + \int_{|\underset{\sim}{r}|=2a}^{\infty}\left[\left\{\langle \underset{\sim}{S}(o|\underset{\sim}{r})\rangle - \underset{\sim}{S}_o\right\}p(\underset{\sim}{r}|o) - \frac{na^3(\alpha-1)}{(\alpha+2)}\langle \underset{\sim}{S}\rangle\cdot\nabla\nabla\frac{1}{r}\right]dV. \quad (6.3)$$

To evaluate the integral, we require an expression for $\langle \underset{\sim}{s}(o/\underset{\sim}{r})\rangle$.

If we can neglect terms of $O(\phi)$, then $\langle \underset{\sim}{S}(o/\underset{\sim}{r})\rangle$ is approximately equal to the dipole strength $\underset{\sim}{S}(\underset{\sim}{o}/\underset{\sim}{r})$ of one of a pair of spheres with separation vector $\underset{\sim}{r}$, alone in an infinite matrix with the far-field boundary condition

$$T \rightarrow \langle \nabla T\rangle\cdot\underset{\sim}{x}$$

at points far from the sphere pair. To show this, we note that $\underset{\sim}{S}(\underset{\sim}{o}/\underset{\sim}{r})$ is given by

$$\underset{\sim}{S}(o|\underset{\sim}{r}) - \underset{\sim}{S}_o = \frac{a^3(\alpha-1)}{(\alpha+2)}\left\{\underset{\sim}{S}(\underset{\sim}{r}|o)\cdot\nabla\nabla\frac{1}{r} + \sum_{k=2}^{\infty}\frac{\mathcal{M}_k(\underset{\sim}{r}|o)}{k!}\overset{(1)}{\nabla}\cdots\overset{(k+1)}{\nabla}\frac{1}{r}\right\}, \quad (6.4)$$

where $\mathcal{M}_i(\underset{\sim}{r}|o)$ denotes the ith multipole strength of the sphere at $\underset{\sim}{r}$. This expression can be obtained in a straightforward manner from the Faxen type formula (3.9) for $\underset{\sim}{S}$. If we neglect the $O(\phi)$ term in (6.2) we see that this expression has the same form as the expression (6.4) for $\underset{\sim}{S}(o/\underset{\sim}{r})$. Similarly, we could formulate expressions for the higher order multipole strengths and in each case the expressions for $\langle\mathcal{M}_i(o|\underset{\sim}{r})\rangle$ and $\mathcal{M}_i(o|\underset{\sim}{r})$ would have the same form. Therefore, neglecting terms of $O(\phi)$, we get

$$\left.\begin{aligned}\langle \underset{\sim}{S}(o|\underset{\sim}{r})\rangle &= \underset{\sim}{S}(o|\underset{\sim}{r}),\\ &\vdots\\ \langle\mathcal{M}_i(o|\underset{\sim}{r})\rangle &= \mathcal{M}_i(\underset{\sim}{o}|\underset{\sim}{r}),\end{aligned}\right\} \quad (6.5)$$

and the expression (6.3) for $\langle \underset{\sim}{S} \rangle$ becomes

$$\langle \underset{\sim}{S} \rangle = \underset{\sim}{S}_0\left(1 + \phi\frac{(\alpha-1)}{(\alpha+2)}\right) + \int_{|\underset{\sim}{r}|=2a}^{\infty} [\{\underset{\sim}{S}(0|\underset{\sim}{r}) - \underset{\sim}{S}_0\}p(\underset{\sim}{r}|0) - a^3\frac{(\alpha-1)}{(\alpha+2)}n\ \underset{\sim}{S}_0 \cdot \nabla\nabla\frac{1}{r}]dV. \qquad (6.6)$$

The average dipole strength $\langle \underset{\sim}{S} \rangle$ can therefore be evaluated from solutions of the two-sphere problem.

From the expressions (1.2.5) and (3.22) for $\langle \underset{\sim}{F} \rangle$ and $\underset{\sim}{S}_0$, we find from (6.6) that the bulk flux density is given by

$$\begin{aligned} \langle \underset{\sim}{F} \rangle = &-k\langle \nabla T \rangle - \frac{3\phi k(\alpha-1)}{\alpha+2}\langle \nabla T \rangle\left(1 + \phi\frac{(\alpha-1)}{\alpha+2}\right) \\ &+ n\int_{|\underset{\sim}{r}|=2a}^{\infty} [\{\underset{\sim}{S}(0|\underset{\sim}{r}) - \underset{\sim}{S}_0\}p(\underset{\sim}{r}|0) - na^3\frac{(\alpha-1)}{\alpha+2}\underset{\sim}{S}_0 \cdot \nabla\nabla\frac{1}{r}]dV, \end{aligned} \qquad (6.7)$$

We can write this expression in the same form as Jeffrey's (1973) result (equation (3.13) in that paper), by noting that the temperature gradient at a point $\underset{\sim}{r}$ due to a single sphere at o in an infinite matrix is given by

$$\nabla T(\underset{\sim}{r}|0) = \langle \nabla T \rangle + \frac{\underset{\sim}{S}_0}{4\pi k} \cdot \nabla\nabla\frac{1}{r} .$$

Combining this result with (6.7) we get

$$\begin{aligned} \langle \underset{\sim}{F} \rangle = &-k\langle \nabla T \rangle - \frac{3\phi k(\alpha-1)}{\alpha+2}\langle \nabla T \rangle\left(1 + \phi\frac{(\alpha-1)}{\alpha+2}\right) \\ &+ n\int_{|\underset{\sim}{r}|=2a}^{\infty} [\{\underset{\sim}{S}(0|\underset{\sim}{r}) - \underset{\sim}{S}_0\}p(\underset{\sim}{r}|0) - 4\pi k n\frac{a^3(\alpha-1)}{\alpha+2}\{\nabla T(\underset{\sim}{r}|0) - \langle \nabla T \rangle\}]dV, \end{aligned}$$

and this is the same as Jeffrey's expressions for $\langle \underset{\sim}{F} \rangle$.

Jeffrey obtained this result using the method which was described in §4.1. To apply that technique it is necessary to obtain a Renormalizing Quantity in order to overcome the problem of the divergence of the integral in the expression (1.1) for $\langle \underset{\sim}{S} \rangle$. The method presented here has the advantage that this Renormalizing Quantity arises naturally from the dipole field term in the expression (3.21) for $\underset{\sim}{S}$, and it is now clear that the convergence difficulties encountered in the past simply do not arise when the dipole field term is included.

4.7 The Effective Elastic Modulus of a Random Suspension of rigid Spheres

We now turn to the problem of determining the effective elastic modulii, correct to $O(\phi^2)$, of a statistically homogeneous random suspension of rigid spherical particles in an elastic matrix. We assume that the material is subjected to a uniform bulk strain $\langle \underset{\approx}{e} \rangle$. The Youngs modulus of the matrix is denoted by E and the Poisson's ratio by ν.

As in the previous section, we begin with an equation relating the dipole strength of a reference sphere to the multipoles associated with the surrounding spheres. This expression for the elastic dipole strength of a rigid sphere can be found from the expression

$$S^j_{pq} = \eta_1 \Big(e_E(\underset{\sim}{x}_0)_{pq} + \frac{a^2}{10} \nabla^2 e_E(\underset{\sim}{x}_0)_{pq} + \frac{\delta_{pq} e_E(\underset{\sim}{x}_0)_{mm}}{5(1-2\nu)} \Big), \qquad (3.23) \text{ repeated}$$

where the constant η_1 is given by (3.24). The external strain field $\underset{\approx}{e}_E(\underset{\sim}{x}_0)$ is the strain tensor which would be obtained at $\underset{\sim}{x}_0$ if the reference sphere could be replaced by matrix material while the stress on the surfaces of the surrounding spheres is held fixed. The quantity $\underset{\approx}{e}_E(\underset{\sim}{x}_0)$ is related to the multipoles of the surrounding particles by equation (3.31), and $\nabla^2 \underset{\approx}{e}_E$ is given by (3.33).

By substituting (3.31) and (3.33) in the expression (3.23) for $\underset{\sim}{S}^j$ we obtain the expression for $\underset{\sim}{S}^j$ in terms of the surrounding multipoles. However, as mentioned in § 4.3, it is preferable to work with the three equations separately.

Taking the average of (3.23), we get

$$\langle S_{pq}\rangle = \eta_1\left(\langle e_E(\underset{\sim}{x}_0)_{pq}\rangle + \frac{a^2}{10}\nabla^2\langle e_E(\underset{\sim}{x}_0)_{pq}\rangle + \frac{\delta_{pq}}{5(1-2\nu)}\langle e_E(\underset{\sim}{x}_0)_{mm}\rangle\right). \tag{7.1}$$

From the expression (3.32) for $\underset{\approx}{e}_E$, we obtain

$$\begin{aligned}\langle e_E(\underset{\sim}{x}_0)_{pq}\rangle = {} & \langle e_{pq}\rangle + \eta_2\langle S_{pq}\rangle + \eta_3\delta_{pq}\langle S_{mm}\rangle + \int_{|\underset{\sim}{r}|=2a}^{\infty}\Big[\Big\{P(\underset{\sim}{r})_{pqmn}\langle S(\underset{\sim}{x}_0+\underset{\sim}{r}|\underset{\sim}{x}_0)_{mn}\rangle \\ & + \sum_{k=2}^{\infty}\frac{1}{k!}\frac{\partial}{\partial x_b}\cdots\frac{\partial}{\partial x_c}P(\underset{\sim}{r})_{pqmn}\langle \mathcal{M}_k(\underset{\sim}{x}_0+\underset{\sim}{r}|\underset{\sim}{x}_0)_{mb\ldots cn}\rangle\Big\}p(\underset{\sim}{x}_0+\underset{\sim}{r}|\underset{\sim}{x}_0) \\ & - n\,P(\underset{\sim}{r})_{pqmn}\langle S_{mn}\rangle\Big]\,dV(\underset{\sim}{r}).\end{aligned} \tag{7.2}$$

We may simplify this equation with the aid of the approximate relations

$$\begin{aligned}\langle e_E(\underset{\sim}{x}_0|\underset{\sim}{x}_0+\underset{\sim}{r})_{pq}\rangle = {} & \langle e_{pq}\rangle + P(\underset{\sim}{r})_{pqmn}\langle S(\underset{\sim}{x}_0+\underset{\sim}{r}|\underset{\sim}{x}_0)\rangle \\ & + \sum_{k=2}^{\infty}\frac{1}{k!}\frac{\partial}{\partial x_b}\cdots\frac{\partial}{\partial x_c}P(\underset{\sim}{r})_{pqmn}\langle \mathcal{M}_k(\underset{\sim}{x}_0+\underset{\sim}{r}|\underset{\sim}{x}_0)_{mb\ldots cn}\rangle \\ & + O(\phi),\end{aligned} \tag{7.3}$$

obtained by averaging (3.32) over all configurations for which there is a sphere at $\underset{\sim}{x}_0$ and another at $\underset{\sim}{x}_0+\underset{\sim}{r}$. From (7.2) and (7.3) we get

$$\begin{aligned}\langle e_E(\underset{\sim}{x}_0)_{pq}\rangle = {} & \langle e_{pq}\rangle + \eta_2\langle S_{pq}\rangle + \delta_{pq}\eta_3\langle S_{mm}\rangle \\ & + \int_{|\underset{\sim}{r}|=2a}^{\infty}\Big[\big\{\langle e_E(\underset{\sim}{x}_0|\underset{\sim}{x}_0+\underset{\sim}{r})_{pq}\rangle - \langle e_{pq}\rangle\big\}p(\underset{\sim}{x}_0+\underset{\sim}{r}|\underset{\sim}{x}_0) - n\,P_{pqmn}(\underset{\sim}{r})\langle S_{mn}\rangle\Big]dV \\ & + O(\phi^2).\end{aligned} \tag{7.4}$$

Similarly, taking the average of (3.33), and using (7.3), we find

$$\langle \nabla^2 e_E(\underset{\sim}{x}_0)_{pq}\rangle = \int_{|\underset{\sim}{r}|=2a}^{\infty}\nabla^2\langle e_E(\underset{\sim}{x}_0|\underset{\sim}{x}_0+\underset{\sim}{r})\rangle_{pq}\,p(\underset{\sim}{x}_0+\underset{\sim}{r}|\underset{\sim}{x}_0)\,dV(\underset{\sim}{r}) + O(\phi^2). \tag{7.5}$$

Substituting the expressions (7.4) and (7.5) for $\langle \underset{\approx}{e}_E\rangle$ and $\langle\nabla^2\underset{\approx}{e}_E\rangle$ in (7.1), we obtain

$$\langle S_{pq}\rangle = S^{\circ}_{pq} + \eta_1\Big(\eta_2\langle S_{pq}\rangle + \delta_{pq}\langle S_{mm}\rangle\Big[\eta_3 + \frac{(\eta_2+3\eta_3)}{5(1-2\nu)}\Big]\Big)$$

$$+ \int\Big[\Big[\langle S(\underset{\sim}{x}_0|\underset{\sim}{x}_0+\underset{\sim}{r})\rangle_{pq} - S^{\circ}_{pq}\Big]p(\underset{\sim}{x}_0+\underset{\sim}{r}|\underset{\sim}{x}_0) - n\eta_1\Big(P(\underset{\sim}{r})_{pqmn}\langle S_{mn}\rangle + \frac{\delta_{pq}}{5(1-2\nu)}P(\underset{\sim}{r})_{kkmn}\langle S_{mn}\rangle\Big)\Big]dV(\underset{\sim}{r}), \tag{7.6}$$

where

$$S^{\circ}_{pq} = \eta_1\Big(\langle e_E\rangle_{pq} + \frac{\delta_{pq}\langle e_E\rangle_{mm}}{5(1-2\nu)}\Big), \tag{7.7}$$

is the average dipole strength of a particle in the limit as $\phi \to 0$.

As in §4.6, we can show that

$$\langle S_{pq}(\underset{\sim}{x}_0|\underset{\sim}{x}_0+\underset{\sim}{r})\rangle = S_{pq}(\underset{\sim}{x}_0|\underset{\sim}{x}_0+\underset{\sim}{r}) + O(\phi), \tag{7.8}$$

where $S_{pq}(\underset{\sim}{x}_0|\underset{\sim}{x}_0+\underset{\sim}{r})$ denotes the dipole strength of one of a pair of spheres, separated by $\underset{\sim}{r}$ and alone in an infinite matrix with an undisturbed uniform strain field $\langle \underset{\approx}{e}\rangle$. With the aid of (7.8) and the expressions (3.26) for η_2 and η_3, we find that equation (7.6) becomes

$$\langle S_{pq}\rangle = S^{\circ}_{pq} + \frac{\pi a^3 n}{3(4-5\nu)}\Big[S^{\circ}_{pq}(13-20\nu) + \delta_{pq}S^{\circ}_{mm}\frac{(58-80\nu)}{10-20\nu}$$

$$+ \int_{|\underset{\sim}{r}|=2a}^{\infty}\Big[\{S_{pq}(\underset{\sim}{x}_0|\underset{\sim}{x}_0+\underset{\sim}{r}) - S^{\circ}_{pq}\}p(\underset{\sim}{x}_0+\underset{\sim}{r}|\underset{\sim}{x}_0) - \frac{10\pi a^3 nE(1-\nu)}{(4-5\nu)(1+\nu)}\Big\{P(\underset{\sim}{r})_{pqmn}S^{\circ}_{mn} + \delta_{pq}P(\underset{\sim}{r})_{kkmn}S^{\circ}_{mn}\Big\}\Big]dV(\underset{\sim}{r}), \tag{7.9}$$

and thus $\langle \underset{\approx}{S}\rangle$ may be calculated with the aid of solutions to the two-sphere problem.

For each of the transport problems we have considered, the dipole field contributes a renormalizing term to the expression for $\underset{\approx}{S}^j$, and without this term the expression would not converge. We shall now show that if the bulk strain tensor has the form

$$\langle e_{ij} \rangle = -\mathcal{E}\,\delta_{ij} \quad , \tag{7.10}$$

corresponding to pure compression, neglect of the dipole field term leads to an expression for the effective modulus of compression K* which is convergent but is nevertheless incorrect.

We begin by deriving the correct expression for K*, based on the expression (7.9) for the average dipole strength. From equations (7.7) and (7.10) we see that the tensor $\underset{\approx}{S}^{o}$ has the isotropic form

$$S^{o}_{pq} = -\delta_{pq}\eta_1\left(1 + \frac{3}{5(1-2\nu)}\right)\mathcal{E} \quad . \tag{7.11}$$

Taking the trace of equation (7.9), we get

$$\langle S_{qq} \rangle = S^{o}_{qq}\left[1 + \frac{\phi(19-20\nu)}{(10-20\nu)}\right] + \int_{|\underset{\sim}{r}|=2a}^{\infty}\Big[\{S_{qq}(\underset{\sim}{x}_0|\underset{\sim}{x}_0+\underset{\sim}{r}) - S^{o}_{qq}\}p(\underset{\sim}{x}_0+\underset{\sim}{r}|\underset{\sim}{x}_0)$$
$$- \frac{10\pi a^3 n E(1-\nu)}{(4-5\nu)(1+\nu)}\{P(\underset{\sim}{r})_{qqmn}S^{o}_{mn}\}\left(1 + \frac{3}{10-20\nu}\right)\Big]\,dV(\underset{\sim}{r}). \tag{7.12}$$

Using the expression (7.11) for $\underset{\approx}{S}^{o}$, we obtain

$$P(\underset{\sim}{r})_{qqmn}S^{o}_{mn} = -\eta_1\left(1 + \frac{3}{(5-10\nu)}\right)\mathcal{E}\,P(\underset{\sim}{r})_{qqmm} = 0 ,$$

where we have used the identity (5.8). Combining this result with (7.12) and substituting the expression (7.11) for $\underset{\sim}{S}^{o}$, we find

$$\langle S_{qq} \rangle = -3\eta_1\mathcal{E}\left(1 + \frac{3}{5-10\nu}\right)\left[1 + \frac{\phi(19-20\nu)}{(10-20\nu)}\right]$$
$$+ \int_{|\underset{\sim}{r}|=2a}^{\infty}\Big[\{S_{qq}(\underset{\sim}{x}_0|\underset{\sim}{x}_0+\underset{\sim}{r}) - S^{o}_{qq}\}p(\underset{\sim}{x}_0+\underset{\sim}{r}|\underset{\sim}{x}_0)\,dV(\underset{\sim}{r}) . \tag{7.13}$$

Although the renormalizing factor has vanished, the integral in (7.13) converges, since

$$S_{qq}(\underset{\sim}{x}_0|\underset{\sim}{x}_0+\underset{\sim}{r}) - S^{\circ}_{qq} = \text{constant} \times P_{qqpp}(\underset{\sim}{r}) + O(\tfrac{1}{r^4})$$
$$= O(\tfrac{1}{r^4}) \quad \text{as } r \to \infty.$$

Substituting (7.13) in the expression (5.2) for K*, and replacing η_1 by the expression (3.24), we find that, correct to $O(\phi^2)$, the effective modulus of compression is given by

$$K^* = K + \frac{3\phi(1-\nu)}{(1+\nu)}K\left(1 + \phi\frac{(19-20\nu)}{(16-20\nu)}\right)$$
$$- \frac{n}{9e}\int_{r=2a}^{\infty}\{S_{qq}(\underset{\sim}{x}_0|\underset{\sim}{x}_0+\underset{\sim}{r}) - S^{\circ}_{qq}\}p(\underset{\sim}{x}_0+\underset{\sim}{r}|\underset{\sim}{x}_0)\,dV(\underset{\sim}{r}). \qquad (7.14)$$

If instead of using the expression (7.9) for <S> we use the incorrect equation

$$\langle S_{pq}\rangle = S^{\circ}_{pq} + \int[S_{pq}(\underset{\sim}{x}_0|\underset{\sim}{x}_0+\underset{\sim}{r}) - S^{\circ}_{pq}]p(\underset{\sim}{x}_0+\underset{\sim}{r}|\underset{\sim}{x}_0)\,dV(\underset{\sim}{r}), \qquad (7.15)$$

based on the assumption that only nearby pairs interact (c.f. equation (1.1)), then on taking the trace of this equation and using the expression (7.11) for S^{o}, we get

$$\langle S_{qq}\rangle = -3\eta_1 e\left(1 + \frac{3}{5-10\nu}\right) + \int[S_{qq}(\underset{\sim}{x}_0|\underset{\sim}{x}_0+\underset{\sim}{r}) - S^{\circ}_{qq}]p(\underset{\sim}{x}_0+\underset{\sim}{r}|\underset{\sim}{x}_0)\,dV(\underset{\sim}{r}). \quad (7.16)$$

Although the integral in (7.15) is non-absolutely convergent, the integral in (7.16) converges and it is tempting to assume that simply because the integral converges, the expression (7.16) for <Sqq> is correct. However, comparing (7.16) with the expression (7.13) (which takes into account the contribution from the dipole field) we see that the term

$$3\eta_1 e\phi\left(\frac{19-20\nu}{10-20\nu}\right)\left(1 + \frac{3}{5-10\nu}\right)$$

does not appear in (7.16). This illustrates a weakness in the renormalization technique described in §4.1 for, since it is designed to overcome the problem of a non convergent integral in the expression (1.1) for $\langle \underset{\sim}{S} \rangle$ it might lead to the belief that any reasonable looking convergent expression is correct.

CHAPTER FIVE

SHEAR INDUCED COAGULATION

5.1 Introduction

From thermodynamic arguments (Verwey and Overbeek (1948)) it can be shown that particles suspended in a liquid have an electric charge. The sign of the charge is determined by the composition of the particles and the solvent, and thus particles composed of the same material tend to repel one another. Opposed to this electrical repulsion is the Van der Waals force of attraction, and the stability of a colloid is determined by the balance between these two forces. This balance can be altered by the addition of electrolyte to the suspension, for the electrical forces diminish as the concentration of ions in the solvent is increased. Thus the particles in a suspension cease to repel each other, and may coagulate, if sufficient electrolyte is added.

The removal of colloidal impurities from a liquid is greatly facilitated by the coagulation of the particles, since the processes of filtration and sedimentation are more effective with larger particles. For most industrial processes, as for example in the purification of water (Harris, Kauffman and Krone (1965)) the liquid is stirred after the addition of the electrolyte. The stirring increases the rate at which particles coagulate, and it is this phenomenon, known as "shear induced coagulation"+, that forms the subject of this chapter.

In particular we shall study coagulation in a dilute suspension in steady shear flow. We assume that the particles are spheres of uniform radius a, and that the electrical forces between the particles are negligible. (The effect of electrical forces is taken up in the next chapter.)

In the initial stages of the process, most of the coagulation takes place between single particles which unite to form "doublets". Our aim is to derive an expression for the "Coagulation rate" $\mathscr{C}$, defined as the number of doublets formed in unit volume of suspension per unit time.

+ sometimes called "shear induced flocculation".

We shall begin by describing the motion of a pair of spheres in a shear flow in the absence of Brownian motion. The Brownian motion of sphere pairs is considered separately in §5.3, and in §5.4 we superpose the two effects to obtain a "pair conservation equation" of the Foker-Planck type. The coagulation rate may be obtained from a solution of this equation.

In §5.5 we discuss this solution for the case of "low" shear rates, and in §5.6 we turn to the problem of solving the pair conservation equation for "high" shear rates. The following four sections are concerned with this problem and finally, in §5.10 we combine the results for low and high shear rates to obtain a semi-quantitative-picture of the effect of shear flow on coagulation rate.

5.2 The Relative velocity of sphere-pairs in Shear flow

In the absence of Brownian motion, the velocity of a particle in the suspension is determined by the shear rate K, and by the positions of the surrounding particles. In a random dilute suspension, the number of particles which have a neighbour within a distance of several radii is much greater than the number which have two or more such neighbours and thus most of the pairs of spheres which coagulate move together on trajectories which are unaffected by the other particles in the suspension. To calculate the effect of shear rate on the coagulation rate we may therefore treat each pair of particles as being alone in an infinite liquid in shear flow.

In this section we shall derive an expression for the velocity of the centre of one member of a sphere pair, relative to the centre of the other. This quantity is termed "the relative velocity of the pair" and is denoted by $\underset{\sim}{V}(\underset{\sim}{r})$, where $\underset{\sim}{r}$ is the vector between the centres of the pair. We assume that the particles are so small that inertial forces may be neglected, and to determine the relative velocity of a pair we must therefore find the velocity $u(\underset{\sim}{x})$ and pressure $p(\underset{\sim}{x})$ which satisfy the Stokes equation

$$\nabla p = \mu \nabla^2 \underset{\sim}{u} \quad , \quad \nabla \cdot \underset{\sim}{u} = 0 \quad , \tag{2.1}$$

at each point in the liquid, where μ is the viscosity.

With a suitably chosen cartesian coordinate system, the outer boundary condition may be written as

$$\underset{\sim}{u}(\underset{\sim}{x}) \approx (-Kx_2, 0, 0) \tag{2.2}$$

at points $\underset{\sim}{x}$ which are a large distance from the sphere-pair. On the surface of the particles the no-slip condition must be satisfied. The relative velocity of the pair is then determined by the condition that there is a given force of attraction between the particles.

Taking advantage of the linearity of the Stokes equations and the boundary conditions, we write

$$\underset{\sim}{V} = \underset{\sim}{V}' + \underset{\sim}{V}'' \tag{2.3}$$

where $\underset{\sim}{V}'$ is the relative velocity of a pair of force-free spheres in an infinite liquid with the outer boundary condition (2.2), and $\underset{\sim}{V}''$ is the relative velocity due to the Van der Waals attraction between a pair of spheres in an infinite liquid which is at rest at points far from the particles.

From the work of Batchelor and Green (1972(a)) on the motion of force-free sphere pairs in a linear flow field we find

$$\underset{\sim}{V}'(\underset{\sim}{r}) = aK\underset{\sim}{U}(\underset{\sim}{r}/a) \tag{2.4}$$

where the components of the non-dimensional velocity $\underset{\sim}{U}$ are

$$\left.\begin{aligned} U_r &= (1 - A(r/a))\frac{r}{a}\sin^2\theta \sin\phi\cos\phi \ , \\ U_\theta &= (1 - B(r/a))\frac{r}{a}\sin\theta\cos\theta\sin\phi\cos\phi , \\ U_\phi &= -\frac{r}{a}\sin\theta\left\{\sin^2\phi + \tfrac{1}{2}B(r/a)(\cos^2\phi - \sin^2\phi)\right\} \end{aligned}\right\} \tag{2.5}$$

and the spherical polar coordinates (r, θ, ϕ) are illustrated in figure (5.1). The origin of the coordinate system is fixed at the centre of one of the spheres, and the line $\theta = 0$ is perpendicular to the plane of the shear flow. The functions A and B are illustrated in figure 2 of Batchelor and Green's (1972(a)) paper. If the spheres are nearly in contact, A and B are given by

$$\left.\begin{aligned} A(r/a) &= 1 - 4.077\frac{h}{a} + O\left(\left(\frac{h}{a}\right)^{3/2}\right) \\ B(r/a) &= .406 + O\left(1/\log\left(\frac{a}{h}\right)\right), \end{aligned}\right\} \tag{2.6}$$

where h is the gap distance, defined by

$$h = r - 2a \quad .$$

The relative velocity due to the Van der Waals attraction between a sphere pair in an infinite liquid which is otherwise at rest is given by

$$\underset{\sim}{V}''(\underset{\sim}{r}) = \frac{G(r/a)}{3\pi\mu a} F(r)\,\hat{r} \tag{2.7}$$

where $\hat{r} = \underset{\sim}{r}/r$, and $F(r)\hat{r}$ is the force acting between the spheres. The mobility function $G(^{r}/a)$ is shown in figure 3 of Batchelor's (1976) paper. We shall only require the form of G for nearly touching pairs, and from Batchelor and Green (1972(a)) this is given by

$$G(r/a) = \frac{2h}{a}\left(1 + O\left(\frac{h}{a}\log\left(\frac{a}{h}\right)\right)\right). \tag{2.8}$$

The Van der Waals force F acting between a pair of spheres may be written in the form (Verwey and Overbeek (1948))

$$F(r) = -\frac{H}{a} f(r/a) \tag{2.9}$$

where H is the Hamaker constant, and

$$f(s) = \frac{1}{6}\left\{\frac{4s}{(s^2-4)^2} + \frac{4}{s^3} - \frac{8}{s(s^2-4)}\right\}. \tag{2.10}$$

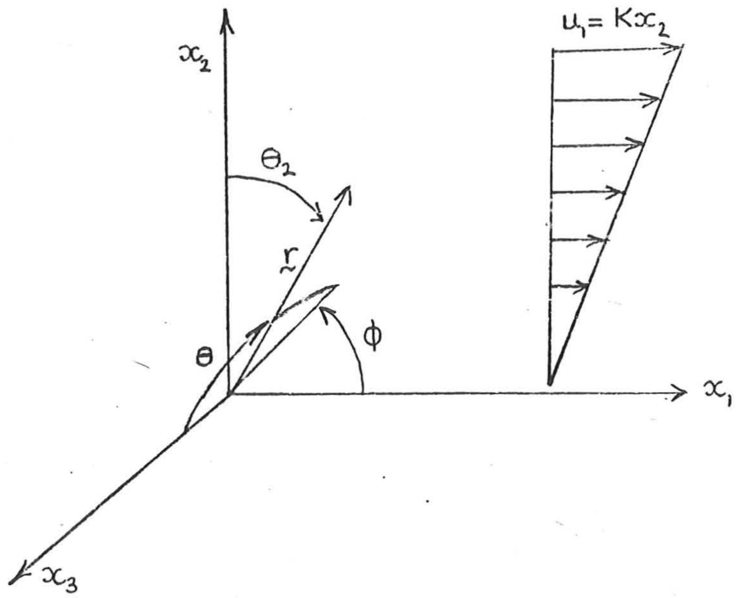

Figure 5.1 The cartesian and polar coordinate systems employed in this Chapter.

(This expression is only valid if the minimum distance between the surfaces of the two spheres is less than 10^{-6} cms. At larger separations the "Retardation Effect" (Verwey and Overbeek (1948)) becomes significant, and the Van der Waals force drops off at a more rapid rate with increasing r than that given by (2.10).) For the case of nearly touching spheres, (2.10) becomes, approximately

$$f(r/a) = \frac{1}{12}\left(\frac{a}{h}\right)^2 \left(1 + O\left(\frac{h}{a}\right)\right). \tag{2.11}$$

The value of the Hamaker constant is determined by the composition of the particles and the solvent, and generally lies in the range

$$10^{-15} < H < 10^{-12} \text{ ergs}$$

(see Ottewill (1973) for review).

Combining the expression (2.7) and (2.9) we obtain

$$\underset{\sim}{V}'' = \frac{-H}{3\pi\mu a^2} G f \hat{r} , \tag{2.12}$$

and using the asymptotic expressions for G and f we find that the Van der Waals attraction causes a pair of nearly touching spheres to move together with a relative velocity given by

$$\underset{\sim}{V}'' = \frac{-H}{18\pi\mu a h}\left(1 + O\left(\frac{h}{a}\log\left(\frac{a}{h}\right)\right)\right)\hat{r}. \tag{2.13}$$

From the expressions (2.4), (2.5) and (2.6) we find that the radial component of the relative velocity due to the shear flow is given by the asymptotic expression

$$V_r' = 8{\cdot}154\, K h \sin^2\theta \sin\phi \cos\phi \left(1 + O\left(\frac{h}{a}\right)\right). \tag{2.14}$$

This quantity decreases linearly with h and is dominated by the term V_r'' if h is sufficiently small. The ratio V_r'/V_r'' is found from (2.13) and (2.14) to be

$$\frac{V_r'}{V_r''} \approx 460\,\frac{\mu a h^2 K}{H}\sin^2\theta \sin\phi \cos\phi \,.$$

For given values of θ and ϕ, the separation h at which V_r'/V_r'' is of order one is proportional to $\left(\frac{H}{\mu a^3 K}\right)^{\frac{1}{2}} a$. Thus if the condition

$$\frac{\mu a^3 K}{H} \gg 1 \tag{2.15}$$

holds, the Van der Waals force only has a significant effect on the motion of nearly-touching sphere pairs (provided that $\sin^2\theta\ \sin\phi\cos\phi$ is of order unity). This observation enables us to simplify the problem of determining the coagulation rate at "high" shear rates, i.e. those shear rates for which the constraint (2.15) is valid. This matter will be discussed more fully in §5.6.

5.3 The Effect of Brownian motion

Each particle in a suspension is subjected to random thermal forces from the surrounding solvent molecules. The way in which a particle responds to an applied force is determined both by the magnitude of the force and by the position of the neighbouring particles, for as a particle moves it interacts hydrodynamically with its neighbours. In the previous section we showed that in a dilute suspension, most of the hydrodynamic interaction occurs between pairs of particles, and each of these pairs is hydrodynamically independent of the surrounding particles. Thus to find the effect of Brownian motion on coagulation we can treat each pair as being alone in an infinite liquid.

The fluctuating thermal forces are random quantities and we can only speak of their effect in a statistical sense, i.e. by considering the Brownian motion of an ensemble of sphere pairs. Such an ensemble is provided by the pairs in a dilute suspension, and in order to describe the effect of Brownian motion on these pairs, it is convenient to introduce the concept of a "Pair Space".

Each pair of spheres in a chosen unit volume of the suspension is represented by two points (x_1, x_2, x_3) and ($-x_1, -x_2, -x_3$) in pair space, where x_1, x_2 and x_3 are the cartesian components of the vector which passes from the centre of one member of the pair to the centre of the other. For the remainder of this chapter we shall use the cartesian axes shown in figure5.1. The points in pair space are obtained by placing the origin of these axes at the centre of each sphere in the unit volume in turn and noting the coordinates of every other sphere in the volume. If n denotes the number of particles in the unit volume, there are n(n-1) points in the pair space. We shall use the term "pair" to denote both the actual sphere pair and the points which correspond to that pair.

The points which correspond to coagulated pairs lie on a sphere of radius 2a, centred on the origin in pair space. This sphere will be referred to as the "central sphere". The number of points which move onto the central sphere in unit time is double the coagulation rate, since each pair of spheres is counted twice.

The density of points in pair space is denoted by $\rho(\underset{\sim}{x})$, and we shall refer to ρ as the "pair distribution function". In the absence of any long range order in the suspension, we have

$$\rho(\underset{\sim}{x}) \rightarrow n^2 \qquad (3.1)$$

as $|\underset{\sim}{x}| \rightarrow \infty$. In other words, the fact that there is a sphere at the origin does not affect the probability of their being another sphere in the unit volume about $\underset{\sim}{x}$, provided $|\underset{\sim}{x}|$ is sufficiently large.

If ρ is non uniform the Brownian motion of the particles leads to a diffusion of points in pair space, and this provides a mechanism for restoring ρ to a uniform value. The flux density vector associated with this diffusion of points in pair space is given by

$$\underset{\sim}{i}_B(\underset{\sim}{r}) = -\frac{kT}{3\pi\mu a}\underset{\approx}{D}'(\underset{\sim}{r}/a).\nabla\rho(\underset{\sim}{r}) \quad , \tag{3.2}$$

where

$$\underset{\approx}{D}'(\underset{\sim}{r}/a) = G(r/a)\hat{r}\hat{r} + H(r/a)(\underset{\approx}{I} - \hat{r}\hat{r}) \ . \tag{3.3}$$

This result is derived by Batchelor (1976), and the functions G and H are illustrated in figure (3) of that paper.

We may now combine the expression (3.2) for the flux due to Brownian motion with the expressions derived in the previous section for the relative velocity of a sphere pair, to obtain a differential equation for ρ . From the solution of this equation we can compute the coagulation rate.

Before proceeding to the derivation of this differential equation for ρ , there is a point which should be cleared up concerning the expression (3.2) for the flux of points in pair space. This result is based on the assumption that the pairs in a suspension form an ensemble of independent pairs. This is not quite correct, for each particle is paired with every other particle to obtain the points in pair space, and since each point does not correspond to a pair of different particles, these points cannot be regarded as an ensemble of independent pairs.

However, the points which lie within a spherical volume of radius r*, centred on the origin, do form an ensemble if

$$r^* \ll \text{average particle separation},$$

that is, if

$$r^* \ll a\phi^{-1/3} \ .$$

This is because the majority of points in this volume each correspond to a unique pair. Thus the expression (3.2) for the flux density vector is valid in this region. We shall assume that the length scale over which ρ is non uniform is << a $\phi^{-1/3}$, and therefore the differential equation for ρ , obtained with the aid of (3.2), gives a valid expression for the pair distribution function.

5.4 The Pair Conservation Equation

In the absence of Brownian motion, the points in pair space move with velocity $\underset{\sim}{V}' + \underset{\sim}{V}''$ where $\underset{\sim}{V}'$ is the velocity due to the shear flow and $\underset{\sim}{V}''$ is the velocity caused by the Van der Waals attraction. The flux density vector associated with this motion is given by

$$\underset{\sim}{i}_H = \rho(\underset{\sim}{V}' + \underset{\sim}{V}'') \tag{4.1}$$

where the subscript "H" stands for "hydrodynamic". It is customary to assume that the Brownian motion of the pairs is unaffected by either the shear flow or the Van der Waals force, and thus the total flux density vector is given by

$$\underset{\sim}{i}_T = \underset{\sim}{i}_H + \underset{\sim}{i}_B . \tag{4.2}$$

Taking the gradient of (4.2) and using the fact that points in pair space are conserved, we get

$$\frac{\partial \rho}{\partial t} = - \nabla \cdot (\underset{\sim}{i}_H + \underset{\sim}{i}_B) . \tag{4.3}$$

For the remainder of the chapter we shall assume that the system is in a "quasi-steady state", i.e.

$$\frac{\partial \rho}{\partial t} \approx 0 . \tag{4.4}$$

Although the number n of single spheres decreases with time, we assume that the time over which n changes appreciably is much longer than the time required to achieve steady state conditions.

Substituting the expressions (2.4), (2.12) and (4.1) for $\underset{\sim}{V}'$, $\underset{\sim}{V}''$ and $\underset{\sim}{i}_H$ in (4.3) and using the expression (3.2) for $\underset{\sim}{i}_B$, we obtain

$$0 = \nabla\cdot\left(\frac{kT}{3\pi\mu a}\,\underset{\approx}{D}'(\underset{\sim}{r}/a)\cdot\nabla\rho(\underset{\sim}{r}) - \rho(\underset{\sim}{r})\left[aK\underset{\sim}{U}(\underset{\sim}{r}/a) - \frac{H}{3\pi\mu a^2}G(r/a)f(r/a)\right]\right). \quad (4.5)$$

This equation, together with the outer boundary condition (3.1) determine ρ uniquely. Equation (4.5) is the "Pair Conservation Equation" referred to in the introduction.

We make use of the fact that both equation (4.5) and the boundary condition (3.1) are linear by introducing a non-dimensional function $\rho_0(\underset{\sim}{r})$ defined by

$$\rho_0(\underset{\sim}{r}) = \rho(\underset{\sim}{r})/n^2\,.$$

Substituting for ρ in (4.5) and transforming to the dimensionless coordinate system

$$x_i' = x_i/a$$

we obtain

$$0 = \nabla'\cdot\left(\frac{kT}{H}\,\underset{\approx}{D}'\cdot\nabla'\rho_0 - \frac{3\pi\mu a^3K}{H}\,\underset{\sim}{U}\rho_0 + Gf\rho_0\right) \qquad (4.6)$$

and the boundary condition (3.1) becomes

$$\rho_0(\underset{\sim}{r}) \longrightarrow 1 \quad \text{as} \quad |\underset{\sim}{r}| \longrightarrow \infty \qquad (4.7)$$

From (4.6) it can be seen that the function $\rho_0(\underset{\sim}{r})$ is determined by the non-dimensional parameters $\frac{kT}{H}$ and $\frac{\mu a^3 K}{H}$.

As mentioned in the previous sections the coagulation rate $\mathcal{C}$ is equal to half the number of points which move onto the central sphere in unit time, and since $\frac{\partial \rho}{\partial t} \approx 0$, we can calculate $\mathcal{C}$ from

$$\mathcal{C} = \frac{1}{2}\oint_{\mathcal{S}} \underset{\sim}{i}_T \cdot \hat{n}\, dA \ , \tag{4.8}$$

where $\mathcal{S}$ denotes a closed surface enveloping the central sphere, dA is an element of that surface and $\hat{n}$ denotes the unit normal directed into the volume enclosed by $\mathcal{S}$.

Replacing $\underset{\sim}{i}_T$ in (4.8) by the expression (4.2) and using (4.1), we get

$$\mathcal{C} = \frac{1}{2}\oint_{\mathcal{S}} (\underset{\sim}{i}_B + \rho(\underset{\sim}{V}' + \underset{\sim}{V}'')) \cdot \hat{n}\, dA \ , \tag{4.9}$$

and with the expressions (2.4), (2.12) and (3.2) for $\underset{\sim}{V}'$, $\underset{\sim}{V}''$ and $\underset{\sim}{i}_B$, (4.9) becomes

$$\frac{\mu \mathcal{C}}{n^2 H} = \frac{1}{2}\oint_{\mathcal{S}} \left(-\frac{kT}{3\pi H}\underset{\approx}{D}' \cdot \nabla' \rho_o + \frac{\mu a^3 K}{H}\rho_o \underset{\sim}{U} - \rho_o \frac{Gf}{3\pi}\right) \cdot \hat{n}\, dA' \tag{4.10}$$

where $dA' = dA/a^2$.

Thus the quantity $\frac{\mu \mathcal{C}}{n^2 H}$ is a function of only two variables, $\frac{kT}{H}$ and $\frac{\mu a^3 K}{H}$. Our aim is to find the form of this function.

We can use the fact that $\mathcal{C}$ is proportional to n^2 to obtain an expression for the evolution of the number density n. With each coagulation, n decreases by two, and thus we have

$$\frac{dn}{dt} = -2\mathcal{C} = -\text{constant} \times n^2$$

and integration of this equation gives

$$\frac{n(t)}{n(0)} = \frac{1}{1 + n(0)(\text{constant})\,t} \tag{4.11}$$

5.5 Coagulation in a Suspension at rest

If there is no bulk flow, the pair conservation equation (4.6) reduces to

$$0 = \nabla' \cdot \left(\frac{kT}{H} \underset{\approx}{D}' \cdot \nabla \rho_0 + \rho_0 G f \hat{r} \right). \tag{5.1}$$

The function ρ_0 has radial symmetry, since equation (5.1) and the boundary condition (4.7) are not altered by a rotation of the coordinate axes. Equation (5.1) therefore becomes

$$0 = \frac{d}{dr}\left(r^2 \left\{ \frac{kT}{H} G \frac{d\rho_0}{dr} + \rho_0 G f \right\} \right), \tag{5.2}$$

where we have replaced $\underset{\approx}{D}'$ by the expression (3.3). Integration of (5.2) yields

$$\frac{c}{Gr^2} = \frac{kT}{H} \frac{d\rho_0}{dr} + \rho_0 f , \tag{5.3}$$

where c is a constant.

Using the "Method of Variation of Parameters" (Kreyszig (1968)) we find that the general solution to (5.3) is

$$\rho_0 = \left\{ A + \frac{Hc}{kT} \int_{r_1}^{r} \frac{\exp(HV/kT)dr}{Gr^2} \right\} \exp\left\{ -\frac{HV}{kT} \right\} , \tag{5.4}$$

where A, and r_1 are constants, and

$$V(r) = -\int_r^\infty f(r) dr$$

is the potential associated with the Van der Waals force. From the asymptotic expression (2.11) for f we find

$$V\left(\frac{h}{a}\right) \sim \frac{-a}{12h} \quad \text{as} \quad \frac{h}{a} \to 0 , \tag{5.5}$$

where $h = r-2a$. The quantity $\exp\{-\frac{HV(r)}{kT}\}$ diverges as $r \to 2$, and for ρ_o to be an integrable function we require

$$\lim_{r\to 2}\left(A + \frac{Hc}{kT}\int_{r_1}^{r}\frac{\exp(HV/kT)\,dr}{Gr^2}\right) \to 0 ,$$

or

$$A = \frac{Hc}{kT}\int_{2}^{r_1}\frac{\exp(HV/kT)\,dr}{Gr^2} .$$

Substituting this expression for A in (5.4) we get

$$\rho_o = \frac{Hc}{kT}\left\{\int_{2}^{r}\frac{\exp(HV'/kT)\,dr'}{G'r'^2}\right\}\exp\left\{-\frac{HV(r)}{kT}\right\} . \tag{5.6}$$

The asymptotic form of ρ as $r \to 2$ is found by replacing G and V by the asymptotic expressions (2.8) and (5.5), which gives

$$\rho_o(h) \sim (\text{constant})\, h \exp\left(-\frac{H}{12kTh}\right) \quad \text{as } h \to 0 . \tag{5.7}$$

This asymptotic result also holds for a suspension in shear flow, for the velocity of points due to Van der Waals attraction diverges as $h \to o$ and we may neglect the effect of shear flow on the motion of points in a thin layer surrounding the central sphere. The value of the constant in (5.7) will of course depend on the shear rate.

The constant c which appears in the expression (5.6) for the pair distribution function of a suspension at rest is determined by the boundary condition (4.7), which gives

$$c = \left(\frac{kT}{H}\right) \Big/ \int_{2}^{\infty}\frac{\exp(\frac{HV}{kT})\,dr}{Gr^2} \tag{5.8}$$

Taking the surface $\mathcal{S}$ which appears in the expression (4.10) for $\mathcal{C}$ to be a sphere of radius r (>2) about the central sphere, we get

$$\begin{aligned}\frac{\mu\mathcal{C}}{n^2H} &= 2\pi r^2\left[\frac{kT}{3\pi H}G\frac{d\rho_o}{dr} + \rho_o\frac{Gf}{3\pi}\right] \\ &= \frac{2}{3}c\end{aligned} \tag{5.9}$$

where we have used the expression (5.3) for c. Substituting (5.8) in the above expression we obtain

$$\frac{\mu \ell}{n^2 H} = \frac{2}{3}\frac{kT}{H} \Big/ \int_2^{\infty} \frac{\exp\left(\frac{HV}{kT}\right) dr}{G(r) r^2} \quad . \tag{5.10}$$

This result was first obtained by Derjaguin and Muller (1967).

The expression (5.10) for $\frac{\mu \ell}{n^2 H}$ takes a particularly simple form in the limit as $\frac{kT}{H} \to \infty$. To find this asymptotic form, we begin by noting that the quantity $\exp\left\{\frac{HV(r)}{kT}\right\}$ is approximately unity unless $\frac{r-2a}{a} \ll 1$, in which case V(r) has a large negative value. We let $\bar{r}$ denote the minimum value of r at which $\exp\left\{\frac{HV}{kT}\right\} \approx 1$, i.e.

$$\exp\left\{\frac{HV(r)}{kT}\right\} \geqslant 1 - \Delta \quad \text{for} \quad r \geqslant \bar{r} \tag{5.11}$$

where $\Delta \ll 1$.

Replacing $\exp\left\{\frac{HV(r)}{kT}\right\}$ by unity for $r > \bar{r}$ in the integral in (5.10) we get

$$\int_2^{\infty} \frac{\exp\left\{\frac{HV}{kT}\right\} dr}{G(r) r^2} \approx \int_2^{\bar{r}} \frac{\exp\left\{\frac{HV}{kT}\right\} dr}{G(r) r^2} + \int_{\bar{r}}^{\infty} \frac{dr}{G(r) r^2} \quad . \tag{5.12}$$

We can estimate $\bar{r}$ by expanding $\exp\left\{\frac{HV}{kT}\right\}$ in (5.11) in a Taylor series about $\frac{HV}{kT} = 0$, which gives

$$V(\bar{r}) \approx -\frac{\Delta kT}{H},$$

and with the asymptotic expression (5.5) for V, this becomes

$$\bar{h} \approx \frac{H}{12 \Delta kT} \tag{5.13}$$

where $\bar{h} = \bar{r} - 2$.

Combining the estimate (5.13) for $\bar{h}$ with the asymptotic expressions (2.8) and (5.5) for G and V, we find that the expression (5.12) has the asymptotic form

$$\int_2^\infty \frac{\exp\{HV/kT\}}{Gr^2}\,dr \sim \frac{1}{8}\log\left(\frac{kT}{H}\right) + O(1) \quad \text{as } \frac{kT}{H} \to \infty \; .$$

Substituting this asymptotic formula for the integral in (5.10) we obtain

$$\frac{\mu \mathscr{C}}{n^2 H} \sim \frac{16}{3}\frac{kT}{H}\Big/\log\left(\frac{kT}{H}\right) \qquad \text{as } \frac{kT}{H} \to \infty, \tag{5.14}$$

or

$$\mathscr{C} \sim \frac{16\, n^2 kT}{3\mu \log\left(\frac{kT}{H}\right)} \qquad \text{as } \frac{kT}{H} \to \infty .$$

Thus the coagulation rate is only weakly dependent on H if $\frac{kT}{H} \gg 1$.

We can obtain the asymptotic form of the expression (5.8) for $\mathscr{C}$ as $\frac{kT}{H} \to 0$ by noting that in this limit, the integral in (5.8) is dominated by the contributions from the region $r \gg 1$, and therefore we may replace G and V in that integral by the approximate expressions

$$G \approx 1 \qquad\qquad \text{(see Batchelor (1976))},$$

and

$$V(r) \approx -\frac{16}{9r^6},$$

where the approximate expression for V was obtained from the formula (2.1) for f and the definition of V. Substituting the above expressions in equation (8.1), we find

$$\frac{\mu \mathscr{C}}{n^2 H} \sim c\left(\frac{kT}{H}\right)^{5/6} \qquad \text{as } \frac{kT}{H} \to 0 \; , \tag{5.15}$$

where

$$c = \left(\frac{9}{16}\right)^{1/6} \int_0^\infty e^{(-x^6)}\,dx$$

This asymptotic formula is only valid for very small particles ($a < 10^{-8}$ cm), since it is based on the formula (2.10) for $f(r/a)$ which is only valid if the particle spearation is less than 10^{-6} cms.

The expression (5.10) gives the leading term in the expansion of $\frac{\mu \mathscr{C}}{n^2 H}$ in powers of $\frac{\mu a^3 K}{H}$. The coefficient of the odd powers of

$\frac{\mu a^3 K}{H}$ in this expansion must be zero, since the coagulation rate is not affected by a reversal of the flow direction, and thus the curve of coagulation rate versus shear rate has zero slope at $K = 0$. We shall not attempt to determine the coefficient of the $(\frac{\mu a^3 K}{H})^2$ term in the expression for $\frac{\mu \ell}{n^2 H}$, since this will only predict the perturbations in the coagulation rate cause by "slow" shear flows, and instead we shall concentration on the more interesting problem of coagulation at high shear rates.

5.6 The High Shear Regime

From the pair conservation equation (4.6) it can be seen that the ratio

$$\frac{\text{Brownian diffusion flux}}{\text{Convective flux due to shear flow}}$$

is proportional to $\frac{kT}{\mu a^3 K}$. Thus if the condition

$$\frac{\mu a^3 K}{kT} \gg 1 \tag{6.1}$$

holds, the Brownian motion of the particles may be neglected. It follows that the quantity $\frac{\mu \ell}{n^2 H}$ is only a function of the variable $\frac{\mu a^3 K}{H}$.

The remainder of this chapter is devoted to the problem of finding the form of this function for the case

$$\frac{\mu K a^3}{H} \gg 1 \quad . \tag{6.2}$$

Shear rates which satisfy the constraints (6.1) and (6.2) are termed "high" shear rates.

In §5.2 it was shown that if the condition (6.2) is satisfied, only the nearly touching sphere-pairs are affected by the Van der Waals force. Thus equation (4.6) may be approximated by

$$\nabla' \cdot (\underset{\sim}{U} \rho_0) = 0 \quad , \tag{6.3}$$

except in a thin layer surrounding the centre sphere. This is the pair-conservation equation for force-free spheres in a shear flow which has been solved by Batchelor and Green (1972(b)).

In this section we will show how the coagulation rate may be obtained by combining Batchelor and Green's results with expressions for the relative trajectories of the nearly-touching spheres which are affected by both shear flow and Van der Waals attraction. The problem of determining the motion of such pairs is simplified by the fact that the stress is much larger in the thin layer of liquid between the spheres than elsewhere in the liquid, and the force exerted by this layer on either sphere is a simple function of the relative velocity of the spheres and the minimum thickness of the liquid layer.

Before describing this technique for determining $\mathcal{C}$ we shall briefly outline the relevant results of Batchelor and Green's (1972(a) and (1972(b)) work on the motion of force-free sphere pairs in a bulk flow.

By integrating equations (2.4) and (2.5) for the relative velocity of a sphere-pair, Batchelor and Green obtained the following expressions for the trajectory of a point in pair space, in the absence of Brownian motion and Van der Waals attraction:

$$\frac{r_3(r)}{R_3} = \exp\left\{\int_r^\infty \frac{A(r') - B(r')}{(1 - A(r'))r'}\, dr'\right\}, \tag{6.4}$$

and

$$r_2(r)^2 = \frac{r_3(r)^2}{(R_3)^2}\left\{(R_2)^2 + \int_r^\infty \frac{B(r')(R_3)^2 r' dr'}{(1 - A(r'))\, r_3(r')^2}\right\}, \tag{6.5}$$

where $r_2 = r \sin\theta \sin\phi$, and $r_3 = r\cos\theta$ (see figure (5.1)). The constants R_2 and R_3 are the values taking by r_2 and r_3 at a point on the trajectory an infinite distance upstream.

The trajectories of force-free pairs which lie in the plane of the shear flow ($\theta = \pi/2$) are illustrated in figure (5.2). (This is a

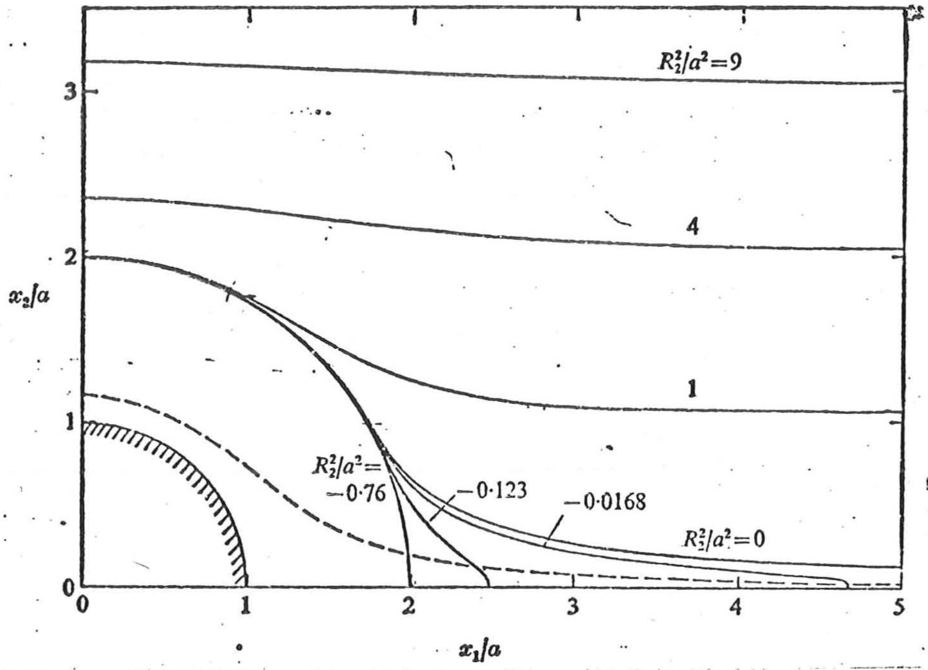

Figure 5.2 The trajectories in the plane $X_2 = 0$ of points in pair space in the absence of Brownian motion and Van Der Waals' attraction. The circle $r = 2$ is the surface of the central sphere. The trajectories for which $(R_2)^2 < 0$ are closed, and the boundary of the region of closed trajectories is formed by rotating the $R_2 = 0$ line about the X_2 axis.

reproduction of figure (4) of Batchelor and Green's (1972(a) paper.)

From this figure it can be seen that there is a region of closed trajectories surrounding the central sphere. The quantity R_2 associated with trajectories in this region is imaginary, and pairs which move on these trajectories execute closed orbits about the central sphere. If there is a force of attraction between the particles the pairs which lie in this region will eventually coagulate, since they will be drawn closer to the central sphere with each pass. Even though there are no closed trajectories if there is a force of attraction between the particles, we shall continue to refer to this region as "the region of closed trajectories".

From figure (5.2) it can be seen that trajectories are "squeezed together" near the top of the central sphere and this is the reason that the shear flow assists in the coagulation process; pairs which move along trajectories such as the $\frac{R_2}{a} = 1$ trajectory shown in figure (5.2) pass very near to the central sphere and only a slight force of attraction is required to cause these pairs to coagulate.

In the second of their papers, Batchelor and Green (1972(b)) found that the solution to the pair conservation equation (6.3) is given by

$$p_0(\underline{r}) = q(r) \tag{6.6}$$

where

$$q(r) = \frac{1}{1-A(r)} \exp\left\{ \int_r^\infty \frac{3(B(r')-A(r'))dr'}{r'(1-A(r'))} \right\} . \tag{6.7}$$

This result only holds outside the region of closed trajectories. Substitution of the asymptotic expressions (2.6) for A and B in (6.7) gives

$$q(r) \sim \frac{\cdot 234}{\left(\frac{h}{a}\right)^{\cdot 781} \left\{ \log \frac{a}{h} \right\}^{\cdot 29}} \quad \text{as} \quad \frac{h}{a} \to 0 . \tag{6.8}$$

Although we are only concerned with the case of shear flow, it should be noted that the expressions (6.6), (6.7) and (6.8) are valid for any type of linear bulk flow. The fact that q diverges as $h \to o$ is a reflection of the tendency for bulk flows to push particles together, and thus any bulk motion of a suspension assists the coagulation process.

This completes the outline of the relevant results of Batchelor and Green's papers. We shall now show how $\mathcal{C}$ may be obtained with the aid of these results.

As mentioned earlier, the Van der Waals forces only affect the motion of pairs which lie in a region surrounding the central sphere. We let $\mathcal{L}$ denotes a surface which encloses this region, and we denote the volume which lies between $\mathcal{L}$ and the central sphere by $V(\mathcal{L})$. In the region outside $\mathcal{L}$, pairs move along the trajectories given by (6.4) and (6.5). If a pair enters $V(\mathcal{L})$ and does not become attached to the central sphere, it leaves the region on a trajectory which has different R_2 and R_3 values from that trajectory on which it entered $V(\mathcal{L})$. Those pairs which leave $V(\mathcal{L})$ and pass into the region of closed trajectories will eventually coagulate, since they will be drawn closer to the central sphere each time they pass through $V(\mathcal{L})$.

We have assumed that the density of points in pair space does not vary with time, and therefore the coagulation rate is equal to the number of pairs which enter $\mathcal{L}$ per unit time from outside the region of closed trajectories in the half space $x_2 > o$ and eventually become attached to the central sphere.

To translate this into a mathematical expression, we take the surface $\mathcal{S}$ which appears in the expression (4.10) for $\mathcal{C}$ to be that surface formed by the part of $\mathcal{L}$ which lies outside the region of closed trajectories together with the part of the boundary of the region of closed trajectories which lies beyond $\mathcal{L}$. This surface is illustrated in figure (5.3).

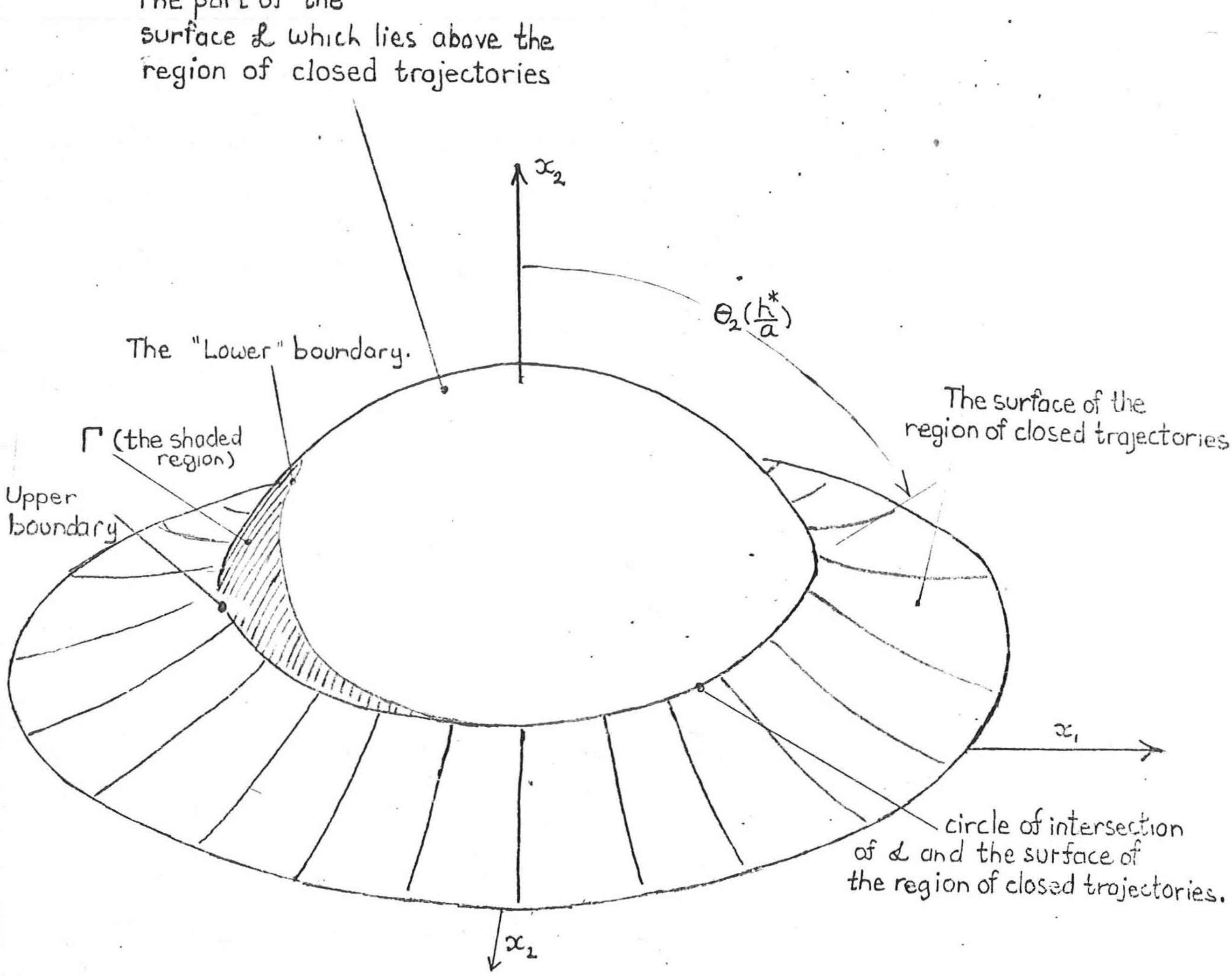

<u>Figure 5.3</u> The surface $\mathcal{S}$ in pair space, defined in §5.6.

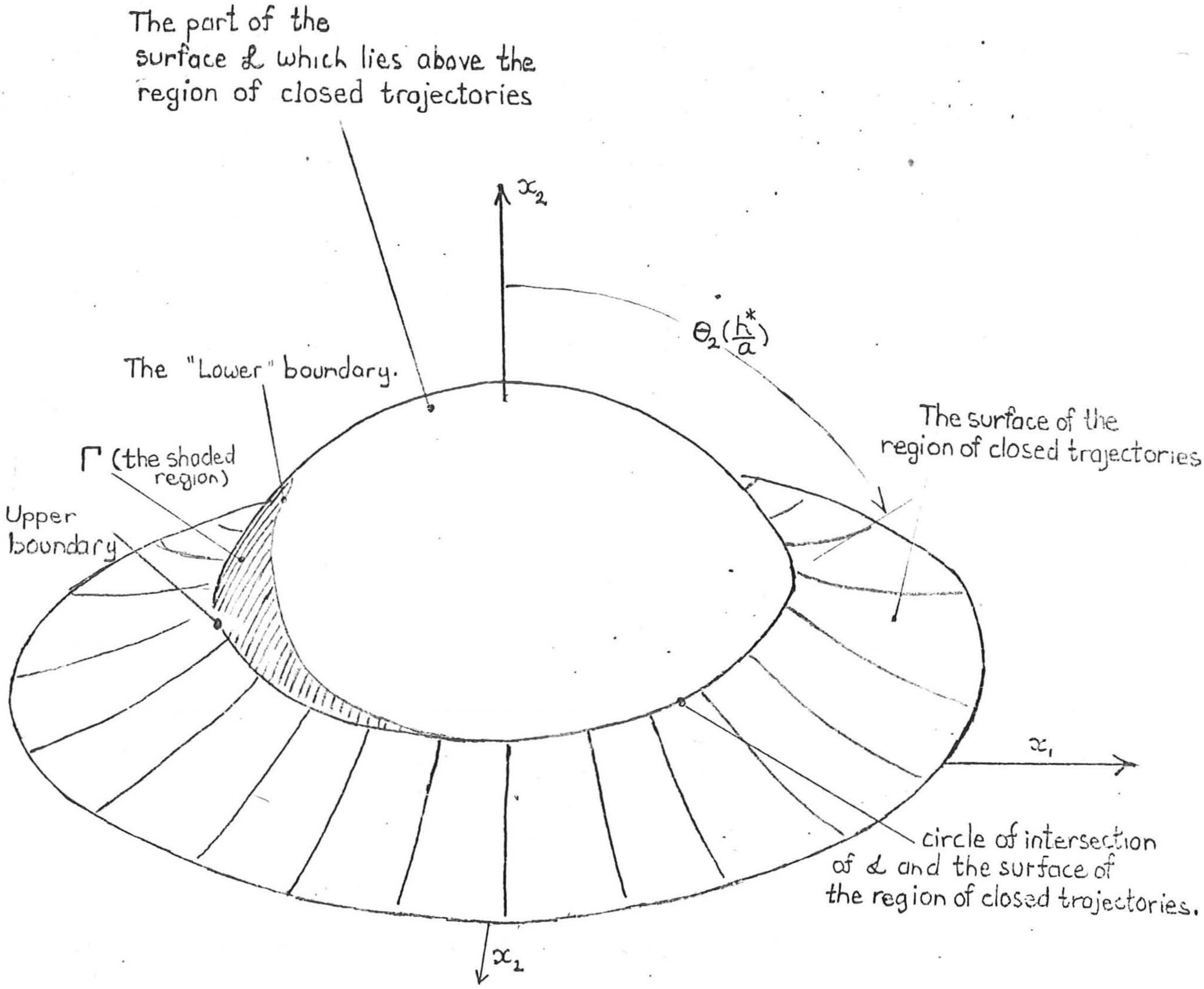

Figure 5.3 The surface $\mathcal{S}$ in pair space, defined in §5.6.

The pairs which lie outside $\mathcal{L}$ are effectively force-free and therefore pairs can only enter $\mathcal{S}$ through the part of that surface which coincides with $\mathcal{L}$.

Those pairs which coagulate enter $\mathcal{S}$ through a portion of the surface denoted by Γ. This region is shown in figure (5.3). The pairs which cross Γ either become attached to the central sphere or pass out of $V(\mathcal{L})$ in the region of closed trajectories. The Van der Waals forces are unimportant beyond $V(\mathcal{L})$ and therefore pairs cross Γ with the velocity $\underset{\sim}{V}'$ given by the expressions (2.4) and (2.5).

The coagulation rate $\mathcal{C}$ is equal to the rate at which pairs pass through Γ, i.e.

$$\mathcal{C} = n^2 \int_{\Gamma} \rho_0 \underset{\sim}{V}' \cdot \hat{n} \, dA \ , \tag{6.9}$$

where $\hat{n}$ denotes the unit normal directed into $V(\mathcal{L})$ and dA is an element of the surface Γ. The distribution function ρ_0 at a point in pair space is determined by the history of the motion of the pairs which arrive at that point. Pairs which cross Γ come from a region in which Van der Waals forces are insignificant and therefore the quantity ρ_0 in (6.9) is given by the expression (6.6), (6.7) and (6.8) derived by Batchelor and Green.

Substitution of the expression (2.4) for V' and (6.6) for ρ_0 in (6.9) gives

$$\mathcal{C} = aKn^2 \int_{\Gamma} q(r) \underset{\sim}{U}(\underset{\sim}{r}) \cdot \hat{n} \, dA \ , \tag{6.10}$$

where the non-dimensional velocity $\underset{\sim}{U}$ is given by (2.5).

We are free to choose any shape for $\mathcal{L}$, provided that the surface $\mathcal{S}$ (of which $\mathcal{L}$ forms a part) encloses the region in which the Van der Waals forces are significant. Since q depends only on $|\underset{\sim}{r}|$, we choose for $\mathcal{L}$ a sphere of radius r*, centred on the origin. The expression (6.10) then becomes

$$\mathscr{C} = -aKn^2q(r^*)\int_{\Gamma(r^*)} U_r(\underset{\sim}{r})\,dA \qquad (6.11)$$

where we have replaced the symbol Γ by $\Gamma(r^*)$, to remind us that the region Γ depends on r^*.

If the shear rate K is sufficiently large, the Van der Waals forces only affect pairs which lie in a thin layer around the central sphere. In this case we may choose an r^* which satisfies the constraint

$$r^* - 2a \ll a$$

and the quantities q and U_r in (6.1) can be replaced by their asymptotic forms. The asymptotic expression for U_r is found by substituting the formulae (2.6) for A and B in the first of equations (2.5). Combining the resulting expression with the formulae (6.8) for q and (6.11) for $\mathscr{C}$, we get

$$\mathscr{C} = -\frac{7.64a^3Kn^2(h^*/a)^{.22}}{\{\log(a/h^*)\}^{.29}}\iint_{\Gamma(h^*)} \sin^3\theta\,\sin\phi\,\cos\phi\,d\theta\,d\phi\ , \qquad (6.12)$$

where $h^* = r^*-2a$.

To evaluate the integral in (6.12) we require expressions for the curves which form the boundary of $\Gamma(h^*)$. In the following two sections we will show how this information may be obtained from the expression for the relative trajectories of nearly touching sphere pairs.

5.7 The Boundary of the region of closed trajectories

The pairs which cross $\Gamma(h^*)$ either coagulate immediately or leave $V(\mathcal{L})$ on a trajectory which lies in the region of closed trajectories. Those pairs which leave $V(\mathcal{L})$ on trajectories which lie on the boundary of the region of closed trajectories are the "last" pairs to coagulate, for any pairs which enter $V(\mathcal{L})$ at points further downstream (i.e. at points which have smaller $\emptyset$ values) leave that region on trajectories which lie beyond the region of closed trajectories, and hence these pairs do not return to $V(\mathcal{L})$. It follows that those pairs which leave $V(\mathcal{L})$ and move along the surface of the region of closed trajectories first enter $V(\mathcal{L})$ at points on the Γ- boundary. The part of the Γ- boundary through which these pairs pass will be termed the "lower boundary". The remaining poitions of the boundary of Γ is formed by the line of intersection of $\mathcal{L}$ and the boundary of the region of closed trajectories. This curve is termed the "upper boundary". Both curves are illustrated in figure (5.3).

To find the position of the upper boundary we require a detailed description of the part of the surface of the region of closed trajectories which lies near the central sphere. In this section we shall obtain approximate equations describing this surface, and in the following section we will look at the more difficult problem of locating the lower Γ-boundary.

The boundary of the region of closed trajectories is formed by the family of trajectories given by (6.4) and (6.5) with $R_2 = 0$. The expression for this surface is obtained by setting $R_2 = 0$ in (6.5) and replacing r_3/R_3 by the expression (6.4), which gives

$$r_2(r)^2 = \exp\left\{2\int_r^{\infty}\frac{A(r')-B(r')}{[1-A(r')]}\frac{dr'}{r'}\right\}\int_r^{\infty}\frac{B(r')}{1-A(r')}\left\{\exp\left[2\int_{r'}^{\infty}\frac{B(r'')-A(r'')}{1-A(r'')}\frac{dr''}{r''}\right]\right\}r'dr'. \quad (7.1)$$

This equation may be put in a more convenient form by substituting the expressions (6.7) for q, from which we obtain

$$r_2(r)^2 = \{q(r)(1-A(r))\}^{-2/3}\int_r^{\infty}\frac{B(r')q(r')^{2/3}r'\,dr'}{(1-A(r'))^{1/3}}. \quad (7.2)$$

This is the equation of an axisymmetric surface, formed by rotating the line $R_2 = 0$ in figure (5.2) about the x_2 axis.

Substituting $r = 2a + h$, and $r_2 = 2a\cos\theta_2$ in (7.2), where θ_2 is the polar angle measured from the x_2 axis (see figure (5.1)), we obtain an expressions relating the θ_2 and h values of points on the surface. With the aid of the tabulated values of the functions A, B and q given by Batchelor and Green (1972(a), 1972(b)), we have computed from (7.2), the angle θ_2 for various values of h/a, and the results are given in table 5.1.

$\Theta_2(h/a)$	h/a	(h/a) approx
0^o	4×10^{-5}	4×10^{-5}
11.4^o	5×10^{-5}	4.9×10^{-5}
33.9^o	2.5×10^{-4}	2.1×10^{-4}
51.3^o	2.5×10^{-3}	2.55×10^{-3}
58.7^o	7.5×10^{-3}	8.8×10^{-3}

Table 5.1 The polar angle Θ_2 of points on the surface of the region of closed trajectories as a function of the distance h of those points from the surface of the central sphere. The quantities (h/a) approx are calculated with the aid of the approximate expresssion (7.11) for the surface of the region of closed trajectories.

From figure (5.3) it can be seen that the spherical shell $\mathcal{L}$ intersects the region of closed trajectories on a circle about the x_2 axis. The angle Θ_2 of points on that circle is found by substituting $r = 2a + h^*$ (the radius of $\mathcal{L}$) and $r_2 = 2a \cos \Theta_2$ in equation (7.2). We denote this angle by $\Theta_2(h^*/a)$. With the aid of figure (5.1) it can be seen that

$$\sin\Theta \sin\phi = \cos\Theta_2$$

and therefore the (Θ, ϕ) coordinates of points on the upper boundary of Γ are related by

$$\phi_u(\Theta) = \pi - \sin^{-1}\left\{\frac{\cos\Theta_2(h^*/a)}{\sin\Theta}\right\} \quad (7.3)$$

where $\phi_u(\Theta)$ denotes the azimuthal angle of a point on the upper boundary.

The integral in the expression (7.2) is difficult to evaluate, and as we shall be requiring $\Theta_2(h^*/a)$ for a number of h^*/a values, it is convenient to replace (7.2) by a simpler approximate expression, valid for $h^*/a \ll 1$.

As mentioned earlier, the boundary of the region of closed trajectories is obtained by rotating the line $\left(\frac{R_2}{a}\right)^2 = 0$, shown in figure (5.2), about the x_2 axis. This line represents the trajectory of a force-free sphere pair in the plane of the flow, and the approximate equation for the part of this line which lies close to the central sphere may be obtained from the approximate form of the expressions (2.4) and (2.5), for nearly-touching pairs. Substituting the asymptotic formulae (2.6) for A and B in (2.5) and using (2.4), we get the approximate equations of motion

$$\frac{dr}{dt} \left(= V_r'\right) = 8{\cdot}154\, K \sin^2\theta \sin\phi \cos\phi\, h \quad , \tag{7.4}$$

$$\frac{d\theta}{dt} \left(= \frac{V_\theta'}{r}\right) = {\cdot}594\, K \sin\theta \cos\theta \sin\phi \cos\phi \quad , \tag{7.5}$$

and

$$\frac{d\phi}{dt} \left(= \frac{V_\phi'}{r\sin\theta}\right) = -K\left[{\cdot}797 - {\cdot}594 \cos^2\phi\right] \quad . \tag{7.6}$$

In deriving these expressions we have neglected $O(1/\log(a/h))$ terms and thus the equations are only strictly valid for extremely close pairs. Although we only require in this section the equation of a trajectory in the plane of the flow ($\theta = \frac{\pi}{2}$), we shall solve these equations for the general case, as this solution will be required in §5.8.

Substituting $r = 2a + h$ in (7.4) and dividing by (7.6), we obtain

$$\frac{\partial h}{\partial \phi} = -\frac{8{\cdot}154 \sin^2\theta \sin\phi \cos\phi\, h}{{\cdot}797 - {\cdot}594 \cos^2\phi} \quad , \tag{7.7}$$

and dividing (7.5) by (7.6) we get

$$\frac{\partial \theta}{\partial \phi} = -\frac{{\cdot}594 \sin\theta \cos\theta \sin\phi \cos\phi}{{\cdot}797 - {\cdot}594 \cos^2\phi} \quad . \tag{7.8}$$

Equation (7.8) is also valid if there is a force of attraction between the spheres, for as this force is radial, it does not affect the rotation of the pair. The solution of (7.8) is found from separation of variables and integration by parts to be

$$\tan\theta(\phi) = \frac{\tan\theta(\pi/2)}{\sqrt{1 - .745\cos^2\phi}} \quad , \tag{7.9}$$

where $\theta(\pi/2)$ denotes the polar angle of the trajectory at $\phi = \pi/2$. The expression (7.9) is the equation of the surface formed by the family of trajectories which intersect the line $\theta = \theta(\pi/2)$, $\phi = \pi/2$. In figure (5.4) we show several curves formed by the intersection of the central sphere with surfaces which satisfy (7.9) for various values of $\theta(\pi/2)$. These lines may be regarded as the trajectories of touching sphere-pairs.

For those who are familiar with the motion of spheroids in a shear flow, we note that the expression (7.9) is identical to the expression for the angular motion of a spheroid with an axis ratio of 1.98.

Eliminating the $\sin^2\theta$ term from (7.7) with the aid of (7.9) and integrating by parts, we get

$$h(\phi) = h(\pi/2)\left\{\frac{1 - .745\cos^2\phi\,\cos^2\theta(\pi/2)}{1 - .745\cos^2\phi}\right\}^{6.87} . \tag{7.10}$$

The large exponent in this expression is a measure of the tendency for the shear flow to push spheres together. To illustrate this effect, we have calculated the ratio $h(\phi)/h(\pi/2)$ for various values and ϕ, and the results are shown in table 5.2.

From this table it can be seen that those pairs which lie in the plane of the shear flow $(\theta = \pi/2)$ are pushed closer together than the pairs for which $\theta(\pi/2) \neq \pi/2$. This suggests that most of the coagulating pairs lie in, or nearly in, the plane of the flow, an observations which shall be verified later in this chapter.

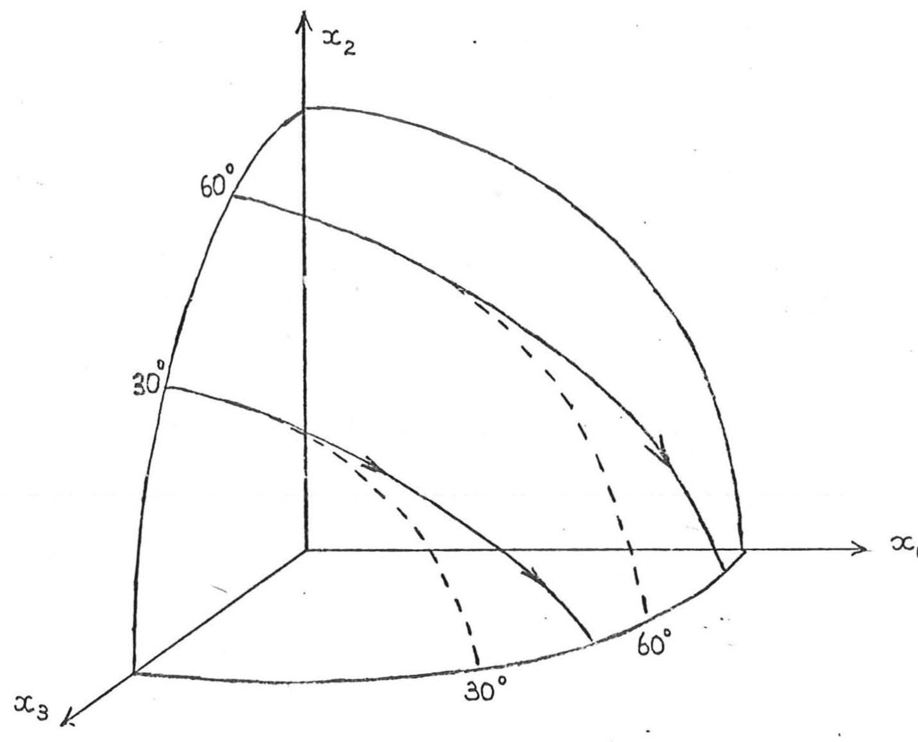

Figure 5.4 The relative trajectories of touching sphere pairs in shear flow. The broken lines are lines of constant θ

ϕ	$\theta(\pi/2)=\pi/2$	$\theta(\pi/2)=1.31$	$\theta(\pi/2)=\frac{\pi}{3}$	$\theta(\pi/2)=\frac{\pi}{4}$
$\pi/2$	1	1	1	1
1.31	1.42	1.39	1.30	1.19
$\pi/3$	4.12	3.78	2.97	2.11
$\pi/4$	24.67	20.68	12.53	5.96
$\pi/6$	276.07	212.85	98.2	29.07

Table 5.2 Values of $h(\phi)/h(\pi/2)$ for trajectories which pass through $\theta = \theta(\pi/2)$ at $\phi = \pi/2$, in the absence of Van der Waals attraction.

We mentioned earlier that the surface of the region of closed trajectories is obtained by rotating the line $R_2 = o$ shown in figure (5.2) about the x_2 axis. This line is a trajectory and may therefore be approximated by an expression of the form (7.10) with $\theta(\pi/2)=\pi/2$. The surface obtained by rotating this line is given by

$$h(\theta_2) = h_{min}\{1 - .745\sin^2\theta_2\}^{-6.87}, \tag{7.11}$$

where h_{min} is the minimum distance separating the boundary of the region of closed trajectories from the central sphere. From table 5.1 it can be seen that

$$h_{min} = 4 \times 10^{-5} a \ . \tag{7.12}$$

Equation (7.11) gives the approximate equation of the surface of the region of closed trajectories. In table 5.1 are shown the values of h/a calculated with the aid of (7.11) and (7.12), and it can be seen that the approximation is quite good even at $h/a = 7.5 \times 10^{-3}$.

From (7.11) we get

$$\sin\theta_2(h^*) = [1{\cdot}34(1 - (\frac{h_{min}}{h^*})^{\cdot 145})]^{\frac{1}{2}} , \quad (7.13)$$

where $\theta_2(h^*)$ is the polar angle characterizing the circle of intersection of the surface (7.11) and the sphere $\mathcal{L}$ of radius $2a + h^*$. Combining this result with (7.3) we find that the θ, ϕ coordinates of the upper boundary of Γ are given by

$$\phi_u(\theta) = \pi - \sin^{-1}\left\{\frac{\sqrt{1{\cdot}34(h_{min}/h^*)^{\cdot 145} - {\cdot}34}}{\sin\theta}\right\} . \quad (7.14)$$

This is the expression for the upper boundary of Γ which will be used in the evaluation of the integral in the expression (6.12) for $\mathcal{C}$, and we now turn to the problem of determining the position of the lower Γ- boundary.

5.8 The trajectories of nearly touching sphere-pairs

Performing the integration with respect to ϕ in the expression (6.12) for $\mathcal{C}$, we get

$$\frac{\mu\mathcal{C}}{n^2 H} = 3{\cdot}82\left(\frac{\mu a^3 K}{H}\right)\frac{(h^*/a)^{\cdot 22}}{[\log(a/h^*)]^{\cdot 29}}\int_{\frac{\pi}{2}-\theta_2(h^*)}^{\frac{\pi}{2}}\sin^3\theta[\cos 2\phi_u(\theta) - \cos 2\phi_L(\theta)]\,d\phi . \quad (8.1)$$

where $\phi_L(\theta)$ is the equation of the curve which forms the lower boundary of Γ. To evaluate this integral by a quadrature scheme, we require the values of $\phi_L(\theta)$ at a number of points on the θ -interval ($\pi/2 - \theta_2(h^*)$, $\pi/2$). In this section we shall obtain equations which enable us to determine these values.

By definition, those pairs which enter $V(\mathcal{L})$ at points which lie on the lower boundary of Γ, leave $V(\mathcal{L})$ on trajectories which lie on the boundary of the region of closed trajectories. Hence these pairs pass out of $V(\mathcal{L})$ at points which lie on the line of intersection of $\mathcal{L}$ and the surface of the region of closed trajectories. From the previous section, this line of intersection is given by

$$\theta_2 = \theta_2(h^*) \quad , \quad \phi < \pi/2 \quad ,$$

where $\theta_2(h^*)$ is given by equation (7.13). Thus we can calculate the point of exit (from $V(\mathcal{L})$) of a trajectory which intersects the lower boundary of Γ, and our aim is to find the point at which that trajectory enters $V(\mathcal{L})$. By finding the entrance points of a number of such trajectories, we can evaluate the expression (8.1).

To find an expression relating the point of entrance of a trajectory into $V(\mathcal{L})$ to the point of exit, we must solve the equations of motion for pairs in $V(\mathcal{L})$. Since these pairs are nearly-touching we may use the asymptotic approximations (2.13), (7.4), (7.5) and (7.6) for $\underset{\sim}{V}'$ and $\underset{\sim}{V}''$. As mentioned previously, the expression (7.9) describing the angular motion of a pair is valid even if there is a force of attraction between the spheres. The expression for $\frac{dh}{dt}$ is obtained by superposing the equations (2.13) and (7.4), which gives

$$\frac{dh}{dt}\left(= V_r' + V_r''\right) = 8{\cdot}154\, K \sin^2\theta \sin\phi \cos\phi\, h - \frac{H}{18\pi\mu a h} \quad . \tag{8.2}$$

Dividing this equation by the expression (7.6) and multiplying the resulting expression by 2h, we get

$$\frac{\partial h^2}{\partial\phi} = -\frac{16{\cdot}31 \sin^2\theta \sin\phi \cos\phi\, h^2}{{\cdot}797 - {\cdot}594 \cos^2\phi} + \frac{H}{9\pi\mu a K({\cdot}797 - {\cdot}594\cos^2\phi)} \quad . \tag{8.3}$$

With the aid of (7.9) we can replace $\sin^2\theta$ by an expression involving ϕ and $\theta(\pi/2)$.

Equation (8.3) can be solved by the Method of Variation of Parameters (Kreyzig (1968)). The first step in this procedure is the solution of the homogeneous equation obtained by neglecting the second term on the right hand side of (8.3). This homogeneous equation is simply the equation for force-free spheres which we solved in the previous section. From (7.10) the homogeneous solution $h_0(\phi)$ is given by

$$h_0(\phi)^2 = h_0(\pi/2)^2 \left\{ \frac{1 - \cdot 745 \cos^2\phi \cos^2\theta(\pi/2)}{1 - \cdot 745 \cos^2\phi} \right\}^{13\cdot 73} . \tag{8.4}$$

The final step in the Method of Variation of Parameters involves substituting

$$h^2 = u h_0^2, \tag{8.5}$$

in (8.3), which gives

$$\frac{du}{d\phi} = \frac{H}{9\pi\mu a K h_0(\phi)^2(\cdot 797 - \cdot 594 \cos^2\phi)} ,$$

or

$$u(\phi) = u(\phi_1) + \frac{H}{22\cdot 53 \mu a K} \int_{\phi_1}^{\phi} \frac{d\phi}{h_0(\phi)^2(1 - \cdot 745 \cos^2\phi)} . \tag{8.6}$$

Substituting (8.6) in (8.5) we obtain the general solution to (8.3):

$$h^2(\phi) = \left(u(\phi_1) + \frac{H}{22\cdot 53 \mu a K} \int_{\phi_1}^{\phi} \frac{d\phi'}{h_0(\phi)^2(1 - \cdot 745 \cos^2\phi')} \right) h_0(\phi)^2 \tag{8.7}$$

where h_0 is given by (8.4). We choose ϕ_1 to be the azimuthal angle of the point at which the trajectory enters $V(\mathcal{L})$ and in addition, we let $h_0(\phi)$ denote the trajectory of a force-free pair which enters $V(\mathcal{L})$ at the same point. Thus we have

$$\begin{aligned} h_0(\phi_1) &= h^* , \\ u(\phi_1) &= 1 , \end{aligned} \tag{8.8}$$

and the expression (8.7) becomes

$$h^2(\phi) = \left(1 - \frac{H}{22{\cdot}53\mu a K h_o^2(\pi/2)}\left\{f(\phi_1,\theta(\pi/2)) - f(\phi,\theta(\pi/2))\right\}\right) h_o(\phi)^2 \,, \tag{8.9}$$

where $h_o(\emptyset)^2$ is given by (8.4). The function f is defined by

$$f(\phi,\theta(\pi/2)) = \int_0^{\phi} \frac{(1 - {\cdot}745\cos^2\phi')^{12\cdot73}\, d\phi'}{(1 - {\cdot}745\cos^2\theta(\pi/2)\cos^2\phi')^{13\cdot73}} \,, \tag{8.10}$$

and the form of this function is shown on figure (5.5) for various values of $\theta(\pi/2)$. To obtain these curves we evaluated the integral in (8.10) using a conditionally convergent scheme based on the trapezoidal rule.

In discussing the form of the trajectories given by (8.9) and (8.10), we shall concentrate on the case $\theta(\pi/2) = \pi/2$, for most of the coagulation takes place between pairs which lie in, or nearly in the plane of the shear flow.

The quantity $\{f(\phi_1,\theta(\pi/2)) - f(\phi,\theta(\pi/2))\}$ in (8.9) determines the amount by which the ratio $h(\emptyset)/_{h_o(\emptyset)}$ differs from unity. From figure (5.5) it can be seen that $f(\emptyset, \frac{\pi}{2})$ is approximately constant outside the interval

$$60^\circ < \phi < 120^\circ \,. \tag{8.11}$$

Thus pairs which enter $V(\mathcal{L})$ at points upstream of $\emptyset = 120^\circ$ in the plane of the shear flow, move along the undisturbed trajectories of force-free pairs until the azimuthal angle drops below 120°. The pairs are then drawn towards the central sphere, and if they do not become attached to the central sphere they leave the region given by (8.11) on an undisturbed trajectory with a reduced value of $h_o(\pi/2)$.

The value of $h_o(\pi/2)$ associated with the undisturbed trajectory on which a pair enters $V(\mathcal{L})$ is found by substituting the expression (8.4) for $h_o(\emptyset)$ in the boundary condition (8.8), which gives

$$h^2(\phi) = \left(1 - \frac{H}{22 \cdot 53 \mu a K h_0^2(\pi/2)} \{f(\phi_1, \theta(\pi/2)) - f(\phi, \theta(\pi/2))\}\right) h_0(\phi)^2 , \tag{8.9}$$

where $h_0(\phi)^2$ is given by (8.4). The function f is defined by

$$f(\phi, \theta(\pi/2)) = \int_0^{\phi} \frac{(1 - \cdot 745 \cos^2\phi')^{12 \cdot 73} d\phi'}{(1 - \cdot 745 \cos^2\theta(\pi/2) \cos^2\phi')^{13 \cdot 73}} , \tag{8.10}$$

and the form of this function is shown on figure (5.5) for various values of $\theta(\pi/2)$. To obtain these curves we evaluated the integral in (8.10) using a conditionally convergent scheme based on the trapezoidal rule.

In discussing the form of the trajectories given by (8.9) and (8.10), we shall concentrate on the case $\theta(\pi/2) = \pi/2$, for most of the coagulation takes place between pairs which lie in, or nearly in the plane of the shear flow.

The quantity $\{ f(\phi_1, \theta(\pi/2)) - f(\phi, \theta(\pi/2)) \}$ in (8.9) determines the amount by which the ratio $h(\phi)/h_0(\phi)$ differs from unity. From figure (5.5) it can be seen that $f(\phi, \frac{\pi}{2})$ is approximately constant outside the interval

$$60° < \phi < 120° . \tag{8.11}$$

Thus pairs which enter $V(\mathcal{L})$ at points upstreamof $\phi = 120°$ in the plane of the shear flow, move along the undisturbed trajectories of force-free pairs until the azimuthal angle drops below $120°$. The pairs are then drawn towards the central sphere, and if they do not become attached to the central sphere they leave the region given by (8.11) on an undisturbed trajectory with a reduced value of $h_0(\pi/2)$.

The value of $h_0(\pi/2)$ associated with the undisturbed trajectory on which a pair enters $V(\mathcal{L})$ is found by substituting the expression (8.4) for $h_0(\phi)$ in the boundary condition (8.8), which gives

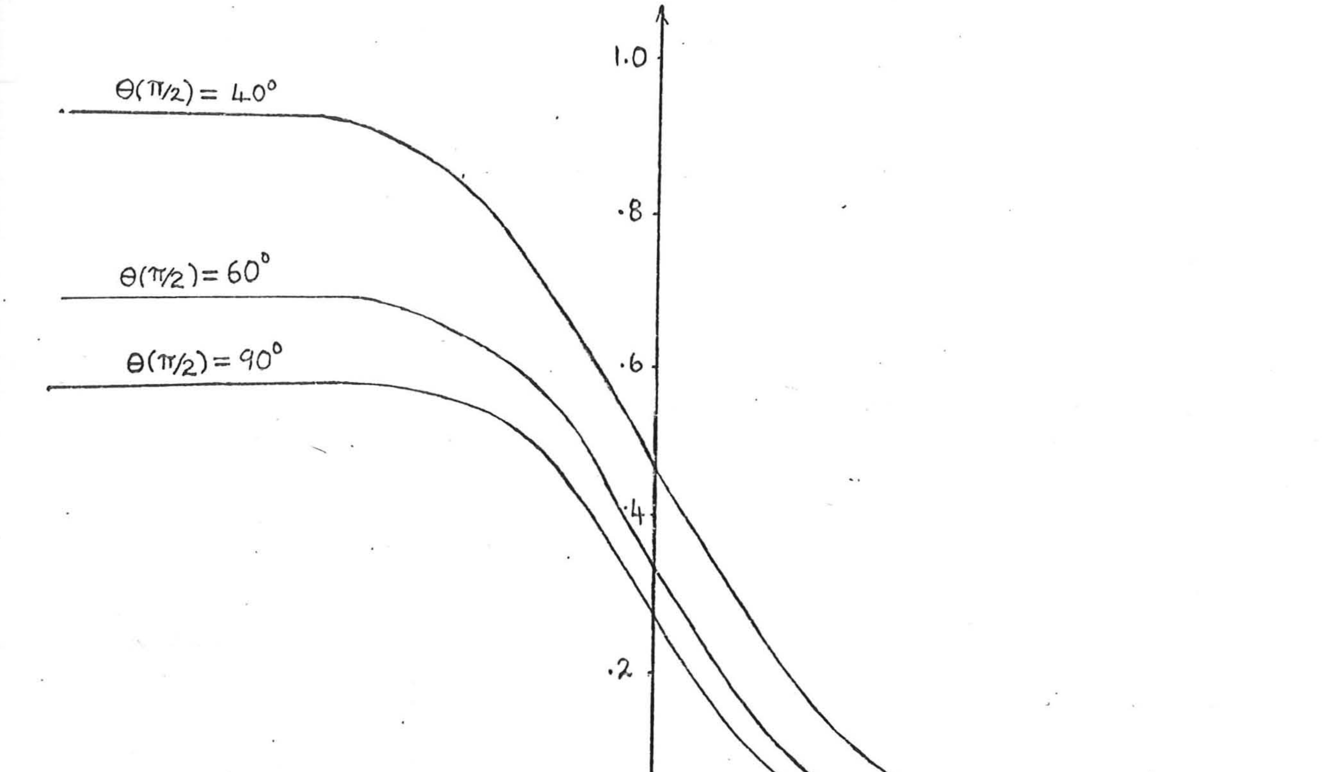

Figure 5.5 The function $f(\phi, \theta(\pi/2))$ which appears in the equation (8.9) describing the trajectories of pairs in V($\mathcal{L}$).

$$h_0(\pi/2) = h^* \left\{ \frac{1 - .745\cos^2\phi_1}{1 - .745\cos^2\phi_1 \cos^2\theta(\pi/2)} \right\}^{6.87} \tag{8.12}$$

The angle $\theta(\pi/2)$ can be related to the polar angle θ_1 at which the trajectory enters V($\mathcal{L}$) with the aid of the expression (7.9) describing the orientation of a nearly-touching sphere-pair, which gives

$$\tan\theta(\pi/2) = \tan\theta_1 \sqrt{1 - .745\cos^2\phi_1} \ . \tag{8.13}$$

Combining the expressions (8.12) and (8.9), we get an expression for h(ϕ) in terms of ϕ_1, $\theta(\pi/2)$ and h*:

$$\left[\frac{h(\phi)}{h^*}\right]^2 = \left(\frac{1 - .745\cos^2\phi\cos^2\theta(\pi/2)}{1 - .745\cos^2\phi}\right)^{13.73} \left\{\left(\frac{1 - .745\cos^2\phi_1}{1 - .745\cos^2\phi_1\cos^2\theta(\pi/2)}\right)^{13.73} - \frac{\xi}{22.53}\left[f(\phi_1,\theta(\pi/2)) - f(\phi,\theta(\pi/2))\right]\right\}, \tag{8.14}$$

where

$$\xi = \frac{H}{\mu a K (h^*)^2} \ , \tag{8.15}$$

and we have replaced $h_0(\phi)^2$ by the expression (8.4).

In figure (5.6) are shown trajectories given by (8.14) for the case $\theta(\pi/2) = \pi/2$, $\xi = 1$.

The angle ϕ_2 at which a trajectory leaves V($\mathcal{L}$) may be found by substituting

$$\phi = \phi_2 \quad \text{and} \quad h = h^*$$

in (8.14), which gives

$$g(\phi_1, \theta(\pi/2)) = g(\phi_2, \theta(\pi/2)) \ , \tag{8.18}$$

where

$$g(\phi,\theta) = \left(\frac{1 - .745\cos^2\phi}{1 - .745\cos^2\theta\cos^2\phi}\right)^{13.73} - \frac{\xi}{22.53} f(\phi,\theta) . \tag{8.19}$$

$$h_0(\pi/2) = h^*\left\{\frac{1-\cdot 745\cos^2\phi_1}{1-\cdot 745\cos^2\phi_1\cos^2\theta(\pi/2)}\right\}^{6\cdot 87} \tag{8.12}$$

The angle $\theta(\pi/2)$ can be related to the polar angle θ_1 at which the trajectory enters V($\mathcal{L}$) with the aid of the expression (7.9) describing the orientation of a nearly-touching sphere-pair, which gives

$$\tan\theta(\pi/2) = \tan\theta_1\sqrt{1-\cdot 745\cos^2\phi_1}\ . \tag{8.13}$$

Combining the expressions (8.12) and (8.9), we get an expression for h($\emptyset$) in terms of $\emptyset_1$, $\theta(\pi/2)$ and h*:

$$\left[\frac{h(\phi)}{h^*}\right]^2 = \left(\frac{1-\cdot 745\cos^2\phi\cos^2\theta(\pi/2)}{1-\cdot 745\cos^2\phi}\right)^{13\cdot 73}\left\{\left(\frac{1-\cdot 745\cos^2\phi_1}{1-\cdot 745\cos^2\phi_1\cos^2\theta(\pi/2)}\right)^{13\cdot 73} - \frac{\xi}{22\cdot 53}\left[f(\phi_1,\theta(\pi/2)) - f(\phi,\theta(\pi/2))\right]\right\}, \tag{8.14}$$

where

$$\xi = \frac{H}{\mu a K (h^*)^2}\ , \tag{8.15}$$

and we have replaced $h_o(\emptyset)^2$ by the expression (8.4).

In figure (5.6) are shown trajectories given by (8.14) for the case $\theta(\pi/2) = \pi/2$, $\xi = 1$.

The angle $\emptyset_2$ at which a trajectory leaves V($\mathcal{L}$) may be found by substituting

$$\phi = \phi_2 \quad \text{and} \quad h = h^*$$

in (8.14), which gives

$$g(\phi_1, \theta(\pi/2)) = g(\phi_2, \theta(\pi/2))\ , \tag{8.18}$$

where

$$g(\phi,\theta) = \left(\frac{1-\cdot 745\cos^2\phi}{1-\cdot 745\cos^2\theta\cos^2\phi}\right)^{13\cdot 73} - \frac{\xi}{22\cdot 53} f(\phi,\theta). \tag{8.19}$$

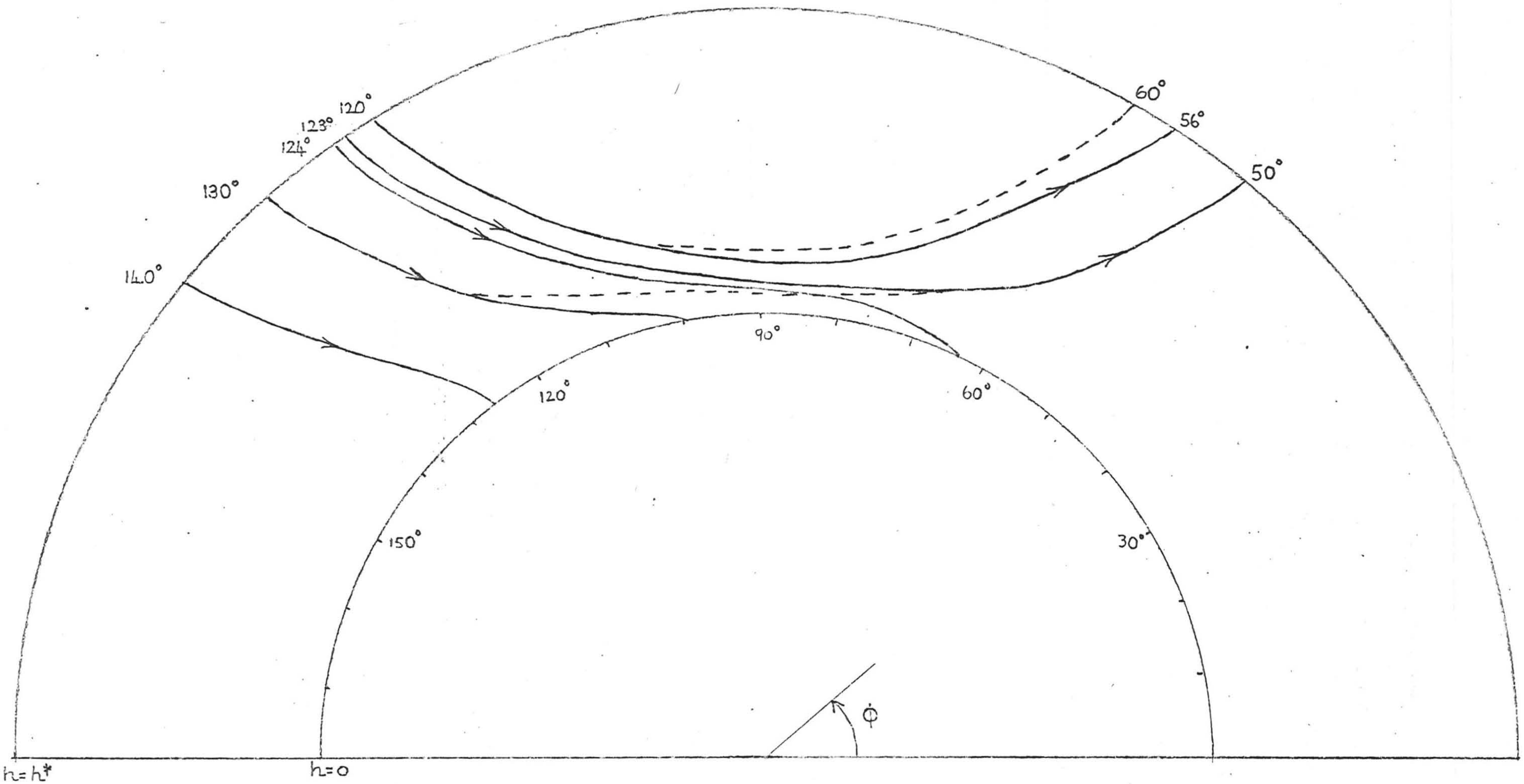

Figure 5.6 The trajectories of nearly-touching pairs which lie in the plane of the shear flow, for $\xi = 1$. (Calculated from equation (8.14)). The broken lines are trajectories of force-free pairs which enter $V(\mathcal{L})$ at $\phi = 130^o$ and $\phi = 120^o$.

The function g is illustrated in figure (5.7). Those pairs which enter $V(\mathcal{L})$ at angles ϕ for which g is negative are drawn onto the central sphere; in other words, these pairs coagulate on their first encounter.

With the aid of the function g we can calculate the coordinates of points on the lower boundary of Γ, for a given value of h^*. Until now, we have left the value of h^* unspecified, and the remainder of this section deals with the problem of choosing a suitable h^*. In §5.9 we combine the results of this and the previous sections to obtain the coagulation rate for a range of $\frac{\mu a^3 K}{H}$ values.

The expression (8.1) for $\mathcal{C}$ is valid if the pairs which pass through Γ are only affected by Van der Waals forces while in the region $V(\mathcal{L})$. This places a restriction on the minimum value of h^*. To estimate this minimum h^*, we recall that pairs which lie in the plane of the flow are only affected by the attractive force in the part of $V(\mathcal{L})$ which lies in the region

$$60^\circ < \phi < 120^\circ .$$

This implies that the point on the lower Γ- boundary in the plane of the flow must have an azimuthal angle of 120° or more if the pairs which enter Γ in the plane of the flow are to be effectively force-free at points outside $V(\mathcal{L})$. We shall take this as the condition for the validity of equation (8.1), for we are mainly interested in the pairs which lie in, or nearly in the plane of the flow.

For a given value of $\frac{\mu a^3 K}{H}$, the minimum value of h^* is that value for which the lower boundary of Γ passes through the point $\phi = 120^\circ$, $\theta = \pi/2$. It is possible to determine this minimum h^* for any value of $\frac{\mu a^3 K}{H}$ by using the expression (7.13) for the angle $\theta_2(h^*)$ at which $\mathcal{L}$ interesects the boundary of the region of closed trajectories together with the equation (8.18) relating the entrance and exit angles of a trajectory. We shall obtain a useful upper bound on the

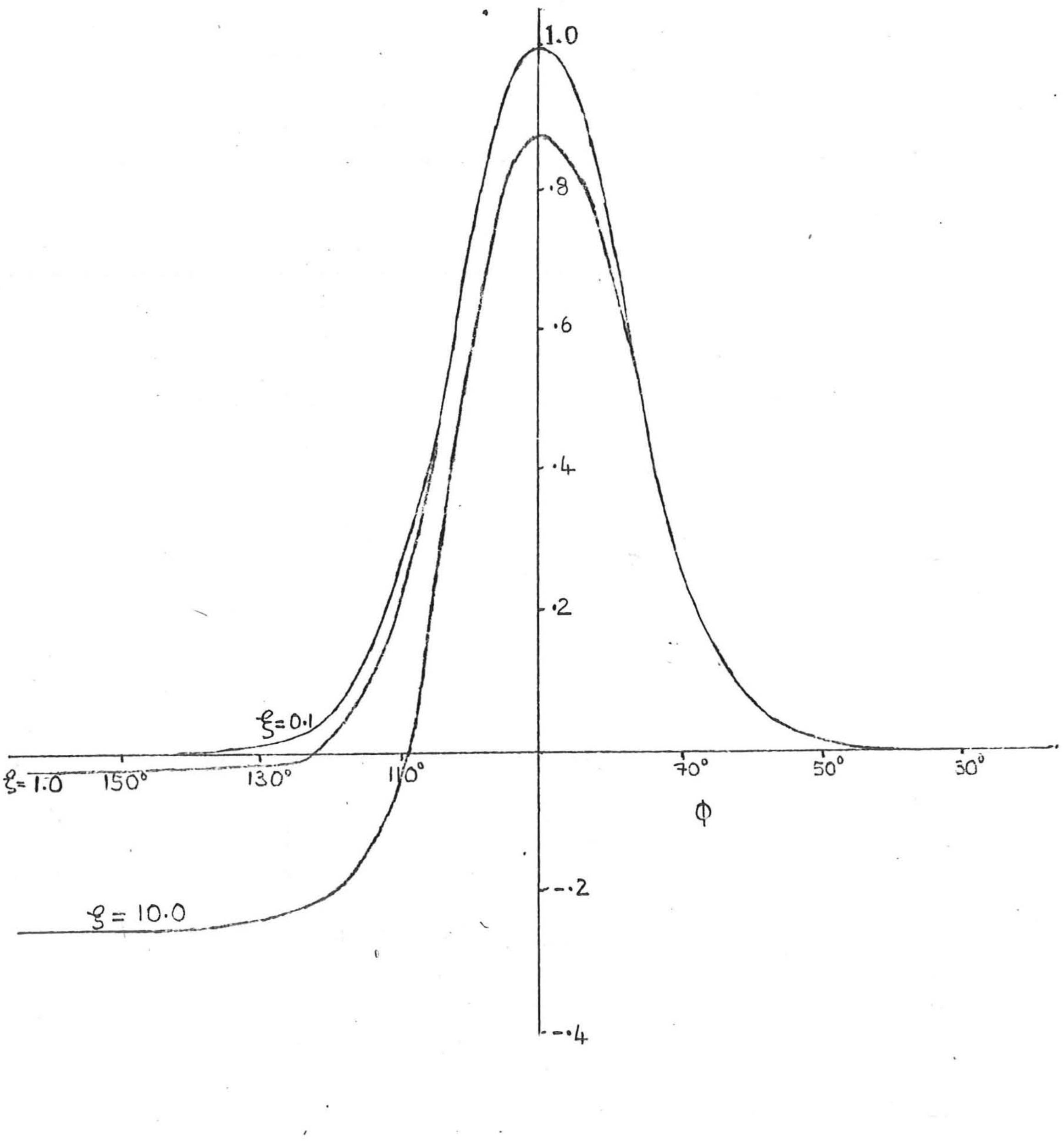

Figure 5.7 The function $g(\phi,\theta(\pi/_2)$ defined in §5.8, for $\theta(\pi/2) = \pi/_2$. The azimuthal angle ϕ_1 at which a trajectory enters $V(\alpha)$ is related to the exit angle ϕ_2 by

$$g(\phi_1,\theta(\pi/2)) = g(\phi_2,\theta(\pi/2)).$$

minimum h^*/a by a more straightforward method.

From figure (5.6) it can be seen that if $\xi = 1$, the trajectory which enters $V(\mathcal{L})$ at $\phi = 120^{\circ}$ leaves at $\phi \approx 56^{\circ}$. Those trajectories which enter upstream of $\phi = 124^{\circ}$ are captured by the central sphere and thus if the boundary of the region of closed trajectories in the plane of the flow intersect $\mathcal{L}$ in the region $\phi < 56^{\circ}$, the lower boundary of Γ lies in the region

$$120^{\circ} < \phi < 124^{\circ},$$

(since these trajectories are "spread out" and leave $V(\mathcal{L})$ in the region $\phi < 56^{\circ}$). If this is the case then the value of h^* is larger than the minimum, and it is this value of h^* (i.e. the value for which $\xi = 1$) which we shall use in the expression (8.1) for $\mathcal{C}$. We are free to use larger values of (h^*/a), but as we have assumed that h^*/a is small, there is no point in doing so.

From the definition (8.15) of ξ, we find that the value of h^*/a to be used in (8.1) is given by

$$\frac{h^*}{a} = \left(\frac{H}{\mu a^3 K}\right)^{1/2} . \tag{8.20}$$

This expression for h^* is only valid if the surface of the region of closed trajectories intersects $\mathcal{L}$ at a point in the sector $\phi < 56^{\circ}$, $\theta = \pi/2$. Substituting $\theta_2 = 34^{\circ}$, and $h_{min} = 4 \times 10^{-4} a$ in the expression (7.11) for the boundary of the region of closed trajectories, we find that the minimum value of h^*/a for which (8.20) is valid is given by

$$\frac{h^*}{a} = 2.5 \times 10^{-3}.$$

Thus a suitable value for the quantity (h^*/a) which appears in the expression (8.1) for $\frac{\mu \mathcal{C}}{n^2 H}$ is given by

$$\frac{h^*}{a} = \max\left[\left(\frac{H}{\mu a^3 K}\right)^{\frac{1}{2}}, 2.5 \times 10^{-3}\right] . \tag{8.21}$$

5.9 The Coagulation Rate

We shall now describe the procedure for evaluating the terms which appear in the expression (8.1) for the coagulation rate.

The thickness h^* of the layer $V(\mathcal{L})$ surrounding the central sphere is given by

$$\frac{h^*}{a} = \max\left(\sqrt{\frac{H}{\mu a^3 K}}, 2.5\times10^{-3}\right). \qquad \text{(8.21) (repeated)}$$

The surface of this layer intersects the boundary of the region of closed trajectories at points on a circle about the x_2 axis (see figure (5.3)). The polar angle θ_2 of points which lie on this circle is given by equation (7.13), and on combining this with the estimate (7.12) for h_{min}, we find

$$\theta_2\left(\frac{h^*}{a}\right) = \sin^{-1}\left\{\sqrt{1.34\left(1-\left(\frac{4\times10^{-5}a}{h^*}\right)^{.145}\right)}\right\}. \qquad (9.1)$$

The integral in equation (8.1) can only be evaluated numerically, and for this we require the value of $\phi_L(\theta)$ at a number of points on the interval

$$\pi/2 - \theta_2(h^*/a) \leqslant \theta \leqslant \pi/2 \quad ,$$

where $(\phi_L(\theta), \theta)$ denote the angular coordinates of a point on the lower boundary of Γ.

To obtain these values, we begin by selecting a point which lies on the line given by equation (9.1) in the region $\phi < \pi/2$. This point, shown in figure (5.8), has angular coordinates (θ', ϕ'). To show how θ' and ϕ' are related, we use the identity

$$\cos\theta_2 = \sin\theta\sin\phi$$

(see figure (5.1)) which in combination with the expression (9.1) for $\theta_2(h^*/a)$ gives

$$\phi' = \sin^{-1}\left\{\frac{\sqrt{1.34(4\times10^{-5}a/h^*)^{.145} - .34}}{\sin\theta'}\right\} \qquad (9.2)$$

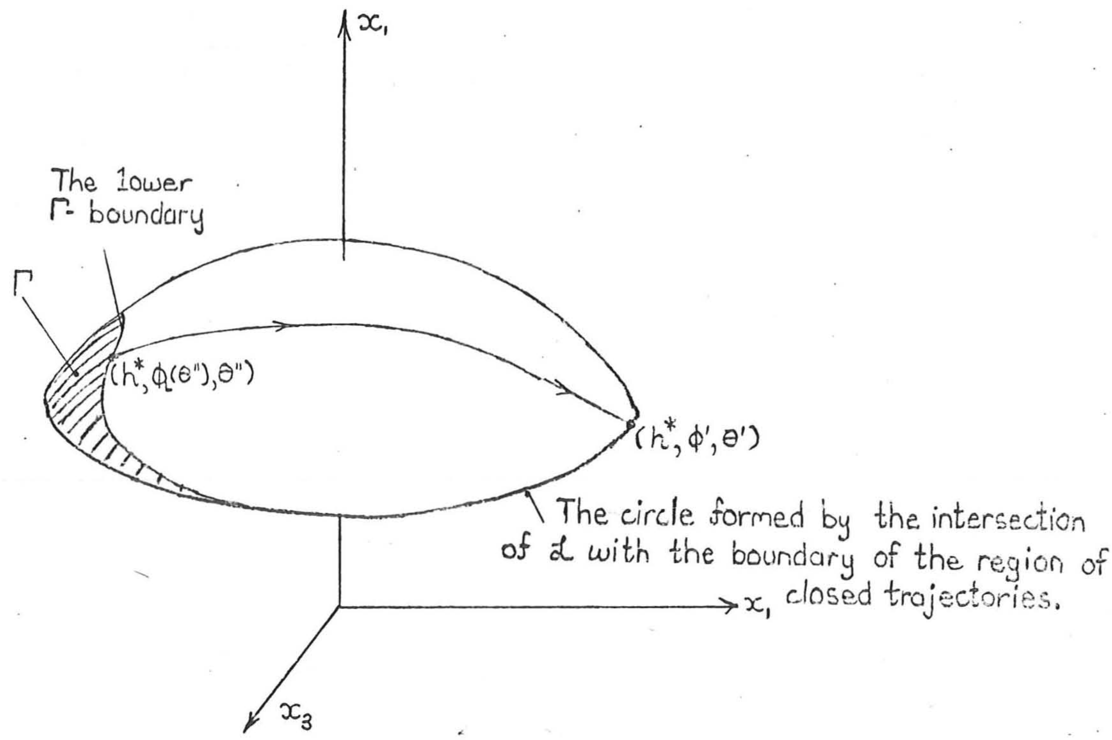

Figure 5.8 A sketch of the trajectory which crosses the lower boundary at $(h^*, \phi_L(\theta''), \theta'')$ and passes through the point (h^*, ϕ', θ') lying on the line of intersection of $\mathcal{L}$ and the boundary of the region of closed trajectories.

The trajectory which passes through the point (θ', ϕ') on the surface $\mathcal{L}$ also passes through a point on the lower boundary of Γ. The polar angle of this point is denoted by θ'' and by definition the corresponding azimuthal angle is $\phi_L(\theta'')$. This point is shown in figure (5.8).

From the equation (8.18) which relates the point at which a trajectory enters $V(\mathcal{L})$ to the point of exit, we find that $\phi_L(\theta'')$ is given by the implicit expression

$$g(\phi_L(\theta''), \theta(\pi/2)) = g(\phi', \theta(\pi/2)) \tag{9.3}$$

where the function g is defined in (8.19) and the angle $\theta(\pi/2)$ is given by

$$\theta(\pi/2) = \tan^{-1}\{(1 - \cdot 745\cos^2\phi')^{1/2}\tan\theta'\} \tag{9.4}$$

This last expression comes from equation (7.9). Also from (7.9) we find that

$$\theta'' = \tan^{-1}\left\{\frac{\tan\theta(\pi/2)}{\sqrt{1-\cdot 745\cos^2\phi_L(\theta'')}}\right\} \tag{9.5}$$

Thus with the adi of (9.3), (9.4) and (9.5) we can obtain the coordinates of a point on the lower boundary of Γ given the coordinates of a point on the line of intersection of $\mathcal{L}$ and the boundary of the region of closed trajectories.

By repeating this procedure for a number of values of θ' in the range

$$\pi/2 - \theta_2(\tfrac{h^*}{a}) < \theta' < \pi/2$$

we obtain the coordinates $(\phi_L(\theta''), \theta'')$ of a set of points which lie on the lower boundary of Γ. Combining this with the values of $\phi_u(\theta'')$

calculated with the aid of (7.14) we can obtain the values of the integrand in (8.1) at a set of points over the range of integration. The integral can then be evaluated by using a suitable quadrature, and combining the result with the expression (8.21), for h^*/a, we can calculate $\frac{\mu \ell}{\Omega^2 H}$ from (8.1).

The values of $\frac{\mu \ell}{\Omega^2 H}$ obtained by this method are shown in figure (5.9). In each case, the integral in (8.1) was evaluated by the trapezoidal rule. Convergence was tested by halving the number of grid points, and in each case the subsequent variation in the computed value of $\frac{\mu \ell}{\Omega^2 H}$ was less than one percent.

The limiting coagulation rate

Although the rate at which pairs enter $V(\mathcal{L})$ is proportional to the shear rate K, the coagulation rate is not linear in K because the percentage of the pairs entering $V(\mathcal{L})$ which coagulate decreases with increasing shear rate. In other words, the area of the region $\Gamma \rightarrow 0$ as $\frac{\mu a^3 K}{H} \rightarrow \infty$. Thus the angles $\phi_u(\theta)$ and $\phi_L(\theta)$ which appear in the expression (8.1) for $\frac{\mu \ell}{\Omega^2 H}$ are approximately equal at very large values of $\frac{\mu a^3 K}{H}$, and the integrand in (8.1) is, approximately

$$-2\sin^3\theta \sin 2\phi_u(\theta)\{\phi_u(\theta) - \phi_L(\theta)\} \; . \tag{9.6}$$

Both ϕ_u and ϕ_L are of order unity and thus the accuracy with which we can determine the difference $\{\phi_u - \phi_L\}$ decreases as $\frac{\mu a^3 K}{H}$ increases. For this reason, we have not attempted to compute the values of $\frac{\mu \ell}{\Omega^2 H}$ beyond $\frac{\mu a^3 K}{H} = 10^6$. However, by slightly modifying the procedure described earlier for calculating ℓ, we can determine the limiting value to which $\frac{\mu \ell}{\Omega^2 H}$ asymptotes as $\frac{\mu a^3 K}{H} \rightarrow \infty$.

To obtain this quantity, we use the fact that at very large values of $\frac{\mu a^3 K}{H}$, the trajectories of pairs which cross the lower boundary of Γ are only slightly perturbed by the Van der Waals forces. Thus we

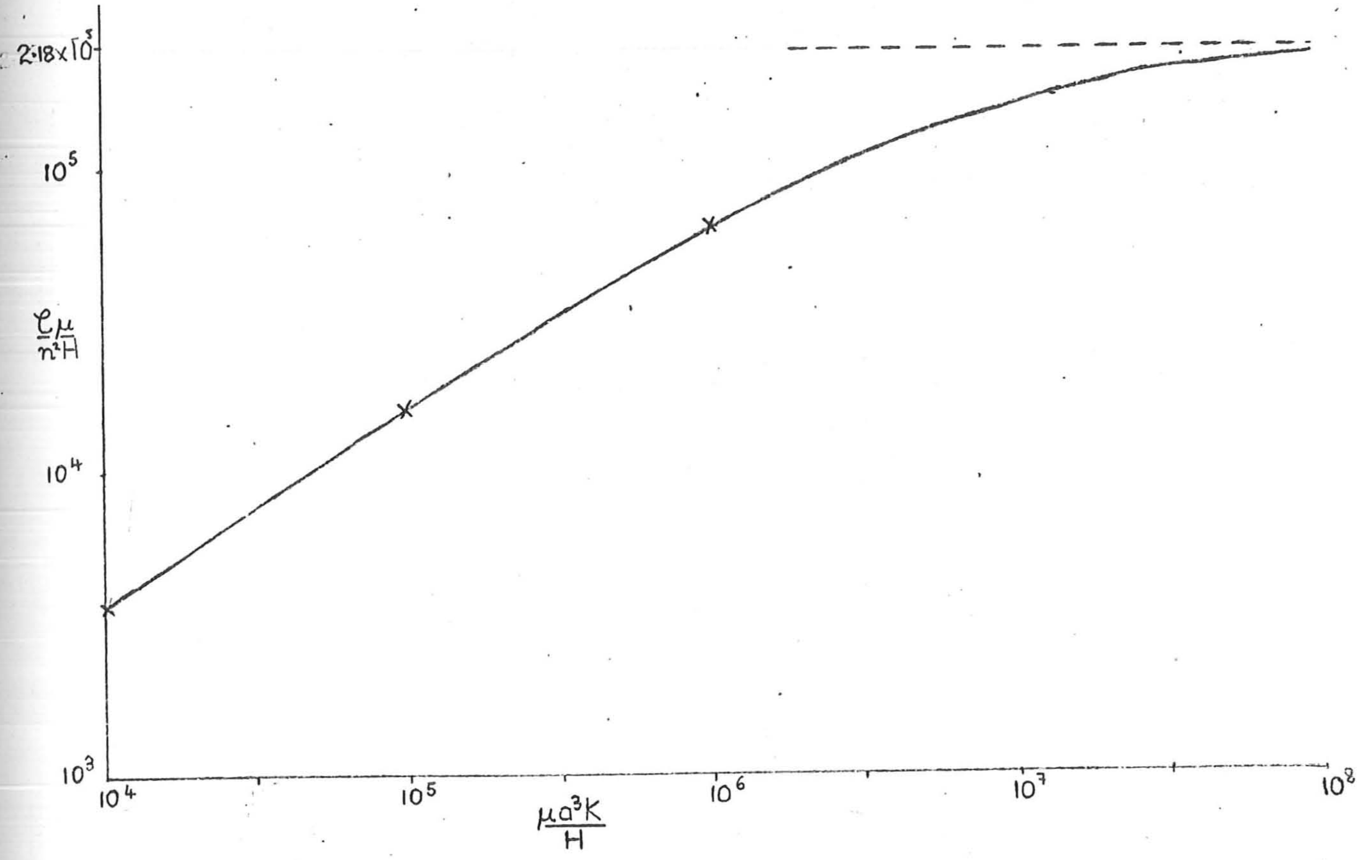

Figure 5.9 The computed values of non-dimensional coagulation rate (marked by crosses).

have $|\theta'' - \theta'| \ll 1$

and $|\phi_L(\theta'') - (\pi - \phi')| \ll 1$,

where, as before, the angles $(\phi_L(\theta''), \theta'')$ denote the coordinates of a point on the lower Γ-boundary through which passes the trajectory that leaves $V(\mathcal{L})$ at the point (h^*, ϕ', θ') (see figure (5.8)).

An approximate expression for the azimuthal angle $\phi_L(\theta'')$ is obtained by substituting

$$g(\phi_L, \theta(\pi/2)) \approx g(\pi - \phi', \theta(\pi/2)) + \left.\frac{\partial g}{\partial \phi}\right|_{\phi = \pi - \phi'} \{\phi_L - (\pi - \phi')\} \ , \tag{9.7}$$

in equation (9.3), which gives

$$\phi_L = \pi - \phi' + \frac{\xi\{f(\pi - \phi', \theta(\pi/2)) - f(\phi', \theta(\pi/2))\}}{22.53 \frac{\partial g}{\partial \phi}} \ , \tag{9.8}$$

where we have used the expression (8.19) for g. Similarly, θ'' can be obtained from (9.4) and (9.5) by neglecting $O((\theta'' - \theta')^2)$ and $O([\phi_L - (\pi - \phi')]^2)$ terms. The value of $\phi_u(\theta'')$ is then obtained with the aid of equation (7.14) and combining this with the value of ϕ_L given by (9.8) we find that $(\phi_u - \phi_L)$ has the form,

$$\phi_u(\theta'') - \phi_L(\theta'') = A(\theta'') \frac{H}{\mu a^3 K} \tag{9.9}$$

Thus the integral in (8.1) is proportional to $\frac{H}{\mu a^3 K}$, and we have calculated the constant of proportionality by calculating the quantity $A(\theta'')$ for a number of values θ'' over the range

$$\pi/2 - \theta_2(\tfrac{h^*}{a}) < \theta'' < \pi/2 \ ,$$

and integrating by the usual quadrature scheme. Substituting the resulting expression for the integral in (8.1), we find that the term $\frac{\mu a^3 K}{H}$ vanishes from the expression, and the non-dimensional coagulation rate has the value

$$2 \cdot 18 \times 10^5 \qquad \text{as} \qquad \frac{\mu a^3 K}{H} \to \infty$$

This limiting value is indicated by a broken line in figure (8.9).

The limiting coagulation rate can also be estimated directly from the expression (4.9), which in the absence of Brownian motion, becomes

$$\mathcal{C} = \frac{1}{2}\int_{\mathcal{S}} \rho(\underset{\sim}{r})(\underset{\sim}{V}'(\underset{\sim}{r}) + \underset{\sim}{V}''(\underset{\sim}{r}))\cdot\hat{n}\,dA \tag{9.10}$$

where $\mathcal{S}$ denotes a closed surface enclosing the central sphere. In this case we take $\mathcal{S}$ to be the surface of the region of closed trajectories. At very high shear rates the pair density function $\rho(\underset{\sim}{x})$ at points on $\mathcal{S}$ has approximately the same value as would be obtained with force-free pairs, and from (6.6) we have

$$\rho(\underset{\sim}{r})\,(= n^2\rho_0(\underset{\sim}{r})) = n^2 q(r) \quad , \tag{9.11}$$

where q(r) is given by (6.7) and has the asymptotic form given by (6.8). Substituting the expression (9.11) for ρ in (9.10) and using the fact that the velocity $\underset{\sim}{V}'$ of force-free pairs is parallel to $\mathcal{S}$ at each point on the surface, we get

$$\mathcal{C} = n^2 \int_{\mathcal{S}^+} q(r)\,\underset{\sim}{V}''(\underset{\sim}{r})\cdot\hat{n}\,dA \tag{9.12}$$

where $\mathcal{S}^+$ denotes the part of $\mathcal{S}$ which lies in the region $x_2 > 0$.

Both q(r) and $\underset{\sim}{V}''(\underset{\sim}{r})$ diverge as $r \to 2a$ and thus the integral in (9.12) is dominated by the contribution from the part of $\mathcal{S}^+$ which is close to the central sphere. In this region $\underset{\sim}{V}''$ and q are given approximately by the asymptotic expression (2.13) and (6.8), and substituting these formulae in (9.12) we obtain

$$\mathcal{C} = \frac{n^2 H}{242\mu a^2}\int_{\mathcal{S}^+} \frac{\hat{r}\cdot\hat{n}\,dA}{(h/a)^{1.78}\{\log(a/h)\}^{.29}} \,. \tag{9.13}$$

The quantity $\hat{r}.\hat{n}dA$ is approximately equal to the projection of the area element dA on the central sphere, i.e.

$$\hat{r}.\hat{n}\,dA = 4a^2 \sin\theta_2 d\theta_2 d\phi_2 \quad ,$$

where ϕ_2 is the azimuthal angle corresponding to the polar angle θ_2, shown in figure (5.1). Substituting this result in (9.13) and using the approximate expression (7.11) which relates the distance h of the surface $\mathcal{S}^+$ from the central sphere to the angle θ_2, we find

$$\frac{\mathcal{C}\mu}{n^2 H} = \frac{1}{9.6}\left(\frac{a}{h_{min}}\right)^{1.78} \int_0^{\pi/2} \frac{(1-.745\sin^2\theta_2)^{12.2} \sin\theta_2 d\theta_2}{\left[\log\left\{\frac{a}{h_{min}}(1-.745\sin^2\theta_2)^{6.87}\right\}\right]^{.29}} \quad , \qquad (9.14)$$

where

$$\frac{h_{min}}{a} = 4 \times 10^{-5}. \qquad \begin{matrix}(7.12)\\(\text{repeated})\end{matrix}$$

Using a conditionally convergent scheme (based on the trapezoidal rule) to estimate the integral in (9.14) we have found

$$\frac{\mathcal{C}\mu}{n^2 H} = 2.04 \times 10^5 \; .$$

As both method for computing the limiting coagulation rate involve simplifying assumptions, the six percent different between the two computed values is quite acceptable.

Previous Theoretical Work

The first theoretical investigation into the effect of shear flow on coagulation was carried out by Smoluchowski (1917), who neglected the hydrodynamic interactions between the pairs. He assumed that particles translate with the bulk fow and coagulated upon "collision" with other particles. Thus the pairs which coagulate lie within a circular cylinder of radius 2a, centred on the x_1 axis in pair space. We shall refer to this cylinder as the "collision cylinder". The coagulation rate is simply equal to the rate at which pairs pass through any cross-sectional area of the collision cylinder, and is given by

$$\mathcal{C} = \frac{16 n^2 K a^3}{3} . \qquad (9.15)$$

Curtis and Hocking (1970) attempted to improve on this analysis by taking into account the hydrodynamic interactions between the particles. These authors realized that only a fraction of those pairs which move within the collision cylinder will in fact coagulate. Unfortunately their work is based on the erroneous expression

$$\mathcal{C} = \frac{16}{3} E n^2 K a^3 \tag{9.16}$$

for the coagulation rate, where E is the fraction of the cross-sectional area of the collision cylinder at points far upstream, through which pass the pairs which eventually coagulate. This expression does not take into account the fact that pairs do not all move with the same velocity. The remaining theoretical section of that paper is devoted to the calculation of the quantity E, referred to as the "collison cross section", and there is no way to compare their results with the values of coagulation rate calculated here.

In addition to the error in the expression (9.16) for $\mathcal{C}$, Curtis and Hocking were unaware of the region of closed trajectories, and hence they did not realize that some of the pairs which do not coagulate on their first encounter coagulate when they are brought together again by the bulk flow.

5.10 Conclusion

In this chapter we have studied the effect of shear rate on coagulation for the cases

$$\frac{\mu a^3 K}{H} \ll 1 \quad ,$$

and

$$\left(\frac{\mu a^3 K}{H} , \frac{\mu a^3 K}{kT}\right) \gg 1 \; .$$

From these investigations we can construct a qualitative picture of the effect of shear on coagulation for the entire range of shear rates.

At zero shear rate, the quantity $\frac{\mu \mathcal{C}}{n^2 H}$ is given by the expression (5.10), which has the asymptotic form

$$\frac{\mu \ell}{n^2 H} \sim \frac{16}{3} \frac{kT}{H} \Big/ \log \frac{kT}{H} \qquad \text{as } \frac{kT}{H} \to \infty . \qquad (5.14)\ \text{(repeated)}$$

In § 5.5 we mentioned that the slope of the curve $\frac{\mu \ell}{n^2 H}$ vs $\frac{\mu a^3 K}{H}$ is zero at $\frac{\mu a^3 K}{H} = 0$ because the coagulation rate is unaffected by the direction of shear.

Combining this information with the results obtained for high shear rates, we find that the curve of $\frac{\mu \ell}{n^2 H}$ is likely to have the form shown in figure (5.10).

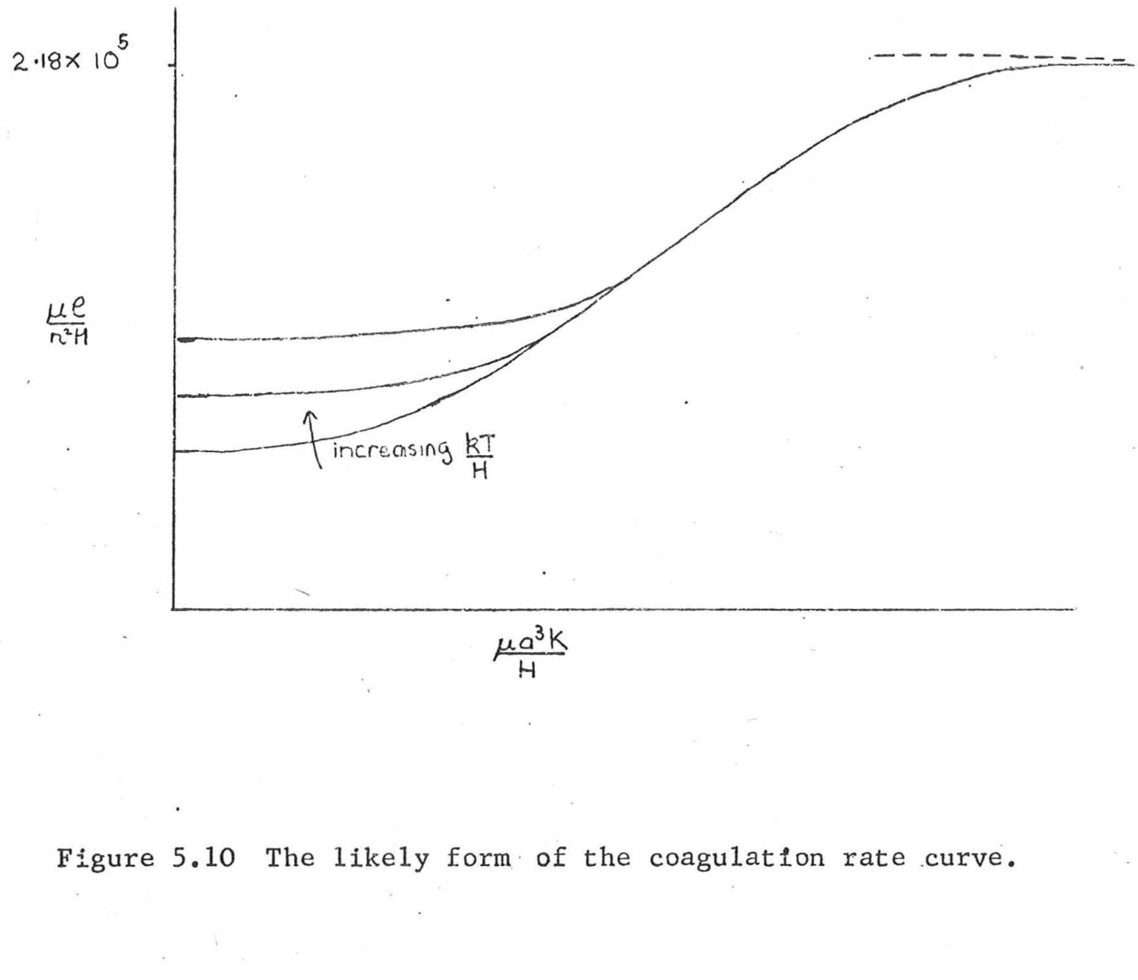

Figure 5.10 The likely form of the coagulation rate curve.

CHAPTER SIX

THE EFFECT OF ELECTRICAL FORCES ON THE MOTION OF PARTICLES IN SHEAR FLOW

6.1 Introduction.

In the previous chapter we mentioned that particles suspended in a liquid are generally charged, and that this charge gives rise to a repulsive force between the particles. It is these electrical forces which are responsible for the stability of most suspensions, but as we were interested in chapter 5 in the process of coagulation, we assumed that the electrical forces had been effectively removed by the addition of electrolyte to the suspension.

This chapter is concerned with the effect of shear flow on a suspension of spherical particles in which there are significant electrical forces. As before, we assume that the suspension is dilute and therefore that interacting pairs of particles are unaffected by the other particles in the suspension. Our aim is to determine the effect of shear rate on the relative motion of these interacting sphere-pairs, in the absence of Brownian motion.

The chapter begins with a description of the electrical force between a pair of spheres in suspension. It is shown that the range of action of this force is characterized by a length D, known as the "Debye length", which depends on the concentration of ions in the suspending medium. We shall be concerned with the case

$$D \ll a$$

where a is the particle radius. If this condition is satisfied, the electrical forces only affect the motion of nearly-touching pairs, and as we have seen in chapter 5, the equations describing the motion of these pairs have a relatively simple form.

In §6.3 we combine the expression for the Van der Waals force between a pair of nearly touching spheres with the formula for the electrical force for the case $D \ll a$, to obtain the total force between a pair of particles. By substituting this result in the expressions derived in the previous chapter for the relative velocity of a nearly-touching sphere-pair we obtain the equations of motion of these pairs, and in §6.4 some numerical solutions to these equations are presented.

It is shown that at low shear rates, the bulk flow simply provides a mechanism for bringing pairs together. The electrical repulsive forces prevent the pairs from coming into contact and instead they orbit each other with an average separation distance of the order of D. These orbits become unstable at higher shear rates and the pairs are torn apart. At still higher shear rates the flow pushes pairs together with such force that some coagulate. In § 6.5 we obtain a lower bound for the shear rate at which the particles are torn apart, and an approximate expression for the shear rate at which pairs begin to coagulate.

6.2 The Electrical force between a pair of spherical particles

In calculating the force between a pair of particles we must take into account not only the charges of the particles but also the distribution and type of ions in the solvent. The ions tend to cluster around particles of opposite charge and so "neutralize" the particle charge. This layer of counterions which surrounds each particle is referred to as "the electrical double layer" and it is the thickness of the double layer which determines the range of action of the electrical force between particles.

In equilibrium, the ions in the solvent are distributed according to the Boltzmann equation. If there are only two types of ion, of valency $+v$ and $-v$ respectively, then their number densities are given by

$$n_-(\underset{\sim}{x}) = n \exp(ev\Psi(\underset{\sim}{x})/kT) , \tag{2.1}$$

$$n_+(\underset{\sim}{x}) = n \exp(-ev\Psi(\underset{\sim}{x})/kT) , \tag{2.2}$$

where n is the number density of ions of either type at great distances from the particles, $\Psi(\underset{\sim}{x})$ is the potential at a point $\underset{\sim}{x}$ in the liquid, e is the charge on an electron, T is the absolute temperature of the system and k is Boltzmann's constant.

The potential ψ is related to the charge density ρ by Poissons equation

$$\nabla^2\psi = -\frac{4\pi\rho}{\varepsilon} \tag{2.3}$$

where ε is the dielectric constant of the solvent. Substituting

$$\rho = e\nu(n_+ - n_-)$$

in (2.3) and using the expression (2.1) and (2.2) for n_+ and n_- we obtain the differential equation for ψ :

$$\nabla^2\psi = \frac{8\pi e\nu n}{\varepsilon} \sinh\left(\frac{e\nu\psi}{kT}\right) . \tag{2.4}$$

If the condition

$$\frac{e\nu\psi}{kT} \ll 1 \tag{2.5}$$

is satisfied, we can replace (2.4) by the linear equation

$$\nabla^2\psi = \frac{\psi}{D^2} , \tag{2.6}$$

where

$$D = \left(\frac{\varepsilon kT}{8\pi n e^2 \nu^2}\right)^{\frac{1}{2}} \tag{2.7}$$

is called the "Debye length". In the work that follows we shall assume that the condition (2.5) holds and therefore that equation (2.6) is valid.

The boundary conditions associated with equation (2.6) are

$$\psi \approx 0 , \quad \text{at points far from the particles,} \tag{2.8}$$

and on the surface of each particle, ψ has the uniform value ψ_0 . In equilibrium, the quantity ψ_0 is determined by the concentration of certain types of ions in the solvent. For example, the potential of Silver Iodide particles in water is determined by the concentration of

Silver or Iodide ions in the solvent (Verwey and Overbeek (1948) pp 47) and is unaffected by the concentration of other ions. The position of the particles has no effect on the value of ψ_0 , and thus if the particle configuration is altered, the charge density on the particle surfaces alters in order that the potential of the particles remains ψ_0.

The solution to equation (2.6) and the associated boundary conditions for a single spherical particle of radius a, alone in an infinite liquid is given by

$$\psi(r) = \psi_0 \frac{a}{r} \exp\left(\frac{a-r}{D}\right), \tag{2.9}$$

where r is the distance from the centre of the particle. The potential decays on a length scale D, and D may be regarded as the "double layer thickness" referred to at the beginning of this section. If the surfaces of a pair of spheres are separated by a distance greater than several Debye lengths, the field of each particle is approximately given by (2.9) and therefore there is no force between the particles.

To find the field ψ surrounding a pair of spheres at smaller separation distances, we must solve equation (2.6), subject to the boundary conditions (2.8) and

$\psi = \psi_0$ on the surface of either sphere.

The charge Q on either particle is related to the potential by Gauss' law

$$Q = \frac{-\varepsilon}{4\pi} \int_A \nabla\psi \cdot \hat{n} \, dA \tag{2.10}$$

where $\hat{n}$ is the unit normal and A denotes the surface of the particle . Verwey and Overbeek ((1948) pp 144) have shown that if ψ satisfies (2.6) the electrical potential energy of the pair of particles is given by

$$V(r) = \psi_0 (Q(\infty) - Q(r)) \tag{2.11}$$

where r denotes the distance between the centres of the spheres, and thus the force acting on either particle is

$$F_R(r) = \psi_0 \frac{dQ(r)}{dr}. \qquad (2.12)$$

Thus from the solution of equation (2.6) for the field ψ surrounding a pair of spheres, we can obtain the electrical force of repulsion between the spheres.

The equation (2.6) for ψ is linear, and from (2.10) it can be seen that Q is proportional to $\varepsilon\psi_0$, and thus (2.12) may be written in the form

$$F_R(r) = \varepsilon\psi_0^2 f_R(r/a, D/a). \qquad (2.13)$$

For the case of "thin double layers" (D << a), the force between the particles is only significant if the particles are nearly touching, and is dominated by the repulsive force between parts of the two surfaces which are nearly in contact. Those surfaces can be locally approximated by parallel flat plates, and with the aid of the expression for the force between a pair of plates, it can be shown that (Verwey and Overbeek (1948) pp 56)

$$F_R(r) = \frac{\varepsilon a \psi_0^2}{2D} \frac{e^{-h/D}}{1 + e^{-h/D}}, \qquad (2.14)$$

where h = r-2a is the minimum distance between the two surfaces.

Formulae for F_R have been obtained for other limiting cases (Russel (1976)) but we are mainly concerned with thin double layers and we shall not repeat these formulae here.

The expression (2.14) for F_R only holds if the linear equation (2.6) for ψ is valid. Verwey and Overbeek (pp 140) solved the exact equation (2.4) for ψ numerically for the case D << a and found that the expression (2.14) for the force is approximately correct if

$$\frac{\nu e \psi_0}{kT} \lesssim 2 .$$

If the ions have a valency of one, this constraint implies

$$\psi_0 \lesssim 50\,\mathrm{mV}.$$

6.3 The net force between a pair of particles

Opposing the electrical repulsion between particles is the Van der Waals force, which for a pair of spherical particles is given by

$$F_A(r/a) = -\frac{H}{a} f_A(r/a) \qquad (5.2.9)\ \text{(repeated)}$$

where

$$f_A(s) = \frac{1}{6}\left\{\frac{4s}{(s^2-4)^2} + \frac{4}{s^3} - \frac{8}{s(s^2-4)}\right\} , \qquad (5.2.10)\ \text{(repeated)}$$

and H is the Hamaker constant.

The force $F_T(^r/a)$ between a pair of particles is the sum of the Van der Waals attraction and the electrical repulsion, which from (5.2.9) and (2.13) is given by

$$F_T(r/a) = \frac{H}{a}\left\{ - f_A(r/a) + \frac{\varepsilon\psi_0^2 a}{H} f_R(r/a, D/a)\right\} . \qquad (3.1)$$

The form of the force-distance curve is thus determined by the parameters

$\frac{\varepsilon\psi_0^2 a}{H}$ and D/a.

If the particles are nearly in contact the Van der Waals force is given approximately by

$$F_A \approx -\frac{Ha}{12h^2} , \qquad \text{(see (5.2.11))},$$

and combining this with the expression (2.14) for the electrical force between a pair of particles with thin double layers, we find that

$$F_T(h') \approx \frac{Ha}{12D^2}\left\{\frac{-1}{h'^2} + \frac{\lambda e^{-h'}}{1+e^{-h'}}\right\}, \tag{3.2}$$

where $h' = h/_D$ is the minimum separation distance between the particles in Debye lengths, and

$$\lambda = \frac{6\varepsilon\psi_0^2 D}{H} \ . \tag{3.3}$$

The result (3.2) is valid if both h and D are << a.

Although we are only concerned with the case of spherical particles, we note that the expression (3.2) for F_T holds for any pair of nearly touching particles, provided the surfaces are locally smooth. In this case the quantity a is an effective radius, given by

$$a = \sqrt{b_1 b_2} \ , \tag{3.4}$$

where b_1 and b_2 appear in the quadratic expression for the thickness of the liquid layer between the particles (c.f. 2.4.1.)). This result follows from the fact that both the Van der Waals and electrical force between a pair of nearly touching particles are dominated by the forces between the parts of the particles which are nearly in contact.

From (3.2) it can be seen that the form of the force-distance curve for a pair of nearly-touching particles is determined only by the parameter λ . Several such curves are illustrated in figure (6.1) for different λ values, and from that figure it can be seen that if

$$\lambda > 2.08 \tag{3.5}$$

there is a repulsive force between particles over an intermediate range of separations. Thus for any $\lambda > 2.08$ there are two separation distances at which $F_T = 0$. The larger of these separations corresponds to a stable equilibrium point and is denoted by h_E.

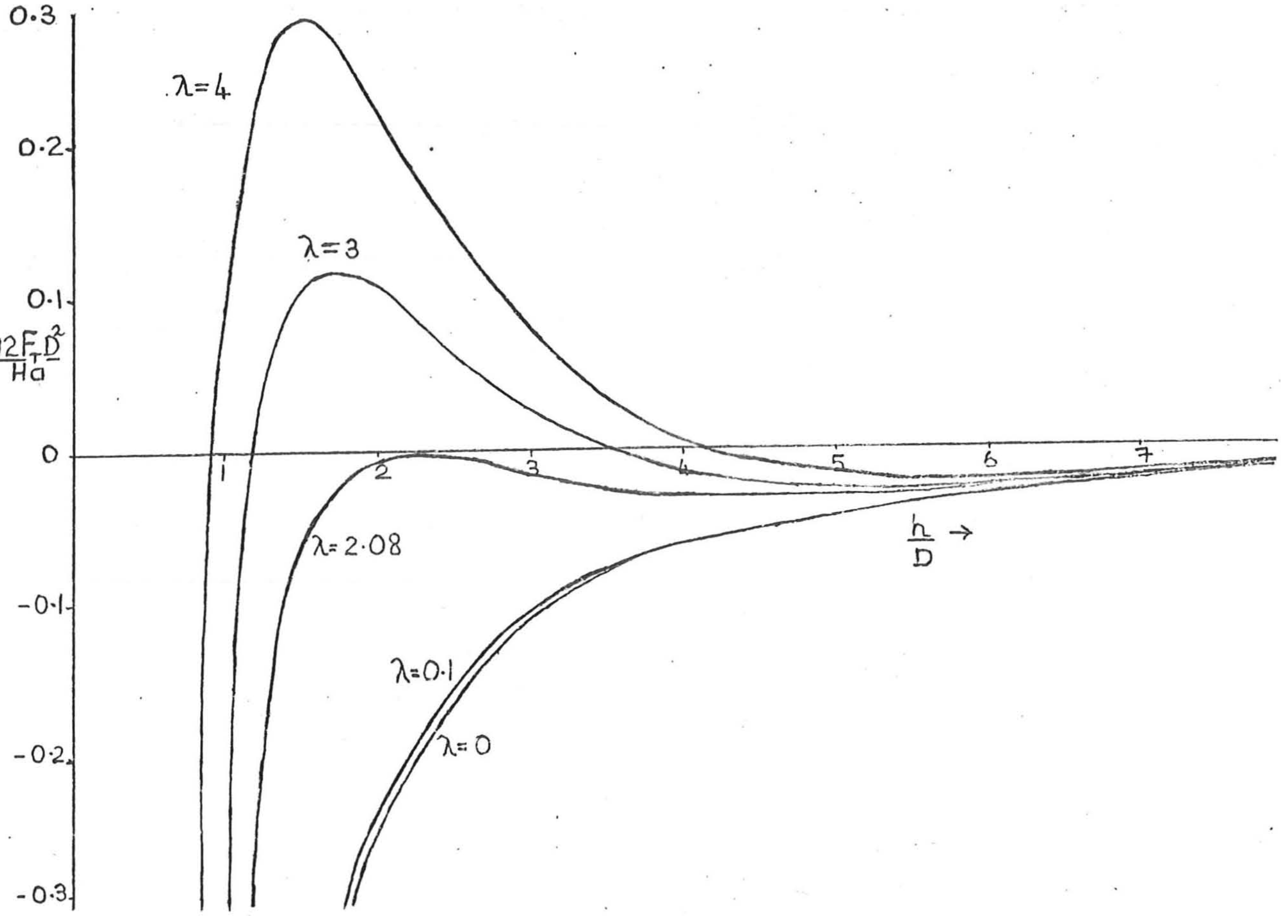

Figure 6.1 Curves describing the variation of the force F_T between a pair of particles with separation h, for various values of the parameter λ . Positive values of F_T correspond to repulsion between particles.

Substituting the expression (3.3) for λ in (3.5), we find that for $\psi_0 = 50$ mV, and H = 10^{-15} ergs the constraint (3.5) is satisfied if

$$D > .015 \text{ microns} .$$

In deriving these results we have assume that $D/_a \ll 1$, and thus if $\lambda = 2.08$, the formula (3.2) for F_T is only valid if

$$a \gtrsim 1 \text{ micron}.$$

From (3.3) it can be seen that λ is proportional to D and therefore as λ increases, the range of particle sizes for which (3.2) is valid decreases.

Before proceeding to the description of the relative motion of sphere pairs in shear flow under the action of the force given by (3.2), we shall pause to consider the implications of an assumption made in chapter five. In that chapter it was assumed that the electrical forces between the particles could be removed by the addition of sufficient electrolyte to the solvent. From figure (6.1) it can be seen that, for the case of thin double layers, the assumption is valid if

$$\lambda < 0.1$$

and with the aid of the expressions (3.3) for λ and (2.6) for D, this becomes

$$n > 10^{-1} \text{ moles}/_{\text{litre}} , \quad \text{for } \psi_0 = 50\text{mV},$$

which for the case of NaCl is equivalent to a concentration of 5.8 gms/$_{\text{litre}}$.

6.4 The relative motion of sphere pairs in shear flow

In this section we shall describe the effect of electrical and Van der Waals forces on the relative motion of nearly-touching sphere pairs in a shear flow. We assume that the expression (3.2) for the force between a pair of particles is approximately valid, even though the particles are in motion. Russel (1976) has shown that this is the case of both the Electric Hartman number $\dfrac{\varepsilon\psi_0^2}{4\pi\mu\omega kT}\dfrac{a}{D}$ and the Peclēt number $\dfrac{aU}{\omega kT}$ are small, where w is the mobility of the ions and U is here the typical velocity in the thin liquid layer between the spheres.

The requirement that the Peclet number be small places a restriction on the magnitude of the velocity difference $\underset{\sim}{V}$ between the centres of the sphere-pair. By the methods of lubrication theory it can be shown that the component of $\underset{\sim}{V}$ along the line of centres of the pair V_r gives rise to a velocity of order $V_r\sqrt{\frac{a}{h}}$ in the liquid layer. Superposed on this squeezing motion is a shearing motion which arises because spheres slide over one another as the pair rotates in the shear flow. This motion is unaffected by the force between the spheres and from expressions derived by Batchelor and Green (1972(a) §5) it can be shown that this sliding motion gives rise to a velocity in the liquid layer of order $\frac{aK}{\log(a/h)}$, where K is the shear rate. Thus if the Peclet number is to be small, we must have

$$\frac{a^2K}{\omega kT\log(\frac{a}{h})} \ll 1 \quad \text{and} \quad V_r a\sqrt{\frac{a}{h}}\Big/\omega kT \ll 1 .$$

In the work that follows, we shall assume that these constraints are satisfied, and therefore that the expression (3.2) for the force between a nearly touching pair is valid.

If the suspension is at rest, the force F_T between the pairs causes them to move with a relative velocity V", given by

$$\underset{\sim}{V}''(\underset{\sim}{r}) = \frac{G(r/a)}{3\pi\mu a} F_T \hat{r} , \qquad (5.2.7)\ (\text{repeated})$$

where $\hat{r}$ is the unit vector in the direction of the line of centres of the pair. If the pair are nearly in contact, G may be replaced in this expression by the formula (5.2.8) and on substituting the expression (3.2) for F, we obtain

$$\underset{\sim}{V}''(h') = \frac{Hh}{18\pi\mu a D^2}\left\{\frac{\lambda e^{-h'}}{1+e^{-h'}} - \frac{1}{h'^2}\right\} . \qquad (4.1)$$

The relative velocity of a sphere pair in shear flow under the action of the force F_T, is found by combining (4.1) with the expressions (5.2.4) and (5.2.5) for the relative velocity of a force-free pair in shear flow, and on substituting the asymptotic formulae (5.2.6) for A and B we get

$$\frac{dh'}{dt} = 8\cdot154 \sin\phi \cos\phi \sin^2\theta \, h' + \beta\left(\frac{\lambda e^{-h'}}{1+e^{-h'}} - \frac{1}{h'^2}\right)h' \quad , \qquad (4.2)$$

$$\frac{d\phi}{dt} = -[\cdot797 - \cdot594 \cos^2\phi] \quad , \qquad (4.3)$$

and

$$\frac{d\theta}{dt} = \cdot594 \sin\theta \cos\theta \sin\phi \cos\phi \quad , \qquad (4.4)$$

where $\beta = \frac{H}{18\pi\mu a D^2 K}$

t is the time in units of K^{-1}, and the angles θ and ϕ describing the orientation of the vector $\underset{\sim}{r}$ between the centres are illustrated in figure (5.1).

As mentioned in chapter 5, the rate of rotation of a sphere pair is not altered by the force between the particles, and the angular motion of the pairs is described by

$$\tan\theta(\phi) = \frac{\tan\theta(\pi/2)}{\sqrt{1 - \cdot745 \cos^2\phi}} \quad , \qquad \begin{matrix}(5.7.9)\\ \text{(repeated)}\end{matrix}$$

where $\theta(\frac{\pi}{2})$ is the azimuthal angle of the pair at $\phi = \frac{\pi}{2}$.

Dividing (4.2) by (4.3) and eliminating $\sin\theta$ with the aid of (5.7.9), we obtain the differential equation for h':

$$\frac{dh'}{d\phi} = \frac{-\beta h'\left(\frac{\lambda e^{-h'}}{1+e^{-h'}} - \frac{1}{h'^2}\right)}{\cdot797 - \cdot594\cos^2\phi} - \frac{8\cdot154 \sin\phi\cos\phi\tan^2\theta(\frac{\pi}{2})\,h'}{(\cdot797 - \cdot594\cos^2\phi)(1+\tan^2\theta(\frac{\pi}{2}) - \cdot745\cos^2\phi)} \quad . \qquad (4.5)$$

By numerically integrating this equation we have obtained the relative trajectories of sphere pairs for various values of β, λ and

$\Theta(\pi/2)$. In order to describe these trajectories we shall again use the concept of a pair space together with the notation introduced in § 5.3. Thus the "trajectory of a pair" is the path followed by the point in pair space which corresponds to that pair[+].

Since equation (4.5) is only valid for nearly-touching spheres, we can only describe the trajectories of pairs which lie in a thin layer surrounding the central sphere. A family of such trajectories for $\beta = 307$, $\lambda = 10$ and $\Theta(\pi/2) = \pi/2$ are illustrated in figure (6.2). From that figure it can be seen that pairs which enter the region $h/D < 12$, $\phi > \frac{\pi}{2}$ move onto a common closed trajectory. Although we cannot describe the motion of the pairs which are not nearly touching, we can show that the only pairs which execute closed trajectories in the plane of the flow for this value of (λ, β) are those which move on the closed trajectory shown in figure (6.2). To prove this assertion, we note that any pair which moves on a closed trajectory must pass through "the region of closed trajectories" defined in §5.6, and once in that region, the pair cannot escape without passing into the region $h < h_E$, where there is a force of repulsion between the particles. From figure (6.2) it can be seen that all pairs which enter the region $h < h_E$ move onto the closed trajectory and therefore this is the only closed trajectory in the plane of the flow.

The trajectories of pairs for $\beta = 307$, $\lambda = 10$ and $\Theta(\frac{\pi}{2}) \neq \frac{\pi}{2}$ are similar to those shown in figure (6.2), except that the closed trajectory is more circular at lower values of $\Theta(\frac{\pi}{2})$. Thus for $\lambda = 10$ and $\beta = 307$, the shear flow brings pairs together and thereafter the pairs execute closed orbits with a mean separation of order h_E.

As β is increased (i.e. as shear rate is decreased) beyond 307 the closed trajectory becomes less distorted, as can be seen from figure (6.3).

[+] There are actually two points associated with each pair, here we refer to the point which lies in the half-space $x_2 > 0$.

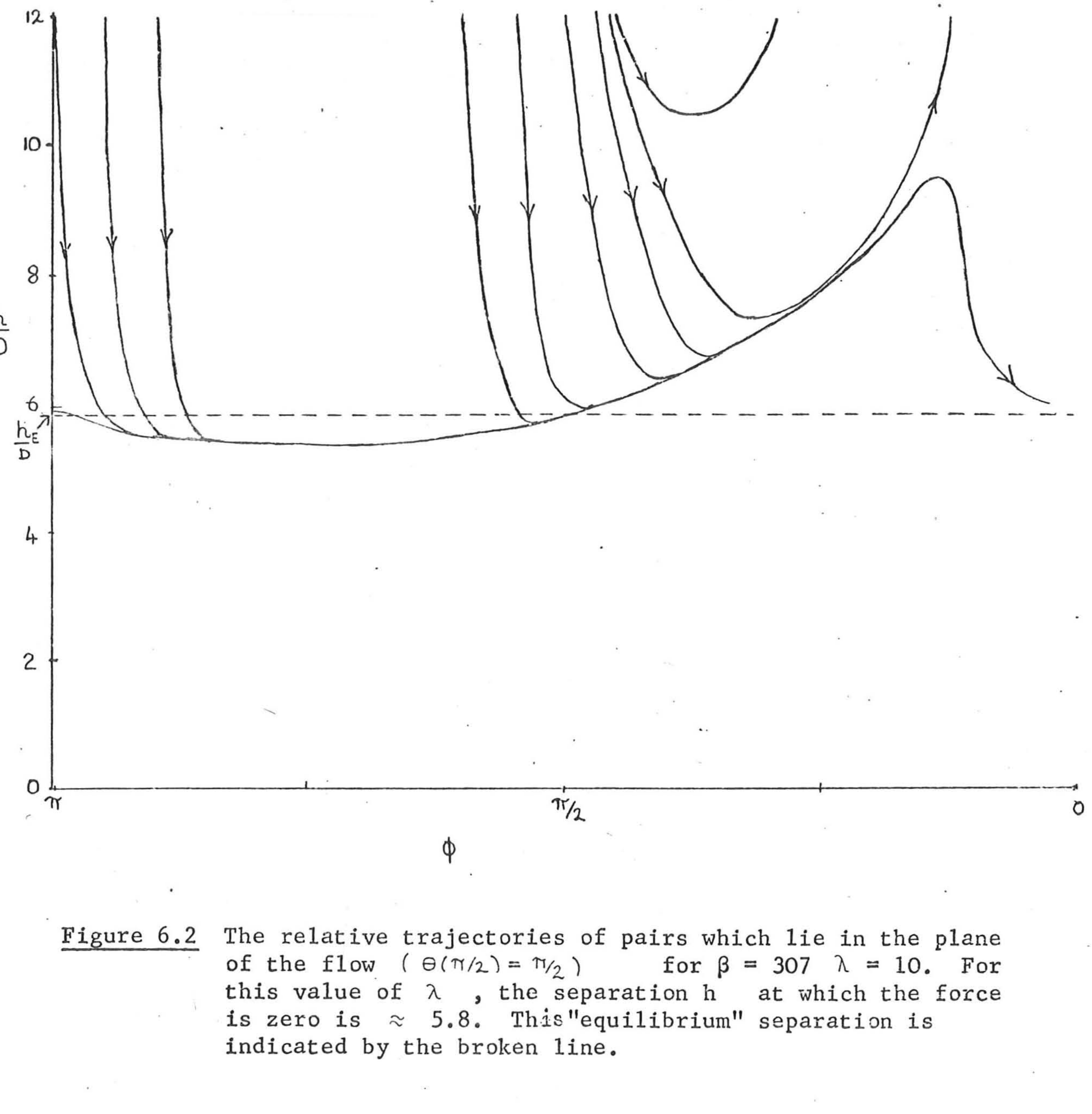

Figure 6.2 The relative trajectories of pairs which lie in the plane of the flow ($\theta(\pi/2) = \pi/2$) for β = 307 λ = 10. For this value of λ , the separation h at which the force is zero is $\approx$ 5.8. This "equilibrium" separation is indicated by the broken line.

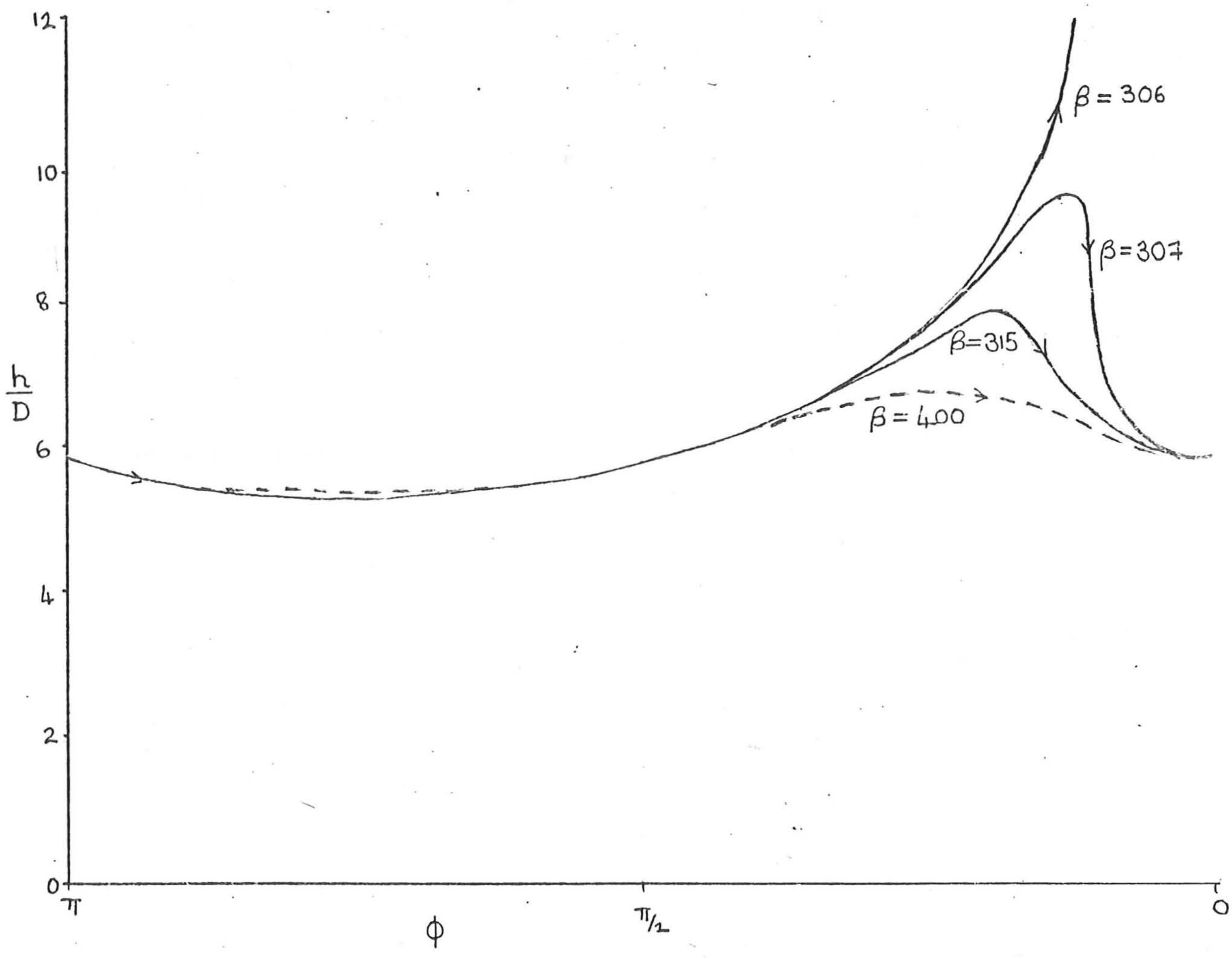

Figure 6.3 The effect of variations in β on the common trajectory for $\Theta(\pi/2) = \pi/2$, λ = 10. For $\beta \gtrsim 307$, this common trajectory is also the only closed trajectory in the plane of the flow.

However if β is decreased below 307, the closed trajectory for $\lambda = 10$ $\Theta(\frac{\pi}{2}) = \frac{\pi}{2}$ appears to become unstable (see figure (6.3)), and pairs on this trajectory move apart rapidly in the region $\phi < \frac{\pi}{4}$ and are soon separated by a distance of many Debye lengths.

We cannot predict the path of the trajectories beyond this point, for unless D/a is extremely small, the equations (4.2), (4.3) and (4.4) are not valid at these large separations. The value of β at which the closed trajectory is pulled into the region $h/D \gg 1$ (where the electrical forces are negligible) is denoted by $\beta^*(\lambda, \Theta(\pi/2))$. It seems likely that the Van der Waals attraction may hold pairs on closed orbits for $\beta < \beta^*$ and that at a critical value of β (which depends also on D/a) the pairs are torn apart by the flow. The quantity β^* provides an upper bound for this critical value, and in the following section we shall obtain an approximate formula for β^*.

For $\beta < \beta^*$ some of the pairs which enter the region in which the electrical forces are significant still join a common trajectory (see figure (6.4)), but as β decreases the fraction of pairs which move onto this common trajectory decreases, and the angle ϕ at which that trajectory leaves the region of significant electrical forces increases.

Finally, at extremely high shear rates, the pattern of the trajectories changes again, for pairs are pushed together with such force by the shear flow that some are able to overcome the repulsive force and coagulation occurs. The value of β at which pairs begin to coagulate is denoted by $\beta^{**}(\phi, \Theta(\frac{\pi}{2}))$. The form of the trajectories at these very high shear rates is illustrated in figure (6.5) for the case $\lambda = 10$, $\beta = 1$ ($< \beta^{**}$) and $\Theta(\pi/2) = \pi/2$.

6.5 Approximate formulae for β^* and β^{**}

By numerically integrating equation (4.5) for a number of values of β, with λ and $\Theta(\pi/2)$ held fixed, we have been able to determine

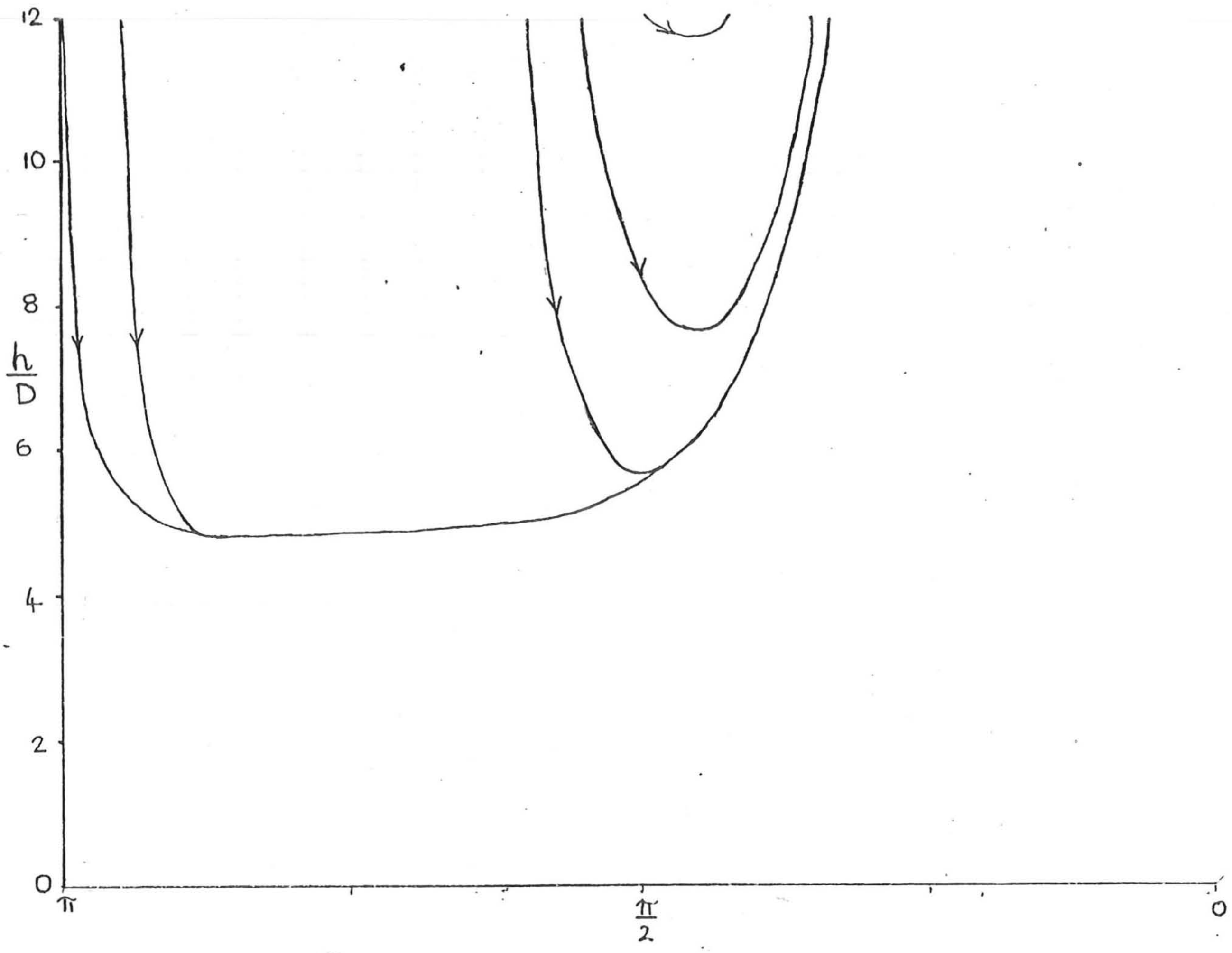

<u>Figure 6.4</u> Trajectories in the plane of the flow for $\lambda = 10$, $\beta = 100$.

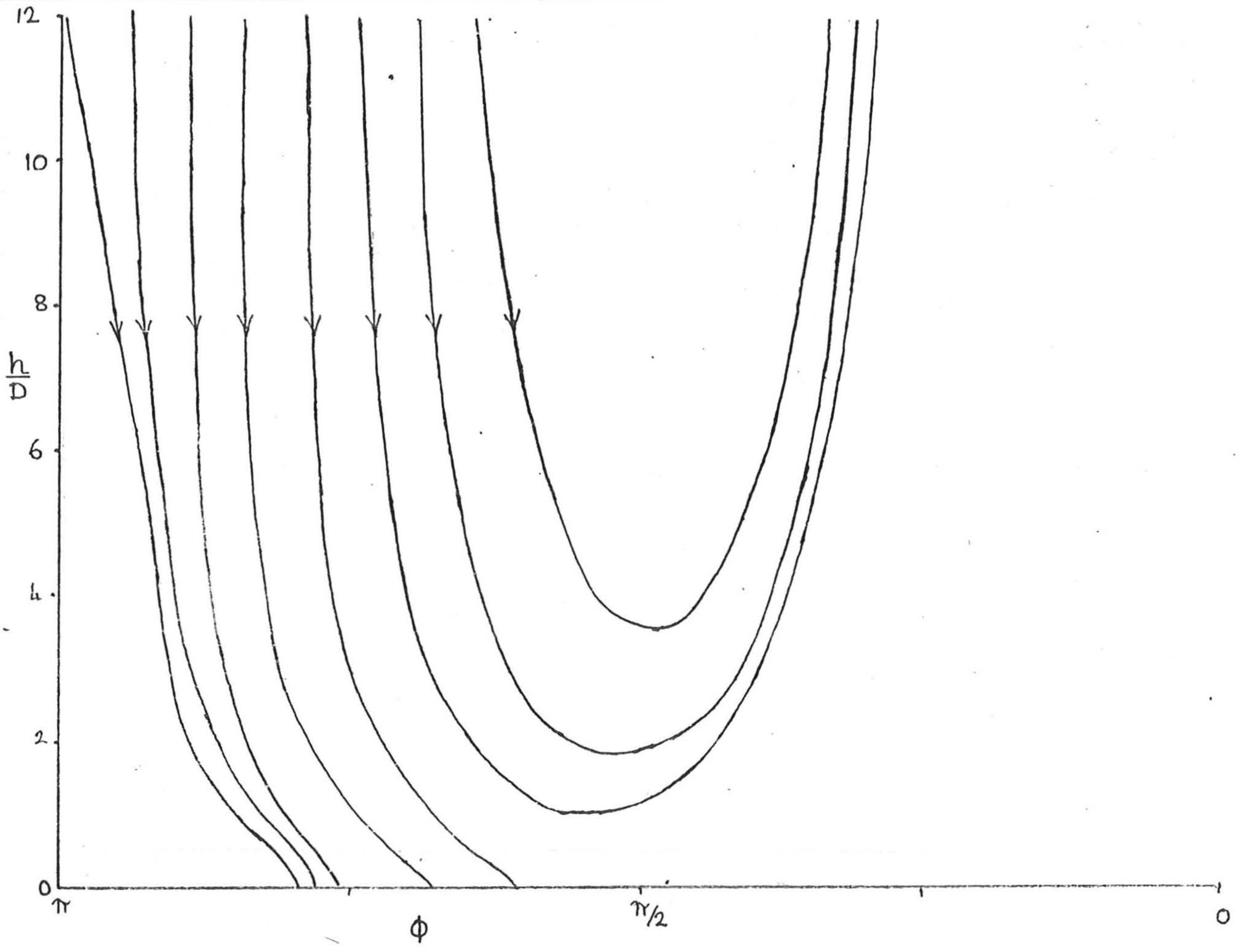

Figure 6.5 At very high shear rates, some pairs coagulate. The trajectories shown in this figure are those of pairs which lie in the plane of the flow for $\lambda = 10$, $\beta = 1$.

β^* and β^{**} for values of λ and $\theta(\pi/2)$. The results, for $\theta(\pi/2) = \pi/2$ are shown in figure (6.6). From that figure it can be seen that as $\lambda \to 2.08$ from above $(\beta^* - \beta^{**}) \to 0$, and for $\lambda < 2.08$ the phenomena described in the previous section do not occur; pairs simply coagulate at all shear rates.

Although it does not seem possible to obtain expression for β^* and β^{**} directly from the equation of motion of the pairs, we can obtain useful bounds for these quantities.

We begin by rewriting equation (4.5) in the form

$$\frac{dh'}{d\phi} = \frac{-\beta h' F(h')}{\cdot 797 - \cdot 594 \cos^2\phi} - \frac{8\cdot 154 \sin\phi \cos\phi \tan^2\theta(\frac{\pi}{2}) h'}{(\cdot 797 - \cdot 594\cos^2\phi)(1 + \tan^2\theta(\frac{\pi}{2}) - \cdot 745 \cos^2\phi)} \qquad (5.1)$$

where $F(h') = \frac{12 D^2 F_T(h')}{Ha} = \frac{\lambda e^{-h'}}{1 + e^{-h'}} - \frac{1}{h'^2}$ is the non-dimensional force between the pairs.

The pairs move in the direction of decreasing ϕ and therefore if $\frac{dh'}{d\phi}$ is negative at a point, pairs which pass through that point are moving apart. We can divide pair space into regions in which pairs are moving apart or coming together. The intersection of these regions with the $\theta = \frac{\pi}{2}$ plane is shown in figure (6.7) for $\beta = 210$, $\lambda = 3$.

On the boundaries of these regions $\frac{dh'}{d\phi} = 0$ and therefore the coordinates (h', ϕ) of points on the boundaries satisfy

$$F(h') = \frac{-8\cdot 154 \sin\phi \cos\phi \tan^2\theta(\frac{\pi}{2})}{\beta(1 + \tan^2\theta(\frac{\pi}{2}) - \cdot 745 \cos^2\phi)} \qquad (5.2)$$

From figure (6.7) it can be seen that for $\beta = 210$ and $\lambda = 3$ there is no way for pairs to pass from the region B to the region A, for between these regions there is an area in which $\frac{dh'}{d\phi} > 0$. Thus there is a stable closed trajectory for this value of β.

The coordinates of points which lie on the boundaries of these regions for $\lambda = 3$ may be found from (5.2) together with the force distance curve for $\lambda = 3$ shown in figure (6.1). If $\phi < \frac{\pi}{2}$, the expression (5.2)

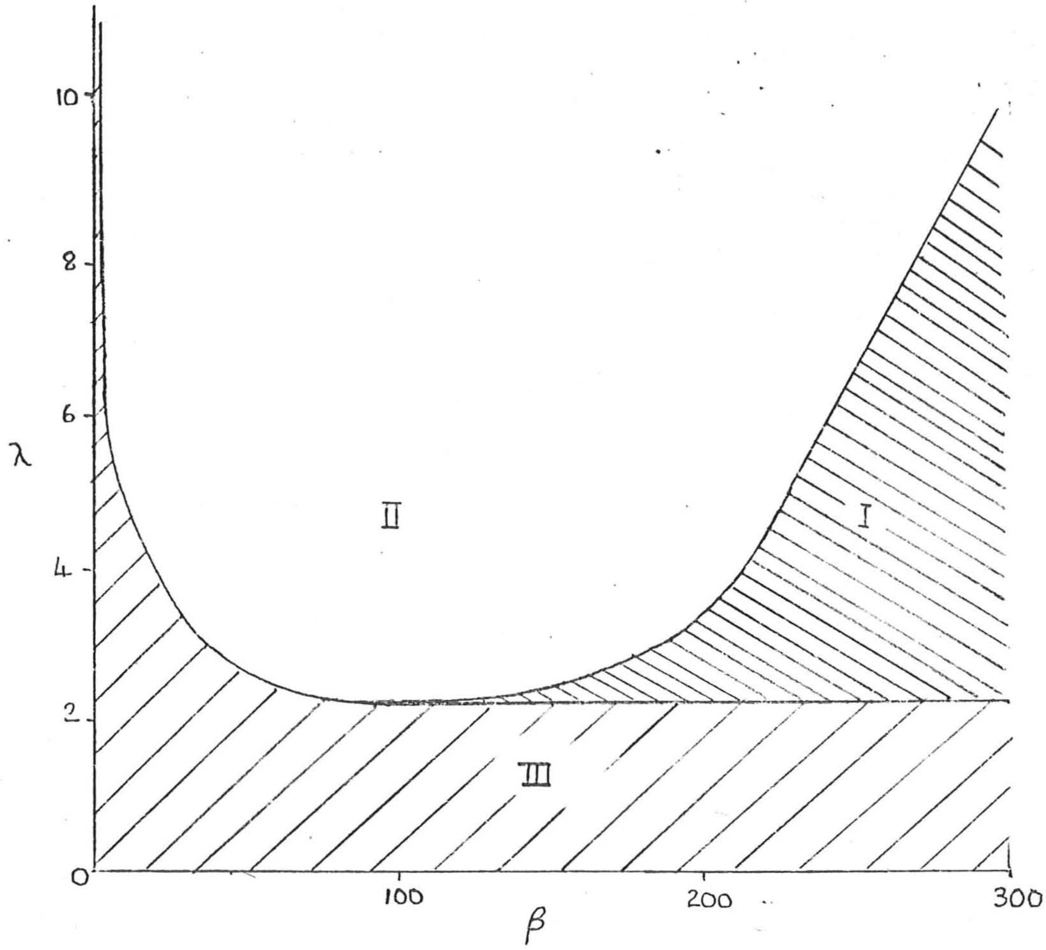

Figure 6.6 The variation of β^* and β^{**} with λ , for $\theta(\pi/2) = \pi/2$. If $\lambda > 2.08$, then at low shear rates ($\beta > \beta^*$), the point (β,λ) lies in region I and the flow brings pairs onto a closed trajectory with average separation of order h_E . For $\beta < \beta^{**}$, (β,λ) lies in region II and the flow pushes the pairs together with such force that some coagulate. Finally, if $\beta^{**} < \beta \leqslant \beta^*$ (region II) the pairs either orbit each other with an average separation $\gg h_E$, or are pulled apart by the flow, depending on the value of D/a

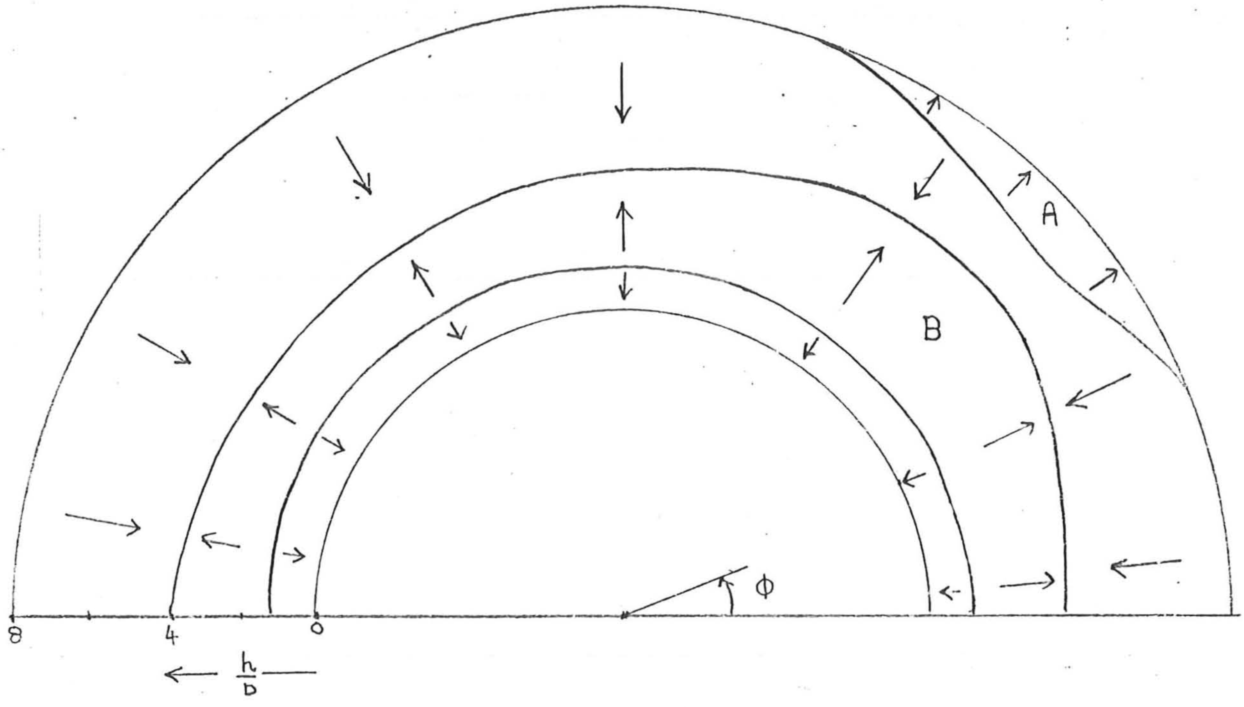

Figure 6.7 We can divide pair space into regions in which pairs move together or apart. The intersection of these regions with the $\theta = \pi/2$ plane is shown in this figure for the case $\lambda = 3$, $\beta = 210$ and $h/D < 8$. It can be seen that no trajectories can pass from region B to region A and hence there is a unique closed trajectory at this value of β.

for $F(h')$ is negative and from figure (6.1) it can be seen that there are at most 3 values of h' (for a given ϕ) which satisfy (5.2). If β is decreased with ϕ held fixed, two of those points converge and eventually meet at the local minimum of the force curve. Hence as β is decreased the regions A and B come together.

The angle ϕ at which the regions first touch is the angle at which

$$\frac{\sin\phi\cos\phi}{1+\tan^2\theta(\pi/2) - \cdot 745\cos^2\phi}$$

is a maximum. On determining this angle and substituting in (5.2), we find that the value of β at which A and B first come into contact is given by

$$\beta = \frac{4.077\sin^2\theta(\pi/2)}{F_{min}(\lambda)\sqrt{1 - \cdot 745\cos^2\theta(\pi/2)}} \tag{5.3}$$

where $F_{min}(\lambda)$ is the local minimum value of F (i.e. the maximum attractive force for $h > h_E$). At values of β below that given by (5.3) the closed trajectory may become unstable, for pairs can cross from B to A. Thus the expression (5.3) gives an upper bound for β^*.

Similarly it can be shown that an upper bound of β^{**} is given by

$$\frac{4.077\sin^2\theta(\pi/2)}{F_{max}(\lambda)\sqrt{1 - \cdot 745\cos^2\theta(\pi/2)}}, \tag{5.4}$$

where $F_{max}(\lambda)$ is the maximum non-dimensional repulsive force between the pairs.

By comparing the bounds (5.3) and (5.4) with the computed values of β^* and β^{**}, we have found that both quantities are approximately given by

$$(\beta^*, \beta^{**}) = \frac{3.6.\sin^2\theta(\pi/2)}{(F_{min}(\lambda), F_{max}(\lambda))\sqrt{1 - \cdot 745\cos^2\theta(\pi/2)}}. \tag{5.5}$$

I have been unable to find in the literature any previous investigation into the affect of electrical and Van der Waals forces on the motion of particles in shear flow, and the work presented here is merely a preliminary investigation into this subject. One possible topic for future research is the determination of the critical shear rate at which pairs are torn apart by the flow. This quantity has some practical value for if a suspension is left standing for some time, the force between the particles will draw many of them together and they will then be held by the force at the equilibrium separation distance h_E. To "redisperse" the suspension by shear flow we must shear it at a rate in excess of this critical shear rate; at lower shear rates, the shear flow will simply assist the forces in bringing particles together.

REFERENCES

Abromowitz, M. and Stegun, I.A., 1968 Handbook of Mathematical functions Dover, New York.

Atkinson, K.E. 1976 A Survey of Numerical Methods for the Solution of Fredholm integral equations of the second kind. S.I.A.M.

Adams, D.J. and Matheson, A.J. 1972 Computation of dense random packing of hard spheres. J. Chem. Phys. 56, 1989.

Batchelor, G.K. 1972 Sedimentation in a dilute dispersion of Spheres. J. Fluid Mech. 52(2) 245.

Batchelor, G.K. 1974 Transport properties of two-phase materials with random structure. Ann. Rev. Fluid Mech. 6, 227.

Batchelor, G.K. 1976 Brownian diffusion of particles with hydrodynamic interaction. J. Fluid Mech. 74(1), 1.

Batchelor, G.K. 1977 The effect of Brownian motion on the bulk stress in a suspension of spherical particles. J. Fluid Mech. To be published.

Batchelor, G.K. and Green, J.T. 1972a The hydrodynamic interaction of two small freely-moving spheres in a linear flow field. J. Fluid Mech. 56, 375.

Batchelor, G.K. and Green, J.T. 1972b The determination of the bulk stress in a suspension of spherical particles to order c^2. J. Fluid Mech. 56, 401.

Bernal, J.D. and Mason, J. 1972 Co-ordination of randomly packed spheres Nature 188, 910.

Bertaux, M.G., Bienfait,G. and Jolivet, J., 1975 Etudes des proprietes thermigues des milieux granulaires. Ann. Geophys. 31, 191.

Carter, L.F. 1967 A study of the rheology of suspension of rod shaped particles in a Navier-Stokes liquid. Ph.D. Thesis, University of Michigan.

Curtis, A.S.G. and Hocking, L.M., 1970 Collision efficiency of equal spherical particles in a shear flow. The influence of London Van der Waals forces. J. Coll. Sci. 66, 1025.

Deissler, R.G. and Boegli, J.S. 1958 An investigation of effective thermal conductivities of powders in various gases. Trans. Amer. Soc. Mech. Engrs. p. 1417.

Derjaguin, E.V. and Muller, V.M. 1967 Doklady Phys. Chem. 176, 738.

Dewey, J.M. 1947 The elastic constants of materials loaded with non-rigid fillers. J. Appl. Phys. 18, 578.

Einstein, A. 1956 Investigations on the theory of Brownian Movement. Dover, New York.

Happel, J. and Brenner, H. 1965 Low Reynolds number hydrodynamics. Noordhoff International Publishing, Leyden.

Harris, H.S., Kaufman, W.J. and Krone, R.E. 1966 Orthokinetic flocculation in water purification. Proc. Amer. Soc. Civil Engrs. Sanitary div. 92, 95.

Jeffrey, G.B. 1912 On a form of the solution of Laplace's equation suitable for problems relating to two spheres. Proc. Roy. Soc. A 87, 109.

Jeffrey, D.J. 1973 Conduction through a random suspension of spheres. Proc. Roy. Soc. A 335, 355.

Jeffrey, D.J. 1974 The bulk properties of suspension Ph.D. Thesis, University of Cambridge.

Keller, J.B. 1963 Conductivity of a medium containing a dense array of perfectly conducting spheres or cylinders or non-conducting cylinders. J. Appl. Phys. 34, 991.

Krieger, I.M. 1972 Rheology of monodisperse latices. Adv. Coll. Int. Sci. 3, 111.

Kreyzig, E. 1968 Advanced Engineering Mathematics. 3rd Ed. Wiley.

Lamb, H. 1932 Hydrodynamics. Cambridge Univ. Press.

Landau, L.D. and Lifshitz, E.M. 1959 Theory of elasticity Pergamon Press.

Leyers, H.J. 1972 Warmeleitung Von losen kugelschutten in stagnierenden Medien. Chem. Ing. Techn. 44, 1109.

McKenzie, D.R. and McPhedran, R.C. 1977 Exact modelling of cubic lattic permittivity and conductivity. Nature 265, 128.

Maxwell, J.C. 1873 Electricity and Magnetism Clarendon Press.

Meredith, R.E. and Tobias, C.W. 1960 Resistance to potential flow through a cubical array of spheres. J. Appl. Phys. 31, 1270.

Ottewill, R.H. 1973 Particulate dispersions Chemic. Soc. Spec. Pat. Report Colloid Science Vol. 2.

Protter, M.H. and Weinberger, H.F. 1967 Maximum principles in differential equations Prentice-Hall.

Rayleigh 1892 On the influence of obstacles arranged in rect. order upon the properties of a medium Phil. May. 34, 481.

Runge, I.Z. 1925 Teck-Phys 6, 61.

Russel, W.B. 1977 The Rheology of suspensions of charged rigid spheres J. Fluid Mech. To be published.

Smoluchowski, M.V. 1917 Z. Phys. Chem. (Leipzig) 1917, 92, 127.

Schuman, T.E.W. and Voxx, V. 1934 Heat flow through granulated material Fuel 13, 249.

Scott, G.D. 1960 Packing of equal spheres Nature 188, 908.

Smith, W.O., Foote, P.D. and Busang, P.F. 1929 Phys. Rev. 24, 1271.

Taylor, G.I. 1932 The viscosity of a fluid containing small drops of another fluid. Proc. Roy. Soc. London. Ser A 138, 41.

Turner, J.C.R. 1973 Electrical conductivity of liquid-fluidized beds. A.I.Ch.E. Symp. Series 69, 115.

Turner, J.C.R. 1976 Two phase conductivity: the electrical conductance of liquid-fluidized beds of spheres. Chem. Eng. Sci. 31, 487.

Verwey, E.J.W. and Overbeek J.Th.G. 1948 Theory of the stability of Lyophobic colloids Elsevier 1948.

A1

Details of the Numerical Solutions of the integral equations in Chapter 2

1. The Solution of equation (2.4.8) for the temperature on the surfaces of a pair of nearly touching, locally spherical particles

The equation to be solved is

$$f(\sigma) = \int_0^\infty \frac{1 - f(\sigma')}{\lambda + \sigma'^2} I(\sigma'/\sigma)\, d\sigma' , \qquad (1)$$

where

$$I(\sigma'/\sigma) = \frac{1}{\pi}\int_0^{2\pi} \frac{\sigma' d\phi}{(\sigma^2 + \sigma'^2 - 2\sigma\sigma'\cos\phi)^{1/2}} = \frac{4\sigma'}{\sigma + \sigma'} K\left(\frac{4\sigma\sigma'}{(\sigma+\sigma')^2}\right) , \qquad (2)$$

and K is the complete elliptic integral of the first kind. The temperature in either particle is approximately uniform at large distances from the contact point (σ = o), i.e.

$$f(\sigma) \longrightarrow 0 \quad \text{as} \quad \sigma \rightarrow \infty ,$$

and thus we may replace equation (1) by the approximate expression

$$f(\sigma) = \int_0^{\sigma_L} \frac{1 - f(\sigma')}{\lambda + (\sigma')^2} I(\sigma'/\sigma) d\sigma' + \int_{\sigma_L}^{\infty} \frac{I(\sigma'/\sigma)\, d\sigma'}{\lambda + \sigma'^2} , \qquad (3)$$

where $\sigma_L >> 1$.

To determine the function f over the range (o, σ_L) we first replace the integral over that interval in equation (3) by a quadrature involving the values of f at a number of grid points. A set of linear equations for the values of f at these grid points is then obtained from the requirement that equation (3) be satisfied at each of the grid points. This method for solving an integral equation is known as "the quadrature technique" (Atkinson 1976).

We have used a quadrature based on a modified rectangle rule, viz

$$\int_0^{\sigma_L} \frac{1-f(\sigma')}{\lambda+\sigma'^2} I(\sigma'/\sigma)\,d\sigma' \approx \sum_{j=0}^{N} \frac{1-f(\sigma_j)}{\lambda+\sigma_j^2} \int_{\sigma_j^*}^{\sigma_{j+1}^*} I(\sigma'/\sigma)\,d\sigma' \quad . \tag{4}$$

where

$$\sigma_j = \frac{\sigma_{j+1}^* + \sigma_j^*}{2} \quad ,$$

and σ_j^* is one of the (N+1) grid points on (o, σ_L). The grid points σ_0^* and σ_N^* are at 0 and σ_L respectively. Equation (4) is approximately valid if the function $\frac{1-f(\sigma)}{\lambda+\sigma^2}$ is approximately constant over each interval $(\sigma_j^*, \sigma_{j+1}^*)$. This function is proportional to the flux density on the surface of either particle and thus it has a sharp maximum of $\sigma = o$, since the particles are nearly in contact at that point. Hence we require a greater density of grid points in the neighbourhood of the origin than elsewhere. A suitable grid point distribution is given by

$$\sigma_j^* = \frac{j}{N} \frac{\sigma_L}{(N+1-j)} \quad . \tag{5}$$

From the expression (2) for the function $I(\sigma'/\sigma)$ we get,

$$\int_0^{\eta} I(\eta'/\eta)\,d\eta' = \frac{4}{\pi}\left\{(\eta^2-1)K(\eta^2) + E(\eta^2)\right\} \quad \text{if} \quad \eta<1 \quad , \tag{6a}$$

and

$$\int_1^{\eta} I(\eta'/\eta)\,d\eta' = \frac{4}{\pi}\left\{\eta E(1/\eta^2) - 1\right\} \quad \text{if} \quad \eta>1 \, , \tag{6b}$$

where E is the complete elliptic integral of the second kind. The coefficients $\int_{\sigma_j^*}^{\sigma_{j+1}^*} I(\sigma'/\sigma)\,d\sigma'$ in equation (3) were calculated with the aid of the relations (6a) and (6b), and polynomial approximations for E and K (Abromowitz and Stegun pp 541-2).

The set of linear equations (3) were solved by a Gaussian elimination technique. Both the setting up of the equations and the solution were carried out on an IBM 370 using double precision.

To evaluate the function $P(\lambda)$ from the computed values for $f(\sigma_j)$, we begin by writing the expression for $P(\lambda)$ in the form

$$P(\lambda) = 2\int_0^{\sigma_L} \frac{f(\sigma)\sigma d\sigma}{\lambda + \sigma^2} + 2\int_{\sigma_L}^{\infty} \frac{f(\sigma)\sigma d\sigma}{\lambda + \sigma^2} \tag{7}$$

The integral over (o, σ_L) in this expression was evaluated from the computed values of $f(\sigma_j)$ using a quadrature which again was based on modified rectangle rule.

To estimate the second integral in the expression (7) for P, we require an asymptotic expression for $f(\sigma)$ as $\sigma \to \infty$. In § 2.4 we found that the leading term in the asymptotic expansion for f is $\frac{2\log\sigma}{\sigma}$. To obtain the next term in this expansion we begin by writing the integral equation (1) for f in the form

$$f(\sigma) = \int_0^{\infty} \frac{I(\sigma'/\sigma)d\sigma'}{\lambda + \sigma'^2} - \int_0^{\infty} \frac{f(\sigma')I(\sigma'/\sigma)d\sigma'}{\lambda + \sigma'^2}, \tag{8}$$

The second integral in this expression is dominated by the contribution from a region surrouding the origin. In that region $I(\sigma'/\sigma) \approx 2\sigma'/\sigma$ (see (2.4.7)) and hence

$$\int_0^{\infty} \frac{f(\sigma')I(\sigma'/\sigma)d\sigma'}{\lambda + \sigma'^2} \sim \frac{P(\lambda)}{\sigma} \quad \text{as} \quad \sigma \to \infty \tag{9}$$

The asymptotic form of the other integral in the expression (8) for $f(\sigma)$ can be easily found by writing the integral in the form

$$\begin{aligned}\int_0^{\infty} \frac{I(\sigma'/\sigma)d\sigma'}{\lambda + \sigma'^2} &= \frac{2}{\sigma}\int_0^{\sigma} \frac{\sigma' d\sigma'}{\lambda + \sigma'^2} + \int_0^{\sigma} \frac{I(\sigma'/\sigma) - 2\sigma'/\sigma}{\lambda + \sigma'^2} d\sigma' + \int_{\sigma}^{\infty} \frac{I(\sigma'/\sigma)d\sigma'}{\lambda + \sigma'^2} \\ &= \frac{\log(\lambda + \sigma^2) - \log(\lambda)}{\sigma} + \frac{1}{\sigma}\left\{\int_0^1 \frac{I(x) - 2x}{\frac{\lambda}{\sigma^2} + x^2} dx + \int_0^1 \frac{I(x)}{\frac{\lambda}{\sigma^2} + x^2}\right\}.\end{aligned} \tag{10}$$

The quantity $I(x) - 2x$ is $O(x^2)$ as $x \to 0$ and thus the contribution to

$$\int_0^1 \frac{I(x) - 2x}{\frac{\lambda}{\sigma^2} + x^2}$$

→ from the region $x^2 < \frac{\lambda}{\sigma^2\Delta}$ where $\Delta \ll 1$, diminishes as $\sigma \to \infty$ (with λ fixed). Beyond this region the quantity $\frac{\lambda}{\sigma^2}$ forms a negligible part of the integrand, and thus the asymptotic form of equation (10) is

$$\int_0^\infty \frac{I(\sigma'/\sigma)\,d\sigma'}{\lambda+\sigma'^2} \sim \frac{2\log\sigma}{\sigma} + \frac{A-\log\lambda}{\sigma} \quad \text{as } \sigma\to\infty \qquad (11)$$

where

$$A = \int_0^1 \frac{I(x)-2x}{x^2}\,dx + \int_1^\infty \frac{I(x)\,dx}{x^2} = 2\cdot 8$$

The value of A was obtained using a conditional convergence scheme based on Simpson's rule.

On combining the asymptotic formulae (9) and (11) with the expression (8) for $f(\sigma)$, we get

$$f(\sigma) \sim \frac{2\log\sigma}{\sigma} + \frac{(2\cdot 8-\log\lambda-P(\lambda))}{\sigma} \quad \text{as } \sigma\to\infty.$$

Finally, on substituting this formula for f in the integral over (σ_L,∞) in the expression (7) for $P(\lambda)$, we find

$$P(\lambda) \approx 2\int_0^{\sigma_L} \frac{f(\sigma)\sigma\,d\sigma}{\lambda+\sigma^2} + \frac{4\log\sigma_L}{\sigma_L} + 2\frac{(4\cdot 8-\log\lambda-P(\lambda))}{\sigma_L}, \qquad (12)$$

and from this formula we can calculate $P(\lambda)$ from the computed values $f(\sigma_j)$.

The accuracy of the computed value of $P(\lambda)$ was checked by calculating P with 45 and then with 90 grid points, and in each case, the two computed values differed by less than one percent. Varying the value of σ_L also had a negligible effect on the value of $P(\lambda)$, provided σ_L was neither too large or too small (if σ_L is "too small" the error involved in replacing equation (1) by (3) is significant, and if σ_L is "too large" the grid points are too widely spaced and the relation (4) is not valid).

2. <u>The solution of equation (2.5.6) for the temperature and flux density over the surfaces of a pair of spheres, pressed together to form a flatspot</u>

We have solved the integral equation

$$f_1(\eta) = -\int_0^1 g_1(\eta') I(\eta'/\eta)\, d\eta' - \frac{1}{\beta}\int_1^\infty \frac{f_1(\eta') I(\eta'/\eta)}{L(\eta')}\, d\eta'$$

$$+ \frac{1}{\beta}\int_1^\infty [1 - f_0(\eta')]\left\{\frac{1}{L(\eta')} - \frac{1}{\eta'^2}\right\} I(\eta'/\eta)\, d\eta', \tag{13}$$

numerically, using similar methods to those employed in the solution of equation (1) for nearly-touching spheres. In this case the unknown functions are $g_1(\eta)$ for $0 < \eta < 1$ and $f_1(\eta)$ for $1 < \eta < \infty$. The quantity $f_0(\eta)$ is the solution to equation (1) for $\lambda = 0$, (and with the variable σ replaced by $\eta (= \sigma/\beta)$) and on the interval $0 < \eta < 1$ we have $f_1 = 1 - f_0$.

In order to simplify the program for solving the equation (13) numerically, we define

$$g_1(\eta) = \frac{1}{\beta}\left\{ \frac{f_1(\eta)}{L(\eta)} - \left[\frac{1}{L(\eta)} - \frac{1}{\eta^2}\right](1 - f_0(\eta))\right\}, \tag{14}$$

and equation (13) then reduces to

$$f_1(\eta) = -\int_0^\infty g_1(\eta') I(\eta'/\eta)\, d\eta' . \tag{15}$$

The aim is to find the function $g_1(\eta)$ which satisifes this equation together with the constraints

$$f_1(\eta) = 1 - f_0(\eta) \quad \text{for} \quad \eta \leqslant 1 \tag{16a}$$

and

$$f_1(\eta) = \beta g_1(\eta) L(\eta) + \beta\left[1 - \frac{L(\eta)}{\eta^2}\right] \quad \text{for} \quad \eta > 1 . \tag{16b}$$

This last constraint is obtained from the expression (14) for g_1.

On the assumption that the contribution to the integral in (15) from the region $\eta \gg 1$ is negligible we replace this integral equation by

$$f_1(\eta) = -\int_0^{\eta_L} g_1(\eta') I(\eta'/\eta)\, d\eta' , \tag{17}$$

where $\eta_L >> 1$.

The integral in (17) is then replaced by a quadrature, based on a modified rectangle rule and we get

$$f_1(\eta_i) = \sum_{j=0}^{N} g(\eta_j) \int_{\eta_j^*}^{\eta_{j+1}^*} I(\eta'/\eta)\, d\eta' , \quad i = 0, \ldots, N+1 \tag{18}$$

where $\eta_j = \frac{\eta_{j+1}^* + \eta_j^*}{2}$. On replacing $f_1(\eta_i)$ by the appropriate expression (16a) or (16b) we obtain a set of simultaneous equations for $g_1(\eta_i)$

The function $g_1(\eta)$ has a sharp maximum at the edge of the contact circle ($\eta = 1$) and this maximum becomes more pronounced as $\beta \to \infty$. Thus the grid points must be closely spaced in the neighbourhood of $\eta = 1$; a suitable distribution of grid points is given by

$\eta_i = 1 + (\eta_L - 1)\left\{\frac{(i - N_1)}{(N - N_1)}\right\}^m$ for points outside the contact circle, and

$\eta_i = 1 - (1 - i/N_1)^n$

for the (N_1 + 1) points on the contact circle where n,m > 1. By varying the parameters m and n we can adjust the grid point distribution; as m and n increase the points move towards the edge of the contact circle.

As before the simultaneous equations were set up and solved on the IBM 370, using a Gaussian elimination technique. The functions $\mathcal{H}_c(\beta)$ and $\Delta\mathcal{H}_m(\beta)$ (defined by equations (2.5.8) and (2.5.9) were calculated from the computed values of $g_1(\eta_j)$ and $f_0(\eta_j)$ using a simple quadrature, again based on a modified rectangle rule.

To test the accuracy of the computed results we first calculated the values of $\mathcal{H}_c(\beta)$ and $\Delta\mathcal{H}_m(\beta)$ using 50 or 60 grid points. The number of grid points was then doubled (with N_1/N fixed) and the computations repeated. The computed values of $\mathcal{H}_c$ and $\Delta\mathcal{H}_m$ were considered to be acceptable if the relative variations in these values caused by increasing the number of grid points (generally from 50 to 100) or by doubling or halving η_L, were less than one percent. The values of the grid parameters n, m and η_L which were used in obtaining these "acceptable" values of $\mathcal{H}_c$ and $\Delta\mathcal{H}_m$ were selected, for each value of β, by trial and error.

As mentioned earlier, the function g_1 develops a sharp peak at $\eta = 1$ as $\beta \to \infty$. Thus the number of grid points required to obtain acceptable values of $\mathcal{H}_c$ and $\Delta\mathcal{H}_m$ increases with β, and for this reason we have only calculated $\mathcal{H}_c$ and $\Delta\mathcal{H}_m$ up to $\beta = 100$.

A2

The numerical solution of the integral equation (3.2.16)

In this section we describe the steps involved in the solution of the equation

$$1 = \alpha\left(\frac{h}{a} + \eta^2\right)g(\eta) + \frac{2}{\pi}\int_{-\infty}^{\infty} g(\eta')\log|\eta'-\eta|\,d\eta' , \qquad \text{(3.2.16) repeated}$$

for the flux density g between a pair of parallel cylinders which are nearly in contact with each other.

Although the limits of the integral in (3.2.16) extend to $\pm\infty$ the integral is dominated by the contribution from a small region surrounding the origin. Hence we may approximate the integral by

$$\frac{2}{\pi}\int_{-1}^{1} g(\eta')\log|\eta-\eta'|\,d\eta' ,$$

where the limits ± 1 are both convenient and large enough to contain the small interval which provides the dominant contribution to the integral. As g is an even function of η we only require values of g in the range (0,1) and the equation (3.2.16) may be rewritten as

$$1 = \alpha\left(\frac{h}{a} + \eta^2\right)g(\eta) + \frac{2}{\pi}\int_0^1 g(\eta')\{\log|\eta-\eta'| + \log(\eta+\eta')\}\,d\eta' \qquad (1)$$

Using a modified rectangle rule, the integral in (1) is replaced by a finite sum involving the values of g at selected grid points in $0 < \eta < 1$, and equation (1) becomes

$$1 = \alpha\left(\frac{h}{a} + \eta_i^2\right)g(\eta_i) + \frac{2}{\pi}\sum_{j=1}^{N} g(\eta_j)\int_{\eta_j^*}^{\eta_{j+1}^*}\{\log|\eta_i-\eta| + \log|\eta_i+\eta|\}\,d\eta \qquad (2)$$

$$= A_{ij}\,g(\eta_j) ,$$

where $$A_{ij} = \alpha\left(\frac{h}{a} + \eta_i^2\right)\delta_{ij} + \frac{2}{\pi}\int_{\eta_j^*}^{\eta_{j+1}^*}\{\log|\eta_i-\eta| + \log(\eta_i+\eta)\}\,d\eta ,$$

$$\eta_j^* = (j/N)^m \qquad (3)$$

and $$\eta_j = \frac{1}{2}(\eta_j^* + \eta_{j+1}^*) \quad .$$

The integer N in the expression (3) for the grid points is equal to the number of grid points in (0,1) and the exponent m determines the concentration of points about the origin. As g has a sharp maximum at the origin, m is chosen to be greater than one in order that there be more points where $d^2g/d\eta^2$ is largest. The set of simultaneous equations (2) with $\alpha = 10^4$, were solved on the IBM 370 using Gaussian elimination for various values of $^h/a$. The non-dimensional flux between the cylinders is given by

$$\mathcal{H}(\alpha, \frac{h}{a}) = 2\alpha \int_0^\infty g(\eta)\, d\eta$$

and with the usual rectangle rule this is approximated by

$$2\sum_{j=1}^{N} g(\eta_j)(\eta_{j+1} - \eta_j) \quad .$$

The errors involved in the approximation of equation (3.2.16) by (1) decrease as the number of grid points is increased, and we may estimate the error in $\mathcal{H}$ by observing the variation in the computed values of $\mathcal{H}$ as the mesh size decreases. In each case the relative variation in $\mathcal{H}(10^4, h/a)$ caused by increasing N from 30 to 60 was less than one percent.

Appendix A3

Deriving the Faxén-type expression (4.3.13) for the elastic dipole strength of a rigid sphere

The starting point for this derivation is the expression (4.2.9) for the displacement at a point in the suspension. On converting the integral over the volume V_j in (4.2.9) into a surface integral, and using the fact that $\underset{\approx}{\tau} = \underset{\approx}{\sigma}$ at points in a rigid particle, we get

$$\underset{\sim}{u}(\underset{\sim}{x}) = \int_{\Gamma_j} \underset{\approx}{G}(\underset{\sim}{x}-\underset{\sim}{x}')\cdot\underset{\approx}{\sigma}(\underset{\sim}{x}')\cdot\hat{n}\, dA(\underset{\sim}{x}') + \underset{\sim}{u}_E(\underset{\sim}{x}) \tag{1}$$

where $\underset{\sim}{u}_E(\underset{\sim}{x})$ is given by (4.3.12). The "external field" $\underset{\sim}{u}_E(\underset{\sim}{x})$ is the displacement which would be obtained at $\underset{\sim}{x}$ if the reference spheres (i.e. sphere j) could be replaced by matrix material, with the stress on the surfaces of the surrounding spheres held fixed.

Our aim is to derive an expression relating the dipole strength of the reference sphere to the field $\underset{\sim}{u}_E$. Since the sphere is rigid, we have

$$\underset{\sim}{u}(\underset{\sim}{x}) = \underset{\sim}{U} + \underset{\sim}{\Omega}\times(\underset{\sim}{x}-\underset{\sim}{x}_0) \tag{2}$$

at points $\underset{\sim}{x}$ on the surface of the sphere. Taking the first moment of equation (1) with respect to the centre $\underset{\sim}{x}_0$ of the reference sphere, we get

$$\begin{aligned}\int_{\Gamma_j} \underset{\sim}{u}(\underset{\sim}{x})(\underset{\sim}{x}-\underset{\sim}{x}_0)\, dA(\underset{\sim}{x}) = &\int_{\Gamma_j'}\left\{\int_{\Gamma_j} \underset{\approx}{G}(\underset{\sim}{x}-\underset{\sim}{x}')\cdot\underset{\approx}{\sigma}(\underset{\sim}{x}')\cdot\hat{n}(\underset{\sim}{x}')(\underset{\sim}{x}-\underset{\sim}{x}_0)\, dA(\underset{\sim}{x})\right\} dA(\underset{\sim}{x}') \\ &+ \int_{\Gamma_j} \underset{\sim}{u}_E(\underset{\sim}{x})(\underset{\sim}{x}-\underset{\sim}{x}_0)\, dA(\underset{\sim}{x}) .\end{aligned} \tag{3}$$

From (2) we get

$$\int_{\Gamma_j} u(\underset{\sim}{x})_m(\underset{\sim}{x}-\underset{\sim}{x}_0)_k\, dA(\underset{\sim}{x}) = \frac{4\pi a^4}{3}\,\epsilon_{imk}\Omega_i \tag{4}$$

To find $\int_{\Gamma_j} \underset{\sim}{u}_E(\underset{\sim}{x})(\underset{\sim}{x}-\underset{\sim}{x}_0)\,dA(\underset{\sim}{x})$, we expand $\underset{\sim}{u}_E(\underset{\sim}{x})$ in a Taylor series about $\underset{\sim}{x}_0$,

$$\int \underset{\sim}{u}_E(\underset{\sim}{x})(\underset{\sim}{x}-\underset{\sim}{x}_0)\,dA(\underset{\sim}{x}) = \underset{\sim}{u}_E(\underset{\sim}{x}_0)\int(\underset{\sim}{x}-\underset{\sim}{x}_0)\,dA + \nabla\underset{\sim}{u}_E(\underset{\sim}{x}_0)\cdot\int(\underset{\sim}{x}-\underset{\sim}{x}_0)(\underset{\sim}{x}-\underset{\sim}{x}_0)\,dA + \ldots \tag{5}$$

Evaluating the coefficients in this expression and using the identity

$$\nabla^4\underset{\sim}{u}(\underset{\sim}{x}) = \underset{\sim}{0}$$

associated with the elasticity equations, (Landau and Lifshitz (1970) pp 18) we get

$$\int_{\Gamma_j} \underset{\sim}{u}_E(\underset{\sim}{x})(\underset{\sim}{x}-\underset{\sim}{x}_0)\,dA = \frac{4\pi a^4}{3}\left(\nabla\underset{\sim}{u}_E(\underset{\sim}{x}_0) + a^2\nabla^2\nabla\underset{\sim}{u}_E(\underset{\sim}{x}_0)\right) \tag{6}$$

This result is valid for any displacement field which satisifies the elasticity equations in Γ_j, and thus we have

$$\begin{aligned}\int_{\Gamma_j}\left\{\underset{\approx}{G}(\underset{\sim}{x}-\underset{\sim}{x}')\cdot\underset{\approx}{\sigma}(\underset{\sim}{x}')\cdot\hat{n}(\underset{\sim}{x}')\right\}(\underset{\sim}{x}-\underset{\sim}{x}_0)\,dA(\underset{\sim}{x}) \\ = \frac{4\pi a^4}{3}\left(\nabla\underset{\approx}{G}(\underset{\sim}{x}'-\underset{\sim}{x}_0) + \frac{a^2}{10}\nabla^2\nabla\underset{\approx}{G}(\underset{\sim}{x}'-\underset{\sim}{x}_0)\right)\cdot\underset{\approx}{\sigma}(\underset{\sim}{x}')\cdot\hat{n}(\underset{\sim}{x}').\end{aligned} \tag{7}$$

We can use this result to evaluate the remaining term in equation (3). Integrating (7) with respect to $\underset{\sim}{x}'$, over the surface of the sphere, we get

$$\begin{aligned}\int_{\Gamma_j}\left[\int_{\Gamma_j}\underset{\approx}{G}(\underset{\sim}{x}-\underset{\sim}{x}')\cdot\underset{\approx}{\sigma}(\underset{\sim}{x}')\cdot\hat{n}(\underset{\sim}{x}')(\underset{\sim}{x}-\underset{\sim}{x}_0)\,dA(\underset{\sim}{x})\right]dA(\underset{\sim}{x}') \\ = \frac{4\pi a^4}{3}\int_{\Gamma_j}\left[\nabla\underset{\approx}{G}(\underset{\sim}{x}'-\underset{\sim}{x}_0) + \frac{a^2}{10}\nabla^2\nabla\underset{\approx}{G}(\underset{\sim}{x}-\underset{\sim}{x}_0)\right]\cdot\underset{\approx}{\sigma}(\underset{\sim}{x}')\cdot\hat{n}(\underset{\sim}{x}')\,dA(\underset{\sim}{x}').\end{aligned} \tag{8}$$

From the definition (4.1.6) for G, we get

$$\begin{aligned}\frac{\partial G_{jk}(\underset{\sim}{x}'-\underset{\sim}{x}_0)}{\partial x_i} + \frac{a^2}{10}\nabla^2\frac{\partial G_{jk}(\underset{\sim}{x}'-\underset{\sim}{x}_0)}{\partial x_i} = \frac{1+\nu}{8\pi E(1-\nu)a^3}\Big\{\delta_{jk}(\underset{\sim}{x}'-\underset{\sim}{x}_0)_i\frac{(18-20\nu)}{5} \\ -\frac{2}{5}\delta_{ij}(\underset{\sim}{x}'-\underset{\sim}{x}_0)_k - \frac{2}{5}\delta_{ik}(\underset{\sim}{x}'-\underset{\sim}{x}_0)\Big\}.\end{aligned} \tag{9}$$

Substituting the expression (9) in the integrand in equation (8) we find

$$\int_{\Gamma_j}\Big[\int_{\Gamma_j} \underset{\approx}{G}(\underset{\sim}{x}-\underset{\sim}{x}')\cdot\underset{\approx}{\sigma}(\underset{\sim}{x}')\cdot\hat{n}(\underset{\sim}{x}')(\underset{\sim}{x}-\underset{\sim}{x}_0)\,dA(\underset{\sim}{x})\Big]\,dA(\underset{\sim}{x}')$$

$$= \frac{-a(1+\nu)}{30E(1-\nu)}\left\{(16-20\nu)\underset{\approx}{S}^j - 2(\text{trace}\,\underset{\approx}{S}^j)\underset{\approx}{I}\right\}. \qquad (10)$$

Replacing each of the terms in equation (3) by the corresponding expressions (4), (6) and (10), we get

$$\frac{4\pi a^4}{3}\epsilon_{mik}\Omega_m = -\frac{a(1+\nu)}{30E(1-\nu)}\left\{(16-20\nu)S^j_{ik} - 2\delta_{ik}S^j_{mm}\right\}$$
$$+\frac{4\pi a^4}{3}\left(\frac{\partial u_E(x_0)_i}{\partial x_k} + \frac{a^2}{10}\frac{\partial^2}{\partial x_m^2}\frac{\partial}{\partial x_k}u_E(x_0)_i\right), \qquad (11)$$

and taking the symmetric part of this expression, we obtain

$$\frac{a(1+\nu)}{30E(1-\nu)}\left\{(16-20\nu)\underset{\approx}{S}^j - 2(\text{trace}\,\underset{\approx}{S}^j)\underset{\approx}{I}\right\} = \frac{4\pi a^4}{3}\left(\underset{\approx}{e}_E(x_0) + \frac{a^2}{10}\nabla^2\underset{\approx}{e}_E(x_0)\right). \qquad (12)$$

Taking the trace of this expression, and using the identity

$$\nabla^2(\text{trace}\,\underset{\approx}{e}_E) \;(=\nabla^2(\nabla\cdot\underset{\sim}{u}_E)) = 0,$$

(Landau and Lifshitz (1970), pp 18), we get

$$\text{trace}\,\underset{\approx}{S}^j = \frac{4a^2E(1-\nu)}{(1+\nu)(1-2\nu)}\,\text{trace}[\underset{\approx}{e}_E(x_0)].$$

Substituting this expression in equation (12), we obtain the Faxen-type formula:

$$\underset{\approx}{S}^j = \frac{10\pi a^3E(1-\nu)}{(4-5\nu)(1+\nu)}\left[\underset{\approx}{e}_E(x_0) + \frac{a^2}{10}\nabla^2\underset{\approx}{e}_E(x_0) + \underset{\approx}{I}\,\frac{\text{trace}[\underset{\approx}{e}_E(x_0)]}{5(1-2\nu)}\right].$$

Appendix A4

The Derivation of equation (4.4.7)

The aim is to derive an expression for the third-order thermal multipole strength of a sphere $\mathcal{M}_3^j$ in a statistically homogeneous suspension. This is obtained from a combination of a Faxén type expression which relates $\mathcal{M}_3^j$ to the external field T_E, and the expression (4.3.2) for T_E.

From equation (4.3.4), we get

$$\frac{\partial}{\partial x_i}\frac{\partial}{\partial x_j}\frac{\partial}{\partial x_k}T(\underset{\sim}{x}_0)=\frac{\partial}{\partial x_i}\frac{\partial}{\partial x_j}\frac{\partial}{\partial x_k}T_E(\underset{\sim}{x}_0)-\frac{(1-\alpha^{-1})}{4\pi k}\int_{\Gamma_j}\frac{\partial}{\partial x_i'}\frac{\partial}{\partial x_j'}\frac{\partial}{\partial x_k'}\left(\frac{1}{r}\right)\underset{\sim}{F}.\hat{n}\,dA\Big|_{\underset{\sim}{x}=\underset{\sim}{x}_0}. \qquad (1)$$

The minus sign in front of the integral comes from replacing $\frac{\partial}{\partial x_i}$ by $-\frac{\partial}{\partial x_i'}$. Substituting

$$\frac{\partial}{\partial x_i'}\frac{\partial}{\partial x_j'}\frac{\partial}{\partial x_k'}\frac{1}{r}=\frac{3}{r^5}\left(\delta_{jk}r_i+\delta_{ki}r_j+\delta_{ij}r_k\right)-\frac{15r_ir_jr_k}{r^7},$$

(where $r_i\equiv(\underset{\sim}{x}-\underset{\sim}{x}_0)_i$) in the integrand in (1), we find

$$\frac{\partial}{\partial x_i}\frac{\partial}{\partial x_j}\frac{\partial}{\partial x_k}T(\underset{\sim}{x}_0)=\frac{\partial}{\partial x_i}\frac{\partial}{\partial x_j}\frac{\partial}{\partial x_k}T_E(\underset{\sim}{x}_0)-\frac{3}{4\pi ka^5}\left\{\delta_{ij}S_k+\delta_{ik}S_j+\delta_{ij}S_k\right\}$$
$$+\frac{15}{4\pi ka^7}(\mathcal{M}_3)_{ijk} \qquad (2)$$

where $\underset{\sim}{S}$ and $\mathcal{M}_3$ are the dipole and 3rd order multipole strength of the reference sphere (for convenience, the superscript j has been dropped).

Another expression for $\frac{\partial}{\partial x_i}\frac{\partial}{\partial x_j}\frac{\partial}{\partial x_k}T(\underset{\sim}{x}_0)$ can be obtained by differentiating the expression (4.3.5) for T, which gives .

$$\frac{\partial}{\partial x_i}\frac{\partial}{\partial x_j}\frac{\partial}{\partial x_k} T(\underset{\sim}{x}_0) = \frac{1}{4\pi\alpha k}\int_{\Gamma_j} \frac{\partial}{\partial x_i'}\frac{\partial}{\partial x_j'}\frac{\partial}{\partial x_k'}\left(\frac{1}{r}\right)_{\underset{\sim}{x}=\underset{\sim}{x}_0} \underset{\sim}{F}\cdot\hat{n}\,dA + \frac{1}{4\pi}\int_{\Gamma_j} T\frac{\partial}{\partial x_i'}\frac{\partial}{\partial x_j'}\frac{\partial}{\partial x_k'}\frac{\partial}{\partial x_m'}\frac{1}{r}\, n_m\, dA$$

$$= \frac{3}{4\pi(\alpha-1)ka^5}\{\delta_{jk}S_i + \delta_{ik}S_j + \delta_{ij}S_k\} - \frac{15(\mathcal{M}_3)_{ijk}}{4\pi k(\alpha-1)a^7}$$

$$+ \frac{3}{\pi a^6}\left\{\delta_{jk}\int Tr_i\,dA + \delta_{ik}\int Tr_j\,dA + \delta_{ij}\int Tr_k\,dA\right\} + \frac{15}{\pi a^8}\int r_i r_j r_k T\,dA\,. \tag{3}$$

Expanding T in a Taylor series about $\underset{\sim}{x}_0$ and using the fact that $\nabla^2 T = 0$, we find

$$\int_{\Gamma_j} r_i T\,dA = \frac{4\pi a^4}{3}\frac{\partial T(\underset{\sim}{x}_0)}{\partial x_i}\,,$$

and

$$\int r_i r_j r_k T\,dA = \frac{4\pi a^8}{105}\frac{\partial}{\partial x_i}\frac{\partial}{\partial x_j}\frac{\partial}{\partial x_k}T(\underset{\sim}{x}_0) + \frac{4\pi a^6}{15}\left[\delta_{jk}\frac{\partial T(\underset{\sim}{x}_0)}{\partial x_i} + \delta_{ik}\frac{\partial T(\underset{\sim}{x}_0)}{\partial x_j} + \delta_{ij}\frac{\partial T(\underset{\sim}{x}_0)}{\partial x_k}\right]$$

Substituting these expressions in (3), we get

$$\frac{\partial}{\partial x_i}\frac{\partial}{\partial x_j}\frac{\partial}{\partial x_k}T(\underset{\sim}{x}_0) = -\frac{35(\mathcal{M}_3)_{ijk}}{4\pi k(\alpha-1)a^7} - \frac{7}{4\pi k(\alpha-1)a^5}\{\delta_{jk}S_i + \delta_{ik}S_j + \delta_{ij}S_k\}$$

$$+\frac{7}{a^2}\left[\delta_{jk}\frac{\partial T(\underset{\sim}{x}_0)}{\partial x_i} + \delta_{ij}\frac{\partial T(\underset{\sim}{x}_0)}{\partial x_k} + \delta_{ik}\frac{\partial T(\underset{\sim}{x}_0)}{\partial x_j}\right]. \tag{4}$$

Eliminating $\frac{\partial}{\partial x_i}\frac{\partial}{\partial x_j}\frac{\partial}{\partial x_k}T(\underset{\sim}{x}_0)$ from the above expression with the aid of (2), we obtain

$$\mathcal{M}_3 = \frac{4\pi k a^7(\alpha-1)}{15(\alpha+4/3)}\nabla\nabla\nabla T_E(\underset{\sim}{x}_0) + [\cdot\cdot\cdot\cdot\cdot]\,. \tag{5}$$

This is required Faxen type expression for $\mathcal{M}_3$. The square brackets in (5) enclose terms of the form

$$\delta_{jk}\frac{\partial T}{\partial x_i} \qquad (6)$$

The coefficient of $(\mathcal{M}_3)_{jki}$ in equation (4.4.1) is

$$\frac{(\alpha-1)a^3}{6(\alpha+2)}\sum_m \frac{\partial}{\partial x_j'}\frac{\partial}{\partial x_k'}\frac{\partial}{\partial x_i'}\frac{\partial}{\partial x_n'}\frac{1}{r^m},$$

and the contribution to (4.4.1) from terms of the form (6) is

$$\frac{(\alpha-1)}{6(\alpha+2)}\sum_m\left(\frac{\partial}{\partial x_i'}\frac{\partial}{\partial x_n'}\nabla'^2\frac{1}{r^m}\right)\frac{\partial T}{\partial x_i} = 0,$$

These terms are therefore of no interest to us, and for the remainder of this section we shall ignore the square bracketed term in equation (5).

To evaluate the expression (5) for $\mathcal{M}_3$, we require $\nabla\nabla\nabla T_E(\underset{\sim}{x}_0)$ The external field T_E is given by the expression (4.3.2). With the aid of the identity (4.3.3) and the divergence theorem we can rewrite (4.3.2) as

$$T_E(\underset{\sim}{x}) = \sum_{\substack{i\\ i\neq j}}\frac{(1-\alpha^{-1})}{4\pi k}\int_{\Gamma_i}\frac{\underset{\sim}{F}\cdot\hat{n}}{r}dA + \frac{1}{4\pi k}\int_{\Gamma_b}\left\{\frac{\langle \underset{\sim}{F}\rangle\cdot\hat{n}}{r} + k\langle T\rangle\nabla'\left(\frac{1}{r}\right)\cdot\hat{n}\right\}dA.$$

From this equation we find

$$\nabla\nabla\nabla T_E(\underset{\sim}{x}_0) = -\sum_{\substack{i\\ i\neq j}}\frac{(1-\alpha^{-1})}{4\pi k}\int_{\Gamma_i}\nabla'\nabla'\nabla'\frac{1}{r}\,\underset{\sim}{F}\cdot\hat{n}\,dA$$
$$-\frac{1}{4\pi k}\int_{\Gamma_b}\left\{\nabla'\nabla'\nabla'\frac{1}{r}\langle \underset{\sim}{F}\rangle\cdot\hat{n} + k\langle T\rangle\nabla'\nabla'\nabla'\nabla'\frac{1}{r}\cdot\hat{n}\right\}dA. \qquad (7)$$

The integral over the macroscopic boundary Γ_b in this equation may be neglected. To show this, we take Γ_b to be a sphere of radius R. By assumption, $\langle\nabla T\rangle$ is uniform throughout the material, and as the material is homogeneous, $\langle \underset{\sim}{F}\rangle$ is also uniform. The term $\nabla'\nabla'\nabla'\frac{1}{r}$ is $O(\frac{1}{r^4})$ as $r\to\infty$, and thus

$$\int\nabla'\nabla'\nabla'\frac{1}{r}\underset{\sim}{F}\cdot\hat{n}\,dA = O\left(\frac{1}{R^2}\right) \text{ as } R\to\infty$$

Similarly $\langle T(\underset{\sim}{x})\rangle - \langle T(\underset{\sim}{x}_0)\rangle \left(= \langle \nabla T\rangle\cdot(\underset{\sim}{x}-\underset{\sim}{x}_0)\right) = O(R)$ on Γ_b' , and since

$\nabla'\nabla'\nabla'\nabla'\frac{1}{r} = O(\frac{1}{R^5})$ on Γ_b' we have

$\int \langle T\rangle \nabla'\nabla'\nabla'\nabla'\frac{1}{r}\cdot \hat{n}\, dA = O(\frac{1}{R^2})$ as $R \longrightarrow \infty$.

Thus the integral over Γ_b in equation (7) vanishes as $R \rightarrow \infty$ and (7) becomes

$$\nabla\nabla\nabla T_E(\underset{\sim}{x}_0) = -\sum_{\substack{i\\ i\neq j}} \frac{(1-\alpha^{-1})}{4\pi k}\int_{\Gamma_i'} \nabla'\nabla'\nabla'\frac{1}{r}\, \underset{\sim}{F}\cdot\hat{n}\, dA \,. \tag{8}$$

Combining this result with equation (5), we get

$$\mathcal{M}_3 = \frac{-a^7(\alpha-1)^2}{15(\alpha+\frac{4}{3})\alpha}\sum_{\substack{i\\ i\neq j}}\int_{\Gamma_i}\nabla'\nabla'\nabla'\frac{1}{r}\, \underset{\sim}{F}\cdot\hat{n}\, dA \,, \tag{9}$$

and expanding the term $\nabla'\nabla'\nabla'\frac{1}{r}$ in a Taylor series about $\underset{\sim}{x}^i$ (the centre of sphere i), we obtain

$$\mathcal{M}_3 = -\frac{(\alpha-1)a^7}{15(\alpha+\frac{4}{3})}\sum_{\substack{i\\ i\neq j}}\left\{\underset{\sim}{S}^i\cdot\nabla'\nabla'\nabla'\nabla'\frac{1}{r^i} + \sum_{k=2}^{\infty}\frac{\mathcal{M}_3^k}{k!}\overset{(1)}{\nabla'}\ldots\overset{(k+3)}{\nabla'}\frac{1}{r^i}\right\} \,. \tag{10}$$